Comparative Studies on Enamel Hypoplasia in the Siwalik Rhinocerotidae (Mammalia)

Ghazala Roohi

Department of Zoology, University of the Punjab,
Quaid-e-Azam Campus, Lahore, Pakistan

May, 2013

Comparative Studies on Enamel Hypoplasia in the Siwalik Rhinocerotidae (Mammalia)

By

Ghazala Roohi

Under the supervision of

Prof. Dr. Muhammad Akhtar
Prof. Dr. Syed Mahmood Raza

A thesis submitted to the University of the Punjab in Partial Fulfillment of the requirements for the degree of
Doctor of Philosophy in Zoology

Department of Zoology
University of the Punjab
Quaid-e-Azam Campus
Lahore, Pakistan

May, 2013

Dedication

I dedicate this thesis to my Beloved Parents

Certificate of Approval

This is to certify that the research work described in this thesis entitled "*Comparative studies on Enamel Hypoplasia in the Siwalik Rhinocerotidae (Mammalia)*" is the original work of Ghazala Roohi and has been carried out under our supervision. We have personally gone through all the data/results/materials reported in the manuscript and certify their correctness/authenticity. We further certify that the material included in this thesis has not been used in part or full in a manuscript already submitted or in process of submission in partial/complete fulfillment of the award of any other degree from any other institution. We also certify that the thesis has been prepared under our supervision according to the prescribed format and we endorse its evaluation for the award of Ph.D. degree through the official procedures of the University of the Punjab.

Prof. Dr. Muhammad Akhtar
Chairman
Department of Zoology
University of the Punjab
Quaid-e-Azam Campus
Lahore

Prof. Dr. Syed Mahmood Raza
Program Coordinator
Tertiary Education Support Program (TESP)
Higher Education Commission
Sector H-9
Islamabad

Comparative studies on Enamel Hypoplasia in the Siwalik Rhinocerotidae (Mammalia)

Abstract

Enamel Hypoplasia (failure for the enamel to form properly), a tooth defect during development, provides a permanent record of systematic stress during early life. Research on enamel defects can provide an insight into environmental conditions present during the growing years of an extinct animal's life. Anthropologists and paleontologists have carried out studies on incidence and distribution of Linear Enamel Hypoplasia to assess the health status of past populations. The present study on Enamel Hypoplasia in Siwalik Rhinoceroses is being conducted for the first time on Siwalik mammals. Dental defects are known in many mammalian taxa but their potential use in paleontological interpretations has not previously been explored in Siwalik mammals. This study is based on examination of a total of 1754 Rhinocerotid teeth housed in major museums and institutes of Pakistan, France, UK and the USA. The Neogene Rhino collections collected from the Potwar Plateau, Sulaiman Range, Bugti Hills, Kirthar Range and the Siwalik Hills housed at the GSP, PMNH, PUPC, MNHN, MHNT, AMNH, PMHU, YPNHM, and the NHM, London, were investigated. Recent Rhino teeth have also been examined at MNHN, Paris and the Harvard Museum of Comparative Zoology (MCZ).

Each and every tooth in the collections was examined for the presence or absence of Enamel Hypoplasia (EH) and description of each defect, its position on the tooth crown, the number of occurrences on the tooth, and the position of the defected tooth in each jaw were recorded. A total 1754 Rhinocerotid teeth comprising 846 fossils Rhino teeth and 908 recent Rhino teeth were examined. The 846 fossil Rhinocerotid teeth included 21 incisors, 2 canines, 43 deciduous premolars, 283 premolars, and 497 molars, whereas the recent Rhino teeth included 15 incisors, 32 canines, 486 premolars, and 375 molars. The 846 fossil teeth calculated for MNI (minimum number of individuals) indicated 337 animals whereas the recent Rhinos teeth are from 45 animals. In fossil Rhinos, 34 teeth had hypoplasia and in recent only 6 teeth are found with EH. EH are recorded almost in equal numbers on the buccal as well as on the lingual side in the fossil or recent specimens studied. Most of the EH are of Linear type which are more prominent and

common. 5 cases of semicircular EH have also been noted which, except one, are on the lingual side. The teeth having hypoplasia in this study show that 87% of EH occurs on permanent teeth, whereas 13% are in deciduous teeth. Among the deciduous teeth, 60% occurrences are on the dP4, which is the last one to erupt among the deciduous teeth of rhinoceroses. EH position on the crown from the cementoenamel junction (i.e. neck), indicate EH in most of the teeth occurred at a late developmental stage. One possible inference, based on the location of EH on the tooth and the position of the tooth in the jaw, is that Enamel Hypoplasia occurred when the animal was not dependent upon mother's nutrition. Therefore, the animal was under some sort of physiological stresses perhaps triggered by external factors.

The ~25 Myr to about 2 Myr fauna of Rhinocerotids dental material examined and analyzed in this study, covers a wider geographical region from the Bugti Hills in central Pakistan to the Pabbi Hills in north-eastern Pakistan, and all the way to the Siwalik Hills in India. This study includes 14 Rhino species from the earliest radiation in the late Oligocene in the Bugti Hills to the still living *Rhinoceros sondaicus* in the Upper Pliocene rocks of the Pabbi Hills and the Siwalik Hills. The 34 species showing hypoplasia occur almost at all the intervals of the Neogene. It is difficult to directly correlate the hypoplasia occurrences with global or regional climate changes but there exists some relationship, which is discussed here. The Rhino species with EH are apparently more prevalent at four time periods; around 22-20 Myr, ~16 Myr, 12-8 Myr and ~2 Myr in the Pliocene. It has been argued that climate, especially seasonality with prolonged draught periods, might have been the cause of stress for these animals having hypoplasia. It would, however, bring credence to the hypothesis proposed here that climate change has caused the EH in Rhinos if other mammalian taxa are also examined for the same time span.

Acknowledgements

My interest in paleontology was first sparked during my M.Sc. studies in Zoology Department, University of the Punjab, Lahore, Pakistan. I took several courses in paleontology and did a research project on "Siwalik *Tragulidae*" supervised by Professor Dr. Muhammad Sarwar. During my initial years (1986-87) as a Research Associate in the Earth Sciences Division of Pakistan Museum of Natural History (Islamabad), Dr. S. Taseer Hussain (Director General), Dr. S. Mahmood Raza (Curator) and Dr. S. Rafiqul Hassan Baqri, Director continuously encouraged and trained me to focus on paleontological research. Dr. John Barry, Peabody Museum of Harvard University encouraged me to pursue this enamel hypoplasia studies and helped me invaluably with my research.

I have many people to thank for their advice, collaboration and camaraderie throughout this research. First I would like to express my deepest gratitude to Prof. Dr. Syed Mahmood Raza for his able guidance, suggestions and fruitful discussions throughout the study period. I am also obliged to Prof. Dr. Muhammad Akhtar for his kind support, inspiration and encouragement throughout this study.

The research work was carried out in Pakistan, France, UK and USA. The financial support of the French Embassy, Islamabad for internship at the Paris Museum and Toulouse University to start this research work on enamel hypoplasia is gratefully acknowledged, and the academic guidance of Dr. Pierre-Olivier Antoine (now at University of Montpelier) and Dr. Grégoire Métais (Museum National d'Histoire Naturelle) was pivotal for initiating the laboratory investigations.

Special thanks to Dr. A. Majid Khan (University of the Punjab); Dr. Munir-ul-Haq (Geological Survey of Pakistan); Dr. David Pilbeam, Dr. John C. Barry, Dr. Larry Flynn, and Dr. Michele Morgan of the Peabody Museum Harvard University; Judith Galkin (American Museum of Natural History); Judith Chupasko and Catherine Weisel (Museum of Comparative Zoology, Harvard University); Dr. Christopher Norris and Daniel Brinkman (Peabody Museum of Natural History, Yale University); and Andrew Currant, *Jessica McDonald and* Roula Pappa (Natural History Museum, UK), for their help and support to facilitate the study of Rhino collections in their respective institutions. I wish to acknowledge Dr. John Barry, Dr. Lawrence Flynn, and Dr. A. Majid Khan for their guidance and discussion on the Siwaliks paleontology and geology.

I am grateful to the Chairman, Pakistan Science Foundation and the Director General of Pakistan Museum of Natural History and the Director, Earth Sciences Division for their consistent encouragement. I also wish to thank my colleague Mr. Hamid Dawood Akbar for editing this volume with unfailing energy and enthusiasm.

Syed Munir Hussain Shah and Faisal Rehman are thanked for helping in preparation of figures, tables and photographs. I am also grateful to all officers and staff of the Earth Sciences Division.

I must thank to dear Nageen and my loving family (sister, brothers, nieces, and nephews) and my friends who prayed day and night for the successful completion of this work.

Finally, I want to dedicate this thesis to my beloved parents, Mr. M. Zafarullah (Late) and Mrs. Shamim Farhat who provided vigorous and enthusiastic support towards its completion.

Comparative studies on Enamel Hypoplasia in the Siwalik Rhinocerotidae (Mammalia)

Contents

Page #

List of Tables

List of Figures

List of Abbreviations

American Museum of Natural History, New York	AMNH
Dental Enamel Hypoplasia	DEH
Enamel Hypoplasia	EH
European Mammalian Neogene Zones	MN
Geological Survey of Pakistan	GSP
Harvard Museum of Comparative Zoology	MCZ
Linear Enamel Hypoplasia	LEH
Minimum Number of Individuals	MNI
Muséum d' Histoire Naturelle, Toulouse	MHNT
Muséum National d' Histoire Naturelle, Paris	MNHN
Natural History Museum, London	NHM
Pakistan Museum of Natural History	PMNH
Peabody Museum Harvard University	PMHU
Punjab University Paleontology Collection, Lahore	PUPC
Semi Circular Enamel Hypoplasia	SEH
Stratigraphic Committee of Pakistan	SCP
Yale Peabody Natural History Museum	YPNHM

Chapter – 1

INTRODUCTION

1.1 Introduction

Hypoplasia, derived from the Greek *hypo* (low) and *plasis* (molding or forming), is used for under or incomplete development of a tissue or organ. Although the term is not always used precisely, it usually refers to an inadequate or below-normal number of cells, thereby leaving permanent marks on hard tissues (e.g. tooth enamel) which can well be studied in fossil tooth as well. There are a few other terms related to tissue development, which often are confused with hypoplasia. For instance, hypoplasia is similar to aplasia, but less severe. It is technically not the opposite of hyperplasia, i.e. too many cells. Hypoplasia is a congenital condition, while hyperplasia generally refers to excessive cell growth later in life.

Hypoplasia, in general, is caused by environmental or physiological stresses in an animal life at that particular time when the growth was taking place. However, in bones, which grow for quite a long period of time in an animal's life, the stress marks are healed up in later ages and hence the record is covered up or obliterated. Tooth development in this respect is unique as enamel, unlike bone, does not remodel and stress marks (such as linear groves, pits, etc.) can be tied up with its chronological development; making enamel perfect archive for development stress (Goodman and Rose, 1990). The fossilized tooth with Enamel Hypoplasia thus has the potential of providing a unique perspective into environmental conditions present during the growing years of an extinct animal's life, which indirectly reflects the climatic conditions prevailing during that period of time.

Enamel Hypoplasia has been widely studied in hominid and non-hominid primates, domestic pigs, wild boars, suids, and bison as an indicator of generalized physiological stress during tooth development (Goodman and Rose, 1990; Guatelli-Steinberg, 2000, 2003, 2004; King *et al*., 2002; Larsen, 1997; Moggi-Cecchi and Crivella, 1991; Skinner and Goodman, 1992; Skinner and Hopwood, 2004; Dobney and Ervynck, 2000; Dobney *et al*., 2004; Franz-Odendaal, 2004; Franz-Odendaal *et al*., 2004; Mead, 1999 and Niven *et al*., 2004).

The presence or absence of Enamel Hypoplasia in fossil dentition has recently caught up the attention of paleontologists for an additional but reliable indicator for local paleoecological conditions and on regional scale paleoenvironmental changes (Bratlund, 1999; Mead, 1999; Franz-Odendaal, 2004; Franz-Odendaal *et al.*, 2003).

The study presented here is the first attempt to analyze the Rhinocerotids tooth for Enamel Hypoplasia in the remarkably complete and fossil-rich Neogene Siwalik rock sequence of the Potwar Plateau (northern Pakistan) and coeval rocks of the Sulaiman Range, Bugti Hills and the Kirthar Range. Whereas, the tooth development and morphology of Enamel Hypoplasia will be discussed in the Chapter 3, a comprehensive summary on the Neogene Siwalik rocks of the Potwar Plateau and coeval formations in other parts of the Indus Basin is presented here. The term 'Siwalik' and 'Siwaliks' have been commonly used in the thesis. The term Siwalik is used to indicate the rocks exposed in the Potwar Plateau and the adjoining regions (e.g. Pabbi Hills, Siwalik Hills). The term Siwaliks however, is used for Neogene continental rocks exposed in other regions of the Indus Basin or for the entire Himalayan belt.

1.2 Objectives of the Present Study

The Hypoplasia analysis can shed crucial information of the physiologic stress that the individual has gone through at or during the natal stages and in the formative (weaning) years. The core cause of the stress is generally perceived to be the prevailing climate during the early part in the life of the animal, thereby causing physiological stress. The pilot studies of hypoplasia in the recent Rhinocerotidae will be taken up to compare the hypoplasia occurrences in recent and fossil Rhinocerotidae.

Studies of enamel defects in fossil (pre-Holocene) teeth are much less common. Dental defects are known in many mammalian taxa, their potential use in paleontological interpretations has not been much explored by paleontologists. Therefore, the proposed investigations would be the first detailed study providing relationship between hypoplasia and the environment in Rhino fauna from the Neogene rocks of Pakistan. This information integrated with studies on other taxa will help in interpreting paleo-climate changes in the South Asian subcontinent.

The analysis presented here is based upon study of 1754 Rhinocerotid teeth housed in major museums and institutes of Pakistan, France, USA and UK. I have examined the entire Neogene

Rhino collections from the Potwar, Sulaiman Range, Bugti Hills, and the Kirthar Range housed at the Geological Survey of Pakistan (GSP), Pakistan Museum of Natural History (PMNH), Punjab University Paleontology Collection (PUPC), Muséum National d'Histoire Naturelle (MNHN), Museum d' Histoire Naturelle (MHNT), American Museum of Natural History (AMNH), Peabody Museum Harvard University (PMHU), Yale Peabody Natural History Museum (YPNHM), and the Natural History Museum (NHM) London. Recent Rhino teeth have also been examined at Laboratoires de Paléontologie et d 'Anatomie Comparée in the Muséum National d'Histoire Naturelle (MNHN), and Harvard Museum of Comparative Zoology (MCZ).

1.3 Outline of the Thesis

This thesis, after a brief introduction of the purpose and objectives of this study in Chapter 1, focuses on three major topics; the Neogene Siwaliks, the Enamel Hypoplasia in Siwaliks and recent Rhinocerotids, and the paleoecological and climate inference from the Rhinos with Enamel Hypoplasia in the Siwaliks. Chapter 2 gives a synopsis of the Neogene Siwalik rocks of Pakistan, with brief discussion on the stratigraphy, mammalian fauna and biostratigraphy of the Neogene sediments exposed in the western Himalayan Foreland Belt including the Potwar Plateau, Sulaiman Range and Bugti Hills, and the Kirthar Range. The background and evolution of the Siwalik rock-formation nomenclature has specially been added, as it is felt that even the present researcher invariably use the names of the Siwalik rocks of the Potwar Plateau to denote them as time unit as well. For this reason, stratigraphy of the Neogene 'Siwaliks' rocks in other contiguous regions, namely the Sulaiman Range, Bugti Hills and the Kirthar Range have also been dealt with separately. Faunal assemblages and the biostratigraphy integrates all these separate regions and shows clearly that rock-names in one region can be coeval to a different set of formation names of contrasting composition in the other region. An attempt has been made to tabulate stratigraphic ranges of all Neogene Rhinocerotids from Siwaliks and coeval rocks of India and Pakistan and correlated in turn with European Mammalian Neogene (MN) Zones. It is interesting to note that Rhinoceros which first appeared in South Asia around 25 million years ago are still continuing their presence in the region though only represented by two species *Rhinoceros sondaicus* and *R. unicornis*.

Chapter 3 addresses the main focus of this study, i.e. Enamel Hypoplasia study of the Siwalik Rhinocerotids dentition. The Enamel Hypoplasia analysis of fossil mammals has recently been attracting the attention of paleontologists and is the first of its kind for the Siwalik mammals.

This chapter therefore gives the background information on hypoplasia, its genesis, and a brief account of the little work done on fossil mammals' dentitions. In contrast to all the previous studies done on fossil sites representing a very short time period, this study includes examination of all the Siwaliks Rhinocerotids spread over the past 25 million years ago to recent. The present study is based on the macroscopic investigation with careful measurement of the number, location, and shape of the linear enamel hypoplasia. The details of the 1754 Rhinocerotids teeth examined including 846 fossil Rhino teeth from Siwaliks of India and Pakistan, and another 908 teeth of four species of Recent Rhinos, are also given in Chapter 3. Except the Siwalik collections residing in India, all other notable collections of Siwaliks Rhinos in the leading natural history museum and institutions of France, UK, USA, and Pakistan have been examined for this study. The recent rhinocerotids dentition at the Museum of Comparative Zoology, Harvard University and the Natural History Museum, Paris were also studied.

Chapter 4 documents and describes each and every tooth with Enamel Hypoplasia among the 1754 teeth examined. A total of 34 teeth from the 846 specimens of Siwaliks Rhinos have been found with Enamel Hypoplasia, known from different time periods throughout the Neogene and almost from all the geographical locations, namely Sevalik Hills (India), Potwar Plateau, Sulaiman Range and the Bugti Hills. Enamel Hypoplasia is found to be mostly on permanent cheek teeth, a trend that was noted on the Recent Rhinos as well. An attempt was made to assess the effects of the hypoplasia development with the longevity of the animal by making age estimates of those animals represented by jaw fragments having hypoplasia as well as non-hypoplasia teeth. Although the sample size is quite small, it can safely be postulated that hypoplasia development in the formative ages did not adversely affect the later life.

The Chapter 5 is synthesis of the information gathered and inferred from the study on the hypoplasia of the fossil Rhinos of the Siwaliks ranging in age from ~25 Myr ago to ~2 Myr ago, with the climatic and paleoecological changes of the region during the Neogene. The ages of each of the Rhino specimen with hypoplasia were carefully estimated and tabulated in the stratigraphic column. A broad clustering of common hypoplasia occurrences in several species of Rhinos have been noted at different time periods. The next step was to ascertain whether these particular geologic times of higher occurrence of hypoplasia in Siwaliks Rhinos can be compared and contrasted with information on other Siwalik mammalian groups and regional geological and climatic events. Based on selected review of Neogene climate change, paleogeographic developments, and paleoecology of South Asia along with studies on a few Siwalik mammals (for

example see Morgan 1994; Nelson 2007), and integrated it with information of Siwaliks Rhinos, a synthesis has been presented on climate and biotic changes during the Neogene in Pakistan and adjoining regions.

The published research work based on some of the material described in the thesis has been included as Appendix 1, in compliance with Ph.D. rules and regulation of the University of the Punjab.

Chapter – 2

STRATIGRAPHY AND PALEONTOLOGY OF NEOGENE ROCKS

2.1 Siwalik Group

The name 'Sivalik Hills' (derived from Siva, the Hindu God) was first introduced by Cautley (in Falconer 1832) in the context of the discovery of vertebrate faunas in the low, northwest-southeast trending hills between the Ganges and the Yamuna rivers. Later Falconer and Cautley (1868) used the term 'Sivalik Hills' in a geographical sense "to designate that range of lower elevation which stretches along the southwest foot of the Himalayan mountains, for the greatest part of their extent from the Indus to Brahmaputra, where these rivers respectively debouch from the hills into the plains of Indus". However, from the very beginning, the term 'Siwalik' ('Sivalik' or 'Sewalik' spellings were in vogue until 1879) was always meant to denote the upper part of the Tertiary rocks, which dominantly are of freshwater origin and contain abundant vertebrate faunas (Falconer, 1832; Medlicott, 1864; Falconer and Cautley, 1868; see Sahni and Mathur, 1964 for details). In 1864 Medlicott on the basis of the relative predominance of clays or sandstones, proposed a threefold division of his 'Siwalik series' exposed in the areas between the Ravi and Ganges Rivers. His divisions were the Lower Siwalik or Nahan (sandstones with shales and clays), the Middle Siwalik (clays, sandstones and conglomerates), and the Upper Siwalik (sandstone and conglomerate); all of them gradationally pass into one another. Wynne in 1877 found Medlicott's classification (1864) of the 'Subhimalayan Series inappropriate for the Tertiary of the Salt Range and the Potwar, and instead divided the sequence into the 'Nummulitics', the 'Murrees', and the 'Siwalik' series. Wynne used the term Siwalik exactly in the same context as Meddlicot proposed, i.e., for the upper Tertiary freshwater rocks. Hence as Cotter (1933) has aptly remarked "the term Siwalik is therefore a transported term, and its use by A.B. Wynne for the Potwar rocks implies a correlation with the rocks of the Himalayan foothills which in view of the fact that the geology of the intervening country was then, and still is imperfectly known, was perhaps somewhat daring". Wynne divided the Potwar Siwaliks on the basis of minor mineralogical differences into an Upper and a Lower division. The former consisting of conglomerates, dull colored clays, and soft sandstones, while the later is characterized by soft clays and sandstones which he also called Red and Grey Series (Figure 2.1).

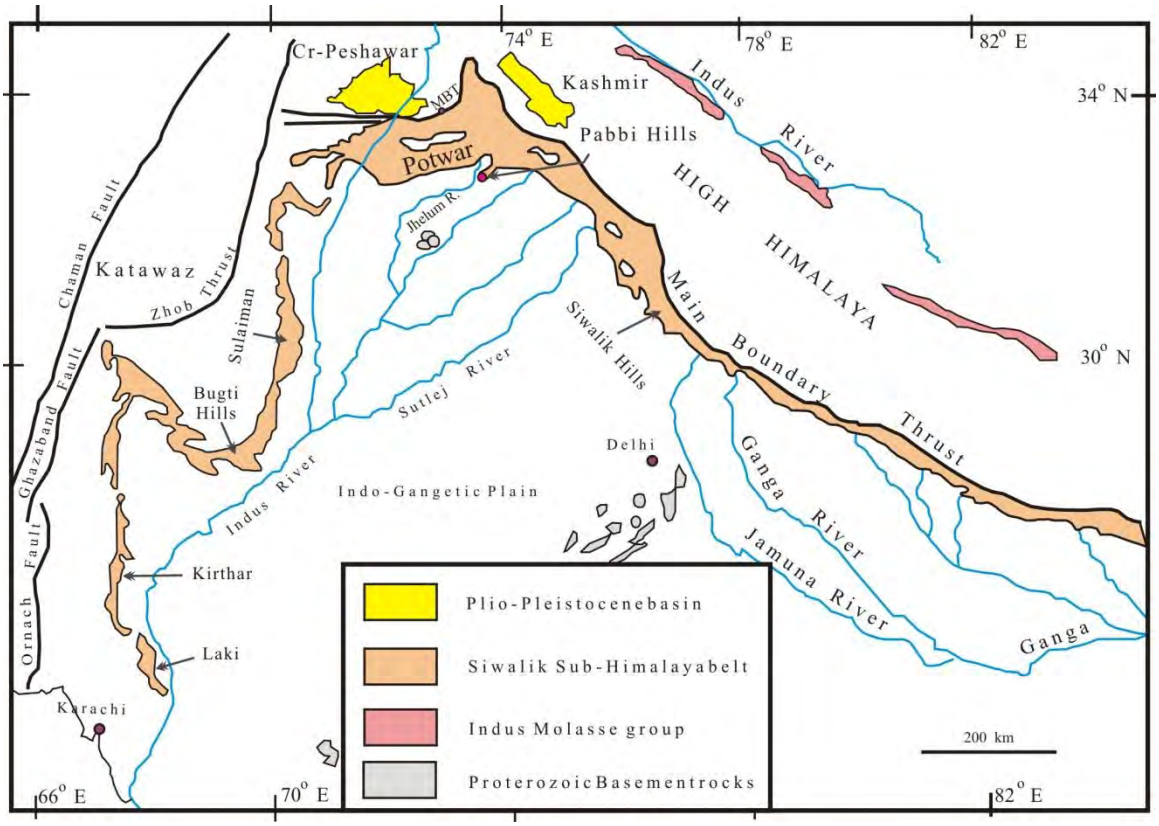

Figure 2.1 Generalized geological map of Pakistan and northern India, showing distribution of the Neogene "Siwalik" and coeval rocks (Modified from Raza, unpublished).

The most important and long lasting contribution to the understanding of the Siwalik rocks was made by Guy E. Pilgrim who as the Chief Paleontologist of the Geological Survey of India worked for at least thirty year on these deposits. He divided the Siwaliks of the Potwar Plateau into the Lower, Middle, and Upper units and suggested that since the sequence is fossiliferous throughout and quite thick, that the Salt Range (i.e. the Potwar Plateau) be the type area. He called these units the "Salt Range System" (Pilgrim, 1910b). He correlated other freshwater deposits of the Subhimalayas with the Potwar sequence and proposed that correlations "may be guided by fossils, or lithological evidences, or stratigraphic considerations". Pilgrim's proposal was apparently not different from those suggested earlier by Medlicott, Wynne, and others but it has two important aspects. First, prior to Pilgrim, all classifications were intended to be more or less local application; and second, for the first time fossils were incorporated in the definition and recognition of various units. Later, in 1913, Pilgrim refined his classification and proposed a

further subdivision of the three units into several zones, which with a few modifications have been used since then (Table 2.1).

Table 2.1 Neogene Formations in various regions of the Indus Basin discussed in the text and appropriate correlation with European MN Zones. Compiled from Raza *et al*. (1984); Hussain *et al*. (1992); Barry *et al*. (2002) and Antoine *et al*. (2013).

Table 2.1

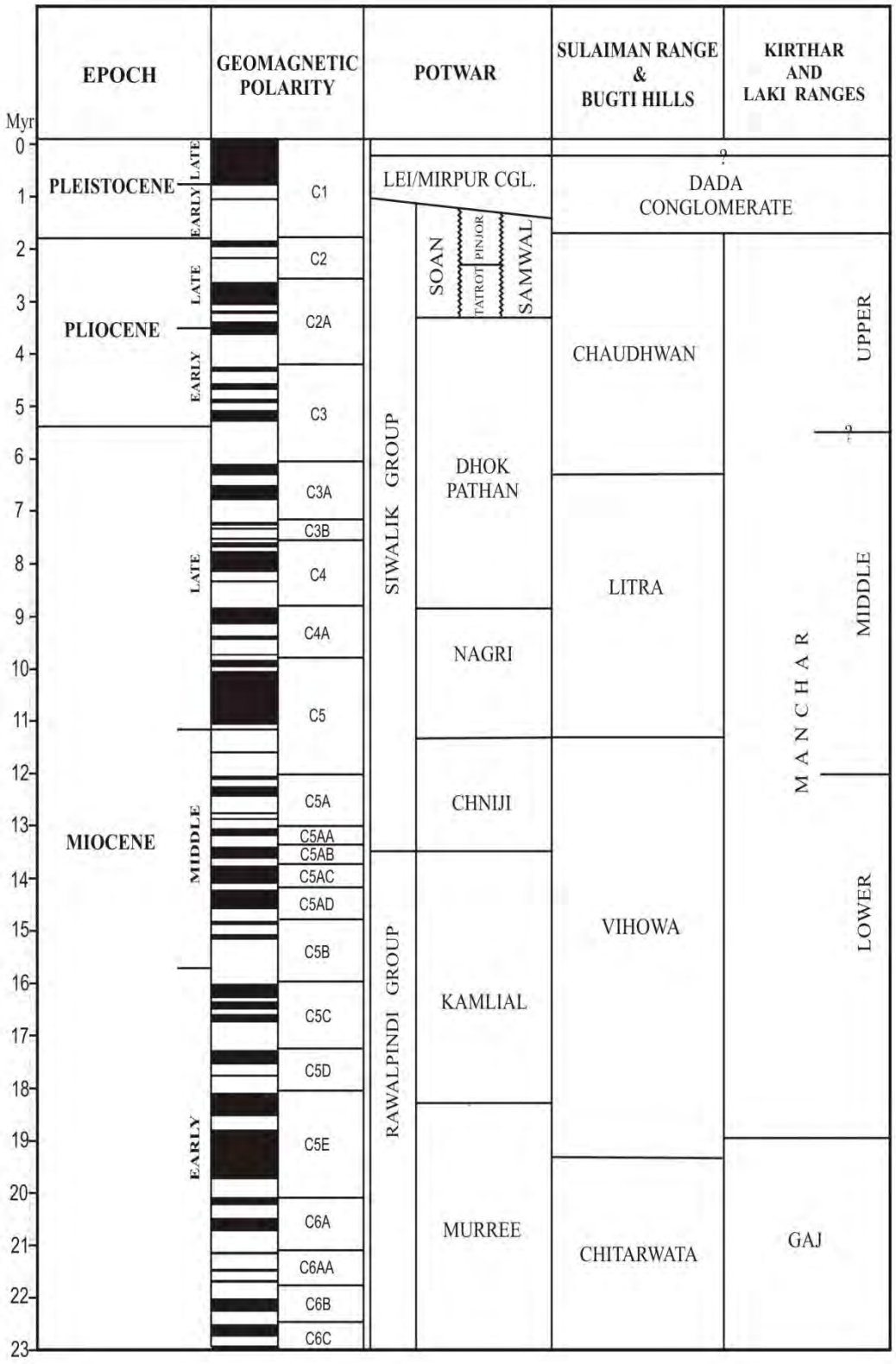
EPOCH
GEOMAGNETIC POLARITY
POTWAR
SULAIMAN RANGE & BUGTI HILLS
KIRTHAR AND LAKI RANGES
Myr
PLEISTOCENE
LATE
EARLY
PLIOCENE
LATE
EARLY
MIOCENE
LATE
MIDDLE
EARLY
C1
C2
C2A
C3
C3A
C3B
C4
C4A
C5
C5A
C5AA
C5AB
C5AC
C5AD
C5B
C5C
C5D
C5E
C6A
C6AA
C6B
C6C
LEI/MIRPUR CGL.
SOAN
TATROT
PINJOR
SAMWAL
SIWALIK GROUP
RAWALPINDI GROUP
DHOK PATHAN
NAGRI
CHNIJI
KAMLIAL
MURREE
DADA CONGLOMERATE
CHAUDHWAN
LITRA
VIHOWA
CHITARWATA
MANCHAR
UPPER
MIDDLE
LOWER
GAJ

This new scheme was based on additional fossil collections in the Potwar Plateau as well as in the Punjab (Himachel Pradesh) region, and therefore in the definition of his 'Zones' fossils from both areas are incorporated as if they are from one continuous section on the assumption that unique homotaxial units can be correlated with unique lithological characteristics. There are clearly many problems with Pilgrim's scheme, which prevent its successful use on a regional scale. First, the fossiliferous horizons, even in his type sections, are separated by large intervals of unfossiliferous strata, and second, the boundaries were drawn between the different zones at what he considered significant and more or less isochronous lithological changes. Pilgrim (1910) observed that rapid lateral changes of the fluvial rocks questioned the correlative value of the lithological features but later (1913) he considered certain lithological characters as secure indices of correlations, even over widely separated areas. Since the distribution of fossils is sporadic, both laterally and vertically, correlations were often attempted on the basis of type area lithology of different zones. Pilgrim (1913: 268-270), seems to have firmly believed that the appearance of red nodular clays and concretionary pseudo-conglomerates in the Siwalik successions is an isochronous feature providing a natural boundary that is valid all over the Siwalik terrain for separating the Middle Siwaliks from the Lower Siwaliks. Similarly, the presence of thick conglomerate bed has been taken as a feature exclusively of the Upper Siwaliks, and "ridge forming" sandstone to be diagnostic of the Kamlial zone.

In spite of all the problems of demarcating clear boundaries between certain zones in the field, Pilgrim's classification had been used by all students of the Siwalik whether engaged in regional mapping (e.g. Pinfold, 1918; Pascoe, 1920; Wadia, 1928; Cotter, 1933) or those interested exclusively in faunas (e.g. Colbert, 1935; Osborn, 1936; Lewis, 1937a; Prasad, 1964; and others). It is quite evident that until recently, rock, faunal, and temporal criteria and definitions have been entwined in discussion of Siwalik geology, causing great confusion. Colbert (1935), Lewis (1937a) and Pilbeam *et al*. (1977) has given excellent discussion of this problem, which need not to be repeated here. Pilgrim's zones have something of the status of 'stages' of current stratigraphic usage, i.e. chronostratigraphic units of relatively minor rank representing a body of rock strata that is unified by being formed during a specific interval of geological time which on average ranges from 3 to 10 million years (Hedberg, 1976: 70-72). Colbert (1935) used Pilgrim's subdivisions as true zones of modern usage that is, based exclusively on faunas. To avoid duplicating terminology he favored the terms Lower Siwalik, Middle Siwalik and Upper Siwalik for regional mapping purposes. Lewis (1937a) on the other hand using the same 1933 North American Stratigraphic Committee's report as Colbert did, restricted Pilgrim's terminologies to actual formations. He gave

type localities and brief descriptions of lithologies but also included some faunal elements as part of the definition. In essence, Lewis's scheme did not differ much from that of Cotter except that it was intended for broader use from the Potwar to the Punjab (Himachal Pradesh), and both are equivalent to 'stages' of the current usage.

Pilgrim's nomenclature, in spite of all the ensuring problems, is well established in the literature and has to be kept in some form. It is felt that one possible solution of this dilemma would be to restrict his terminology to rock stratigraphic usages defined on the basis of type area lithologies. By the very nature of fluvial deposits, it can hardly be expected that identical facies would demarcate the boundaries everywhere. Once a formation is properly defined at its type area, strike mapping into contiguous areas would be the best course. In the Potwar Plateau, exposures are good, physical continuity exists, and a number of reliable base maps are available, so that strike mapping from the type areas is possible. Therefore, it should not be difficult to develop a sound lithostratigraphic framework. A separate set of nomenclature will be required to define biostratigraphic and chronostratigraphic aspects.

The Stratigraphic Committee of Pakistan (SCP: Fatmi, 1973), drawing principally upon Lewis's classification, formalized names such as Chinji, Nagri, etc., exclusively as lithostratigraphic terms. The SCP divided the entire molassic sequence into a lower Rawalpindi Group and an upper Siwalik Group; the former includes the Murree and the Kamlial Formations whereas the later comprises Chinji, Nagri, Dhok Pathan, and Soan formations (Table 2.1).

Since the Committee followed Lewis's scheme their recommendations also inherited some of the basic flaws of the earlier scheme. The formations were defined on their broad lithologic characteristics but the contacts, even in their type sections, were not clearly defined. Also, type sections of all the component formations were proposed in different and separate areas with the notable exceptions of the Chinji and the Nagri type sections which are in one continuous section in the Chinji-Nagri areas in southern Potwar. However, the Committee has made an important contribution by explicitly excluding faunas from the formational definitions. The SCP initiatives were later led to a comprehensive literature-based review of non-marine Neogene rocks of Pakistan but erroneously extended the Potwar "Siwalik" lithostratigraphic nomenclature to other coeval rocks of the Khisor-Bhiattani Range, Sulaiman Range, Kirthar Range and other parts of the Lower Indus Basin (Cheema *et al*., in Shah, 1977; Shah, 2009).

Since1973, collaborative research between the Geological Survey of Pakistan and the Yale Peabody Museum (now Harvard Peabody Museum) has been in progress in the Potwar Plateau, aimed at a better understanding of the geological and faunal history of the Siwalik Group in particular, and of South Asia, in general (*see* Pilbeam *et al*., 1977, 1979; Raza, 1983; Khan *et al*., 1997, Barry *et al*., 2002; Behrensmeyer *et al*., 2007). A synopsis of the Neogene rock sequence of the Potwar, Sulaiman and Kirthar ranges is given in Figure 2.1.

2.2 Potwar Siwalik

The Siwalik Miocene fluvial sediments in Potwar Plateau have been divided into Kamlial, Chinji, Nagri, Dhok Pathan and Soan formations (oldest to younger) Figure 2.2.

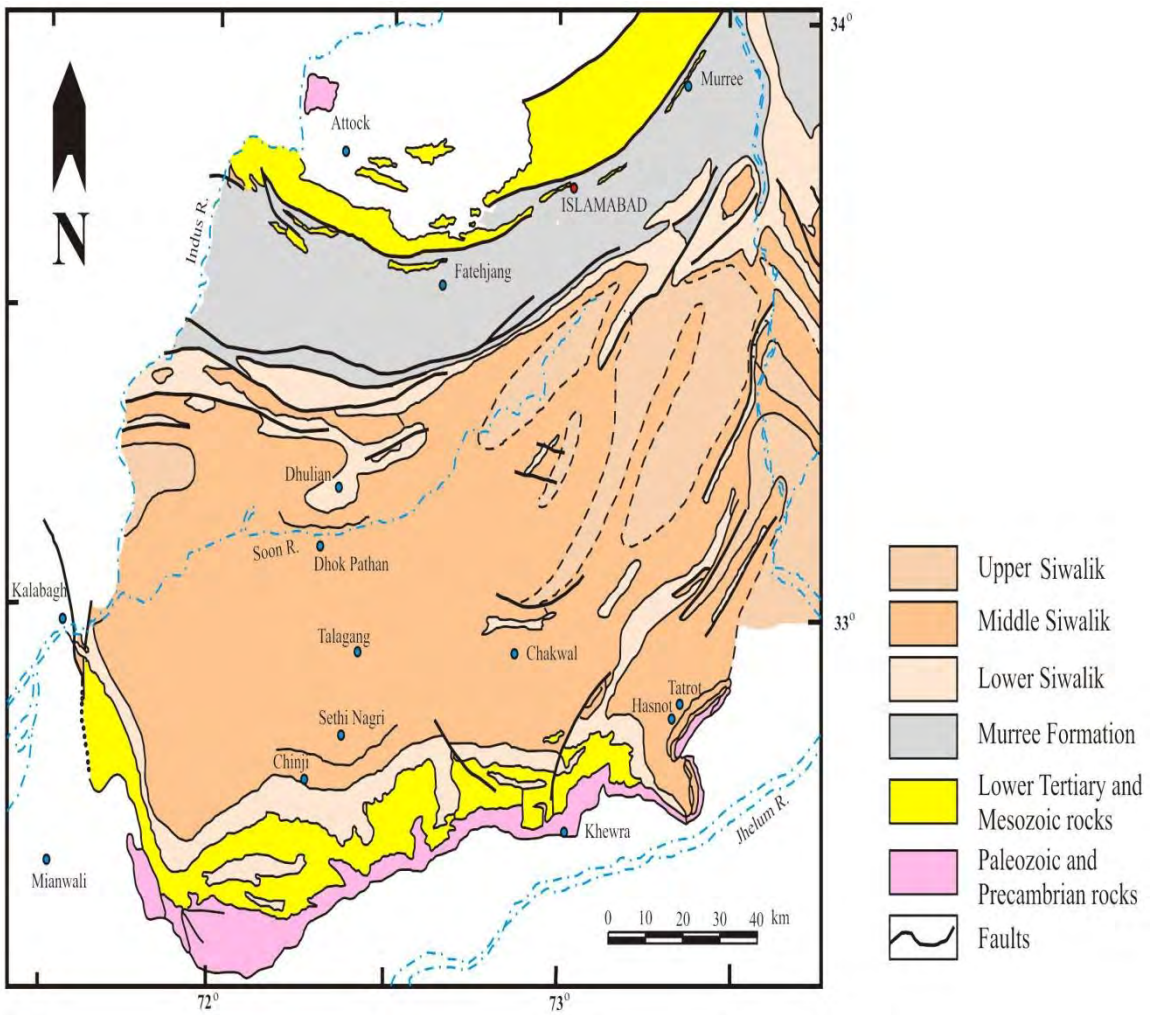

Figure 2.2 Generalized Geological map of the Potwar Plateau.

2.2.1 Kamlial Formation

The "Kamlial beds" of Pinfold (1918) have been formally established as Kamlial Formation by the Stratigraphic Committee of Pakistan (Shah, 1977). The Kamlial Formation consists of purple-grey and dark brick-red sandstone which is medium to coarse grained and contains interbeds of hard purple shale and yellow and purple intraformational conglomerate. It is widely distributed in the Kohat and Potwar areas and has also been recognized in the Jammu Hills.

2.2.2 Chinji Formation

Pilgrim (1913) proposed the name "Chinji Zone" to designate the upper faunal subdivision of his "Lower Siwalik". Lewis (1937) upgraded it as Chinji Formation and the name was accepted as such by the Stratigraphic Committee of Pakistan.

The formation consists of red clay with subordinate ash grey or brownish grey sandstone. The sandstone is fine to medium grained, occasionally gritty, cross-bedded and soft. At some places, scattered pebbles of quartzite and thin lenses of intraformational conglomerate are found at different horizons throughout the formation. The proportion of clay and sandstone in interbeds is variable from place to place e.g., in the Shinghar Range (in the Kohat-Potwar Province) the formation is mainly composed of reddish brown or reddish grey sandstone with subordinate clay interbeds. However, the formation essentially represents an argillaceous facies where the sandstone bands rarely attain 16 m thickness but clay bands may be as much as 60 m thick (Raza, 1983; Friend *et al*., 2001).

2.2.3 Nagri Formation

The "Nagri Formation" of Lewis (1937) has been accepted as such by the Stratigraphic Committee of Pakistan. It consists of sandstone with subordinate clay conglomerate. The sandstone is greenish grey medium to coarse grained, cross-bedded and massive. In places, the sandstone is bluish grey dull red with salt and pepper" pattern, calcareous, and moderately to poorly cemented. The clay is sandy or silty chocolate brown or reddish grey and pale orange, the proportion of which

varies from section to section. The conglomerate bed has highly varied thickness and composition in different areas and contains pebbles of quartzite, schists, and other granitic rocks.

2.2.4 Dhok Pathan Formation

The name “Dhok Pathan” was introduced by Pilgrim (1913) in a biostratigraphic sense) for the upper subdivision of the Middle Siwalik in the northeast Punjab. Cotter (1933) redefined the unit as Dhok Pathan Formation, which was adopted by the Stratigraphic Committee of Pakistan for application in the Kohat-Potwar Province.

The formation is typically represented by monotonous cyclic alternations of sandstone and clay beds. The sandstone is commonly grey, light grey, gleaming white or reddish brown and occasionally rusty orange, greenish yellow, yellowish grey, chocolate colored, calcareous and sandy. Minor intercalations of yellowish brown siltstone are common. Conglomerate in the form of lenses and a layer is an essential character of the upper part. The thickness of one sandstone-clay cycle varies from 6 to 60 m.

2.2.5 Soan Formation

In the northwest Punjab the “Upper Siwalik” of Medlicott (1864), which was later divided biostratigraphically into “Tatrot” and “Pinjor” zones or stages by Pilgrim (1913), has been formally named “Soan Formation” by the Stratigraphic Committee of Pakistan. However, the name Soan Formation did not get much acceptance among the researcher for the post-Dhok Pathan sequence at it shows substantial lateral lithological variations in different areas of the Potwar and other adjacent regions. For example, the name ‘Tatrot Formation’ has been used on the southeastern Potwar region whereas the name ‘Samwal Formation’ was introduced in Mangla-Bhimber region in Kashmir by Hussain *et al*., 1992. The formation consists essentially of compact massive conglomerate with subordinate interbeds of varicolored sandstone siltstone and or clay. The proportion of different rock type varies within short distances. The conglomerate consists of a variety of pebbles and boulders of different sizes. The conglomerate of Kohat-Potwar province is massive and consists mainly of pebbles and boulders of “Margala Hill” type grey limestone, quartzite, porphyritic rocks, sandstone, gneiss, schist, diabasic, etc. The pebbles and boulders range

in size from 5 to 30 cm commonly claystone and sandstone are intercalated, The claystone is orange, brown, pale pinkish or red and soft, the sandstone is grey, greenish grey, coarse grained and soft (Cheema *et al*., 1977).

2.3 Sulaiman Range and Bugti Hills

The Sulaiman Range is a north-south-trending band of rugged mountains defining the boundary between Balochistan and Punjab province and extends in to the Khyber Pakhtoonkhwa Province (Figure 2.3).

The continental series of the Sulaiman Range, and especially of its south-and west extension into the Bugti Hills, has been fairly well investigated (e.g. Pilgrim, 1912; Forster-Cooper, 1924; Hemphill and Kidwai, 1973; Raza and Meyer, 1984; Welcomme *et al*., 2001, Antoine *et al*., 2013). The recent researches in the Sulaiman Range and Bugti Hills region has greatly benefitted by the seminal researches of the Harvard-GSP Team on biostratigraphy and magneto-stratigraphy on the Siwaliks of in the Potwar Plateau. In 1990s, Professor Lindsay of Arizona University with his team from Harvard University, Pakistan Museum of Natural History (PMNH) and Geological Survey of Pakistan (GSP) initiated geological and paleontological studies in the Dalana area are, central Sulaiman Range which was later (in 2001) extended further up north in the Zinda Pir Dome areas by Raza *et al*., (Freidman *et al*., 1992; Lindsay *et al*., 2000, 2005; Raza *et al*., 2002; and references therein) The first collection of small mammals comprising of important data from the Bugti Hills and Sulaiman Range was described by Jacobs *et al*. (1981) and Flynn, Jacobs, and Cheema (1986).

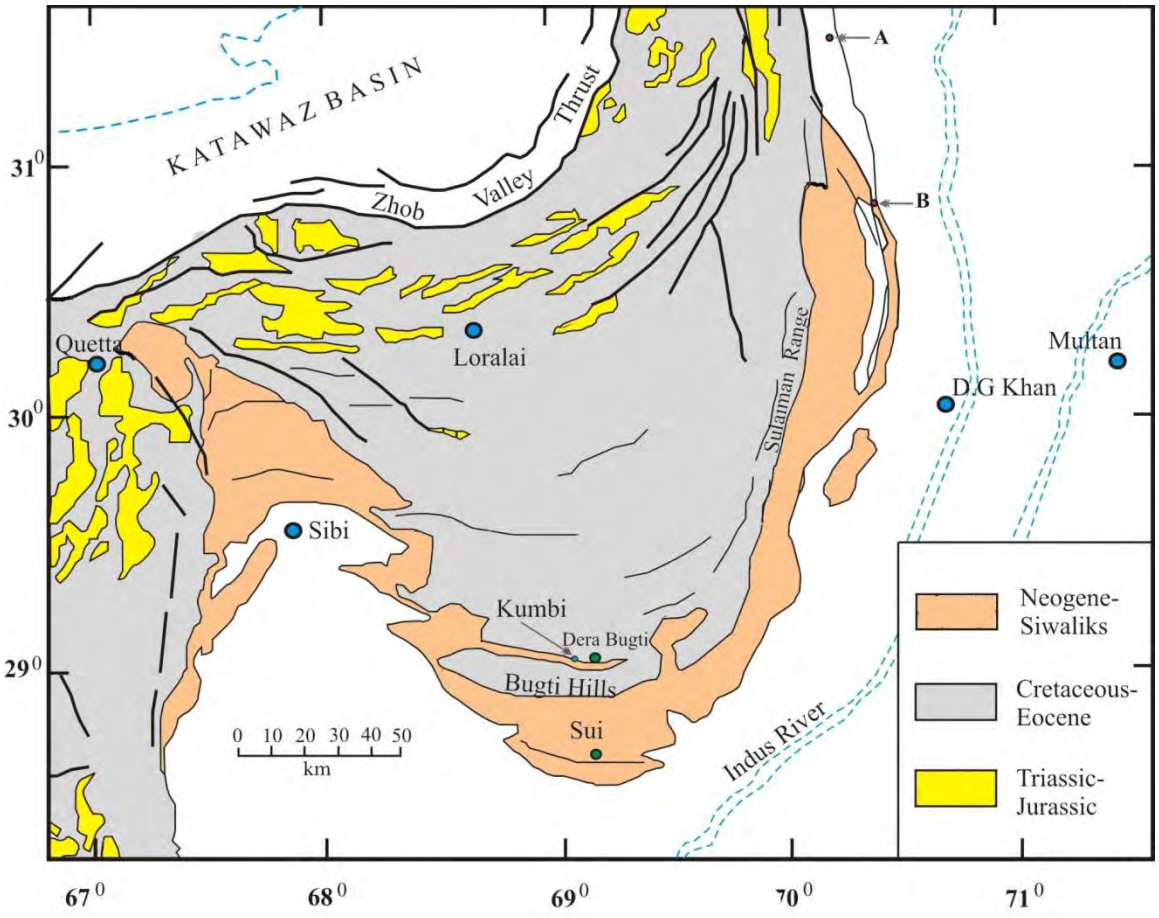

Figure 2.3 Geological map of the Middle Indus Basin. The areas marked A and B are the type localities of Chaudhwan Formation (area A) and of Litra, Vihowa and Chitarwata formations (area B) designated by Hemphill and Kidwai (1973). Modified after Raza *et al*. (2002).

In 1995 a French team led by Jean-Loup Welcomme started work in the Bugti Hills with the objective of establishing a proper lithostratigraphic framework in order to determine the stratigraphic provenance of spectacular collections made by Pilgrim and Forster-Cooper nearly a century ago. It was generally considered that Early Miocene non-marine deposits lay unconformably on the marine upper Eocene rocks (for e.g. Raza and Meyer, 1984). The French Team paleontological work provided the first unambiguous evidence of (fossiliferous) Oligocene deposits in the Bugti Hills lay uncoformably over the Eocene rocks but passing gradationally up into the Early Miocene sediments (Welcomme and Ginsburg, 1997; Welcomme *et al*., 1997). The studies of Welcomme *et al*. (1999, 2001) led to a re-examination of the age of the Zinda Pir sequence (Lindsay *et al*., 2005) which had important biostratigraphic implications for the entire

Sulaiman Province as well as to the geological development of the entire West Himalayan fore-land basins, especially the evolution of the Indus paleo-drainage and its tributaries (Downing and Lindsay, 2005; Metais *et al*., 2009). The Neogene sediments of the Sulaiman Province are divided in to four formations, which are described below.

2.3.1 Chitarwata Formation (Late Oligocene to earliest Miocene)

The Chitarwata Formation in the Sulaiman Range consists of red, gray, and green mudstone and subordinate amounts of brownish yellow sandstone and siltstone (Hemphill and Kidwai, 1973). In the Zinda Pir Dome area, the formation has been divided in to lower, middle and upper parts with distinct lithology and fauna and in parts can be traced southwards to the Bugti Hills (Raza and Meyer, 1984; Downing *et al*., 1993; Lindsay *et al*., 2005; Metais *et al*., 2009). In the Zinda Pir area, the Chitarwata Formation is up to 480 m thick but pretty condensed in the Bugti Hills. The lower and middle units recognized in the Zinda pir area (Lindsay *et al*., 2005) and the 'Bugti Member' of the Bugti Hills (Metais *et al*., 2009) are considered similar faunally and temporally. The upper part of the Chitarwata Formation in both areas is referred to the earliest Miocene (i.e., roughly corresponding to the Aquitanian marine stage or Agenian European Land Mammal Age; Antoine *et al*., 2010). In the Bugti Hills, the upper member of the Chitarwata Formation is richest stratigraphic interval in terms of fossil vertebrates. Large mammal remains in other parts of the Sulaiman Range are scarce, although they occur in various localities (Raza *et al*., 2002; Barry *et al*., 2005; Lindsay *et al*., 2005).

2.3.2 Vihowa Formation (Late Early Miocene-Middle Miocene)

The Vihowa Formation is composed of grey sandstone and red-brown mudstone with rare thin conglomerate interbeds, which often contains fragmentary unidentifiable bones and teeth. It is 720 m thick in the Zinda Pir Dome but thins to 100-200 m in the Bugti Hills (Raza *et al*., 2002; Antoine *et al*., 2013). Mammalian fauna though fewer in number are found from all parts of the formation. The lower part of the Vihowa Formation in the Bugti Hills contains late Early Miocene fauna which are not known form other parts of Pakistan whereas the fauna from the middle and

upper parts indicate Middle Miocene age, coeval to the Chinji fauna of Potwar Plateau (Welcomme *et al*., 2001; Metais *et al*., 2009; Orliac *et al*., 2009; Antoine *et al*., 2010). Large mammals are scarce, but they occur in various localities (Raza *et al*., 2002; Barry *et al*., 2005; Lindsay *et al*., 2005).

2.3.3 Litra Formation (Late Miocene)

Raza *et al*. (2002) described Litra Formation as a thick vertically stacked laterally extensive finning upward sandstone sequence with thin dull red brown siltstone on top. It contains thin beds of varicolored paleosols, which can be traced laterally for several tens to hundreds of meters. It is 1700 m thick in the Zinda Pir area (Raza *et al*., 2002). The Litra Formation records the first appearance of *Hipparion* sp., which is securely dated in the Potwar Plateau at 10.2 Myr (Raza *et al*., 2002; Antoine *et al*., 2013). These localities yielded large mammal fauna similar to the fauna observed in lower part of the Middle Siwaliks in the Potwar Plateau (Antoine *et al*., 2013).

2.2.4 Chaudhwan Formation (Post Miocene; Pliocene-Pleistocene)

The Chaudhwan Formation is 1500 m thick in Zinda Pir and is composed of massive conglomerate and pebbly sandstone with subordinate medium and fine-grained gray sandstone and grayish brown siltstone (Raza *et al*., 2002). In the Bugti area, consists essentially of boulder conglomerates and fluvial terraces but its composition and thickness is highly variable depending on local tectonic context. No mentionable mammalian fauna has been reported form the Chaudhwan Formation except that Welcomme *et al*. (1997) mentioned egg shells of an unidentified struthioniform (Ostrich) from the Bugti Hills. Crochet *et al*. (2009) report prehistoric rock paintings in the vicinity of Lundo with anthropomorphic, geometric, and zoomorphic (e.g., cervid and felid) sketches attesting to favorable climatic conditions in the area around the Last Glacial Maximum and during subsequent periods.

2.4 Kirthar Range

The most complete Cenozoic sequence preserved on the Indian subcontinent is in the Kirthar province of Pakistan, which is the southernmost sedimentary province of the Indus Basin.

In the Kirthar province the Oligocene sediments are well developed as the marine Nari and Gaj Formations and pass gradationally into the fluvial beds of the overlying Miocene Manchar Formations (Blanford, 1879, 1883; Raza *et al*., 1984) formations (Figure 2.4) also have diverse assemblages of marine and terrestrial fossils, they are crucial for biostratighraphic correlations between southern Asia and other parts of Old World. These deposits along with the Bugti Hill fauna document an important phase in the development of the mammalian faunas of the subcontinent: a phase during which a variety of ruminant and non-ruminant first appeared in southern Asia. It is with these appearances that the classic Siwalik fauna first became established.

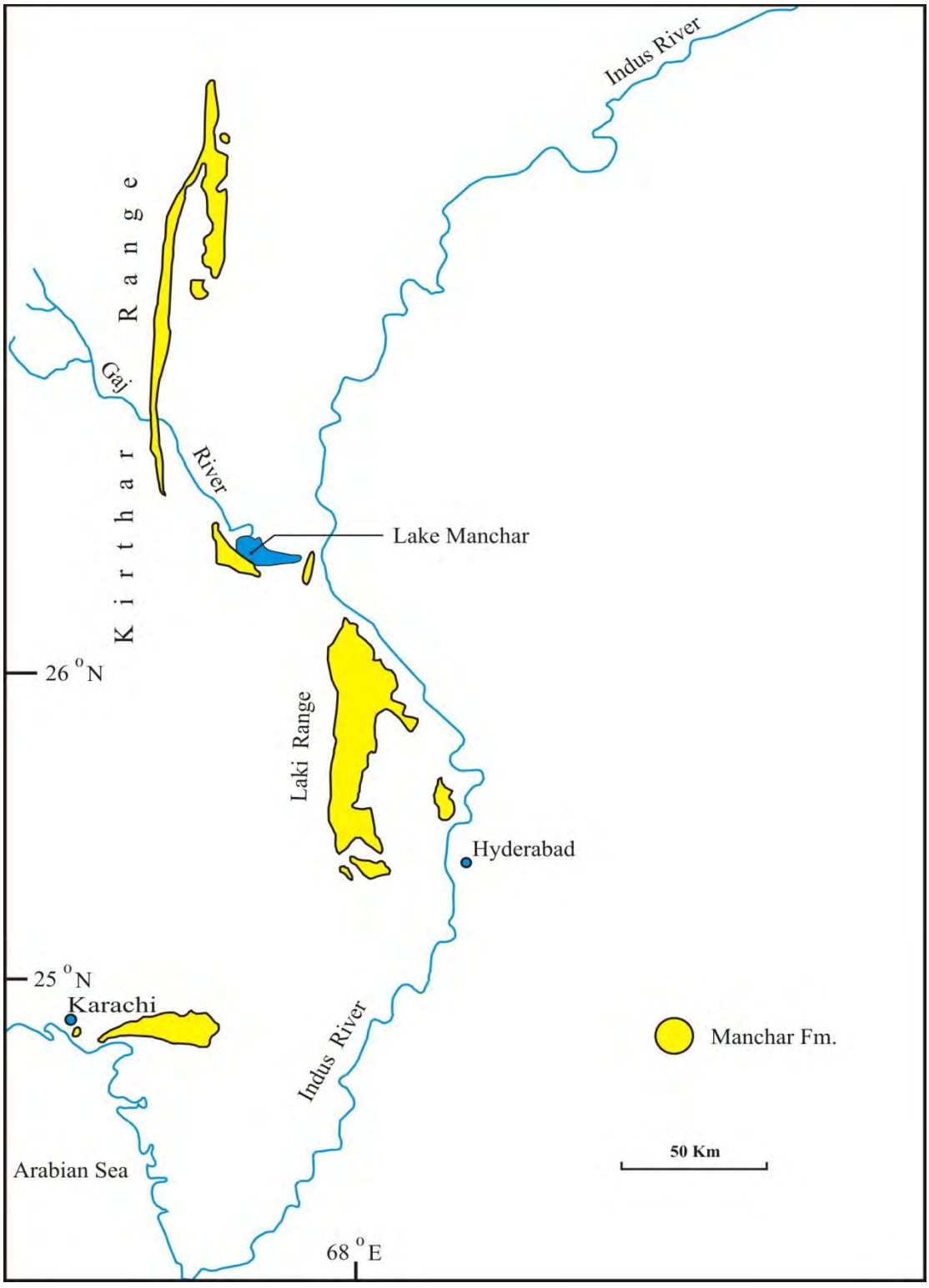

Figure 2.4 Map of Kirthar and Laki Ranges showing the outcrop areas of the Manchar Formation (after Raza *et al*., 1984).

2.4.1 Manchar Formation

The Manchar Formation is composed of alternating cycles of sandstone and silt, with thin beds of conglomerate that increase in thickness and frequency upward in the sequence. It is more than 2000 m thick in the Kirthar Range but thins out rapidly eastwards (Raza *et al*., 1984). It has a transitional contact with the underlying Gaj Formation recording a gradual change from the shallow marine-estuarine Gaj rocks passing upwards to fluvial Manchar Formation. Most of the vertebrate faunas reported form the Manchar Formation comes from the outcrops in the Lakhi Range near Sehwan Sharif, which are similar to Chinji, Nagri and Dhok Pathan Formations of the Potwar Plateau (Raza *et al*., 1984; Hussain *et al*., 1992) Manchar Formation, thus, spans most of the Miocene period and may extend into the Pliocene as well.

2.5 Biostratigraphy

The ambiguous demarcation and mixing of lithological and faunal characteristics of the otherwise red-and-grey repetitive sandstone and mudstone couplets composing the 'Siwalik' rocks in the past, has recently been clearly separated and properly defined by the extensive collaborative research under the umbrella of the Geological Survey of Pakistan and Harvard University working in the Potwar Plateau since 1973. The meticulous placing of each faunal locality, in-depth systematic studies of several key mammalian families, secure age determination by extensive paleomagnetic analysis and absolute-age methods, and tieing up of the fossil localities with paleomagnetic time-scale have defined well established biostratigrpahic divisions of the entire Siwalik sequence (for example see Barry *et al*., 1982, 2002; Flynn *et al*., 1999; Pilbeam *et al*., 1996; and references therein). The biostratigraphic zonation are mostly done by documenting the First Local Appearance (FLA) in different local sections as well as documenting observed ranges of a number key taxa on a regional scale. The Siwalik rocks of the Potwar Plateau ranging from the Middle Miocene to Pliocene are the best studied and serve as standard biostratigraphic zonation for the entire Sub-Himalayan belt (Pilbeam *et al*., 1979; Barry *et al*., 1982, 2002). Recent work in the Sulaiman Range established late Oligocene through Middle Miocene biostratigraphic zonation of the non-marine Neogene rocks of the region (Raza and Meyer 1984; Raza *et al*., 2002; Antoine *et al*., 2013; and references therein). Antoine *et al*., (2013) have identified four successive faunal Assemblages in the Bugti Hills and Sulaiman Range. These are constrained mainly by the First Appearances of selected few rhinocerotids, equids and proboscideans species as well as by a wide

range of various rodent families. The current understanding of the biostratigraphic zonation of the Neogene rocks of Pakistan and Western India has been summarized in Figure 2.5 (Antoine *et al*., 2013; Barry *et al*., 1982; Hussain *et al*., 1992; Patnaik, 2013).

Figure 2.5 Generalized biostratigraphy of Neogene Siwaliks (Sources: Barry *et al*., 1982; Hussain *et al*., 1992; Antoine *et al*., 2013; Patnaik, 2013).

Figure. 2.5

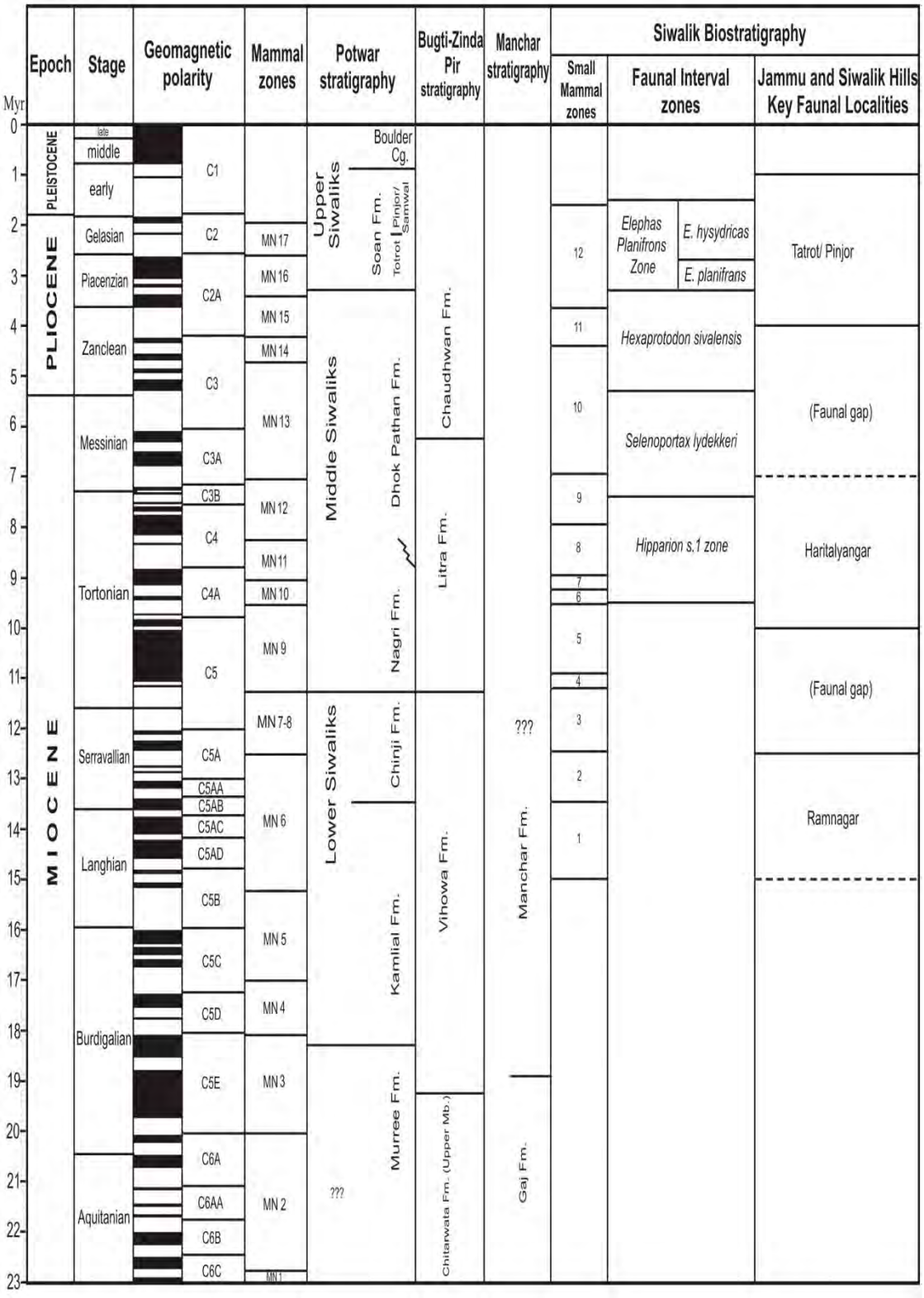
Myr
Epoch
Stage
Geomagnetic polarity
Mammal zones
Potwar stratigraphy
Bugti-Zinda Pir stratigraphy
Manchar stratigraphy
Siwalik Biostratigraphy
Small Mammal zones
Faunal Interval zones
Jammu and Siwalik Hills Key Faunal Localities
PLEISTOCENE
PLIOCENE
MIOCENE
late
middle
early
Gelasian
Piacenzian
Zanclean
Messinian
Tortonian
Serravallian
Langhian
Burdigalian
Aquitanian
C1
C2
C2A
C3
C3A
C3B
C4
C4A
C5
C5A
C5AA
C5AB
C5AC
C5AD
C5B
C5C
C5D
C5E
C6A
C6AA
C6B
C6C
MN 17
MN 16
MN 15
MN 14
MN 13
MN 12
MN 11
MN 10
MN 9
MN 7-8
MN 6
MN 5
MN 4
MN 3
MN 2
MN 1
Upper Siwaliks
Boulder Cg.
Soan Fm.
Pinjor/ Samwal
Totrot
Middle Siwaliks
Dhok Pathan Fm.
Nagri Fm.
Lower Siwaliks
Chinji Fm.
Kamlial Fm.
Murree Fm.
???
Chaudhwan Fm.
Litra Fm.
Vihowa Fm.
Chitarwata Fm. (Upper Mb.)
???
Manchar Fm.
Gaj Fm.
12
11
10
9
8
7
6
5
4
3
2
1
Elephas Planifrons Zone
E. hysydricas
E. planifrans
Hexaprotodon sivalensis
Selenoportax lydekkeri
Hipparion s.1 zone
Tatrot/ Pinjor
(Faunal gap)
Haritalyangar
(Faunal gap)
Ramnagar

2.6 Siwaliks Mammalian Fauna

The extensive paleontological research in the Potwar Plateau, the Sulaiman Range including the Bugti Hills, and the Kirthar-Lakhi Range carried out in the past three decades have greatly improved the systematics of different taxa as well as their temporal ranges and spatial distribution. The careful collection in the field with exact tying up of their stratigraphic occurrences and with secure paleomagnetic dates have established a good succession of various faunal assemblages which are time successive over a wider geographical area.

The Miocene Siwalik and coeval mammal fauna includes species from at least 13 orders and more than 50 families (Flynn *et al*., 1995; Barry *et al*., 2002; Raza *et al*., 2002; Lindsay *et al*., 2005; Antoine *et al*., 2013; and references therein). They interpreted faunal changes with respect to evidence for global and local climatic change, and intercontinental migrations. At least nineteen of these families are currently present in the Indo-Pakistan subcontinent (Roberts, 1997; Nanda, 2008). The orders include Insectivora, Scandentia, Chiroptera, Pholidota, Primates, Rodentia, Lagomorpha, Creodonta, Carnivora, Tubulidentata, Proboscidea, Artiodactyla, and Perissodactyla; the last one is discussed further here.

2.7 Siwaliks Perissodactyla

Perissodactyls in the Neogene continental sediments of Pakistan are represented by three families, Equidae, Chalicotheriidae, and Rhinocerotidae; rhinocerotids being the most common and occur ubiquitously throughout the Neogene sequence almost from all over the region (Figure 2.6).

The order dominates the faunas from the Chitarwata and Vihowa formations in the Bugti Hills and Sulaiman Range. Chalicotheres are represented by a single relatively uncommon, long-lived species *Chalicotherium salinum* (Pickford, 1982) in the Potwar Siwaliks and by *Phyllotillon naricus* and *C. pilgrimi* in the Bugti Hills (Antoine *et al*., 2013). Rhinocerotids are represented by several genera and species throughout the sequence (Heissig, 1972) whereas the Equids once they appear in South Asia become quite abundant in fossil record and also fairly well diverse in species composition.

Figure 2.6 Biostratigraphical ranges of Rhinocerotidae (this study) from the Neogene "Siwaliks" of Pakistan and the Siwalik Hills (India). Bugti Hills and Sulaiman Rhinocerotids from Antoine *et al*., (2013). Biostratigraphic ranges of Rhinocerotids in this study are estimated from various sources (Colbert, 1935; Hussain *et al*., 1992; Barry *et al*., 2002; Nanda, 2008; Khan, A.M., 2009). Cross (x) indicate exact ages of the specimen studied.

Figure. 2.6

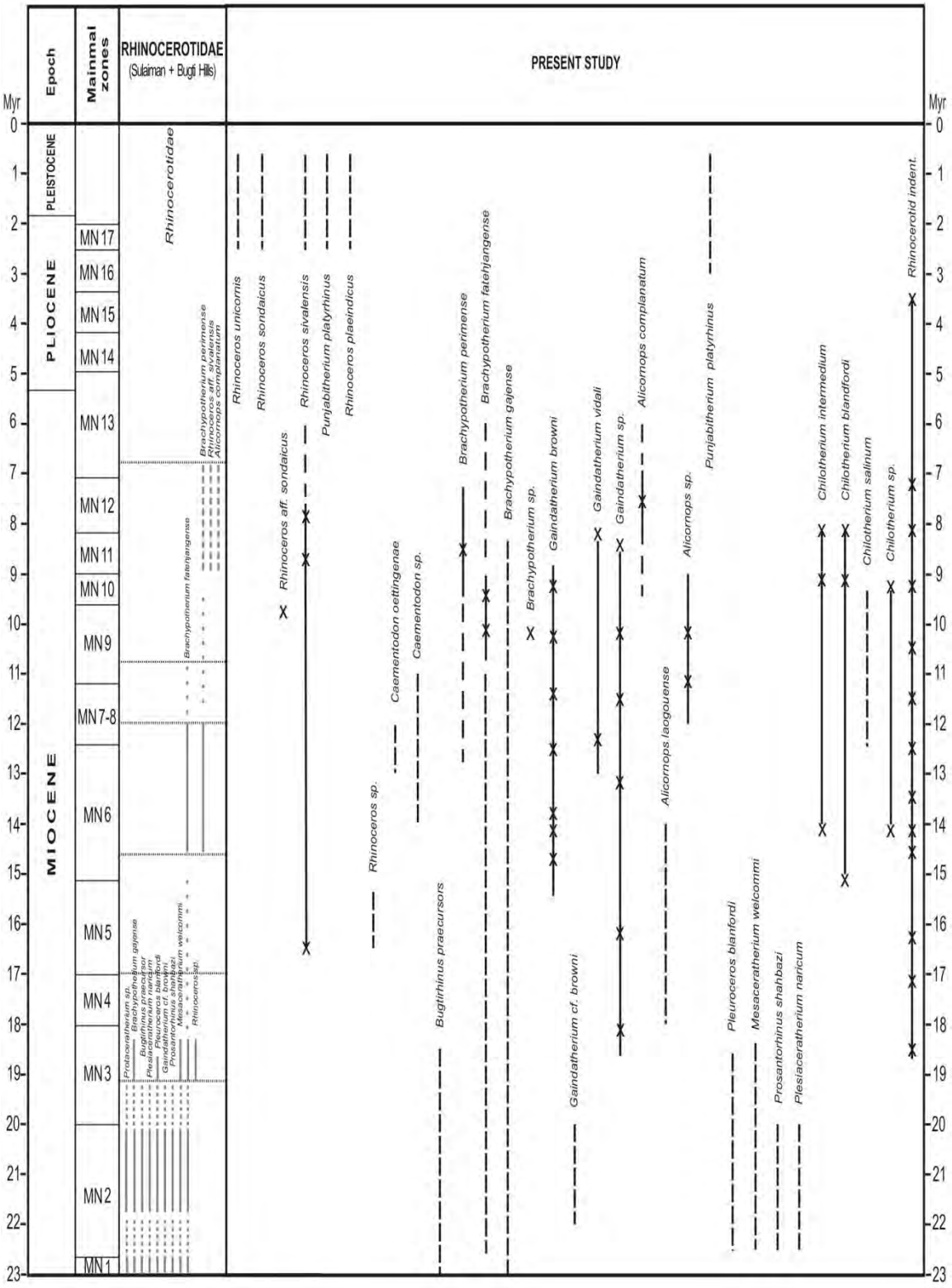
Myr
Epoch
Mainmal zones
RHINOCEROTIDAE
(Sulaiman + Bugti Hills)
PRESENT STUDY
PLEISTOCENE
PLIOCENE
MIOCENE
MN17
MN16
MN15
MN14
MN13
MN12
MN11
MN10
MN9
MN7-8
MN6
MN5
MN4
MN3
MN2
MN1
Rhinocerotidae
Protaceratherium sp.
Brachypotherium gajense
Bugtirhinus praecursors
Plesiaceratherium naricum
Pleuroceros blanfordi
Gaindatherium cf. browni
Prosantorhinus shahbazi
Mesaceratherium welcommi
Rhinoceros sp.
Brachypotherium fatehjangense
Brachypotherium perimense
Rhinoceros aff. sivalensis
Alicornops complanatum
Rhinoceros unicornis
Rhinoceros sondaicus
Rhinoceros aff. sondaicus
Rhinoceros sivalensis
Punjabitherium platyrhinus
Rhinoceros plaeindicus
Rhinoceros sp.
Caementodon oettingenae
Caementodon sp.
Bugtirhinus praecursors
Brachypotherium perimense
Brachypotherium fatehjangense
Brachypotherium gajense
Brachypotherium sp.
Gaindatherium browni
Gaindatherium cf. browni
Gaindatherium vidali
Gaindatherium sp.
Alicornops complanatum
Alicornops laogouense
Alicornops sp.
Punjabitherium platyrhinus
Pleuroceros blanfordi
Mesaceratherium welcommi
Prosantorhinus shahbazi
Plesiaceratherium naricum
Chilotherium intermedium
Chilotherium blandfordi
Chilotherium salinum
Chilotherium sp.
Rhinocerotid indent.

2.8 Siwaliks Rhinocerotidae

Khan A. M. (2009) has carried out a review of the Siwalik rhinocerotids with additional collections from the Potwar Plateau housed at the PUPC. He listed 19 species in the Siwalik sequence whereas described 9 species based on material at the PUPC, adding new information to the known classification and evolutionary trends of the Family Rhinocerotidae in South Asia. Antoine in a series of papers from 2000 to recent has described the systematics of new rhino fossils of late Oligocene to Miocene age collected from the Bugti Hills by the French team led by Welcomme as well as included the undescribed collections of the Harvard-GSP Team and analyzed their evolutionary and geo-biogeography trends in the global context (Table 2.2).

Table 2.2 List of Rhinocerotid taxa whose dental materials were examined for hypoplasia, collected earlier from various parts of Pakistan and northern India. This study also includes rhinocerotids from the Bugti Hills-Sulaiman Range studied by Antoine *et al*. (2013) and from the Potwar Plateau-Mirpur by Khan, A. M. (Unpublished PhD thesis 2009).

Potwar (Khan, A.M., 2009)	**Bugti and Sulaiman** (Antoine *et al*., 2013)	**Present Study**
Rhinoceros sondaicus *Rhinoceros sivalensis* *Punjabitherium platyrhinus* *Gaindatherium browni* *Gaindatherium vidali* *Alicornops complanatum* *Alicornops laogouense* *Chilotherium intermedium* *Brachypotherium perimense*	*Bugtirhinus praecursor* *Plesiaceratherium naricum* *Pleuroceros blanfordi* *Gaindatherium* cf. *browni* *Prosantorhinus shahbazi* *Mesaceratherium welcommi* *Brachypotherium fatehjangense* *Brachypotherium perimense* *Brachypotherium gajense* *Protaceratherium* sp. *Rhinoceros* aff. *sivalensis* *Rhinoceros* sp. *Alicornops complanatum*	*Rhinoceros unicornis* *Rhinoceros sondaicus* *Rhinoceros* aff. *sondaicus* *Rhinoceros sivalensis* *Rhinoceros plaeindicus* *Rhinoceros sp.* *Caementodon oettingenae* *Caementodon* sp. *Bugtirhinus praecursors* *Brachypotherium perimense* *Brachypotherium fatehjangense* *Brachypotherium gajense* *Brachypotherium* sp. *Gaindatherium browni* *Gaindatherium* cf. *browni* *Gaindatherium vidali* *Gaindatherium* sp. *Alicornops complanatum* *Alicornops laogouense* *Alicornops* sp. *Punjabitherium platyrhinus* *Pleuroceros blanfordi* *Mesaceratherium welcommi* *Prosantorhinus shahbazi* *Plesiaceratherium naricum* *Chilotherium intermedium* *Chilotherium blandfordi* *Chilotherium salinum* *Chilotherium* sp. Rhinocerotid indet. **RECENT RHINOS** *Ceratotherium simum simum* *Ceratotherium simum* *Rhinoceros sondaicus* *Rhinoceros unicornis* *Diceros bicornis* *Dicerorhinus sumatrensis*

Heissig (2003) has reported the diversity and species composition of rhinoceroses in three regions of different faunal history including the Siwaliks of Pakistan. He included at least 5 genus, namely *Chilotherium, Brachypotherium, Aprotodon, Rhinoceros, Gaindatherium*, and *Caementodon* from the Siwaliks of Potwar Plateau which was also supported by Khan A. M. (2009). The Siwalik Rhinocerotid fauna from the Potwar Plateau includes *Brachypotherium*

perimense, *Chilotherium blanfordi*, *Didermoceros* aff. *sumatrensis*, *Didermoceros* aff. *abeli*, *Aceratherium* sp., *Eurhinoceros* sp. inc. sed., *Gaindatherium browni*, *Gaindatherium vidali*, *Caementodon oettingenae*, *Aprotodon fatehjangense*, *Eurhinoceros* aff. *sondaicus*, *Chilotherium intermedium complanatum*, *Chilotherium intermedium intermedium*, *Rhinoceros* (Rhinoceros) aff. *sivalensis*, *Rhinoceros sivalensis*, *Punjabitherium platyrhinus*, *Pliotriplopus chinjiensis*, and *Rhinoceros kendengindicus* (Khan A. M., 2009).

Two species of *Aceratherium* and *Chilotherium* from the Bugti Hills was first documented by Forster-Cooper (1934). Many rhinocerotid genera of Oligocene and Miocene fossiliferous formations of Bugti Hills were described by Antoine (2002a and b); Antoine *et al*. (2004); Metais *et al*. (2009); Antoine and Welcomme (2000). They identified an exceptionally rich Rhinocerotids assemblages consisting of *Protaceratherium* sp., *Plesiaceratherium* sp., *Hoploaceratherium* sp., *Aprotodon blanfordi*, *Brachypotherium perimense*, *Dicerorhinus shahbazi*, *Dicerorhinus* cf. *abeli* and *Coementodon oettingenae*.

Rhinos diversity declines from the latest Miocene onward and resulted in nearly complete disappearance of the *Aceratheriinae*, except for the presence of *Chilotherium* in Asia throughout the Pliocene (Cerdeño, 1998).

2.9 Taphonomy

In Siwalik the fossils productivity strongly influenced by sedimentary facies. The two mud-stone dominated Formations, Chinji and Dhok Pathan contains more fossil localities than the two sandstone-dominated Formations, the Kamlial and Nagri. The comparison of fossils assemblages from different depositional environments of the Chinji and Dhok Pathan Formations generally indicated similar taxonomic and sekelatal-element composition, with floodplain surface assemblages most distinct as compared to the channel environments (Badgley *et al*., 1980, 1995; Raza, 1983). The most productive depositional environments for fossils are abandoned channels lags and fills. Floodplains produced fewer fossils than expected which is thought to be a result climate seasonality reduced the preservation potential of Siwalik fossils in soils (Badgley *et al*., 1995; Behrensmeyer *et al*., 2005). Badgley *et al*. (1995), however, speculate that habitat avoidance by animals of open floodplain habitat may also have contributed to their low fossil productivity. Rhino fossils are found in all types of depositional set-up but generally less in flood-plain soil beds.

They are also well represented in fossil localities by all their skeletal elements, a slight preservational bias towards teeth, podials and phalanges elements (Raza, 1983).

Chapter – 3

HYPOPLASIA AND METHODOLOGY

3.1 Enamel Hypoplasia

Teeth, one of the hardest parts of the skeleton, are often well preserved in the fossil record and are not remodeled after maturation. Enamel and dentin do not regenerate after they mineralize initially. It therefore acts as permanent record of events that occurred during tooth development. The fact that enamel, unlike bone, does not remodel, together with its chronological development and the sensitivity of the ameloblasts, makes enamel perfect archive for development stress (Goodman and Rose, 1990). Furthermore, Serial analyses from top to base of the tooth crown reflect seasonal changes during tooth development in modern and fossil animals (Koch *et al*., 1989; Bryant *et al*., 1994; Fricke and O'Neil, 1996; Stuart-Williams and Schwarcz, 1997; Feranec and Mac-Fadden 2000; Balasse *et al*., 2002).

Dental Enamel Hypoplasia (DEH) is a thinning of tooth enamel resulting from disruptions in the enamel deposition by amelobalsts during crown development (Ensor and Irish, 1995; Guita, 1984; Shafer *et al*., 1983; Yaeger, 1980). This results either in pits and grooves in areas of the tooth or in widespread absence of enamel as a linear band (Berten, 1895; Goodman and Rose, 1990; Hillson, 1996, 1997, 2005; Larsen, 1997). The most visible deficiencies are in the form of linear band noted as Linear Enamel Hypoplasia (LEH). Since hypoplasitic defects are not erased unless the enamel itself is worn away, teeth provide an excellent record of the different types and degrees of environmental stress and influence of the metabolic conditions affecting tooth structure and tooth survival. The causes of structural anomalies are either hereditary, environmental or a combination of both (Gorlin and Goldman, 1970). Teeth are recognized as important indicators of biological interaction, adaptation, behavior and metabolic trauma, which El-Najjar *et al*. (1978) explained to have occurred as follows:

1. Hereditary structural anomalies usually involve both primary and secondary dentition, whereas environmental anomalies affect either the primary or secondary dentition or specific teeth.

2. Hereditary structural anomalies, as a rule, affect either enamel or dentine whereas environmental anomalies affect both enamel and dentine.
3. Hereditary structural anomalies most often cause diffuse or even vertical orientation derangements, whereas environmental structural anomalies are primarily horizontally arranged.

3.2 Linear Enamel Hypoplasia

Linear Enamel Hypoplasia (LEH) is a deficiency in enamel thickness occurring during tooth crown formation. It is typically visible on a tooth's surface as one; two or more horizontal (or transverse) grooves or lines (Figure 3.1). It may also be in the form of linear array of pits, representing a deficiency of enamel formation visible on outer enamel surface (Goodman and Rose, 1991; Skinner and Goodman, 1992). It is the most commonly studied expression of Enamel Hypoplasia.

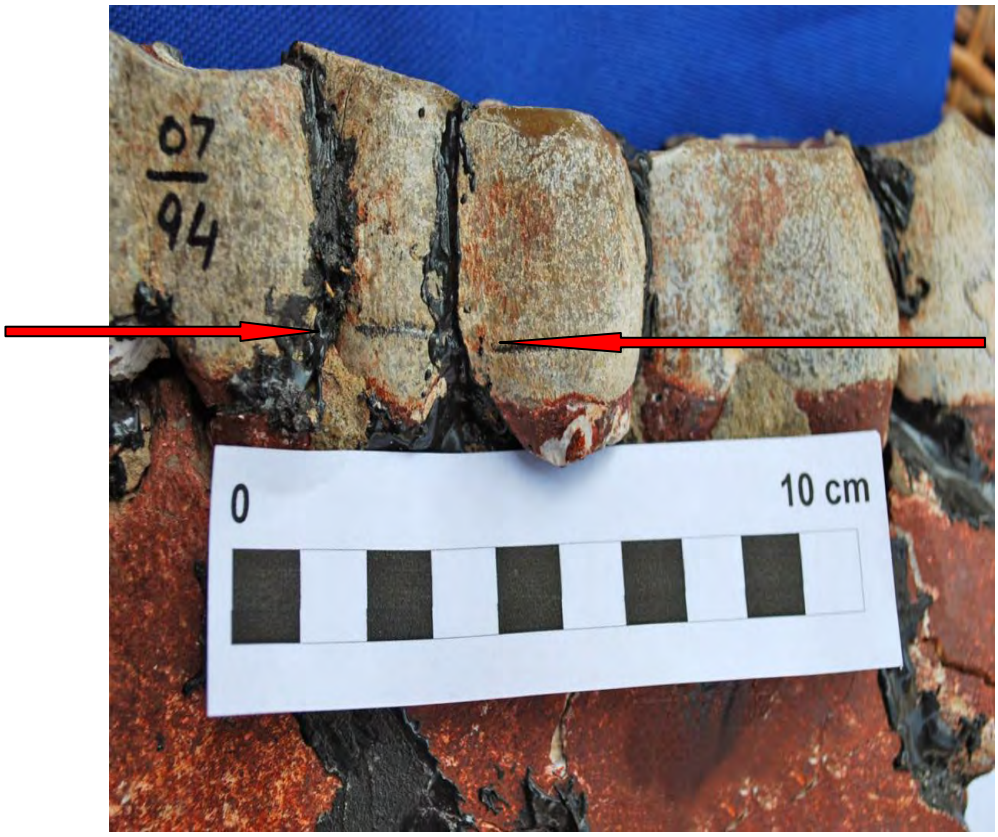

(a)

Figure 3.1 (a) Buccal view of left mandibullary (*Chilotherium intermedium*) and (b) Lingual view of left maxillary (*Rhinoceros sivalensis*) dental set illustrating linear Enamel Hypoplasia (Red Arrows).

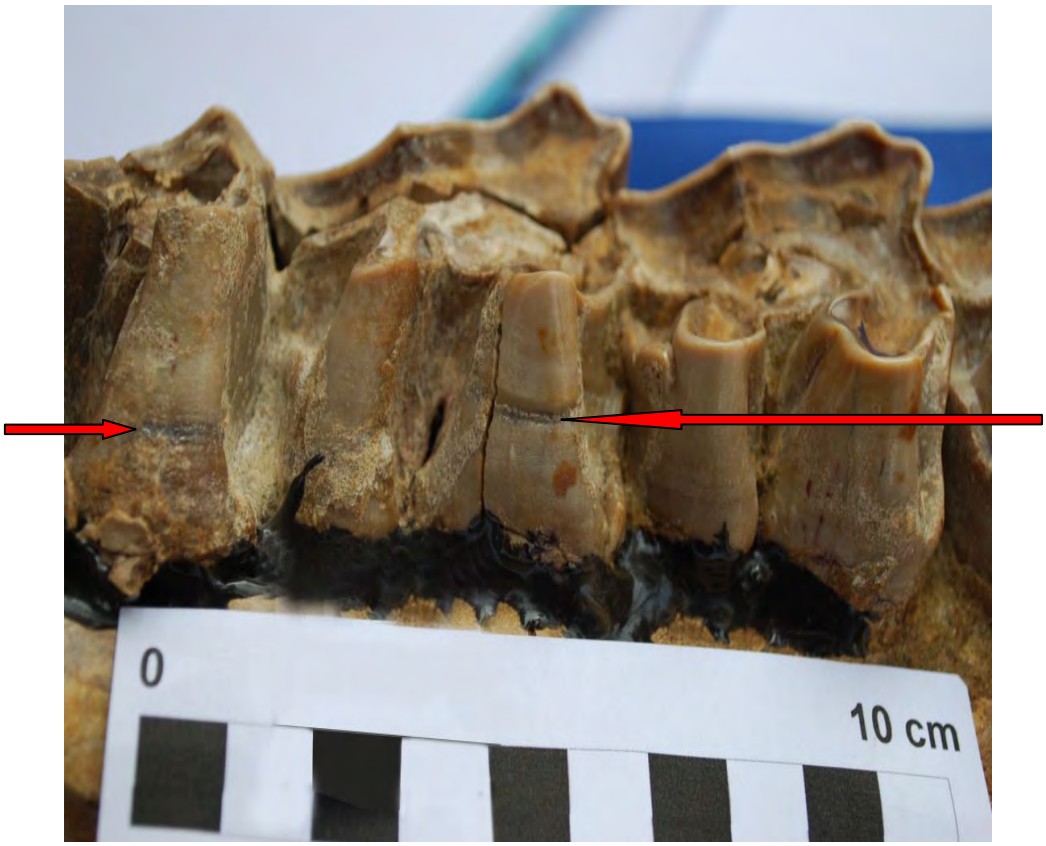

(b)

Figure 3.1 (a) Buccal view of left mandibullary (*Chilotherium intermedium*) and (b) Lingual view of left maxillary (*Rhinoceros sivalensis*) dental set illustrating linear Enamel Hypoplasia (Red Arrows).

It is caused by a physical disruption in the cells (ameloblasts) laying down the enamel (Goodman and Rose, 1990). The disruption is usually caused by systematic (metabolic) stress and this defect is manifested by thinning of the tooth enamel. Enamel essentially forms in two phases: a secretory and a maturation phase (Hillson, 1986). During the initial secretory phase, enamel laid down in an incremental fashion starting at the dentine-enamel junction and proceeding outwards and downwards (Figure 3.2).

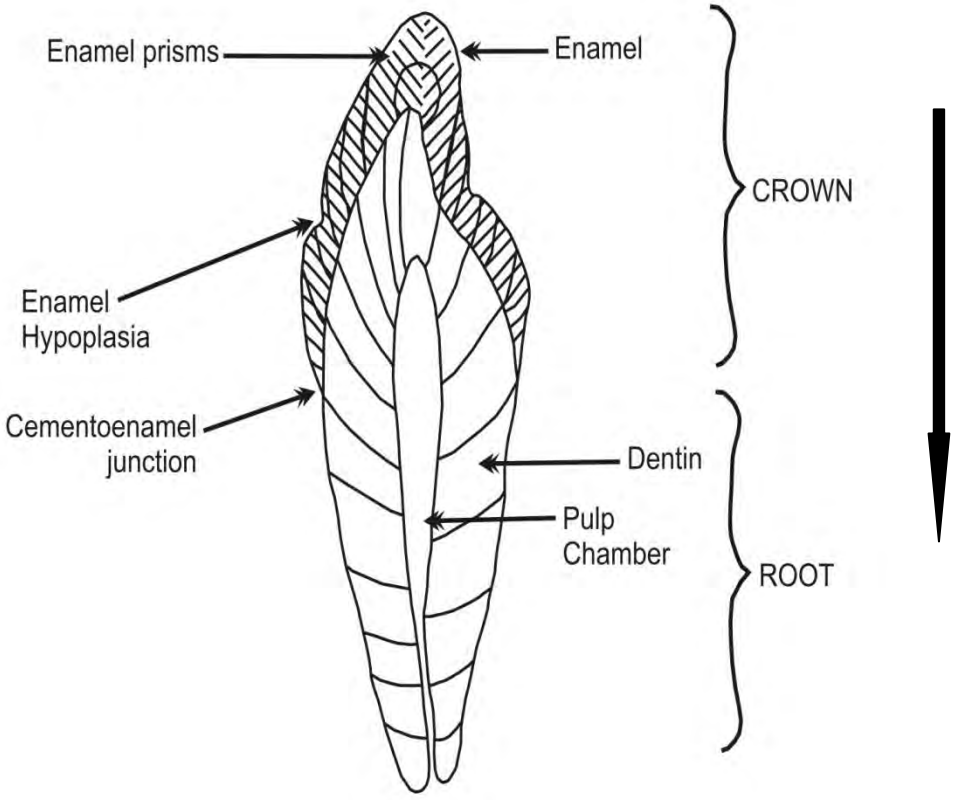

Figure 3.2 Diagrammatic representation of longitudinal section of a tooth. The vertical arrow (extreme right) indicates the direction of crown development from tip to base. (After Goodman and Rose, 1990; Franz-Odendaal *et al*., 2004)

The age at which the defect formed and the timing of the stress episode can be estimated from its position on the tooth crown relative to the root-crown junction. The width of the LEH relates to the duration of the stress episode and its depth is thought to be related to severity (Goodman *et al*., 1980; Suckling, 1989).

3.3 Literature review on Enamel Hypoplasia (EH)

The Linear Enamel Hypoplasia has been widely used as an indicator of period of generalized physiological stress during tooth development in hominid and non-hominid primates (Goodman and Rose, 1990; Guatelli-Steinberg, 2000, 2003,2004; King *et al*., 2002; Larsen, 1997; Moggi-Cecchi and Crivella, 1991; Skinner and Goodman, 1992; Skinner and Hopwood, 2004), domestic pigs and wild boar (Dobney and Ervynck, 2000; Dobney *et al*., 2004), and other extinct or extant ungulate species (Franz-Odendaal, 2004; Franz-Odendaal *et al*., 2004; Mead, 1999 and Niven *et al*. 2004). These studies demonstrated that the analysis of LEH has been a useful means for retrospective assessment of the timing and intensity of systematic stress events during the period in which an individual's dentition is formed, and can thereby contribute to the understanding of past ecological and health conditions.

Enamel Hypoplasia has widely been used for exploring the health status of past human populations (Skinner and Goodman, 1992), and to standardize methodologies, an international index for Enamel Hypoplasia was set up by the Federation Dentaire International (FDI; Federation Dentaire International, 1982). The FDI index recognizes three broad categories of this defect: pits (single or multiple; non-linear), grooves (vertical or horizontal; linear), and areas missing enamel. These defects can be caused by one of three factors: severe physiological stress; localized trauma (such as injury to the jaw) or, in rare instances, it can be inherited. In inherited cases, all teeth will be affected (Stewart and Poole, 1982) and the person is likely to have other congenital abnormalities resulting in an overall low survival rate (Goodman and Rose, 1990). Localized trauma would cause Enamel Hypoplasia in single or adjacent teeth and would not affect the contralateral (uninjured) side of the mouth (Skinner, 1986; Skinner and Hung, 1989). Both inherited cases and those resulting from local injury rarely reported probably because complete skulls with all teeth intact less frequently found in the fossil record. Physiological stress (such as weaning, parturition, nutritional stress, illness, and calf-cow separation) that occurs at a particular ontogenetic stage would affect all teeth developing at the time of the stress and would occur as Linear Enamel Hypoplasia (LEH) (Goodman and Rose, 1990; Neiburger, 1990; Mead, 1999; Dobney and Ervynck, 2000; Lukacs, 2001). Lukacs (2001) in his study of Enamel Hypoplasia of Early Miocene Catarrhines noted that the deciduous teeth in addition to linear hypoplasia show semi-circular enamel hypoplasia defects in primates, which he attributed to physiological stress.

Hypoplasia studies of non-primate mammalian fossils have attracted very little attention; only two notable studies have been found in the literature. The two studies are the North American

Miocene rhinoceros Teleoceras by Mead (1999) and the Early Pliocene Sivathere giraffids from South Africa by Franz-Odendaal *et al*. (2004). Mead (1999) had attributed the high prevalence of EH (87.9%; n=66) on dp^4s of the Teleoceras to severe physiological stress at or very near birth. The *Sivathrium hendeyi* from Langebaanweg South Africa has incidence of LEH restricted to permanent dentition which is thought to be the result of poor environmental condition, possible seasonal nutritional stresses and in some instances stresses at the weaning stage (Franz-Odendaal *et al.* 2004). Based on the distribution, incidence and size of linear defects in each tooth type of the *Sivathrium hendeyi*, Franz-Odendaal *et al*. (2004) suggested that the duration of the stress episodes varied at different times during ontogeny. Almost all herbivore groups at Langebaanweg such as Giraffa, Palaeotragus, Mesembrioportax, Sivatherium, Ceratotherium, Simatherium, Kobus, Demalacra, and Hippopotomidae show variable degree of the LEH development on several tooth types (Franz-Odendaal *et al*., 2003). Several distinct linear defects were observed in the continually erupting hippopotamus tusks, indicating that stress episodes were not confined to the developing years of an animal's life but they also extend into adulthood.

Franz-Odendaal *et al*. (2003) concluded a strong correlation between the presence of Linear Enamel Hypoplasia in a large early Pliocene Langebaanweg faunal assemblage and reduced seasonality (aridity) in Southern Africa. These adverse climate conditions persisted from development and throughout adulthood, and placed several herbivores under severe systematic stress that ultimately resulted in the manifestation of Linear Enamel Hypoplasia. They carried out the high-resolution isotope analyses of teeth enamel, which gave the otherwise unobtainable insights into the weaning behavior of extinct animals, and used as a tool to understand the environmental contexts under which developmental dental disease manifests.

Niven *et al*. (2004) provided a methodology to estimate the ontogenetic and seasonal timing of enamel hypoplasia formation in bison dentition of the butchery/kill sites of Buffalo Creek (Wyoming) and Kaplan-Hoover (Colorado). They concluded that DEH offers indelible and relatively fine-grained records of physiological changes occurring during tooth development. They proposed that physiological stress was exacerbated by specific-age (birth, weaning) and season-specific (below-average forage capacity due to drought and/or winter severity) factors. The combination of the physiological condition of bison and one or more stressors was significant enough to push disruption in tooth development over "threshold level" and manifest in tooth defects in many individuals. These patterns can provide valuable insights into local paleoecological conditions as well as details of the relationship of individual animals to their environment.

Kierdorf *et al*. (2006) while studying the cattle (*Bos taurus*) cheek teeth reported that the occurrence of horizontal lines in coronal cementum and the filling of hypoplasitic enamel defects can cause problems in correct identification of LEH especially near to cervical crown areas, where the coronal cementum is thickest. They recommended that in cattle and other ungulates microscopic examination should be used with macroscopic study to use LEH reliable stress indicator.

Dobney and Ervynck (2000) recorded Linear Enamel Hypoplasia (LEH) on tooth crowns of numerous archeological pig's teeth and construct a chronology of physiological stress for five different archaeological assemblages. Their data showed strong causal relationship between the occurrence of LEH, events in life and seasonal conditions affecting the food intake and energy balance of ancient domestic pigs.

Hussain and Sondaar (1968) while reporting on anomalous features in Hipparion dention from Spain, Potwar Plateau, and Samos (Greece) noted hypoplasia on an "upper (third or fourth) Premolar of *Hipparion concudense"* from Spain. They ascribed the Enamel Hypoplasia due to malnutrition of the mother during the enamel development of the individual.

3.4 Materials

It was realized in the initial stages of this study that the Rhino teeth collections available in Punjab University, PMNH are not sufficient to make a meaningful analysis. Also there were no facilities for studying the Recent Rhino material. Therefore, extensive studies were carried out at all the notable Siwalik collections housed in foreign museums and institutions.

A total of 1754 teeth of extinct (Siwalik Rhinocerotidae) and extant Rhinocerotidae were studied which are housed at the paleontological collections of Geological Survey of Pakistan (GSP), Islamabad, Pakistan; Pakistan Museum of Natural History (PMNH), Islamabad, Pakistan; Punjab University Paleontology Collection (PUPC), Zoology Department, Punjab University, Lahore, Pakistan; Muséum National d'Histoire Naturelle (MNHN), Paris, France; Museum d' Histoire Naturelle (MHNT), Toulouse, France; American Museum of Natural History (AMNH),

New York, USA; Peabody Museum Harvard University (PMHU), USA; Yale Peabody Natural History Museum (YPNHM), New Heaven, USA and Natural History Museum (NHM), London, UK. I personally visited all these institutes to observe the Siwalik paleontological collection present in Pakistan, France, USA and UK and studies 846 Rhino fossil teeth (Table 3.1) to collect the Enamel Hypoplasia data. Whereas, also studied the 908 teeth (Table 3.2) of Recent Rhino collection present at Laboratoires de Paléontologie et d' Anatomie Comparée in the Muséum National d'Histoire Naturelle (MNHN), Paris, France and Harvard the MCZ, Mammalogy Department, Cambridge, Massachusetts, USA.

Table 3.1 List of Siwalik Rhinocerotid taxa and number of teeth studied at Museums and Institutions of Pakistan, France, USA and UK.

1. GSP (Geological Survey of Pakistan), Islamabad, Pakistan

(i)	***Brachypotherium***	
	B. perimense	1
(ii)	Rhinocerotidae indet.	15

2. PMNH (Pakistan Museum of Natural History), Earth Sciences Division, Islamabad, Pakistan

(i)	***Gaindatherium***	
	G. browni	8
	G. vidali	2
(ii)	***Brachypotherium***	
	B. fatehjangense	5
	B. perimense	6
(iii)	***Alicornops***	
	A. complanatum	1
	A. sp.	1
(iv)	***Caementodon***	
	C. sp.	2

(v) ***Bugtirhinus***

B. praecursors 2

(iv) ***Rhinoceros***

R. unicornis 5

3. PUPC (Punjab University Paleontology Collection), Zoology Department, Punjab University, Lahore, Pakistan

(i) ***Alicornops***

A. laogouense 12

A. complanatum 15

A. sp. 1

(ii) ***Gaindatherium***

G. browni 12

G. sp. 2

(iii) ***Brachypotherium***

B. fatehjangense 9

B. perimense 41

(iv) ***Rhinoceros***

R. sondaicus 20

R. sivalensis 15

R. unicornis 7

R. sp. 1

(v) ***Punjabitherium***

P. platyrhinus 6

(vi) ***Chilotherium***

C. *intermedium* 23

(vii) ***Caementodon***

C. sp. 9

4. MNHN (Muséum National d'Histoire Naturelle), Paris, France

(i) ***Brachypotherium***

B. fatehjangense 2

B. perimense 4

	B. sp.	1
(ii)	***Gaindatherium***	
	G. sp.	4
(iii)	***Alicornops***	
	A. sp.	9
(iv)	***Rhinoceros***	
	R. aff. *sondaicus*	1
(v)	Rhinocerotidae indet.	1

5. MHNT (Museum d' Histoire Naturelle), Toulouse, France

(i)	***Alicornops***	
	A. complanatum	6
(ii)	***Pleuroceros***	
	P. blanfordi	40
(iii)	***Brachypotherium***	
	B. fatehjangense	54
	B. gajense	10
(iv)	***Mesaceratherium***	
	M. welcommi	22
(v)	***Gaindatherium***	
	G. cf. *browni*	3
(vi)	***Prosantorhinus***	
	P. shahbazi	6
(vii)	***Plesiaceratherium***	
	P. naricum	6

6. AMNH (American Museum of Natural History), New York, USA

(i)	***Caementodon***	
	C. oettingenae	1

(ii) ***Rhinoceros***

R. sivalensis	1
R. sp.	10

(iii) ***Gaindatherium***

G. browni	31

(iv) ***Chilotherium***

C. *intermedium*	43
C. blandfordi	28
C. salinum	4
C. sp.	8

(v) ***Rhinocerotidae*** 18

7. PMHU (Peabody Museum Harvard University), USA (Harvard – GSP Collection)

(i) ***Rhinoceros***

R. sivalensis	3
R. sp.	1

(ii) ***Gaindatherium***

G. browni	22
G. vidali	4
G. sp.	30

(iii) ***Brachypotherium***

B. perimense	1

(iv) ***Rhinocerotina*** 2

(v) ***Rhinocerotidae*** 39

8. YPNHM (Yale Peabody Natural History Museum), New Heaven, USA (Siwalik Collection)

(i)	***Brachypotherium***	
	B. fatehjangense	1
(ii)	*Rhinoceros* indet.	61

9. NHM (Natural History Museum) Paleontology Department (Siwalik Collection), London, UK

(i)	***Rhinoceros***	
	R. sivalensis	25
	R. plaeindicus	69
	R. sp.	38
(ii)	***Punjabitherium***	
	P. platyrhinus	16

Table 3.2 List of Recent Rhinocerotid taxa and number of teeth studied in France and USA.

1. MNHN (Muséum National d' Histoire Naturelle), Paris, France (Laboratoires de Paléontologie et d 'Anatomie Comparée)

(i)	***Ceratotherium***	
	C. simum simum	2
	C. simum	36
(ii)	***Rhinoceros***	
	R. sondaicus	191
	R. unicornis	99
(iii)	***Diceros***	
	D. bicornis	241

2. Museum of Comparative Zoology (MCZ), Mammalogy Department, Harvard University, Cambridge (MA), USA

(i)	***Ceratotherium***	
	C. simum	44
(ii)	***Rhinoceros***	
	R. sondaicus	26
	R. unicornis	119
(iii)	***Diceros***	
	D. bicornis	126
(iv)	***Dicerorhinus***	24
	D. sumatrensis	

3.5 Methods

Dental terminology of Rhinocerotidae tooth for studying hypoplasia in this thesis follows that of Antoine *et al*. (2010) as shown in the Figure 3.3.

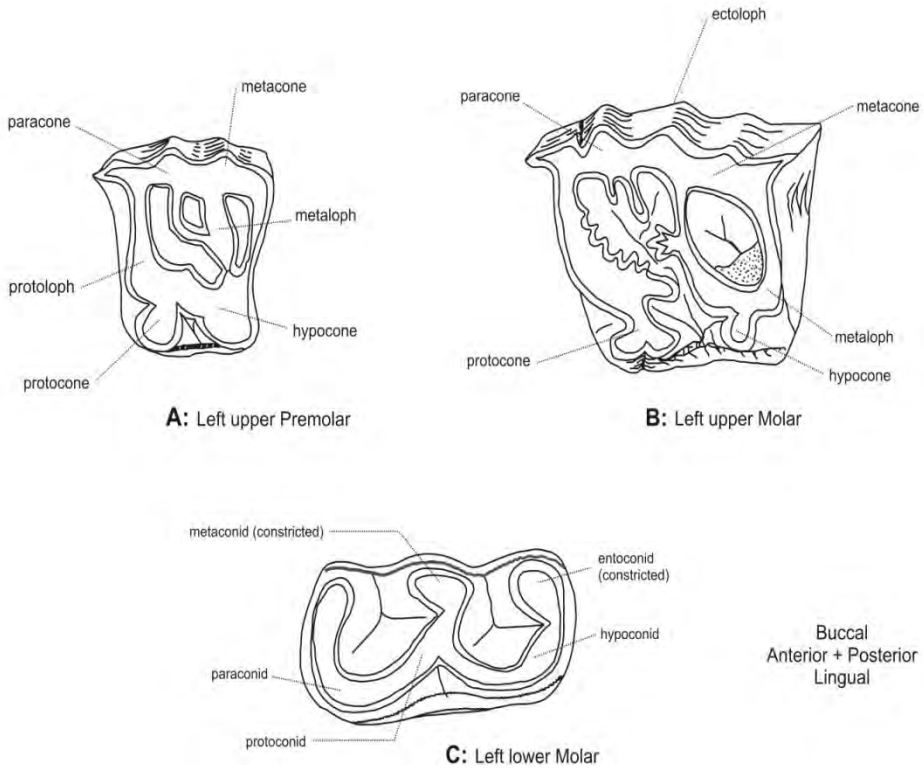

Figure 3.3 Dental terminology of rhinocerotid tooth for studying hypoplasia (After Antoine *et al*., 2010).

All teeth were examined very carefully and macroscopically for the presence or absence of Enamel Hypoplasia (EH) and description of each defect, its position on the tooth crown and the position of the defected tooth in each jaw were recorded. Enamel defects were further classified as Linear Enamel Horizontal (LEH) or Semi-Circular Enamel Hypoplasia (SEH) depression. Linear horizontal and semicircular defects on both lingual and buccal surfaces were also noted down. The position of LEH on the tooth crown heights from the root-crown junctions (neck) was measured.

Extensive photography of buccal and lingual views of each tooth was also undertaken. All measurements were taken in mm.

3.6 Dataset

A total of 1754 teeth were carefully examined which included 846 fossils Rhino teeth and 908 Recent Rhino teeth. These 846 fossil Rhinocerotid teeth included 21 incisors (i), 2 canines (c), 43 deciduous premolars, 283 premolars, and 497 molars (Figure 3.4) whereas recent Rhino teeth included 15 incisors (i) 32 canines (c), 486 premolars, and 375 molars (Figure 3.5). The MNI (minimum number of individuals) for the 846 fossil teeth calculated to be 337 animals whereas; the Recent Rhinos teeth are from 45 animals.

Figure 3.4 Number of teeth examined for EH in fossil Rhinos.

i	c	Dp1	DP2	DP3	DP4	P1	P2	P3	P4	M1	M2	M3
21	**2**	**11**	**7**	**13**	**12**	**25**	**69**	**93**	**96**	**178**	**129**	**190**

Figure 3.5 Number of teeth examined for EH in recent Rhinos**.**

i	c	P1	P2	P3	P4	M1	M2	M3
15	**32**	**72**	**134**	**140**	**140**	**143**	**141**	**91**

A fairly small number of teeth were found with hypoplasia; 39 teeth from a total of 846 teeth had hypoplasia. The recent rhinos showed much less incidence of hypoplasia, only 6 teeth with EH from a total of 908 teeth were examined. The MNI of fossil rhino with EH was calculated to be 34 animals whereas only 3 recent rhinos have EH. The studied material grouped to genus and species level and is given in Table 3.3 to 3.11 (with Enamel Hypoplasia- **highlighted**) and Table 3.12 to 3.22 (without Enamel Hypoplasia).

Table 3.3 **Fossil Rhinocerotidae dental sample (with EH) by genus, jaw and tooth at** PMNH (Pakistan Museum of Natural History), Earth Sciences Division, Islamabad, Pakistan

Taxon	Jaw		p1	p2	p3	p4	m1	m2	m3	Total
Gaindatherium										
G. browni (n=6) (MUS 106)	Mandible (r)	0	1	**1**	**1**	1	1	1	6	

Table 3.4 **Fossil Rhinocerotidae dental sample (with EH) by genus, jaw and tooth at** PUPC (Punjab University Paleontology Collection), Zoology Department, Punjab University, Lahore, Pakistan

Taxon	Jaw	dp4	p1	p2	p3	p4	m1	m2	m3	Total
Alicornops										
A. laogouense (n=5) (PUPC 07/47)	Maxilla (r)	0	0	1	1	1	**1**	1	0	5

Taxon	Jaw	dp4	p1	p2	p3	p4	m1	m2	m3	Total
Gaindatherium										
G. browni (PUPC 07/147)	Maxilla (l)	0	0	0	0	**1**	0	0	0	1

Taxon	Jaw	dp4	p1	p2	p3	p4	m1	m2	m3	Total
Brachypotherium										
B. fatehjangense (PUPC 07/170)	Maxilla (l)	0	0	0	0	**1**	0	0	0	1

Taxon	Jaw	dp4	p1	p2	p3	p4	m1	m2	m3	Total
Brachypotherium										
B. fatehjangense (PUPC 07/173)	Maxilla (l)	**1**	0	0	0	0	0	0	0	1

Taxon	Jaw	dp4	p1	p2	p3	p4	m1	m2	m3	Total
Brachypotherium										
B. perimense (PUPC 07/74)	Mandible (r)	0	0	**1**	0	0	0	0	0	1

Table 3.4: Cont…

Taxon	Jaw	dp4	p1	p2	p3	p4	m1	m2	m3	Total
Brachypotherium										
B. perimense (PUPC 07/152)	Maxilla (r)	**1**	0	0	0	0	0	0	0	1

Taxon	Jaw	dp4	p1	p2	p3	p4	m1	m2	m3	Total
Brachypotherium										
B. perimense		0	0	**1**	0	0	0	0	0	1
	Maxilla (r)									
(PUPC 07/126)										

Taxon	Jaw	dp4	p1	p2	p3	p4	m1	m2	m3	Total
Brachypotherium										
B. perimense		0	0	0	0	0	0	0	**1**	1
	Maxilla (l)									
(PUPC 68/826)										

Taxon	Jaw	dp4	p1	p2	p3	p4	m1	m2	m3	Total
Brachypotherium										
B. perimense		0	0	0	**1**	1	**1**	1	0	4
(n=4)	*Mandible* (r)									
(PUPC 07/54)										

Taxon	Jaw	dp4	p1	p2	p3	p4	m1	m2	m3	Total
Brachypotherium										
B. perimense		0	0	0	0	0	0	0	**1**	1
	Maxilla (l)									
(PUPC 68/529)										

Table 3.4: Cont…

Taxon	Jaw	dp4	p1	p2	p3	p4	m1	m2	m3	Total
Chilotherium										
C. *intermedium*		0	0	0	0	0	0	**1**	0	1
	Mandible (r)									
(PUPC 07/95)										

Taxon	Jaw	dp4	p1	p2	p3	p4	m1	m2	m3	Total
Chilotherium										
C. *intermedium*		0	0	1	**1**	1	1	0	0	4
(n=4)	Mandible (l)									

(PUPC 07/94)

Taxon	Jaw	dp4	p1	p2	p3	p4	m1	m2	m3	Total
Rhinoceros										
R. sivalensis		0	0	0	0	0	0	**1**	0	1
	Mandible (l)									
(PUPC 07/39)										

Taxon	Jaw	dp4	p1	p2	p3	p4	m1	m2	m3	Total
Rhinoceros										
R. sivalensis		0	1	1	1	1	1	**1**	**1**	7
(n=7)	Maxilla (l)									
(PUPC 07/38)										

Taxon	Jaw	dp4	p1	p2	p3	p4	m1	m2	m3	Total
Rhinoceros										
R. sondaicus		0	0	0	0	1	1	1	**1**	4
(n=4)	Mandible (r)									
(PUPC 2010/68)										

Table 3.4: Cont…

Table 3.5 **Fossil Rhinocerotidae dental sample (with EH) by genus, jaw and tooth**
MNHN (Muséum National d'Histoire Naturelle), Paris, France

Taxon	Jaw	dp4	p1	p2	p3	p4	m1	m2	m3	Total
Brachypotherium										
B. fatehjangense (15400)	Mandible (l)	**1**	0	0	0	0	0	0	0	1

Taxon	Jaw	dp4	p1	p2	p3	p4	m1	m2	m3	Total
Gaindatherium										
Gaindatherium sp. (15551)	Mandible (l)	**0**	0	0	0	0	**1**	0	0	1

Taxon	Jaw	d4	p1	p2	p3	p4	m1	m2	m3	Total
Gaindatherium										
Gaindatherium sp. (10468)	Maxilla (r)	**0**	0	0	0	**1**	0	0	0	1

Table 3.6 **Fossil Rhinocerotidae dental sample (with EH) by genus, jaw and tooth**
MHNT (Museum d' Histoire Naturelle), Toulouse, France

Taxon	Jaw	p1	p2	p3	p4	m1	m2	m3	Total
Alicornops									
A. complanatum		0	1	1	**1**	1	1	**1**	6
	Mandible (l)								
(Pak 1606)									

Taxon	Jaw	p1	p2	p3	p4	m1	m2	m3	Total
Pleuroceros									
P. blanfordi		0	**1**	0	0	0	0	0	1
	Maxilla (l)								
(Pak 1031)									

Taxon	Jaw	p1	p2	p3	p4	m1	m2	m3	Total
Pleuroceros									
P. blanfordi		0	0	0	0	**1**	0	0	1
	Maxilla (l)								
(Pak 46 D)									

Taxon	Jaw	p1	p2	p3	p4	m1	m2	m3	Total
Brachypotherium									
B. fatehjangense		0	0	0	0	**1**	0	0	1
	Mandible (r)								
(Pak 1069)									

Taxon	Jaw	p1	p2	p3	p4	m1	m2	m3	Total
Mesaceratherium									
M. welcommi		0	0	0	0	0	0	**1**	1
	Maxilla (r)								
(Pak 1032b)									

Table 3.7 Fossil Rhinocerotidae dental sample (with EH) by genus, jaw and tooth

AMNH (American Museum of Natural History), New York, USA

Taxon	Jaw	p1	p2	p3	p4	m1	m2	m3	Total
Caementodon									
C. oettingenae		0	0	0	**1**	0	0	0	1
AMNH 19591	Maxilla (l)								

Table 3.8 Fossil Rhinocerotidae dental sample (with EH) by genus, jaw and tooth

PMHU (Peabody Museum Harvard University), USA (Harvard – GSP Collection)

Taxon	Jaw	d1	d2	d3	d4	p1	p2	p3	p4	m1	m2	m3	Total
Rhinoceros													
R. sivalensis		0	0	0	0	0	0	0	0	0	0	**1**	1
PMHU - Y 28225	Maxilla (r)												

Taxon	Jaw	d1	d2	d3	d4	p1	p2	p3	p4	m1	m2	m3	Total
Rhinoceros													
R. sp.		0	0	0	0	0	0	0	0	0	**1**	0	1
PMHU - Y 31182	Mandible (r)												

Taxon	Jaw	d1	d2	d3	d4	p1	p2	p3	p4	m1	m2	m3	Total
Gaindatherium													
G. browni		0	0	0	0	0	0	0	0	0	1	**1**	2
(n=2) PMHU - Y 24067 b	Mandible (l)												

Table 3.8: Cont…

Taxon	Jaw	d1	d2	d3	d4	p1	p2	p3	p4	m1	m2	m3	Total

Gaindatherium													
G. sp.		**1**	0	0	0	0	0	0	0	0	0	0	1
	Mandible (l)												
PMHU - Y 7079													

Taxon	Jaw	d1	d2	d3	d4	p1	p2	p3	p4	m1	m2	m3	Total
Brachypotherium													
B. perimense		0	0	**1**	0	0	0	0	0	0	0	0	1
	Mandible (l)												
PMHU - Y 53615													

Table 3.8: Cont…

Table 3.9 **Fossil Rhinocerotidae dental sample (with EH) by genus, jaw and tooth**
YPNHM (Yale Peabody Natural History Museum), New Heaven, USA (Siwalik Collection)

Taxon	Jaw	p1	p2	p3	p4	m1	m2	m3	Total
Brachypotherium									
B. fatehjangense		0	0	0	0	0	**1**	0	1
	Mandible (l)								
YPM VP 049762									

Table 3.10 **Fossil Rhinocerotidae dental sample (with EH) by genus, jaw and tooth**
NHM (Natural History Museum) Paleontology Department (Siwalik Collection), London, UK

Taxon	Jaw	p1	p2	p3	p4	m1	m2	m3	Total
Rhinoceros									
R. sivalensis (n=6) (NHM 39647)	Maxilla (l)	0	1	1	**1**	1	1	1	6

Taxon	Jaw	p1	p2	p3	p4	m1	m2	m3	Total
Punjabitherium									
P. platyrhinus (n=5) (NHM 17996)	Mandible (r)	0	1	**1**	1	1	1	0	5

Taxon	Jaw	p1	p2	p3	p4	m1	m2	m3	Total
Punjabitherium									
P. platyrhinus (n=6) (NHM 28911- Cast)	Maxilla (r)	0	1	**1**	1	**1**	1	1	6

Table 3.11 **Recent Rhinocerotidae dental sample (with EH) by genus, jaw and tooth**
MNHN (Muséum National d' Histoire Naturelle), Paris, France
(Laboratoires de Paléontologie et d 'Anatomie Comparée)

Taxon	Jaw	c	p1	p2	p3	p4	m1	m2	m3	Total
Ceratotherium										
C. simum simum		0	0	0	0	1	0	0	**1**	2
	Mandible (r)									
(MNHN, Paris n0 2005-297)										

Taxon	Jaw	c	p1	p2	p3	p4	m1	m2	m3	Total
Rhinoceros										
R. sondaicus	Maxilla (r)	0	1	1	1	0	0	0	1	4
(MNHN, Paris	Maxilla (l)	0	1	1	1	**1**	1	0	1	6
1985-159)	Mandible (r & l)	0	0	0	2	2	2	2	2	10
	Total	0	2	2	4	3	3	2	4	20

Taxon	Jaw	c	p1	p2	p3	p4	m1	m2	m3	Total
R. sondaicus	Maxilla (r & l)	2	2	2	2	2	2	2	2	16
(MNHN, Paris	Mandible (r)	1	0	1	**1**	**1**	1	1	1	7
A-7971)	Mandible (l)	1	0	1	**1**	**1**	1	1	1	7
	Total	4	2	4	4	4	4	4	4	30

Table 3.12 **Fossil Rhinocerotidae dental sample (**without EH**) by genus, jaw and tooth**
GSP (Geological Survey of Pakistan), Islamabad, Pakistan

Taxon	Jaw	p1	p2	p3	p4	m1	m2	m3	Total
Brachypotherium									
B. perimense		0	0	0	0	1	0	0	1
(n=1)	Mandible								
Rhinocerotidae indet.	Tooth Fragment	15							
(n=15)									

Tablte 3.13 **Fossil Rhinocerotidae dental sample (**without EH**) by genus, jaw and tooth**
PMNH (Pakistan Museum of Natural History), Earth Sciences Division, Islamabad, Pakistan

Taxon	Jaw	I	D4	p1	p2	p3	p4	m1	m2	m3	Total
Gaindatherium											
G. browni	Maxilla	0	0	0	0	0	1	1	0	0	2

(n=2)											
G. vidali	Maxilla	0	1	0	0	0	0	0	0	0	1
(n=2)	Mandible	0	0	0	0	0	0	0	1	0	1
	Total	0	1	0	0	0	0	0	1	0	2
Brachypotherium											
	Maxilla	0	0	0	1	1	0	0	0	0	2
B. fatehjangense	Mandible	0	0	0	0	0	0	1	1	1	3
(n=5)	Total	0	0	0	1	1	0	1	1	1	5
B. perimense	Maxilla	1	0	0	0	0	0	2	0	1	4
(n=6)	Mandible	0	0	0	0	0	0	0	1	1	2
	Total	1	0	0	0	0	0	2	1	2	6
Alicornops											
A. complanatum											
(n=1)	Mandible	0	0	0	0	0	0	0	1	0	1
A. sp.	Mandible	0	0	0	0	0	0	0	0	1	1
(n=1)											
Caementodon	Maxilla	0	0	0	0	1	0	0	0	0	1
C. sp.	Mandible	0	0	0	0	0	0	1	0	0	1
(n=2)	Total	0	0	0	0	1	0	1	0	0	2
Bugtirhinus	Maxilla	0	0	0	0	0	0	0	1	1	2
B. praecursors											
(n=2)											
Rhinoceros	Mandible	0	0	0	0	1	1	1	1	1	5
R. unicornis											
(n=5)											

Table 3.14 **Fossil Rhinocerotidae dental sample (**without EH**) by genus, jaw and tooth**
PUPC (Punjab University Paleontology Collection), Zoology Department, Punjab University, Lahore, Pakistan

Taxon	Jaw	I	d1	d2	d3	d4	p1	p2	p3	p4	m1	m2	m3	Total
Rhinoceros														
R. sondaicus	Maxilla	0	0	0	0	0	0	2	2	1	2	1	1	9
(n=16)	Mandible	0	0	0	0	0	0	0	0	1	2	2	2	7
	Total	0	0	0	0	0	0	2	2	2	4	3	3	16
R. unicornis	Mandible	0	0	0	0	0	0	0	1	2	2	1	1	7
(n=7)														
R. sivalensis	Maxilla	0	0	0	0	0	1	1	1	1	1	1	1	7
(n=7)														
R. sp.	Maxilla	0	0	0	0	0	0	0	0	0	1	0	0	1
(n=1)														
Punjabitherium														
P. platyrhinus	Maxilla	0	0	0	0	0	0	0	1	0	1	0	0	2
(n=6)	Mandible	0	0	0	0	0	0	0	0	1	1	1	1	4
	Total	0	0	0	0	0	0	0	1	1	2	1	1	6
Gaindatherium														
G. browni	Maxilla	0	0	0	0	0	1	1	1	1	2	0	2	8
(n=11)	Mandible	0	0	1	0	0	0	1	0	0	0	0	1	3
	Total	0	0	1	0	0	1	2	1	1	2	0	3	11
G. sp.	Maxilla	0	0	0	0	0	0	0	0	1	0	0	0	1
(n=2)	Mandible	0	0	0	0	0	0	0	0	0	0	1	0	1
	Total	0	0	0	0	0	0	0	0	1	0	1	0	2
Brachypotherium														
B. perimense	Maxilla	0	0	0	0	0	3	0	0	3	3	4	4	17
(n=32)	Mandible	0	0	0	0	0	0	0	5	2	2	3	3	15
	Total	0	0	0	0	0	3	0	5	5	5	7	7	32
Chilotherium														
C. *intermedium*	Maxilla	0	0	0	0	0	0	0	2	1	1	1	1	6
(n=18)	Mandible	0	0	0	1	0	0	1	2	2	3	1	2	12
	Total	0	0	0	1	0	0	1	4	3	4	2	3	18
Alicornops														
A. complanatum	Maxilla	0	0	0	0	0	0	1	1	1	1	0	0	4
(n=15)	Mandible	0	2	0	0	0	0	0	2	3	3	1	0	11
	Total	0	2	0	0	0	0	1	3	4	4	1	0	15
A. laogouense	Maxilla	0	0	0	0	0	0	0	1	1	1	1	1	5
(n=7)	Mandible	0	0	0	0	0	0	0	0	1	1	0	0	2
	Total	0	0	0	0	0	0	0	1	2	2	1	1	7
A. sp.														
(n=1)	Maxilla	1	0	0	0	0	0	0	0	0	0	0	0	1
Brachypotherium														
B. fatehjangense	Maxilla	0	0	0	0	1	0	2	0	0	2	0	0	5
(n=7)	Mandible	0	0	0	0	0	0	0	0	0	0	1	1	2
	Total	0	0	0	0	1	0	2	0	0	2	1	1	7
Caementodon														
C. sp.	Maxilla	1	0	0	0	0	0	2	1	1	0	0	0	5
(n=9)	Mandible	1	0	0	0	0	0	0	0	0	0	2	1	4
	Total	2	0	0	0	0	0	2	1	1	0	2	1	9

Table 3.15 **Fossil Rhinocerotidae dental sample (**without EH**) by genus, jaw and tooth**
MNHN (Muséum National d'Histoire Naturelle), Paris, France

Taxon	Jaw	i	d3	p1	p2	p3	p4	m1	m2	m3	Total
Brachypotherium											
B. perimense (n=4)	Maxilla	0	0	0	1	1	0	1	1	0	4
B. fatehjangense (n=1)	Mandible	0	1	0	0	0	0	0	0	0	1
B. sp. (n=1)	Maxilla	1	0	0	0	0	0	0	0	0	1
Alicornops											
Alicornops sp.	Maxilla	0	0	0	0	2	1	0	0	3	6
(n=9)	Mandible	0	0	0	0	0	0	1	1	1	3
		0	0	0	0	2	1	1	1	4	9
Gaindatherium											
G. sp. (n=2)	Maxilla	0	0	0	1	1	0	0	0	0	2
Rhinoceros											
R. aff. *sondaicus* (n=1)	Maxilla	0	0	1	0	0	0	0	0	0	1
Rhinocerotinae indet (n=1)	Maxilla	1	0	0	0	0	0	0	0	0	1

Table 3.16 **Fossil Rhinocerotidae dental sample (**without EH**) by genus, jaw and tooth**
MHNT (Museum d' Histoire Naturelle), Toulouse, France

Taxon	Jaw	d1	d2	d3	d4	p1	p2	p3	p4	m1	m2	m3	Total
Gaindatherium													
G. cf. *browni*	Maxilla	0	0	0	0	0	0	0	1	0	0	0	1
(n= 3)	Mandible	0	0	0	0	0	0	0	0	2	0	0	2
	Total	0	0	0	0	0	0	0	1	2	0	0	3
Prosantorhinus													
P. shahbazi	Maxilla	0	0	0	0	0	1	0	0	2	1	0	4
(n=6)	Mandible	0	0	0	0	0	0	0	0	0	0	2	2
	Total	0	0	0	0	0	1	0	0	2	1	2	6
Plesiaceratherium													
P. naricum	Maxilla	0	0	0	0	0	0	0	0	0	1	1	2
(n=6)	Mandible	0	0	0	0	0	1	1	0	0	2	0	4
	Total	0	0	0	0	0	1	1	0	0	3	1	6
Mesaceratherium													
M. welcommi	Maxilla	0	0	0	0	0	3	3	1	1	1	0	9
(n=21)	Mandible	0	0	0	0	0	0	1	2	4	2	3	12
	Total	0	0	0	0	0	3	4	3	5	3	3	21
Pleuroceros													
P. blanfordi	Maxilla	0	0	0	0	0	3	5	4	3	2	3	20
(n=38)	Mandible	0	1	1	1	0	2	1	3	2	4	3	18
	Total	0	1	1	1	0	5	6	7	5	6	6	38
Brachypotherium													
B. fatehjangense	Maxilla	0	0	0	0	0	5	5	5	4	4	5	28
(n=53)	Mandible	0	0	3	1	0	3	3	3	3	3	6	25
	Total	0	0	3	1	0	8	8	8	7	7	11	53
B. ganense	Maxilla	0	0	0	0	0	0	2	0	1	0	0	3
(n=10)	Mandible	1	1	1	1	0	0	0	0	1	1	1	7
	Total	1	1	1	1	0	0	2	0	2	1	1	10

Table 3.17 **Fossil Rhinocerotidae dental sample (**without EH**) by genus, jaw and tooth**
AMNH (American Museum of Natural History), New York, USA

Taxon	Jaw	i	d1	d2	d3	d4	p1	p2	p3	p4	m1	m2	m3	Total
Rhinoceros														
R. sivalensis	Maxilla	0	0	0	0	0	0	0	0	0	1	0	0	1
(n= 1)														
R. sp.	Maxilla	1	0	0	0	0	0	0	0	0	2	1	3	7
(n= 10)	Mandible	0	0	0	0	0	0	0	0	0	0	1	2	3
	Total	1	0	0	0	0	0	0	0	0	2	2	5	10
Gaindatherium														
G. browni	Maxilla	1	0	0	0	0	1	2	2	1	3	3	2	15
(n= 31)	Mandible	2	0	0	0	0	1	1	3	2	1	3	3	16
	Total	3	0	0	0	0	2	3	5	3	4	6	5	31
Chilotherium														
C. blanfordi	Maxilla	2	0	0	0	0	1	0	1	0	4	2	2	12
(n= 28)	Mandible	0	0	0	0	0	1	1	2	2	4	3	3	16
	Total	2	0	0	0	0	2	1	3	2	8	5	5	28
C. intermedium	Maxilla	1	0	0	0	0	0	0	0	2	3	3	7	16
(n= 43)	Mandible	0	0	0	0	0	4	4	3	4	4	4	4	27
	Total	1	0	0	0	0	4	4	3	6	7	7	11	43
C. salinum	Maxilla	0	0	0	0	0	0	0	0	0	0	2	1	3
(n= 4)	Mandible	0	0	0	0	0	0	0	0	0	0	1	0	1
	Total	0	0	0	0	0	0	0	0	0	0	3	1	4
C. sp.	Maxilla	0	0	0	0	0	0	0	0	0	1	1	1	3
(n= 8)	Mandible	0	0	0	0	0	0	0	1	1	1	1	1	5
	Total	0	0	0	0	0	0	0	1	1	2	2	2	8
Rhinocerotidae														
(n=18)	Maxilla	1	0	0	1	1	0	0	1	0	1	2	2	9
	Mandible	0	0	0	0	0	0	0	0	1	2	4	2	9
	Total	1	0	0	1	1	0	0	1	1	3	6	4	18

Table 3.18 **Fossil Rhinocerotidae dental sample (**without EH**) by genus, jaw and tooth**
PMHU (Peabody Museum Harvard University), USA
(Harvard – GSP Collection)

Taxon	Jaw	i	d1	d2	d3	d4	p1	p2	p3	p4	m1	m2	m3	Total
Rhinoceros														
R. sivalensis (n= 2)	Maxilla	0	0	0	0	0	0	0	2	0	0	0	0	2
Gaindatherium														
G. browni	Maxilla	0	0	0	0	1	0	1	2	1	3	1	2	11
(n= 20)	Mandible	0	0	0	0	0	0	0	3	1	1	2	2	9
	Total	0	0	0	0	1	0	1	5	2	4	3	4	20
G. vidali	Maxilla	0	0	0	0	0	0	0	0	0	1	1	1	3
(n= 4)	Mandible	0	0	0	0	0	0	1	0	0	0	0	0	1
	Total	0	0	0	0	0	0	1	0	0	1	1	1	4
G. sp.	Maxilla	0	2	1	0	0	1	3	3	0	1	0	0	11
(n= 29)	Mandible	0	1	2	3	1	0	1	1	0	6	2	1	18
	Total	0	3	3	3	1	1	4	4	0	7	2	1	29
Rhinocerotina														
(n= 2)	Maxilla	0	0	0	0	1	0	0	0	0	0	0	0	1
	Mandible	0	0	0	0	0	0	0	0	0	1	0	0	1
	Total	0	0	0	0	1	0	0	0	0	1	0	0	2
Rhinocerotidae														
(n= 39)	Maxilla	0	4	0	0	0	4	0	0	0	10	0	0	18
	Mandible	4	0	1	1	0	2	1	1	1	9	1	0	21
	Total	4	4	1	1	0	6	1	1	1	19	1	0	39

Table 3.19 Fossil Rhinocerotidae dental sample (without EH**) by genus, jaw and tooth**
YPNHM (Yale Peabody Natural History Museum), New Heaven, USA (Siwalik Collection)

Taxon	Jaw	Molars
Rhinoceros indet.		
(Siwalik Collection)	Mandible	26
	Maxilla	35
	Total	61

Table 3.20 Fossil Rhinocerotidae dental sample (without EH**) by genus, Jaw and tooth**
NHM (Natural History Museum) Paleontology Department (Siwalik Collection), London, UK

Taxon	Jaw	i	c	p1	p2	p3	p4	m1	m2	m3	Total
Rhinoceros											
R. sivalensis	Maxilla	0	0	0	1	2	4	4	4	4	19
(n= 19)											
R. plaeindicus	Maxilla	0	0	1	3	3	6	12	11	10	46
(n=69)	Mandible	2	2	2	2	1	4	4	3	3	23
	Total	2	2	3	5	4	10	16	14	13	69
R. sp.	Maxilla	1	0	0	3	4	4	5	4	2	23
(n= 38)	Mandible	0	0	0	0	0	2	5	4	4	15
	Total	1	0	0	3	4	6	10	8	6	38
Punjabitherium											
P. platyrhinus	Maxilla	0	0	0	0	1	1	1	1	1	5
(n= 5)											

Table 3.21 Recent Rhinocerotidae dental sample (without EH**) by genus, jaw and tooth**
MNHN (Muséum National d' Histoire Naturelle), Paris, France
(Laboratoires de Paléontologie et d 'Anatomie Comparée)

Taxon	Jaw	i	c	p1	p2	p3	p4	m1	m2	m3	Total
Diceros											
D. bicornis	Maxilla	0	0	9	13	15	15	16	16	18	102
(n= 241)	Mandible	2	2	10	20	24	24	23	23	11	139
	Total	2	2	19	33	39	39	39	39	29	241
Ceratotherium											
C. simum	Maxilla	0	0	0	4	4	4	4	4	4	24
(n= 36)	Mandible	0	0	2	2	2	2	2	2	0	12
	Total	0	0	2	6	6	6	6	6	4	36
Rhinoceros											
R.sondaicus	Maxilla	0	4	9	12	10	8	12	11	9	75
(n= 141)	Mandible	0	8	6	10	10	10	10	10	2	66
	Total	0	12	15	22	20	18	22	21	11	141
R. unicornis	Maxilla	0	4	5	7	5	7	7	7	4	46
(n= 99)	Mandible	2	4	3	8	8	8	8	8	4	53
	Total	2	8	8	15	13	15	15	15	8	99

Table 3.22 Recent Rhinocerotidae dental sample (without EH**) by genus, jaw and tooth**
Museum of Comparative Zoology (MCZ), Mammalogy Department, Harvard University, Cambridge (MA), USA

Taxon	Jaw	i	c	p1	p2	p3	p4	m1	m2	m3	Total
Diceros											
D. bicornis	Maxilla	0	0	8	12	12	12	12	12	10	78
(n= 126)	Mandible	0	0	2	8	8	8	8	8	6	48
	Total	0	0	10	20	20	20	20	20	16	126
Ceratotherium											
C. simum	Maxilla	0	0	0	4	4	4	4	4	2	22
(n= 44)	Mandible	0	0	0	4	4	4	4	4	2	22
	Total	0	0	0	8	8	8	8	8	4	44
Rhinoceros											
R.sondaicus	Maxilla	0	0	2	2	2	2	2	2	2	14
(n= 26)	Mandible	0	0	2	2	2	2	2	2	0	12
	Total	0	0	4	4	4	4	4	4	2	26
R. unicornis	Maxilla	6	4	2	8	10	10	10	10	4	64
(n= 119)	Mandible	5	2	4	8	8	8	8	8	4	55
	Total	11	6	6	16	18	18	18	18	8	119
Dicerorhinus											
D. sumatrensis	Maxilla	0	0	2	2	2	2	2	2	0	12
(n= 24)	Mandible	0	0	2	2	2	2	2	2	0	12
	Total	0	0	4	4	4	4	4	4	0	24

Chapter – 4

ENAMEL HYPOPLASIA IN SIWALIK RHINOCEROTIDS

4.1 Enamel Hypoplasia in Siwaliks Rhinocerotids

A total of 846 Rhinocerotid fossil teeth were examined for the presence of Enamel Hypoplasia (EH). These Siwaliks Rhinocerotidae materials are housed at the paleontological collections of GSP, PMNH, PUPC, MNHN, MHNT, AMNH, PMHU, YPNHM and NHM.

After careful examination of the teeth, the description of each defect, its position on the tooth crown and the position of the defected tooth in each jaw were recorded. All teeth with enamel defects (linear enamel horizontal - LEH and semi circular enamel depression - SEH) were measured for position of each defect on the tooth crown heights from the root-crown junctions. Linear horizontal and semi-circular defects on both lingual and buccal surfaces were noted down and the position of the defected tooth in each jaw was also recorded. Most of the teeth have more than one linear defect and a maximum number of 7 linear defects were found on any one tooth (Figure 4.7).

Family	Rhinocerotidae OWEN, 1848
Subfamily	Rhinocerotinae OWEN, 1845
Tribe	Teleoceratini HAY, 1885
Genus	*Brachypotherium* ROGER, 1904

Brachypotherium fatehjangense

Material studied: 71 teeth specimens were studied for Enamel Hypoplasia from Siwalik collection housed at PMNH (Table 3.13), PUPC (Table 3.4 and 3.14), MNHN (Table 3.5 and 3.15), MHNT (Table 3.6 and 3.16) and YPNHM (Table 3.9).

Description: Enamel Hypoplasia recorded on five Rhino teeth (Table 4.1) which are:

1. Specimen No. 15400 MNHN. Enamel Hypoplasia recorded on hypoconid of dp4 tooth of left mandible. One linear horizontal enamel depression present at 7 mm above the neck on the buccal side (Figure 4.1).
2. Specimen No. Pak 1069 MHNT. Enamel Hypoplasia recorded on hypoconid of m1 tooth of right mandible. One linear horizontal enamel depression present at 13 mm above the neck on the buccal side (Figure 4.2*)*.
3. Specimen No. PUPC 07/170. Enamel Hypoplasia recorded on protocone of P4 tooth of left maxilla. Two semi-circle enamel depressions present at 5 and 7 mm above the neck on the lingual side (Figure 4.3).
4. Specimen No. PUPC 07/173. Enamel Hypoplasia recorded on protocone of DP4 tooth of left maxilla. Three semi-circle enamel depressions present at 5, 7 and 11 mm above the neck on the lingual side (Figure 4.4).
5. Specimen No. YPM VP 049762. Enamel Hypoplasia recorded on ectoconid of m2 tooth of left mandible. One linear horizontal enamel depression present at 15 mm above the neck on the lingual side (Figure 4.5).

Table 4.1 Comparative measurements of Enamel Hypoplasia in *Brachypotherium fatehjangense.*

No.	**Taxon/ Specimen**	**Enamel Hypoplasia**			**Age (**Myr**)**
		Tooth	**Cusps**	**Location**	
1 F-4	*B. fatehjangense* MNHN, (15400)	dp4	Hypoconid	One LEH 7 mm above the neck	8.468- 8.525
2 F-8	*B. fatehjangense* MHNT, (Pak 1069)	m1	Hypoconid	One LEH 13 mm above the neck	22.5
3 Z-3	*B. fatehjangense* PUPC (07/170)	P4	Protocone	Two SEH 5 and 7 mm above the neck	11.2-10.1
4 Z-7	*B. fatehjangense* PUPC (07/173)	DP4	Protocone	Three SEH 5, 7 and 11 mm above the neck	11.2-10.1
5 Y-1	*B. fatehjangense* YPM VP (049762)	m2	Ectoconid	One LEH 15 mm above the neck	6-7

Figure 4.1 (F-4): *Brachypotherium fatehjangense,* 15400 MNHN.
One LEH, 7 mm above the neck on the buccal side of dp4; scale x 2 of natural size.

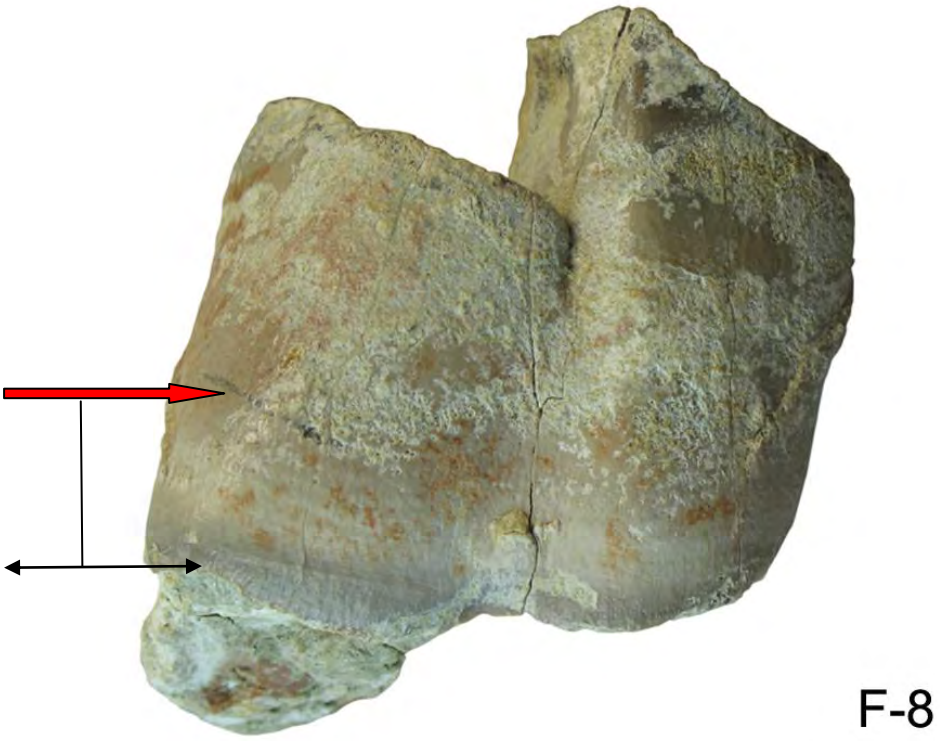

Figure 4.2 (F-8): *Brachypotherium fatehjangense,* Pak 1069 MHNT.
One LEH, 13 mm above the neck on the buccal side of m1; scale x 2 of natural size.

Figure 4.3 (Z-3): *Brachypotherium fatehjangense,* PUPC 07/170. Two SEH, 5 and 7 mm above the neck on the lingual side of P4; scale x 2 of natural size.

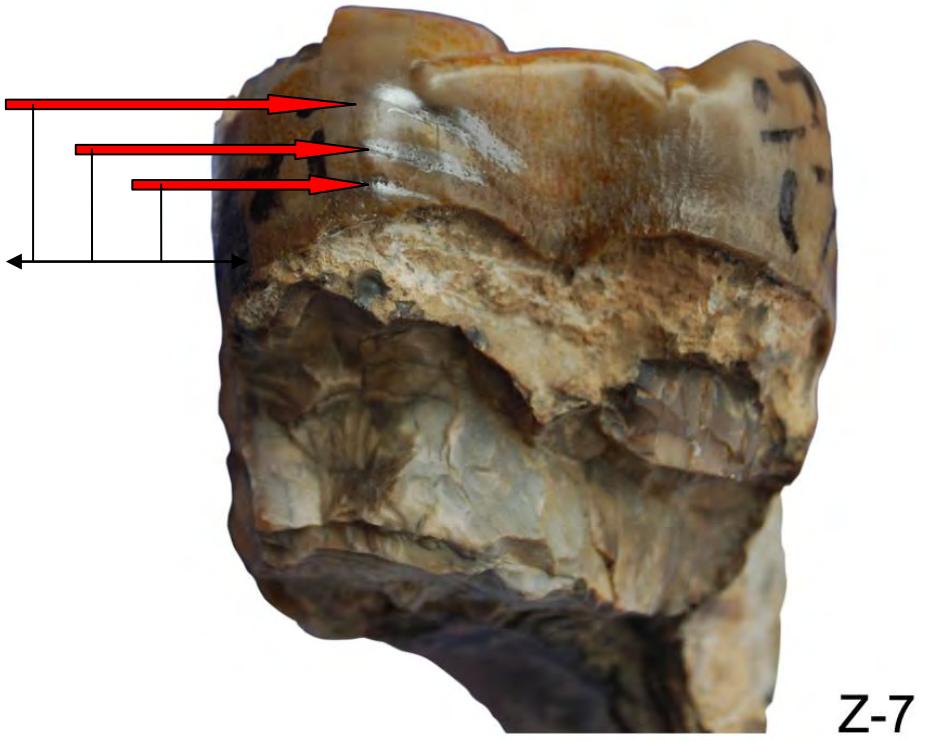

Figure 4.4 (Z-7): *Brachypotherium fatehjangense,* PUPC 07/173.
Three SEH, 5, 7 and 11mm above the neck on the lingual side of DP4; scale x 2 of natural size.

Figure 4.5 (Y-1): *Brachypotherium fatehjangense,* YPM VP 049762.
One LEH, 15 mm above the neck on the lingual side of m2; scale x 3 of natural size.

Brachypotherium perimense

Material studied: 53 teeth specimens were studied for Enamel Hypoplasia from Siwalik collection housed at GSP (Table 3.12), PMNH (Table 3.13), PUPC (Table 3.4 and 3.14), MNHN (Table 3.15) and PMHU (Table 3.8).

Description: Enamel Hypoplasia recorded on eight Rhino teeth (Table 4.2) which are:

1. Specimen No. PUPC (07/74). Enamel Hypoplasia recorded on metaconid and entoconid of p2 tooth of right mandible. On metaconid one linear horizontal enamel depression presents at 15 mm above the neck, whereas, on entoconid two linear enamel depression present at 15 and 20 mm above the neck on the lingual side (Figure 4.6).
2. Specimen No. PUPC (07/152). Enamel Hypoplasia recorded on hypocone and protocone of DP4 tooth of right Maxilla. On hypocone three linear horizontal enamel depression present at 7, 10 and 17 mm above the neck, whereas, on protocone four linear horizontal enamel depression present at 9, 14, 17 and 22 mm above the neck on the lingual side (Figure 4.7).
3. Specimen No. PUPC (07/126). Enamel Hypoplasia recorded on hypocone of P2 tooth of right maxilla. One semi circle enamel depression present at 8 mm above the neck on the lingual side (Figure 4.8).
4. Specimen No. PUPC (68/826). Enamel Hypoplasia recorded on protocone of M3 tooth of left maxilla. One linear horizontal enamel depression present at 15 mm above the neck on the lingual side (Figure 4.9).
5. Specimen No. PUPC (07/54). Enamel Hypoplasia recorded on p3 and m1 teeth of right mandible. Two linear horizontal enamel depressions present at 10 and 20 mm above the neck on hypoconid of p3. Whereas, on m1 EH recorded on protoconid and hypoconid. On protoconid one linear horizontal enamel depression, present at 8 mm above the neck while on hypoconid two linear horizontal enamel depressions present 10 and 15 mm above the neck on the buccal side (Figure 4.10).
6. Specimen No. PUPC (68/529). Enamel Hypoplasia recorded on ecto-metaloph of M3 tooth of left maxilla. One semi circle enamel depression present at 18 mm above the neck on the lingual side (Figure 4.11).
7. Specimen No. PMHU (Y 53615). Enamel Hypoplasia recorded on paraconid of dp3 tooth of left mandible. One linear horizontal enamel depression present at 10 mm above the neck on the buccal side (Figure 4.12).

Table 4.2 Comparative measurements of Enamel Hypoplasia in *Brachypotherium perimense.*

No.	**Taxon/ Specimen**	**Enamel Hypoplasia**			**Age (**Myr**)**
		Tooth	**Cusps**	**Location**	
1 Z-4	*B. perimense* PUPC (07/74)	p2	Metaconid and Entoconid	One LEH 15 mm above the neck. Two LEH 15 and 20 mm above the neck	12.6-11.2
2 Z-5	*B. perimense* PUPC (07/152)	DP4	Hypocone and Protocone	Three LEH 7, 10 and 17 mm above the neck Four LEH 9, 14, 17 and 22 mm above the neck	12.6-11.2
3 Z-6	*B. perimense* PUPC (07/126)	P2	Hypocone	One SEH 8 mm above the neck	12.6-11.2
4 Z-13	*B. perimense* PUPC (68/826)	M3	Protocone	One LEH 15 mm above the neck	12.6-11.2
5 Z-10	*B. perimense* PUPC (07/54)	p3 and m1	Hypoconid Protoconid	Two LEH 10 and 20 mm above the neck One LEH	11-10

			and Hypoconid	8 mm above the neck Two LEH 10 and 15 mm above the neck	
6 Z-14	*B. perimense* PUPC (68/529)	M3	Ecto- Metaloph	One SEH 18 mm above the neck	12.6-11.5
7 H-2	*B. perimense* PMHU (Y 53615)	dp3	Paraconid	One LEH 10 mm above the neck	10.017-10.091

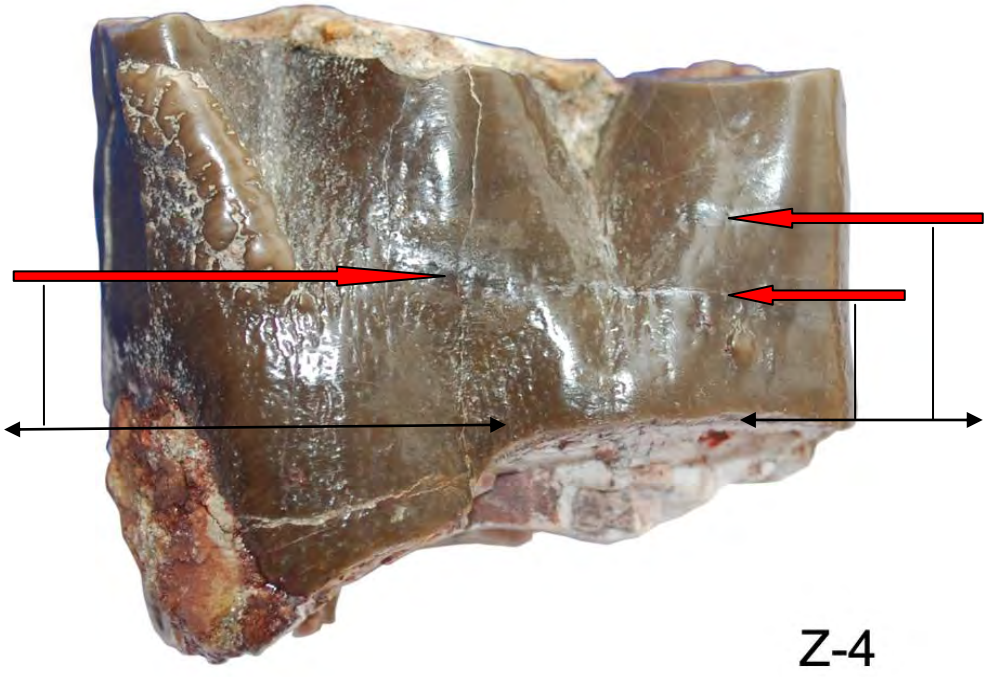

Figure 4.6 (Z-4):*Brachypotherium perimense,* PUPC 07/74. Three LEH, 15 mm and 15, 20 mm above the neck on the lingual side of p2; scale x 1.25 of natural size.

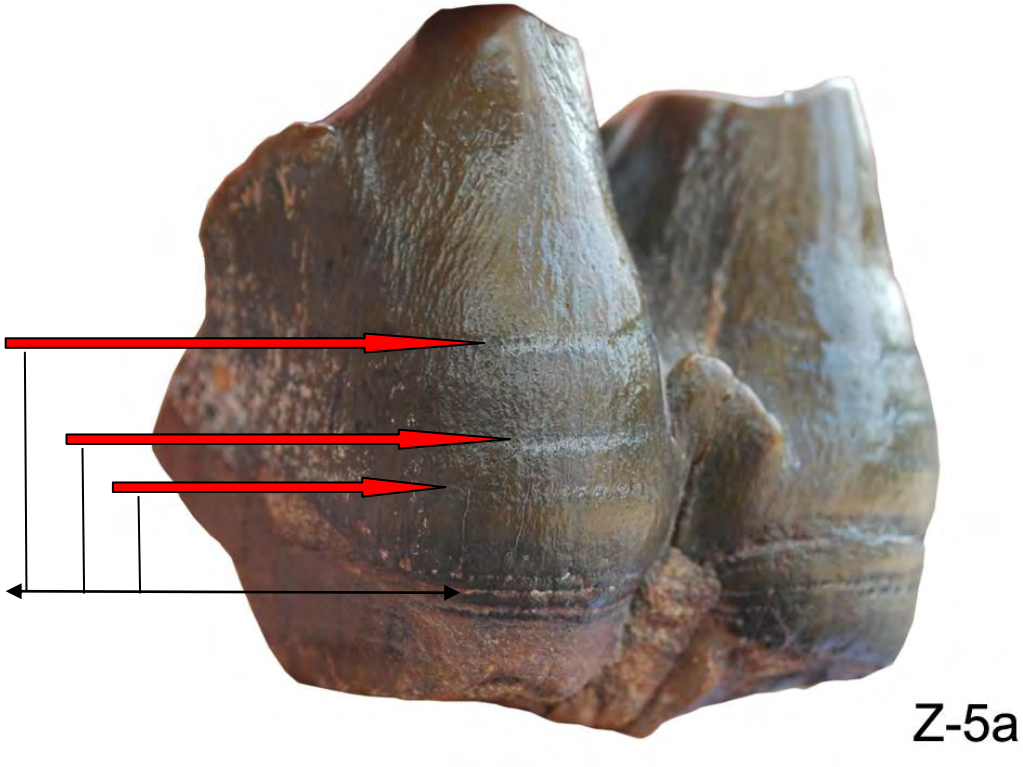

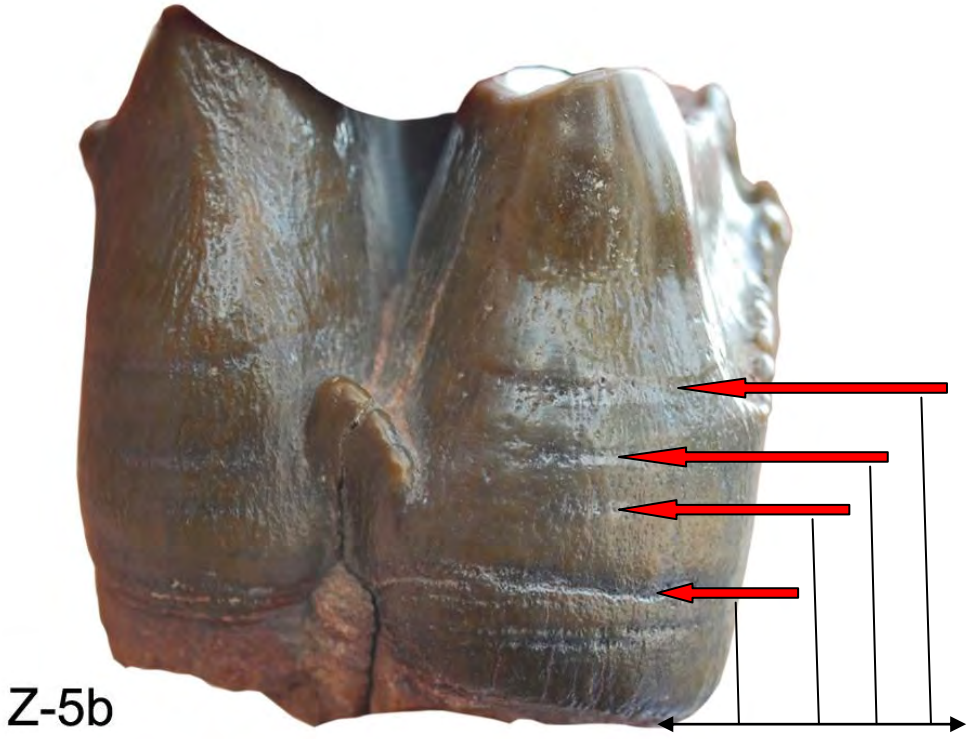

Figure 4.7 (Z-5a,b): *Brachypotherium perimense,* PUPC 07/152. (a) Three LEH, 7, 10,17 mm and (b) Four LEH, 9, 14, 17, 22 mm above the neck on the lingual side of DP4; scale x 2 of natural size.

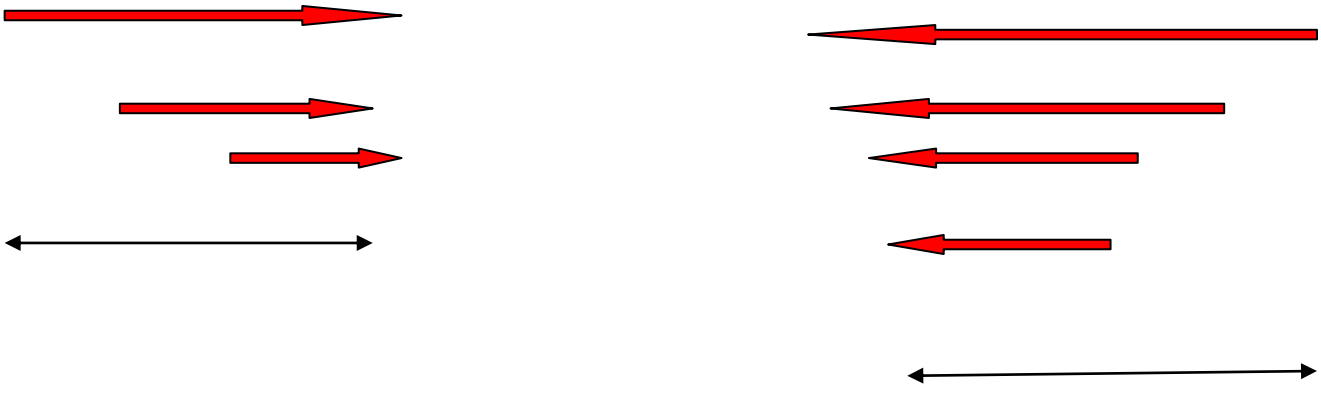

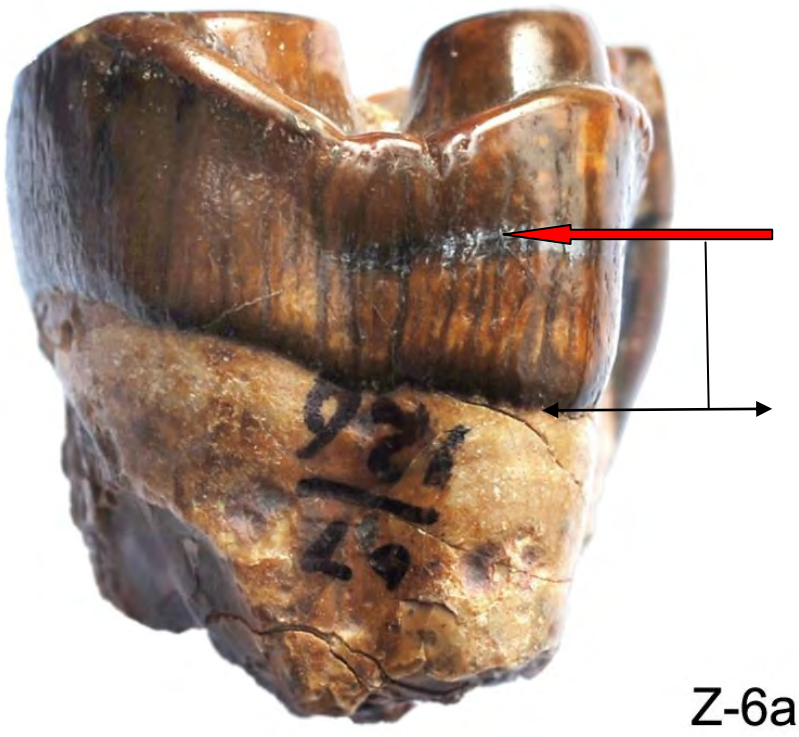

Figure 4.8 (Z-6a): *Brachypotherium perimense,* PUPC 07/126. One SEH, 8 mm above the neck on the lingual side of P2; scale x 3 of natural size.

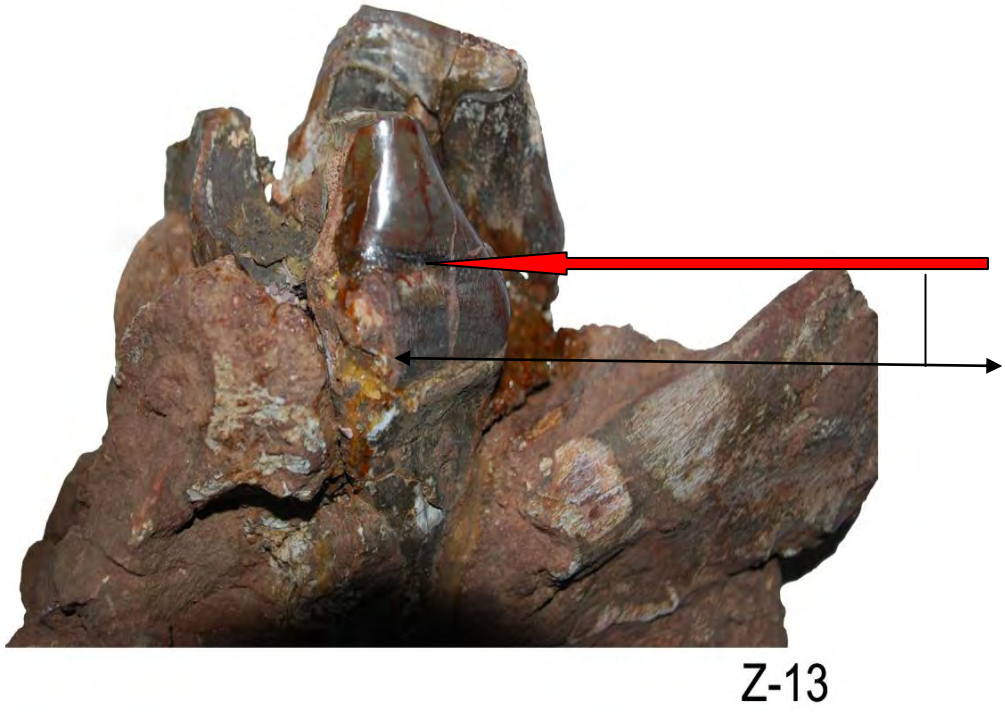

Figure 4.9 (Z-13): *Brachypotherium perimense,* PUPC 68/826.
One LEH, 15 mm above the neck on the lingual side of M3; natural size.

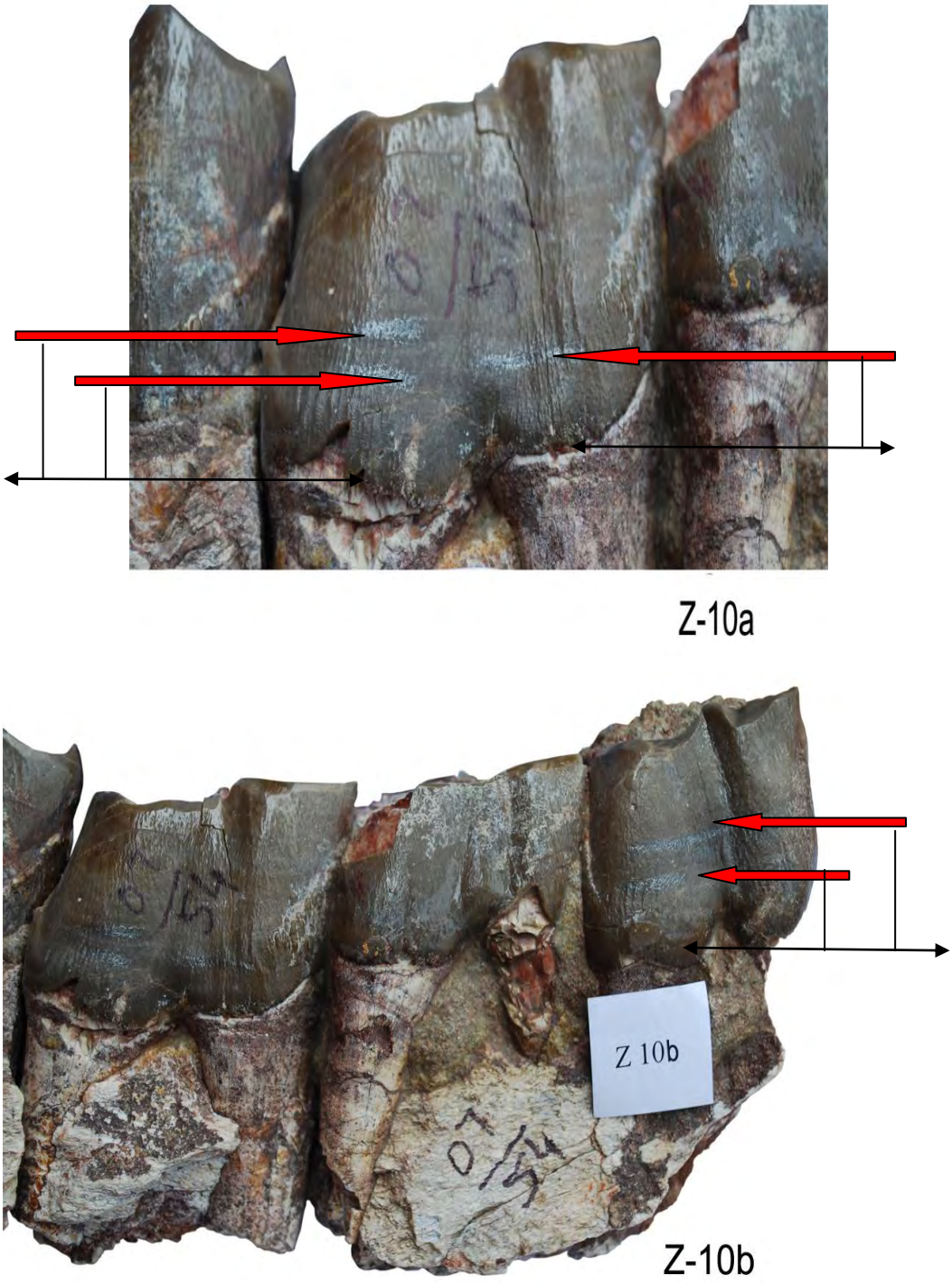

Figure 4.10 (Z-10a,b): *Brachypotherium perimense,* PUPC 07/54.
(a) Three LEH, 8 mm and 10, 15 mm, above the neck on the buccal side of m1, scale x 1.5 of natural size, (b) Two LEH, 10, 20 mm above the neck on the buccal side of p3; almost natural size.

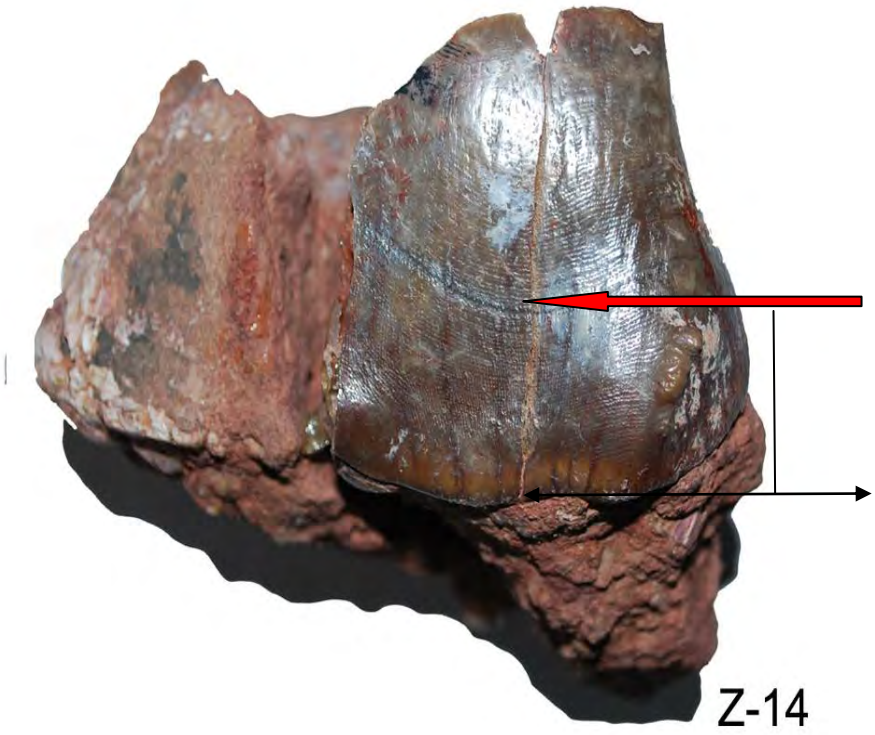

Figure 4.11 (Z-14): *Brachypotherium perimense,* PUPC 68/529. One SEH, 18 mm above the neck on the lingual side of M3; scale x 1.4 of natural size.

Figure 4.12 (H-2): *Brachypotherium perimense,* Y 53615. One LEH, 10 mm above the neck on the buccal side of dp3; scale x 3 of natural size.

Pleuroceros blanfordi

Material studied: 40 teeth specimens were studied for Enamel Hypoplasia from Siwalik collection housed in MHNT (Table 3.6 and 3.16).

Description: Enamel Hypoplasia recorded on two Rhino teeth (Table 4.3) which are:

1. Specimen No. MHNT (Pak 1031). Enamel Hypoplasia recorded on protocone of P2 tooth of left maxilla. One linear horizontal enamel depression present at 11 mm above the neck on the lingual side (Figure 4.13).
2. Specimen No. MHNT (Pak 46 D). Enamel Hypoplasia recorded on protocone of M1 tooth of left maxilla. One linear horizontal enamel depression present at 5 mm above the neck on the lingual side (Figure 4.14).

Table 4.3 Comparative measurements of Enamel Hypoplasia in *Pleuroceros blanfordi.*

No.	**Taxon/ Specimen**	**Enamel Hypoplasia**			**Age (**Myr**)**
		Tooth	**Cusps**	**Location**	
1 F-6	*P. blanfordi* MHNT (Pak 1031)	P2	Protocone	One LEH 11 mm above the neck	22.5
2 F-7	*P. blanfordi* MHNT (Pak 46 D)	M1	Protocone	One LEH 5 mm above the neck	22.5-18.7

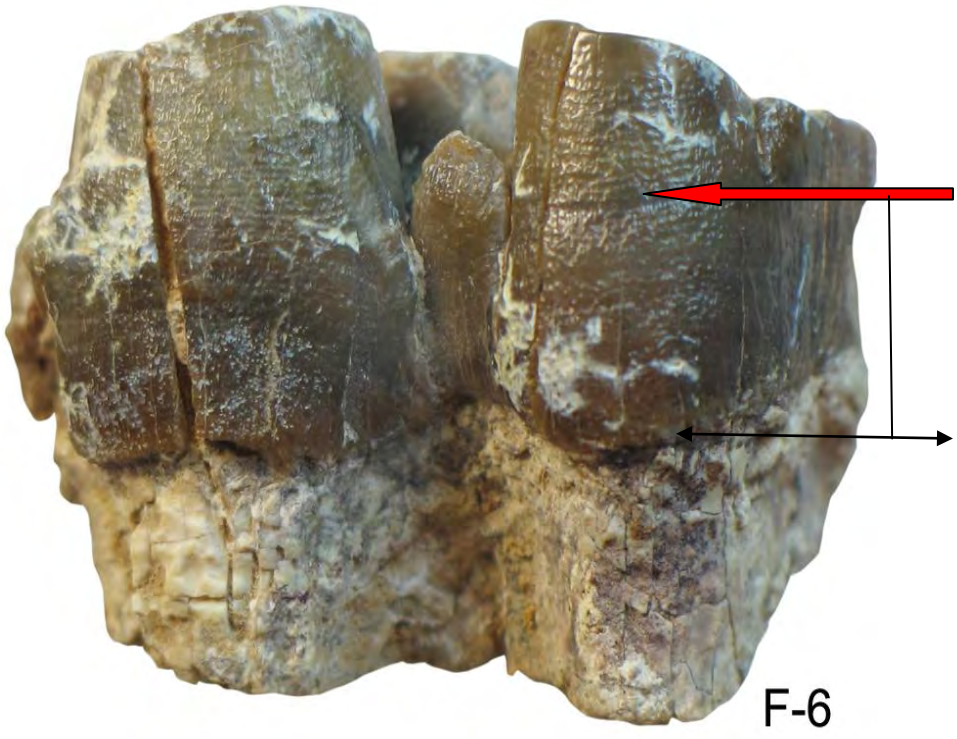

Figure 4.13 (F-6): *Pleuroceros blanfordi,* Pak 1031.
One, LEH 11 mm above the neck on the lingual side of P2;
scale x 3 of natural size.

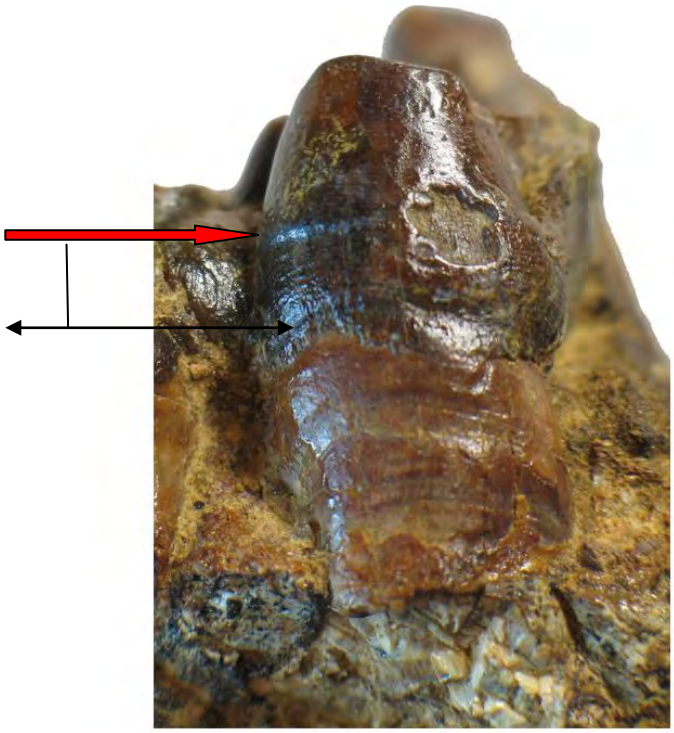

Figure 4.14 (F-7): *Pleuroceros blanfordi,* Pak 46 D. One LEH, 5 mm above the neck on the lingual side of M1; scale x 2 of natural size.

Mesaceratherium welcommi

Material studied: 22 teeth specimens were studied for Enamel Hypoplasia from Siwalik collection housed in MHNT (Table 3.6 and 3.16).

Description: Enamel Hypoplasia recorded on one Rhino tooth (Table 4.4) which is:

1. Specimen No. MHNT (Pak 1032b). Enamel Hypoplasia recorded on protocone and Metaloph of M3 tooth of right maxilla. On protocone two linear horizontal enamel depression present at 9 and 16 mm above the neck, whereas, on metaloph three linear horizontal enamel depression present at 14, 15 and 16 mm above the neck on the lingual side (Figure 4.15).

Table 4.4 Comparative measurements of Enamel Hypoplasia in *Mesaceratherium welcommi.*

No.	**Taxon/ Specimen**	**Enamel Hypoplasia**			**Age (**Myr**)**
		Tooth	**Cusps**	**Location**	
1 F-9	*M. welcommi* MHNT (Pak 1032b)	M3	Protocone Metaloph	Two LEH 9 and 16 mm above the neck Three LEH 14, 15 and 16 mm above the neck	22.5-18.4

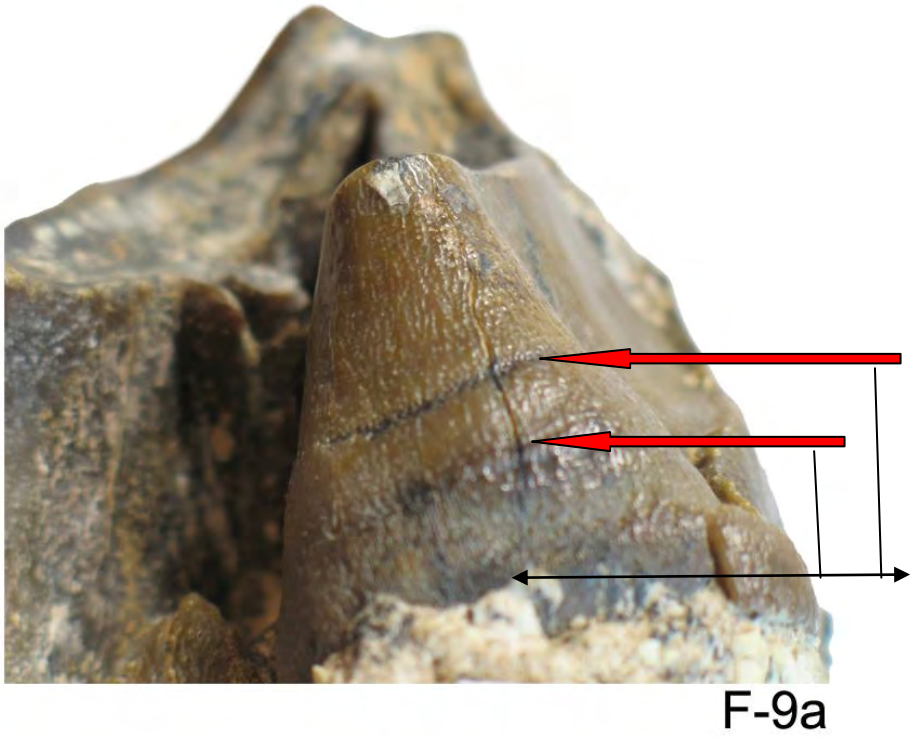

Figure 4.15 (F-9a): *Mesaceratherium welcommi,* Pak 1032b. Two LEH, 9, 16 mm on the protocone above the neck on the lingual side of M3; scale x 1.5 of natural size.

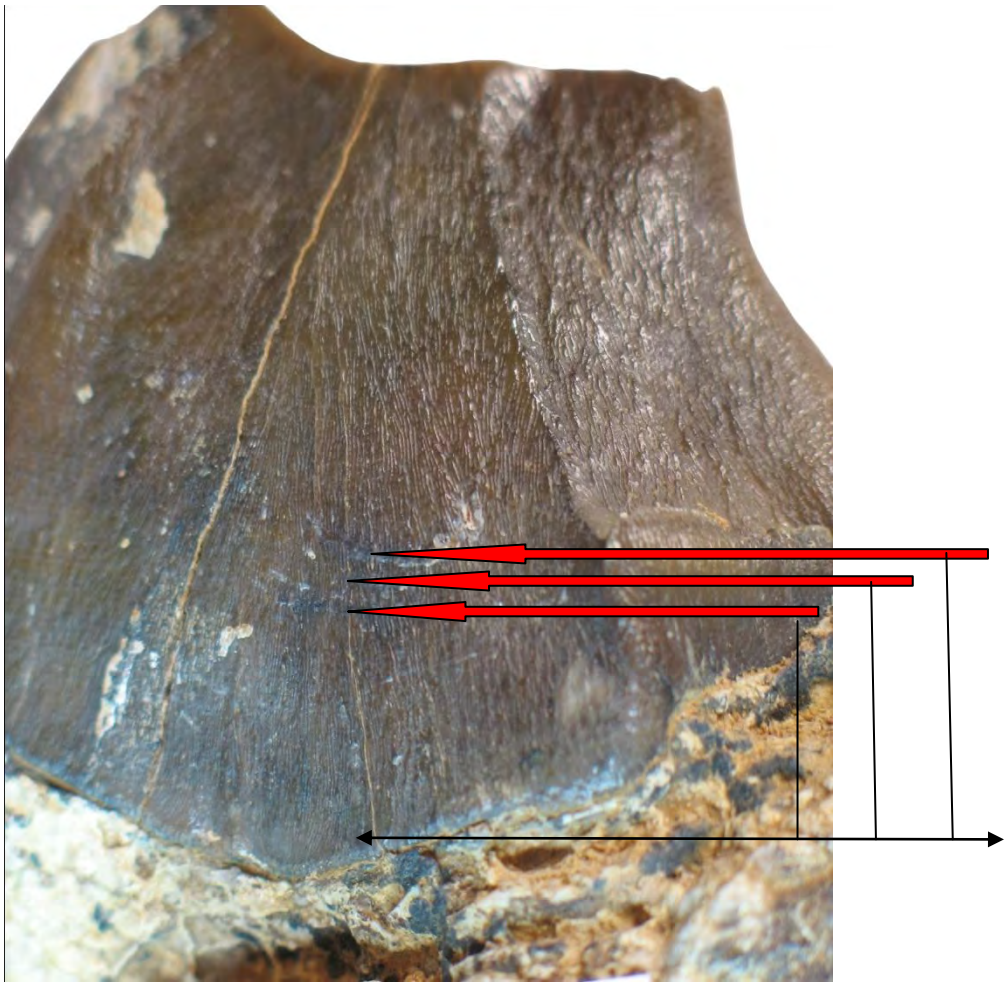

F-9b

Figure 4.15 (F-9b): *Mesaceratherium welcommi,* Pak 1032b.
Three LEH, 14, 15, 16 mm on metaloph above the neck on the lingual side of M3; scale x 2 of natural size.

Family Rhinocerotidae OWEN, 1848

Subfamily Rhinocerotinae OWEN, 1845

Sub-tribe Aceratheriina DOLLO, 1885

Genus *Alicornops* GINSBURG AND GUERIN, 1995

Alicornops complanatum

Material studied: 22 teeth specimens were studied for Enamel Hypoplasia from Siwalik collection housed at MHNT (Table 3.6), PUPC (Table 3.14) and PMNH (Table 3.13).

Description: Enamel Hypoplasia recorded on two Rhino teeth (Table 4.5) which are:

1. Specimen No. MHNT (Pak 1606). Enamel Hypoplasia recorded on p4 and m3 teeth of left mandible. Two linear horizontal enamel depressions present at 10 and 5 mm above the neck on paraconid and hypoconid of p4 respectively. Whereas, on m3 EH recorded on protoconid and one linear horizontal enamel depression present at 13 mm above the neck on the buccal side (Figure 4.16).

Table 4.5 Comparative measurements of Enamel Hypoplasia in *Alicornops complanatum.*

No.	**Taxon/ Specimen**	**Enamel Hypoplasia**			**Age (**Myr**)**
		Tooth	**Cusps**	**Location**	
1 F-1	*A. complanatum* MHNT (Pak 1606)	p4 and m3	Paraconid and Hypoconid Paraconid	One LEH 10 mm above the neck One LEH 5 mm above the neck One LEH 13 mm above the neck	9.4-6

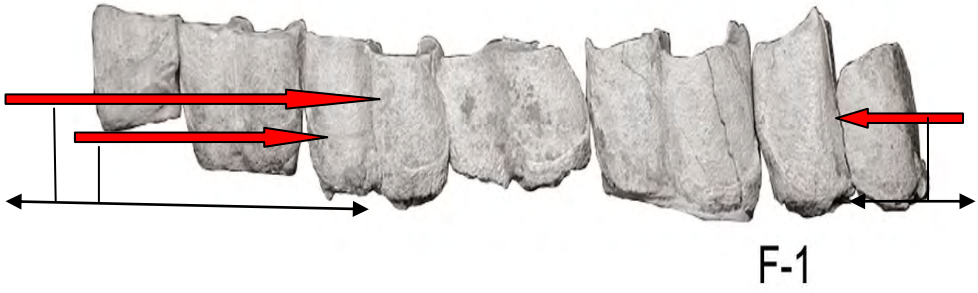

Figure 4.16 (F-1): *Alicornops complanatum,* Pak 1606.
Two LEH, 10 mm and 5 mm above the neck on the buccal side of p4 and one LEH, 13 mm above the neck on the buccal side of m3; scale x 1.3 of natural size.

Alicornops laogouense

Material studied: 12 teeth specimens were studied for Enamel Hypoplasia from Siwalik collection housed in PUPC (Table 3.4 and 3.14).

Description: Enamel Hypoplasia recorded on one Rhino tooth (Table 4.6) which is:

1. Specimen No. PUPC (07/47). Enamel Hypoplasia recorded on protocone and hypocone of M1 tooth of right maxilla. One linear horizontal enamel depression present at 14 mm and 12 mm above the neck on Protocone and Hypocone respectively on the lingual side (Figure 4.17).

Table 4.6 Comparative measurements of Enamel Hypoplasia in *Alicornops laogouense.*

No.	**Taxon/ Specimen**	**Enamel Hypoplasia**			**Age (**Myr**)**
		Tooth	**Cusps**	**Location**	
1 Z-1	*A. laogouense* PUPC (07/47)	M1	Protocone	One LEH 14 mm above the neck	17-14
			Hypocone	One LEH 12 mm above the neck	

Z-1a

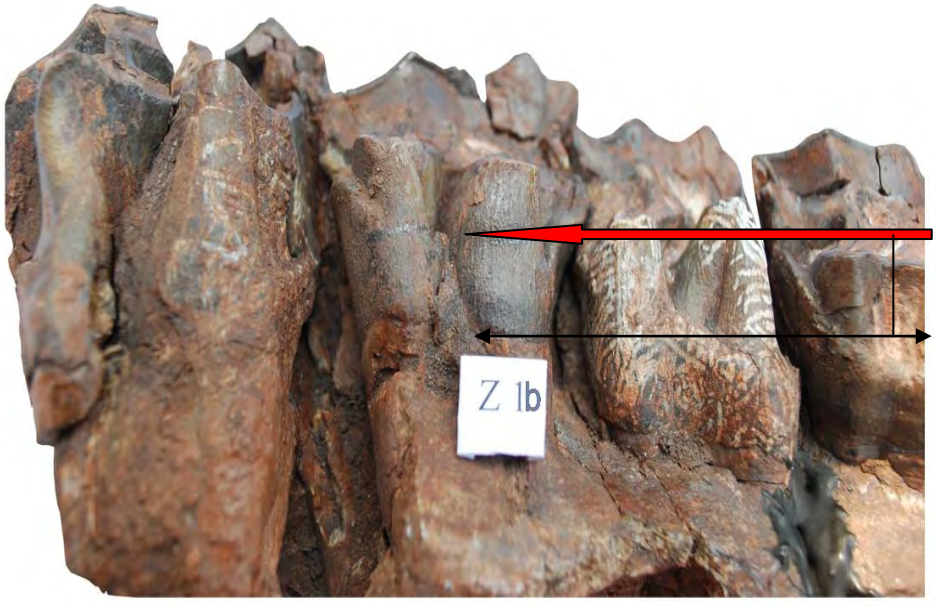

Z-1b

Figure 4.17 (Z-1a,b): *Alicornops laogouense,* PUPC 07/47.
Two LEH, (a) 12 mm and (b) 14mm above the neck on the lingual side of M1; natural size.

Family	Rhinocerotidae OWEN, 1848
Subfamily	Rhinocerotinae OWEN, 1845
Tribe	Rhinocerotini OWEN, 1845
Subtribe	Rhinocerotina OWEN, 1845
Genus	*Gaindatherium* COLBERT, 1934

Gaindatherium browni

Material studied: 76 teeth specimens were studied for Enamel Hypoplasia from Siwalik collection housed at PUPC (Table 3.4 and 3.14), PMNH (Table 3.3 and 3.13) and PMHU (Table 3.8 and 3.18).

Description: Enamel Hypoplasia recorded on four Rhino teeth (Table 4.7) which are:

1 Specimen No. PUPC (07/147). Enamel Hypoplasia recorded on protocone of P4 tooth of left maxilla. Two linear horizontal enamel depressions present at 5 and 9 mm above the neck on the lingual side (Figure 4.18).

2 Specimen No. PMNH (MUS-106). Enamel Hypoplasia recorded on protoconid and Hypoconid of p3 and p4 teeth of right mandible. On both protoconid and hypoconid of p3 one linear horizontal enamel depression is present at 10 and 11 mm above the neck, respectively. Same pattern is observed in p4 where one linear enamel depression is present at 8 and 7 mm above the neck on protoconid and hypoconid, respectively on the buccal side (Figure 4.19).

3 Specimen No. PMHU (Y 24067 b). Enamel Hypoplasia recorded on paraconid and hypoconid of m3 tooth of left mandible. One linear horizontal enamel depression present at 10 mm above the neck on both paraconid and hypoconid on the buccal side (Figure 4.20).

Table 4.7 Comparative measurements of Enamel Hypoplasia in *Gaindatherium browni.*

No.	**Taxon/ Specimen**	**Enamel Hypoplasia**			**Age (**Myr**)**
		Tooth	**Cusps**	**Location**	
1 Z-2	*G. browni* PUPC (07/147)	P4	Protocone	Two LEH 5 and 9 mm above the neck	14-9
2 P-1	*G .browni* PMNH (MUS-106)	p3 and	Protoconid	One LEH 10 mm above the neck	14-9
			Hypoconid	One LEH 11 mm above the neck	
		p4	Protoconid	One LEH 8 mm above the neck	
			Hypoconid	One LEH 7 mm above the neck	
3 H-1	*G. browni* PMHU (Y 24067 b)	m3	Paraconid and Hypoconid	One LEH, each 10 mm above the neck	12.289-12.341

Figure 4.18 (Z-2): *Gaindatherium browni,* PUPC 07/147. Two LEH, 5, 9 mm above the neck on the lingual side of P4; scale x 2 of natural size.

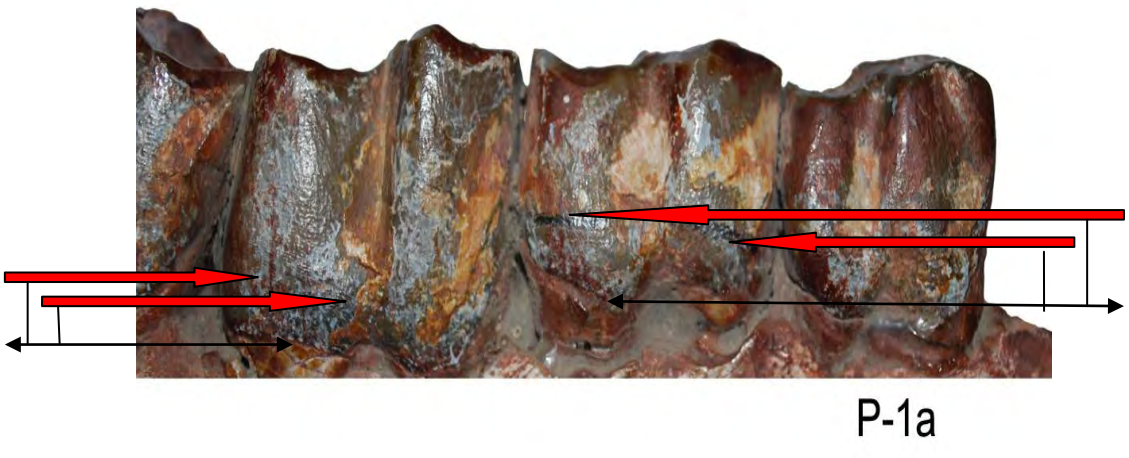

P-1b

Figure 4.19 (P-1a,b): *Gaindatherium browni,* MUS-106.
(a)Two LEH, 10 mm and 11 mm above the neck on the buccal side of p3 and two LEH, 7 mm and 8 mm above the neck on the buccal side of p4; natural size. (b) Buccal view of right mandible; scale x 0.6 of natural size.

H-1a

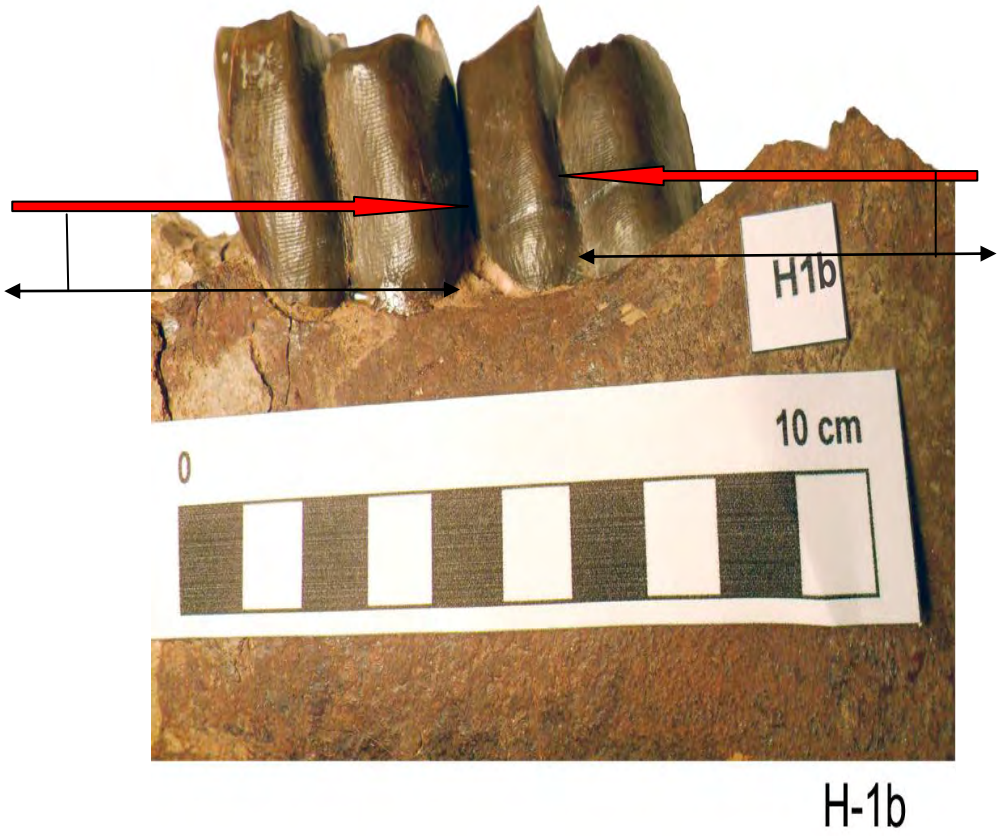

Figure 4.20 (H-1a,b): *Gaindatherium browni,* PMHU Y 24067 b.
(a) Left mandible. (b) Two LEH, 10 mm and 10 mm above the neck on the buccal side of m3; natural size.

***Gaindatherium* sp.**

Material studied: 36 teeth specimens were studied for Enamel Hypoplasia from Siwalik collection housed at PUPC (Table 3.14) MNHN (Table 3.5 and 3.15) and PMHU (Table 3.8 and 3.18).

Description: Enamel Hypoplasia recorded on three Rhino teeth (Table 4.8) which are:

1. Specimen No. PMHU (Y 7079). Enamel Hypoplasia recorded on entoconid and metaconid of dp1 tooth of left mandible. One linear horizontal enamel depression present at 5 mm above the neck on both entoconid and metaconid on the lingual side (Figure 4.21).
2. Specimen No. MNHN (15551). Enamel Hypoplasia recorded on paraconid of m1 tooth of left mandible. One semi circle enamel depression present at 5 mm above the neck on the buccal side (Figure 4.22).
3. Specimen No. MNHN (10468). Enamel Hypoplasia recorded on metacone of P4 tooth of right maxilla. One linear horizontal enamel depression present at 5 mm above the neck on the buccal side (Figure 4.23).

Table 4.8 Comparative measurements of Enamel Hypoplasia in *Gaindatherium* sp.

No.	**Taxon/ Specimen**	**Enamel Hypoplasia**			**Age (**Myr**)**
		Tooth	**Cusps**	**Location**	
1 H-3	*G.* sp. PMHU (Y 7079)	dp1	Entoconid and Metaconid	One LEH 5 mm above the neck	10.017-10.091
2 F-5	*G.* sp. MNHN (15551)	m1	Paraconid	One SEH 5 mm above the neck	8.553-8.616
3 F-3	*G.* sp. MNHN (10468)	P4	Metacone	One LEH 5 mm above the neck	10.017-10.091

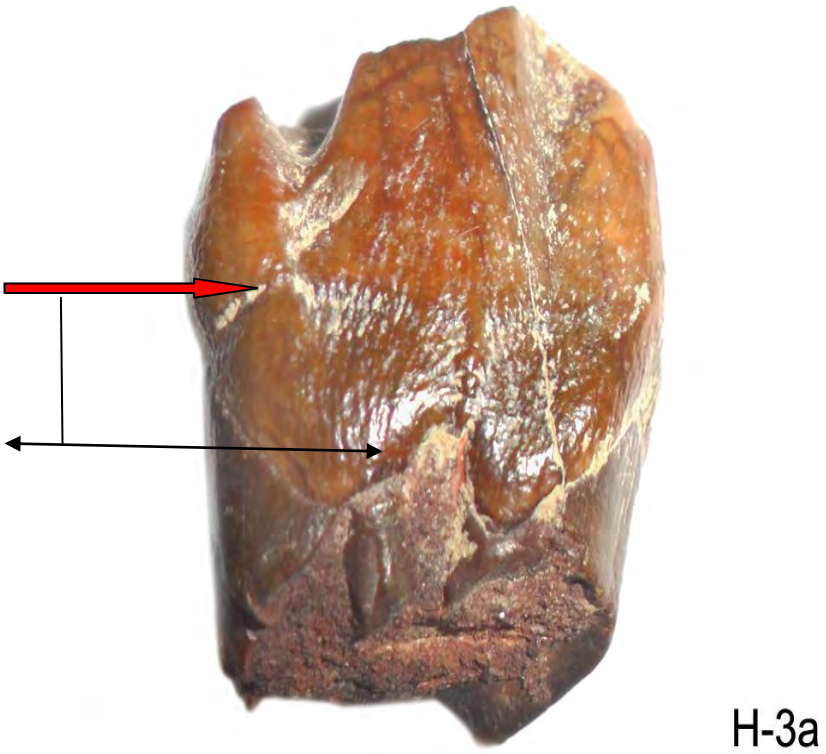

Figure 4.21 (H-3a): *Gaindatherium* sp., PMHU Y 7079.
One LEH, 5 mm above the neck on the lingual side of dp1;
scale x 4 of natural size.

Figure 4.22 (F-5): *Gaindatherium* sp., MNHN 15551.
One SEH, 5 mm above the neck on the buccal side of m1;
scale x 3 of natural size.

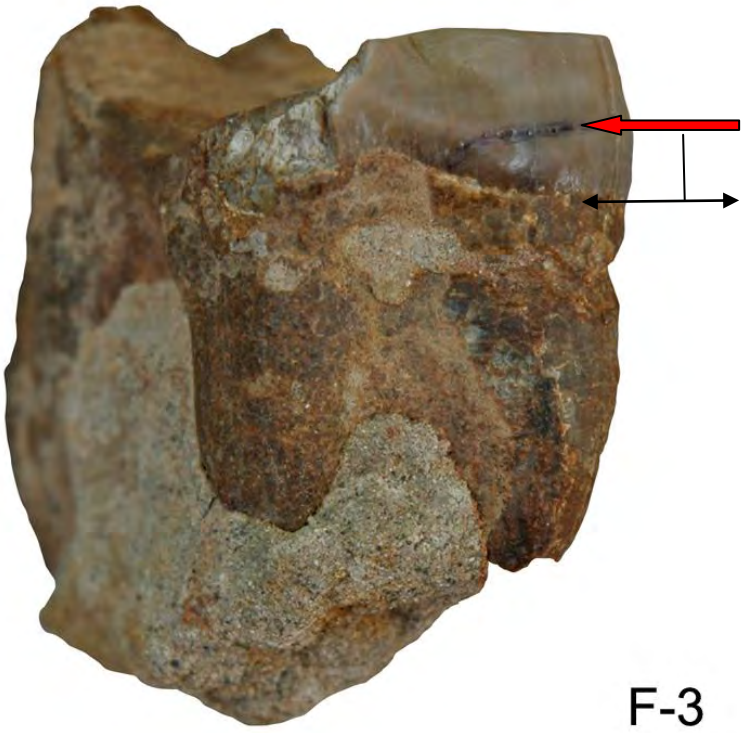

Figure 4.23 (F-3): *Gaindatherium* sp., MNHN 10468.
One LEH, 5 mm above the neck on the buccal side of P4;
scale x 2 of natural size.

Tribe Teleoceratini HAY, 1902

Genus *Chilotherium* RINGSTROM, 1924

Chilotherium intermedium

Material studied: 67 teeth specimens were studied for Enamel Hypoplasia from Siwalik collection housed at PUPC (Table 3.4 and 3.14) and AMNH (Table 3.17).

Description: Enamel Hypoplasia recorded on two Rhino teeth (Table 4.9) which are:

1. Specimen No. PUPC (07/95). Enamel Hypoplasia recorded on hypoconid and protoconid of m2 tooth of right mandible. On hypoconid two linear horizontal enamel depressions present at 10 and 18 mm above the neck, whereas, on protoconid, one linear horizontal enamel depression present at 10 mm above the neck on the buccal side (Figure 4.24).
2. Specimen No. PUPC (07/94). Enamel Hypoplasia recorded on protoconid and hypoconid of p3 tooth of left mandible. On protoconid, one linear horizontal enamel depressions present at 9 mm above the neck, whereas, on hypoconid one linear horizontal enamel depression present at 7 mm above the neck on the buccal side (Figure 4.25).

Table 4.9 Comparative measurements of Enamel Hypoplasia in *Chilotherium intermedium.*

No.	**Taxon/ Specimen**	**Enamel Hypoplasia**			**Age (**Myr**)**
		Tooth	**Cusps**	**Location**	
1 Z-9	C. *intermedium* PUPC (07/95)	m2	Hypoconid Protoconid	Two LEH 10 and 18 mm above the neck One LEH 10 mm above the neck	13.5-8
2 Z-11	*C. intermedium* PUPC (07/94)	p3	Protoconid Hypoconid	One LEH 9 mm above the neck One LEH 7 mm above the neck	13.5-8

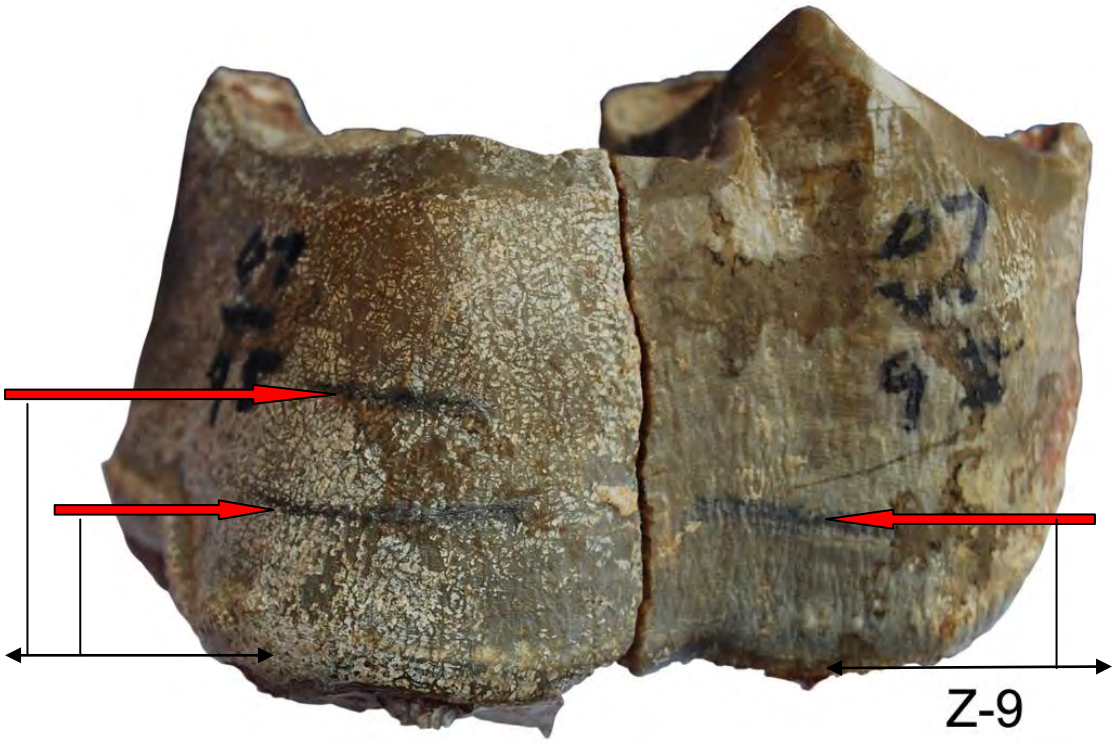

Figure 4.24 (Z-9): *Chilotherium intermedium*, PUPC 07/95. Three LEH, 10, 18 mm and 10 mm above the neck on the buccal side of m2; scale x 2 of natural size.

Figure 4.25 (Z-11): *Chilotherium intermedium*, PUPC 07/94. Two LEH, 9, 7 mm above the neck on the buccal side of p3; natural size.

Family Rhinocerotidae OWEN, 1848

Subfamily Rhinocerotinae OWEN, 1845

Tribe Elassmotheriini

Genus *Caementodon*

Caementodon oettingenae

Material studied: one tooth specimen was studied for Enamel Hypoplasia from Siwalik collection housed in AMNH (Table 3.7).

Description: Enamel Hypoplasia recorded on one Rhino tooth (Table 4.10) which is:

1. Specimen No. AMNH (19591a). Enamel Hypoplasia recorded on metacone of P4 tooth of left maxilla. One linear horizontal enamel depression present at 4 mm above the neck on the buccal side (Figure 4.26).

Table 4.10 Comparative measurements of Enamel Hypoplasia in *Caementodon oettingenae.*

No.	**Taxon/ Specimen**	**Enamel Hypoplasia**			**Age (**Myr**)**
		Tooth	**Cusps**	**Location**	
1 A-1	*C. oettingenae* AMNH (19591a)	P4	Metacone	One LEH 4 mm above the neck	13.5-12

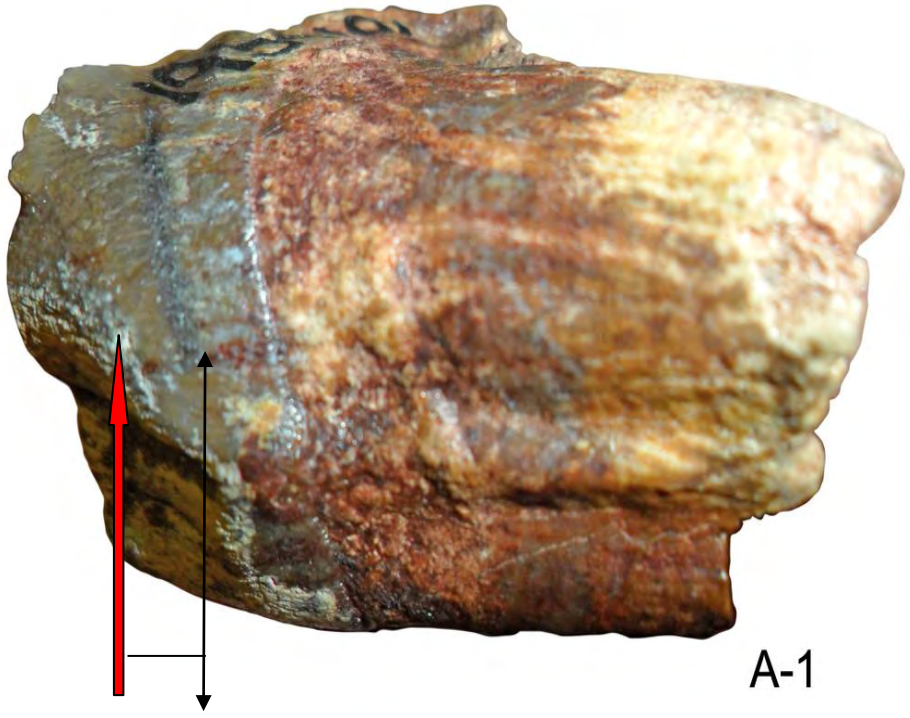

Figure 4.26 (A-1): *Caementodon oettingenae*, AMNH 19591a. One LEH, 4 mm above the neck on the buccal side of P4; scale x 2 of natural size.

Family	Rhinocerotidae OWEN, 1848
Subfamily	Rhinocerotinae OWEN, 1845
Tribe	Rhinocerotini OWEN, 1845
Subtribe	Rhinocerotina OWEN, 1845
Genus	*Rhinoceros* LINNAEUS, 1758

Rhinoceros sivalensis

Material studied: 44 teeth specimens were studied for Enamel Hypoplasia from Siwalik collection housed at PUPC (Table 3.4), NHM (Table 3.10 and 3.20), PMHU (Table 3.8 and 3.18) and AMNH (Table 3.17).

Description: Enamel Hypoplasia recorded on five Rhino teeth (Table 4.11) which are:

1. Specimen No. PUPC (07/39). Enamel Hypoplasia recorded on ectoconid of m2 tooth of left mandible. One linear horizontal enamel depressions present at 15 mm above the neck on the lingual side (Figure 4.27).
2. Specimen No. PUPC (07/38). Enamel Hypoplasia recorded on protocone of M2 and M3 teeth of left maxilla. One linear horizontal enamel depressions present at 15 and 12 mm above the neck on protocone of M2 and M3 teeth respectively on the lingual side (Figure 4.28).
3. Specimen No. NHM (39647). Enamel Hypoplasia recorded on protocone of P4 tooth of left maxilla. One linear horizontal enamel depressions present at 5 mm above the neck on the lingual side (Figure 4.29).
4. Specimen No. PMHU (Y 28225). Enamel Hypoplasia recorded on protocone of M3 tooth of right maxilla. Two linear horizontal enamel depressions present at 23 and 32 mm above the neck on the lingual side (Figure 4.30).

Table 4.11 Comparative measurements of Enamel Hypoplasia in *Rhinoceros sivalensis.*

No.	**Taxon/ Specimen**	**Enamel Hypoplasia**			**Age (**Myr**)**
		Tooth	**Cusps**	**Location**	
1. Z-8	*R. sivalensis* PUPC (07/39)	m2	Entoconid	One LEH 15 mm above the neck	2.6-0.6
2. Z-12	*R. sivalensis* PUPC (07/38)	M2 and M3	Protocone Protocone	One LEH 15 mm above the neck One LEH 12 mm above the neck	2.6-0.6
3. L-4	*R. sivalensis* NHM (39647)	P4	Protocone	One LEH 5 mm above the neck	2.6-0.6
4. H-5	*R. sivalensis* PMHU (Y 28225)	M3	Protocone	Two LEH 23 and 32 mm above the neck	16.565-16.745

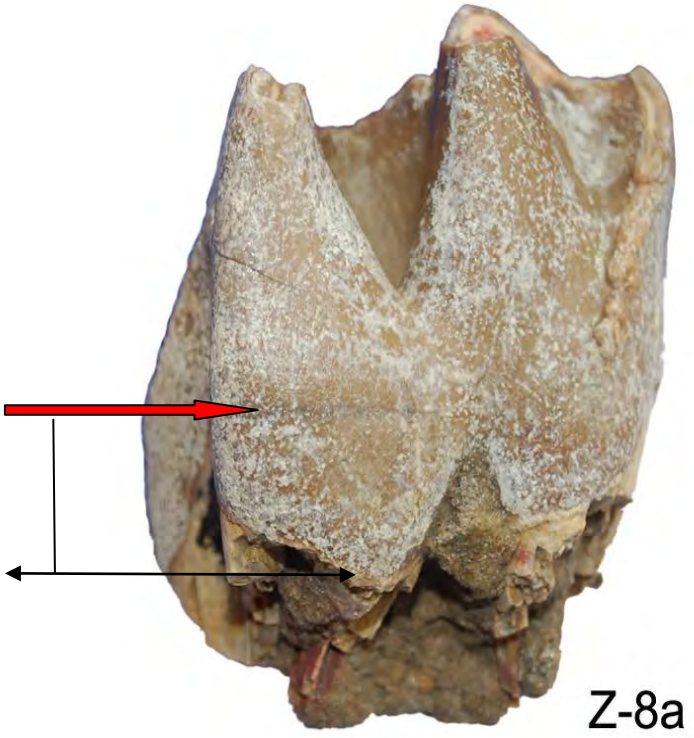

Figure 4.27 (Z-8a): *Rhinoceros sivalensis,* PUPC 07/39. One LEH, 15 mm above the neck on the lingual side of m2; scale x 1.5 of natural size.

Z-12a

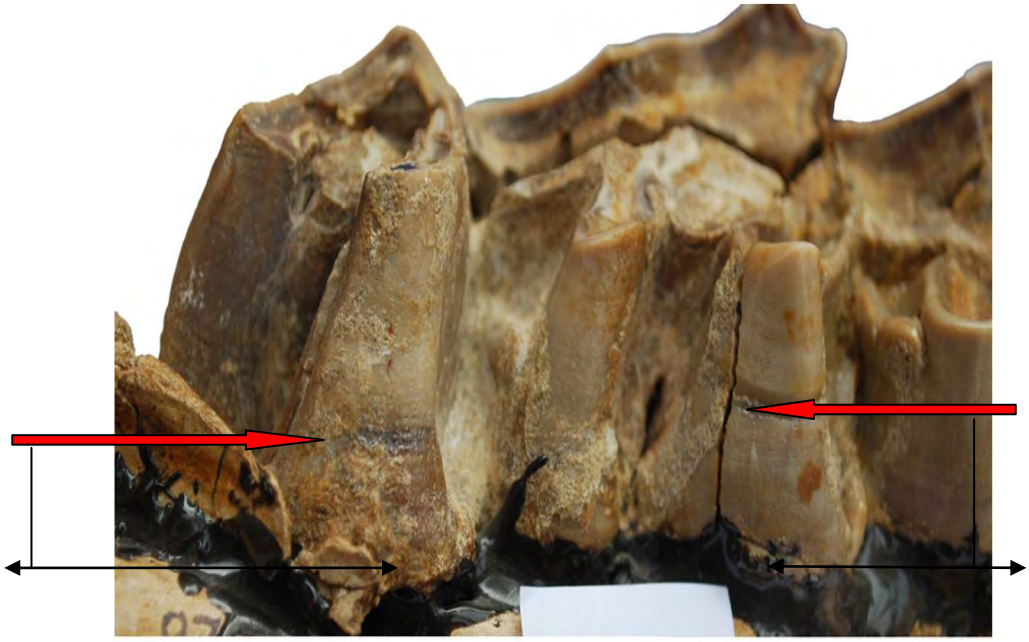

Z-12b

Figure 4.28 (Z-12a,b): *Rhinoceros sivalensis,* PUPC 07/38.
(a) Lingual view of left maxilla (b) One LEH, 15 mm above the neck on the lingual side of M2 and one LEH, 12 mm above the neck on the lingual side of M3; scale x 1.5 of natural size.

L-4a

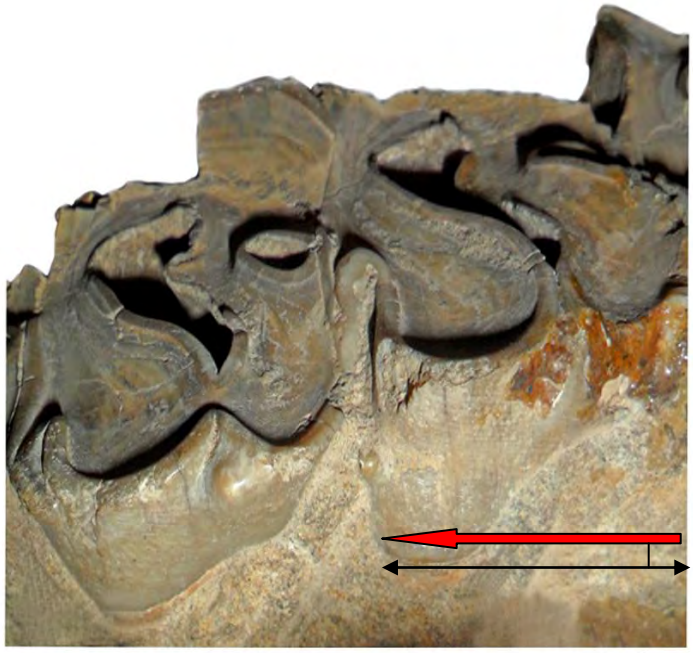

L-4b

Figure 4.29 (L-4a,b): *Rhinoceros sivalensis,* NHM 39647.
(a) Occlusal view of maxilla; ½ of natural size (b) One LEH, 5 mm above the neck on the lingual side of P4; scale x 0.5 of natural size.

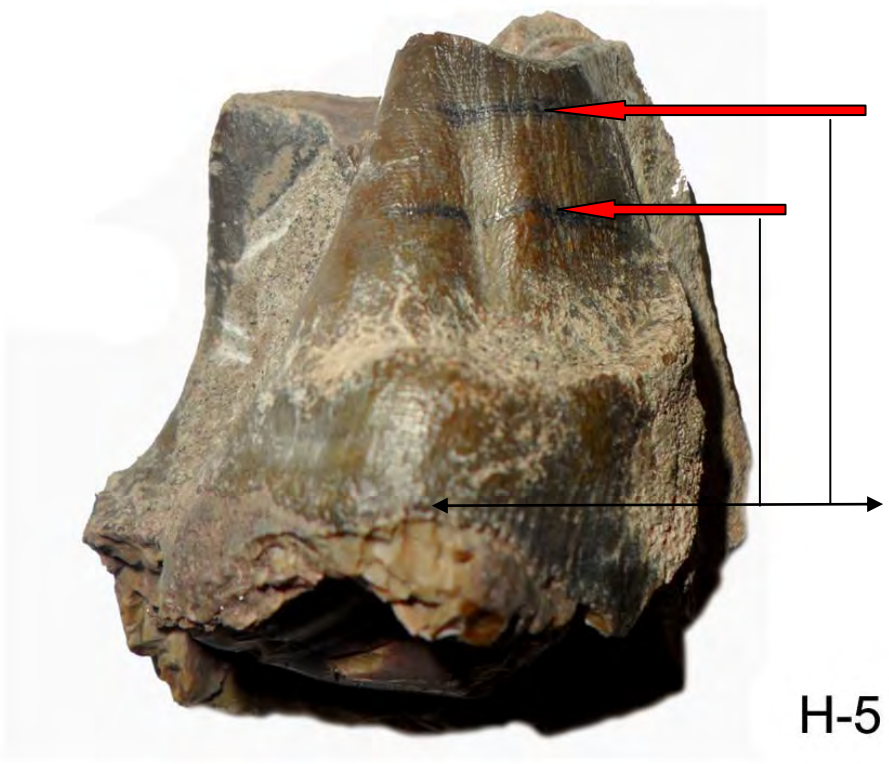

Figure 4.30 (H-5): *Rhinoceros sivalensis,* PMHU Y 28225.
Two LEH, 23, 32 mm above the neck on the lingual side of M3;
scale x 1.5 of natural size.

Rhinoceros sondaicus

Material studied: 21 teeth specimens were studied for Enamel Hypoplasia from Siwalik collection housed in PUPC (Table 3.4 and 3.14).

Description: Enamel Hypoplasia recorded on one Rhino tooth (Table 4.12) which is:

1. Specimen No. PUPC (2010/68). Enamel Hypoplasia recorded on metaconid of m3 tooth of right mandible. One linear horizontal enamel depressions present at 8 mm above the neck on the lingual side (Figure 4.31).

Table 4.12 Comparative measurements of Enamel Hypoplasia in *Rhinoceros sondaicus.*

No.	**Taxon/ Specimen**	**Enamel Hypoplasia**			**Age (**Myr**)**
		Tooth	**Cusps**	**Location**	
1. Z-15	*R. sondaicus* PUPC (2010/68)	m3	Metaconid	One LEH 8 mm above the neck	2.6-0.6

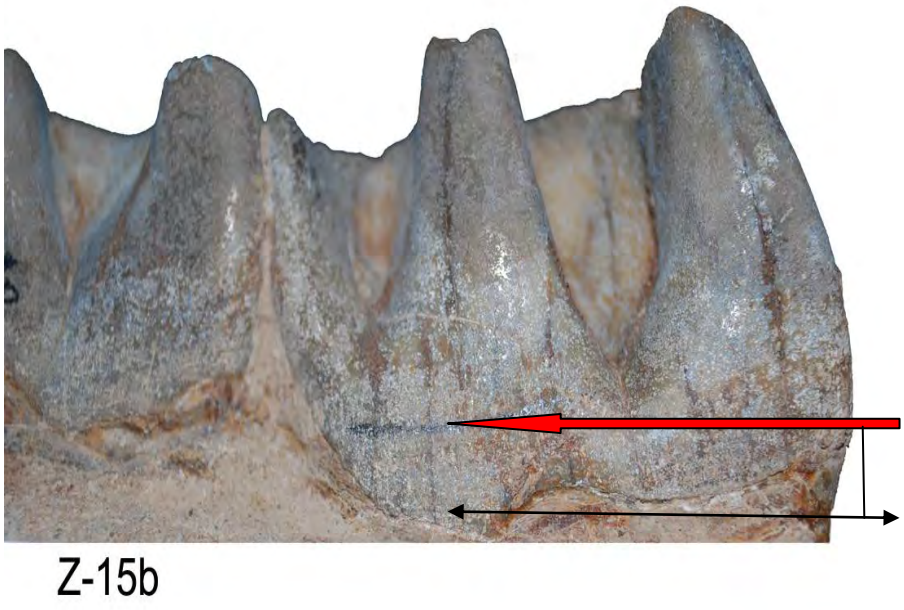

Figure 4.31 (Z-15a,b): *Rhinoceros sondaicus*, PUPC 2010/68.
(a) Lingual view of right mandible; ½ of natural size (b) One LEH 8 mm above the neck on the lingual side of m3; scale x 1.5 of natural size.

***Rhinoceros* sp.**

Material studied: 50 teeth specimens were studied for Enamel Hypoplasia from Siwalik collection housed at PUPC (Table 3.14), NHM (Table 3.20), PMHU (Table 3.8) and AMNH (Table 3.17).

Description: Enamel Hypoplasia recorded on one Rhino tooth (Table 4.13) which is:

1. Specimen No. PMHU (Y 31182). Enamel Hypoplasia recorded on paraconid and hypoconid of m2 tooth of right mandible. Two linear horizontal enamel depressions present at 11 and 9 mm above the neck on paraconid and hypoconid respectively on the buccal side (Figure 4.32).

Table 4.13 Comparative measurements of Enamel Hypoplasia in *Rhinoceros* sp.

No.	**Taxon/ Specimen**	**Enamel Hypoplasia**			**Age (**Myr**)**
		Tooth	**Cusps**	**Location**	
1. H-4	*R.* sp. PMHU (Y 31182)	m2	Paraconid	One LEH 11 mm above the neck	15.947-16.142
			Hypoconid	One LEH 9 mm above the neck	

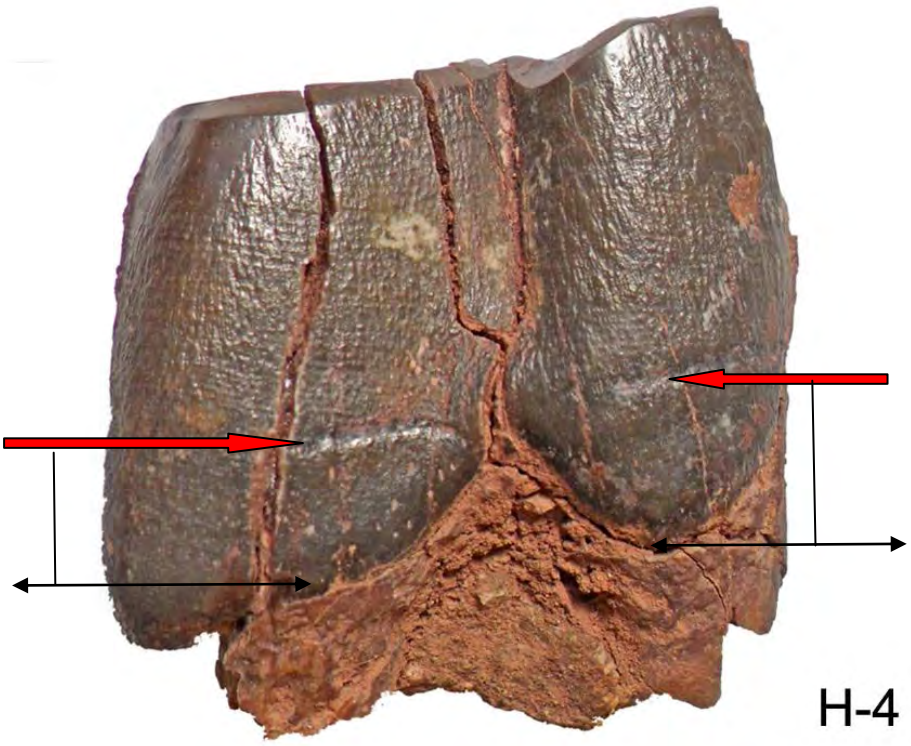

Figure 4.32 (H-4): *Rhinoceros* sp., PMHU Y 31182. Two LEH, 11, 9 mm above the neck on the buccal side of m2; scale x 2 of natural size.

Genus ***Punjabitherium KHAN 1971***

Punjabitherium platyrhinus

Material studied: 16 teeth specimens were studied for Enamel Hypoplasia from Siwalik collection housed in NHM (Table 3.10 and 3.20).

Description: Enamel Hypoplasia recorded on five Rhino teeth (Table 4.14) which are:

1. Specimen No. NHM (17996). Enamel Hypoplasia recorded on paraconid and hypoconid of p3 tooth of right mandible. One linear horizontal enamel depression present at 4 mm above the neck on paraconid, whereas, one linear horizontal enamel depressions present at 5 mm above the neck on hypoconid on the buccal side (Figure 4.33).
2. Specimen No. NHM (28911-cast). Enamel Hypoplasia recorded on protocone and hypocone of P3 and Protocone of M1 teeth of right maxilla. On P3 tooth two linear horizontal enamel depressions present 23 mm above the neck on both protocone and hypocone. Whereas, on protocone of M1 tooth one linear horizontal enamel depression present at 28 mm above the neck on the lingual side (Figure 4.34).

Table 4.14 Comparative measurements of Enamel Hypoplasia in *Punjabitherium platyrhinus.*

No.	**Taxon/ Specimen**	**Enamel Hypoplasia**			**Age (**Myr**)**
		Tooth	**Cusps**	**Location**	
1. L-11	*P. platyrhinus* NHM (17996)	p3	Paraconid Hypoconid	One LEH 4 mm above the neck One LEH 5 mm above the neck	2.6-0.6
2. L-1	*P. platyrhinus* NHM (28911- cast)	P3 and M1	Protocone and Hypocone Protocone	Two LEH One on each cone, each at 23 mm above neck. One LEH 28 mm above the neck	2.6-0.6

Figure 4.33 (L-11a,b): *Punjabitherium platyrhinus*, NHM 17996.
(a) Occlusal view of mandible; ½ of natural size (b) Two LEH, 4 mm and 5 mm above the neck on the buccal side of p3; scale x 1.2 of natural size.

Figure 4.34 (L-1a,b): *Punjabitherium platyrhinus*, NHM 28911 (Cast).
(a) Occlusal view of maxilla; 1/3 of natural size (b) Two LEH, 23 mm each above the neck on the lingual side of P3 and one LEH, 28 mm above the neck on the lingual side of M1; scale x 0.7 of natural size.

4.2 Pilot study of recent Rhinocerotids

A fast-track study on five species of extant rhinocerotids, housed in various museums, were also taken up to record the occurrence of hypoplasia in a complete maxilla and mandible of a given animal, i.e. to see whether the developmental disorder (hypoplasia) affects one tooth or more in the dental battery (Table 3.11 & 3.22). This study was also intended for observing the prevalence of hypoplasia in natural habitats. 45 Cranium belonging to *Rhinoceros sondaicus, R. unincorinis, Ceratotherium simum, C. simum simum, Diceros bicornis* and *Dicerorhinus sumatrensis* were examined and their habitat information were also recorded from the Museum catalogues. All animals were adult and have permanent, fairly worn out, dentition. Most of the Mammalogy collections have Rhino skeletons from zoo or natural parks; therefore it is hard to conjecture about the natural habitats and to draw causal relationship of hypoplasia development with physiological or environmental stress.

Out of 908 teeth examined, only 6 teeth belonging to *R. sondaicus* (2 crania) and *C. simum simum* have hypoplasia (Table 3.11 & 3.22). These animals have a tendency of having hypoplasia on the premolars and more so on the mandibles (Table 4.15). The *C. simum simum* (Figure 4.35) and *R. sondaicus* (Figure 4.36) have hypoplasia on m3 and P4, respectively. The *C. simum simum*, was an adult animal (estimated age 35 years) whereas the *R. sondaicus* was apparently a young-adult at the time of death. However, both the sepcimens record hypoplasia on those teeth, which are known to develop later in the growing years.

One of the *R. sondaicus* (Figure 4.37), a gifted specimen, has hypoplasia on left and right p3 and p4 teeth which is quite a rare occurrence even in the fossil Rhino teeth. The hypoplasia is developed at various satges in the lower half of the teeth indicating that the stressful conditions might have been episodic. Although the early life history is not known but since, the hypoplasia was noted on the permanent premolars, it can be postulated that it might have happened in the Juvenile stage (*sensu* Hillman & Smith, 1986) which could be related to poor dietary conditions because of repeated environmental changes.

Table 4.15 Comparative measurements of Enamel Hypoplasia in Recent Rhinos.

No.	Taxon/ Specimen	Enamel Hypoplasia			Age (Years) (Age estimation adopted from Hillman-Smith, 1986 and Tong, 2001)
		Tooth	Cusps	Location	
1 R-2	*Ceratotherium simum simum* MNHN 2005-297	m3	Protoconid	One LEH 9 mm above the neck	30-38 (Old Adult)
2 R-6	*Rhinoceros sondaicus* MNHN 1985-159	P4	Paracone	One LEH 9 mm above the neck	10-15 (Young Adult)
3 R-12	*Rhinoceros sondaicus* MNHN A-7971	p3 (r) p4 (r) p3 (l) p4 (l) 	Ectolophid Paraconid Paraconid Hypoconid Paraconid	Two LEH 8, 10 mm above the neck Four LEH 7, 9, 11, 13 mm above the neck Two LEH 9, 11 mm above the neck Three LEH 9, 11, 13 mm above the neck Two LEH 7, 9 mm above the neck	20-28 (Adult)

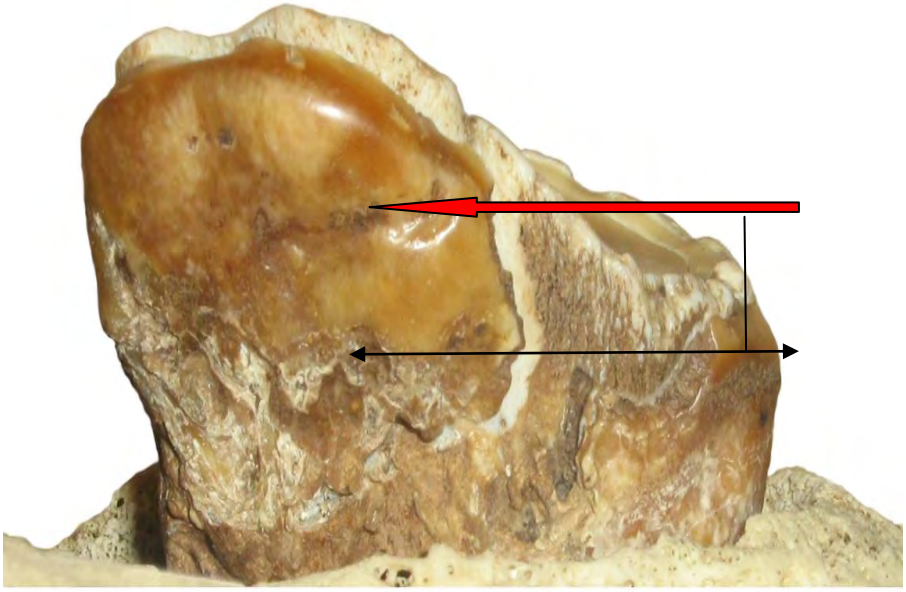

Figure 4.35 (R-2): *Ceratotherium simum simum*, MNHN 2005-297.
One LEH, 9 mm above the neck on the lingual side of m3;
scale x 2 of natural size.

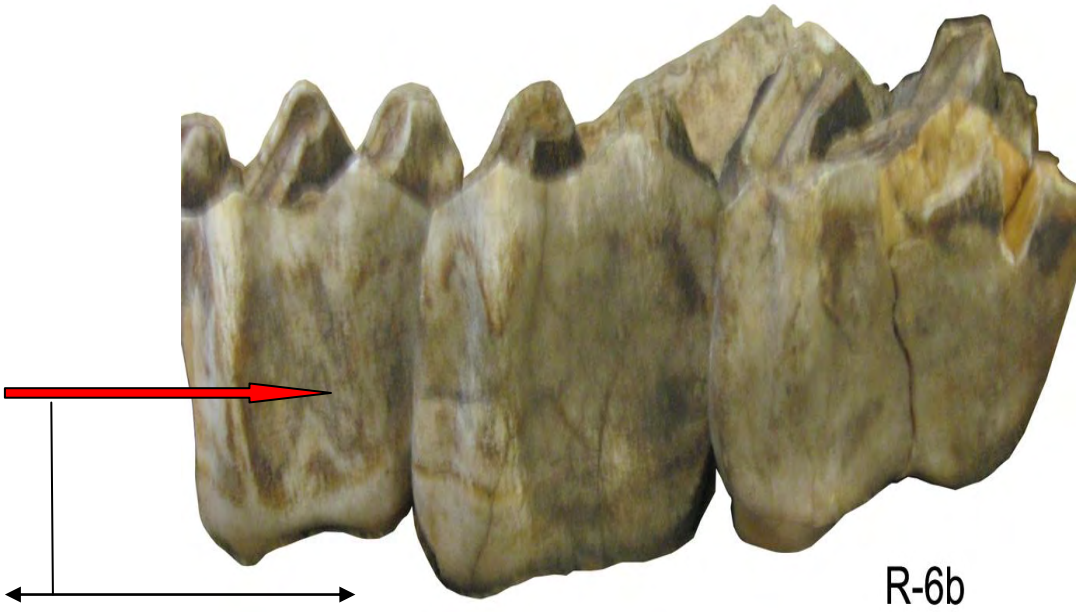

Figure 4.36 (R-6a,b): *Rhinoceros sondaicus*, MNHN 1985-159
(a) Occlusal view of maxilla; scale x 1/3 of natural size (b) One LEH, 9 mm above the neck on the buccal side of P4; scale x 3 of natural size.

R-12a

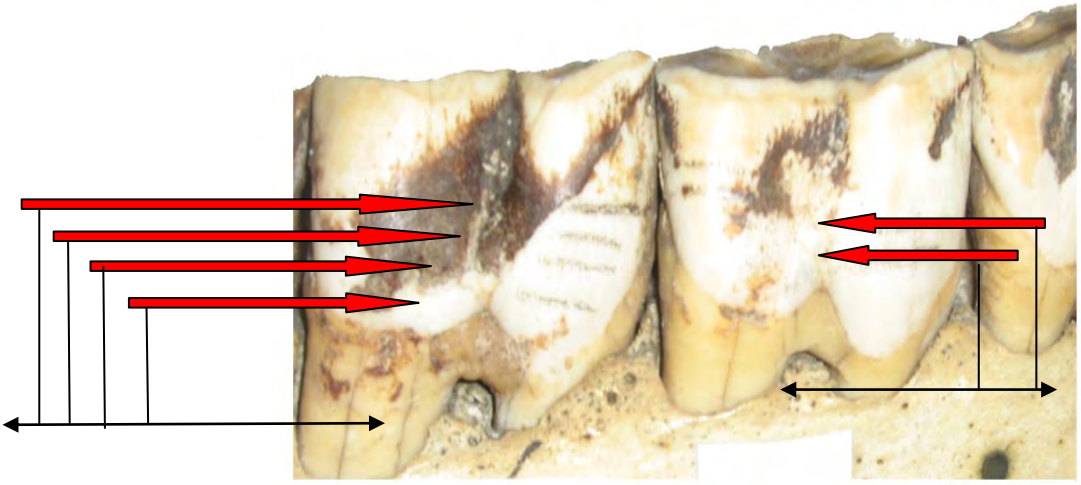

R-12b

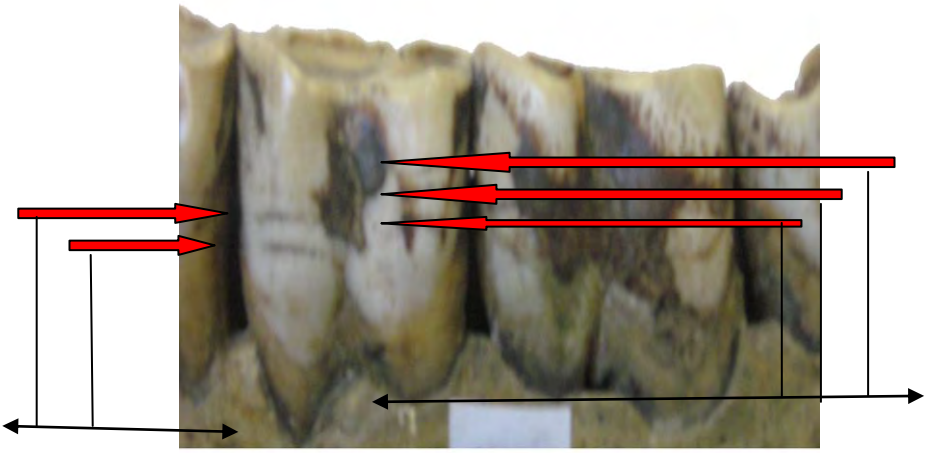

R-12c

R-12d

Figure 4.37 (R-12a,b,c,d,e): *Rhinoceros sondaicus*, MNHN A-7971
(a) Occlusal view of maxilla; scale x ¼ of natural size (b) Two LEH, 8, 10 mm above the neck on the buccal side of p3 and four LEH, 7,9,11,13 mm above the neck on the buccal side of p4 of right mandible; scale x 2 of natural size (c) Five LEH, 9, 11 mm and 9, 11, 13 mm above the neck on the buccal side of p3 of left mandible; scale x 2 of natural size (d) Two LEH, 7, 9 mm above the neck on the buccal side of p4 of left mandible; scale x 3 of natural size and (e) oclusal view of complete mandible showing the teeth with EH; scale x ¼ of natural size.

4.3 **Results & Discussion**

The 34 fossil rhinos belonging to 14 species with hypoplasia reported in this study are from a very wide region of the Himalayan foreland belt and covering almost the whole of Neogene period. There is no such report of any study done of this magnitude. All the previous studies on fossil animals were done on quarry sites or archeological localities where a large sample size accumulated in very short time span. Same is the case with recent population's studies, which is mostly on human beings. However, such studies have given an important insight for analyses of our findings.

The tooth distribution having hypoplasia in this study given in Table 4.16 shows that 87% of EH occurs on permanent teeth, whereas 13% are in deciduous teeth, mostly on the fourth premolar. It may be noted that among the deciduous teeth occurrence, 60% occurrences are on the dP4, which is the last one to erupt among the deciduous teeth (Tong, 2001). It has also been noted that the EH in most of the teeth occurred at a late developmental stage as evidenced from its position on the crown from the cementoenamel junction (i.e. neck). One possible inference, based on the developmental and eruption pattern of Recent Rhinos, is that Enamel Hypoplasia occurred when the animal was not dependent upon mother's nutrition. Therefore, the animal was under some sort of physiological stresses perhaps triggered by external factors.

Table 4.16 Occurrences of EH on different teeth in the studied Rhino specimens.

Dp1	Dp3	Dp4	P2	P3	P4	M1	M2	M3
1	1	3	3	5	7	6	5	8

Though the studied material comprised mostly of isolated teeth but there were 11 animals represented by partial mandible or maxillary fragments. Age estimation was attempted on these 11 animals based on the wear status of the teeth, following the methods devised by Hillman-Smith *et al*., (1986) and Tong (2001). Most of them were adult, around 30 years of age while only two were categorized as 'young adult', estimated to be of 10-15 years of age (Table 4.17). These animals did not show hypoplasia on any particular teeth but was found to be developed on premolar or molar. It appears that hypoplasia does not have any effect on the longevity of an animal.

The 3 cranium of the living species of *R. sondaicus* and *C. simum simum* have given useful insight that hypoplasia could develop on a single tooth of the dental battery, though reasons not well understood as yet. There is one case (Figure 4.37) where hypoplasia has occurred on 3rd and 4th Premolars on both sides of the mandible of an adult with estimated age range of 25-28 years (Hillman-Smith *et al*., 1986; Tong, 2001). Unfortunately there is no contextual information available that weather the sample was taken from the zoo or captured from wild. This individual could have served as a good case of long term environmental stress which seriously affected the animal's growth in its early life.

In the fossil or recent specimens studied, EH are recorded almost in equal numbers on the buccal as well as on the lingual side. Most of the EH are of Linear type which are more prominent and common. 5 cases of Semicircular EH have also been noted which, except one, are on the lingual side. The present study does not support the Dobney and Ervynck (2000) analysis on pigs from archeological sites that EH gets masked or obliterated on the lingual surface because of more abrasion due to the constantly moving tongue and food bolus.

The literature survey shows that Linear Enamel Hypoplasia has been linked to nutritional stress (Neiburger, 1990; Goodman and Rose, 1991; Dobney and Ervynck 2000), birth stress (Goodman and Rose 1991; Mead, 1999), weaning stress (Goodman and Rose, 1991; Dobney and Ervynck 2000), and stress associated with calf-cow separation (Mead, 1999). Similar expalantions have been postulated for incidence of hypoplasia in fossil rhinocerotids, giraffids, and catarrhines monkeys (Mead, 1999; Lukacs, 2001). It is quite likely that hypoplasia occurs in extreme stressful conditions, may be physiologic (mostly in deciduous teeth) or nutritional due to environmental conditions (mostly in adult teeth). In this study, it is suggested that the environemntal factors may have been responsible for the hypoplasia, mostly when the animal was independent of mother's feeding.

Table 4.17 Age estimation of rhinocerotid species having Enamel Hypoplasia. (Age estimation method adapted from Hillman-Smith *et al*. 1986 and Tong, 2001).

Species	Specimen No.	Teeth with Hypoplasia (complete tooth row)	Estimated age of the animal (years)
Brachypotherium perimense	PUPC 07/54	p3 and m1 (p3-m2)	20-28 (Adult)
Alicornops complanatum	MHNT (Pak 1606)	p4 and m3 (p2-m3)	20-28 (Adult)
Alicornops laogouense	PUPC (07/47)	M1 (P2-M2)	10-15 (Young adult)
Gaindatherium browni	PMNH (MUS-106)	p3 and p4 (p2-m3)	25-32 (Adult)
Gaindatherium browni	PMHU (Y 24067 b)	m3 (m2-m3)	20-28 (Adult)
Chilotherium intermedium	PUPC (07/94)	p3 (p2-m1)	20-28 (Adult)
Rhinoceros sivalensis	PUPC (07/38)	M2 and M3 (P1-M3)	25-32 (Adult)
Rhinoceros sivalensis	NHM (39647)	P4 (P2-M3)	25-32 (Adult)
Rhinoceros sondaicus	PUPC (2010/68)	m3 (p4-m3)	20-28 (Adult)
Punjabitherium platyrhinus	NHM (17996)	p3 (p2-m2)	25-32 (Adult)
Punjabitherium platyrhinus	NHM (28911- Cast)	P3 and M1 (P2-M3)	20-28 (Adult)
RECENT RHINOS			
Ceratotherium simum simum	MNHN, 2005-297	m3	30-38 (Adult)
Rhinoceros sondaicus	MNHN, 1985-159	P4	10-15 (Young adult)
Rhinoceros sondaicus	MNHN, A-7971	Right p3 and p4 Left p3 and p4	20-28 (Adult)

Chapter -5

SYNTHESIS AND CONCLUSION

The Rhinocerotids dental material examined and analyzed in this study ranges in age from ~25 Myr to about 2 Myr and covers a wider geographical region from the Bugti Hills in central Pakistan to the Pabbi Hills in north-eastern Pakistan. The early 19th century Rhinocerotids collection from the Siwalik Hills in northern India, described by Falconer and Cautley and presently housed in the British Museum of Natural History, were also studied. This study, thus, includes 14 Rhino species from the earliest radiation in the late Oligocene in the Bugti Hills to the still living *Rhinoceros sondaicus* in the Upper Pliocene rocks of the Pabbi Hills and the Siwalik Hills. The 34 animals showing hypoplasia are recorded almost at all the intervals of the Neogene but there are a few periods where the hypoplasia occurrences have become fairly common (Figure 5.1). In the previous chapter, it was argued that the hypoplasia is in fact related with the environmental stress, which might have affected the nutrition and the food availability. In this chapter, the distribution of Rhinos with EH is being viewed within the framework of a global and regional analysis of Neogene climate change.

Figure 5.1 Biostratigraphical ranges of Rhinocerotidae (this study) from the Neogene "Siwaliks" of Pakistan and the Siwalik Hills (India). Biostratigraphic ranges of Rhinocerotids in this study are estimated from various sources (Colbert, 1935; Hussain *et al*., 1992; Barry *et al*., 2002; Nanda, 2008; Khan, A.M., 2009; Antoine *et al*., 2013). The red line in the individual taxa range shows the occurrence of EH, whereas, black lines indicate the ranges studied without EH. Cross and circles indicate exact ages of the specimens studied.

Figure. 5.1

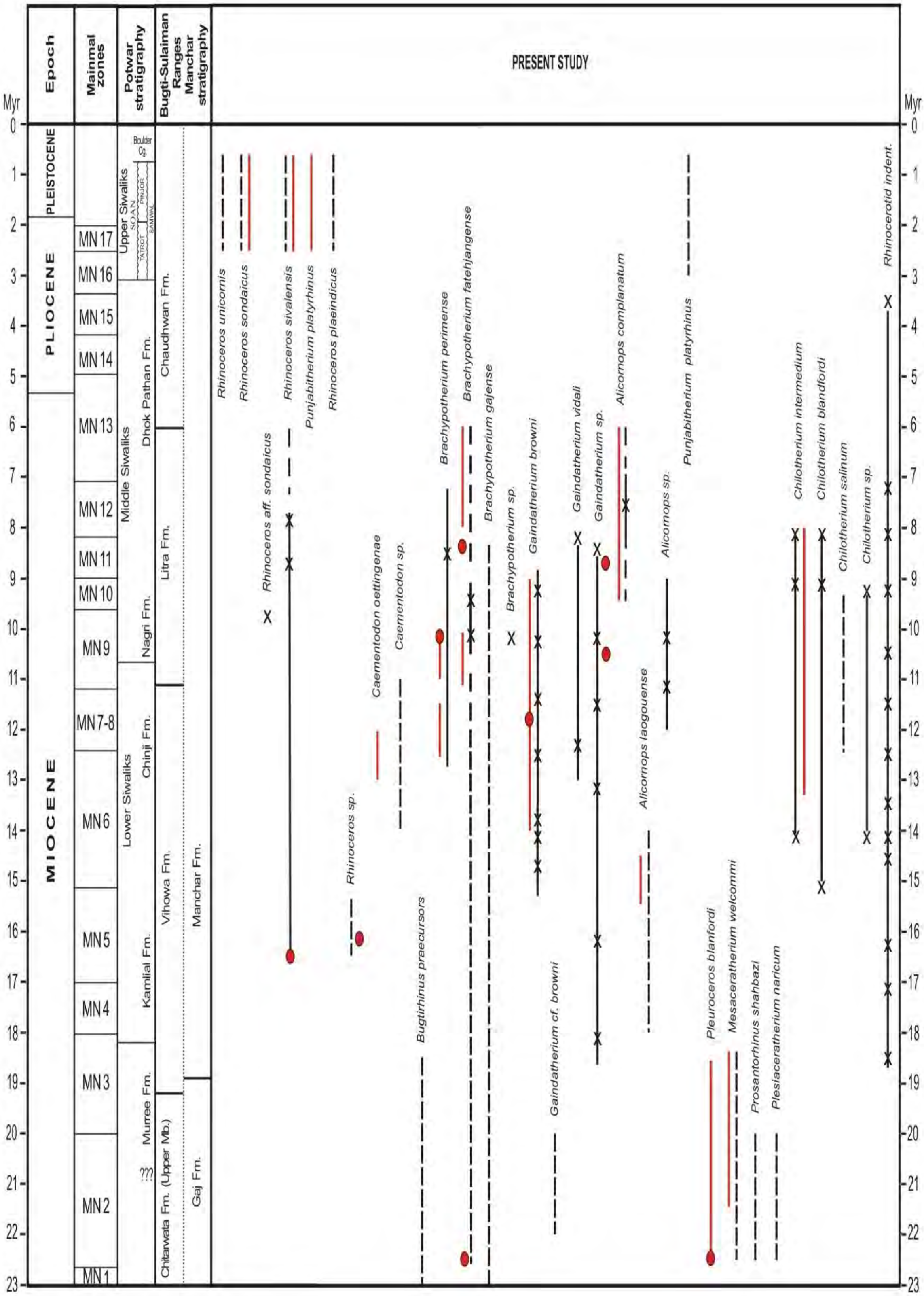

Epoch
Mainmal zones
Potwar stratigraphy
Bugti-Sulaiman Ranges Manchar stratigraphy
PRESENT STUDY
Myr
PLEISTOCENE
PLIOCENE
MIOCENE
MN17
MN16
MN15
MN14
MN13
MN12
MN11
MN10
MN9
MN7-8
MN6
MN5
MN4
MN3
MN2
MN1
Boulder Cg
Upper Siwaliks
SOAN
PINJOR
TATROT
SAMWAL
Middle Siwaliks
Dhok Pathan Fm.
Nagri Fm.
Lower Siwaliks
Chinji Fm.
Kamlial Fm.
Murree Fm.
???
Chaudhwan Fm.
Litra Fm.
Vihowa Fm.
Chitarwata Fm. (Upper Mb.)
Manchar Fm.
Gaj Fm.
Rhinoceros unicornis
Rhinoceros sondaicus
Rhinoceros sivalensis
Punjabitherium platyrhinus
Rhinoceros plaeindicus
Rhinoceros aff. sondaicus
Rhinoceros sp.
Caementodon oettingenae
Caementodon sp.
Bugtirhinus praecursors
Brachypotherium perimense
Brachypotherium fatehjangense
Brachypotherium gajense
Brachypotherium sp.
Gaindatherium browni
Gaindatherium cf. browni
Gaindatherium vidali
Gaindatherium sp.
Alicornops complanatum
Alicornops laogouense
Alicornops sp.
Punjabitherium platyrhinus
Pleuroceros blanfordi
Mesaceratherium welcommi
Prosantorhinus shahbazi
Plesiaceratherium naricum
Chilotherium intermedium
Chilotherium blandfordi
Chilotherium salinum
Chilotherium sp.
Rhinocerotid indent.

5.1 The Neogene Climate pattern

The Neogene period (ca. 24-2.6 Myr) records a succession of profound changes in both the terrestrial and marine realms that led to the modern configuration of climates and environments (e.g. Zachos *et al*., 2001). The global climate during the Oligocene started from a cooler beginning in the early part with rapid expansion of Eastern Antarctic continental ice-sheet, to a general warming trend during the later part (~28-24 Myr) which reduced the extent of Antarctic ice (Zachos *et al*., 2001; Billups and Schrag, 2002). This warming continued in the early Miocene which culminated in the mid-Miocene climate optimum, around 17-15 Myr; being the warmest period in the Neogene. The climate optimum was followed by a gradual cooling, associated with expansion in permanent Antarctic ice sheet by 10 Myr ago and cooling of Antarctic deep waters (Flower and Kennett, 1995; Zachos *et al*., 2001). The coldest period of the Late Miocene may have prevailed around 10.5 Myr. A second cooler period occurred between 9 and 8 Myr Global temperature generally became warmer around 8 Myr and cooler again after 6.5 Myr (Hodell *et al*., 1986; Kennett, 1986; Vincent *et al*., 1985). These changes resulted in defining climatic zones and increased seasonality, especially in the mid-latitude belt (Flower and Kennett, 1994). The climatic deterioration with increased seasonality began in the Late Miocene (11-5 Myr) and continued during the Pliocene as well (Janis, 1993).

One of the key agents of impacting the global climatic deterioration was the intensified uplift of Himalayas and Tibetan Plateau at 11 Myr as a result of the collision of India with Asia, Harrison *et al*., 1993. Prominent changes in terrestrial ecosystems took place in the Late Miocene as more open woodlands began to replace the forests (Potts and Behrensmeyer, 1992), accompanied by the expansion of grasslands and savannas from 7-8 Myr onwards (Cerling *et al.*, 1997). The present paleogeography had all its broad features of land configuration, mountain chains and extent of the continental ice sheets developed by Early Pliocene times.

The Late Miocene tectonic events in South Asia also caused or intensified the Asian Monsoon circulation which now is the dominant feature of South and East Asia climate (Molnar, 2005 and references therein).The Monsoon system during Late Miocene and Early Pliocene time gradually increased in strength but was still weaker than at present day. Monsoon refers to climate conditions where the wind direction is reversed 180 degrees between seasons. The nature of monsoon is different in South and in East Asia. The South Asian monsoon is mainly driven by

seasonal temperature differences. During summer, the low-pressure cells are situated over the northern part of South Asian subcontinent and warm, moist air is drawn towards it from the Indian Ocean. More than half of the humanity and wild life now depends upon the Monsoon system, which is also being affected by the man-induced modern climatic deterioration.

5.2 Neogene paleoenvironmental and climatic changes in South Asia

The collision of India and Asia, which began ~55 Myr (i.e. latest Paleocene) and proceeded from west to east, resulted in the final closure of the Tethys and uplift of the Himalayas (Beck *et al*., 1995; Rowley, 1996; and references therein). By 40 Myr, the two continents appear to have met with full length of ~3000 kms long Indus-Tsangpo Suture zone (Hodges, 2000). Major uplift of the Himalayas occurred during the Middle and Late Miocene. An initial period of rapid uplift around 19 Myr produced large sediment load (Harrison *et al*., 1993). A second period of major uplift began between 12 and 11 Myr and continued until at least 7.5 Myr. Burbank *et al*. (1993) suggested that Himalayan sediment production decreased around 8 Myr.

A vast foreland developed on the southern side of the rising Himalaya, which was continually filled with the detritus eroding out of the ever-growing Himalaya. These terrestrial sediments, called 'Siwaliks' throughout the belt extending from Nepal, northern India to Pakistan, with the mammalian fauna contained in these rocks give a fairly good record of the evolution of the present day wild life, vegetation and the river system of South Asia. The mammalian faunal analysis coupled with studies on stable isotopes of carbon and oxygen in paleosol carbonates and mammalian tooth enamel of the Siwaliks of Indus Basin have provided a good basis for reconstructing the regional paleoenvironmental and paleoclimatic changes during the Neogene (Martin *et al*., 2011; Badgley *et al*., 2008; and references therein). Fossil plants are extremely rare in these sediments except from the Chitarwata Formation and a few reports from the Indian Siwalik belt (De Franceschi *et al*., 2008; Mathur, 1984; Awasthi, 1982; Lakhanpal, 1970), but the microwear studies of mammalian teeth and the stable isotopes of soil carbonate nodules and tooth enamel are reliable proxy for vegetation composition, seasonality and rainfall of the region.

Martin *et al*. (2011) measured carbon and oxygen isotope ratios in fossil mammalian tooth enamel of a few selected Rhinocerotids, Proboscidae and *Hipparion* from the Bugti Hills and along with the published dataset on similar studies from the Miocene Siwalik rocks of Potwar Plateau have reconstructed paleoenvironment and paleoclimate of the Oligocene and Miocene epochs of

Pakistan. The salient features of vegetation and climate change during the Neogene as deciphered form the Siwaliks of Pakistan are described below:

1) Oligocene (~30-23 Myr)

During the Oligocene times the Bugti huge herbivores (e.g. *Paraceratherium bugtiense*) were eating C_3 plants in tropical semi-deciduous forest (Martin *et al*., 2011). The same forested tropical landscape is supported by presence of several complete or fragmentary fossil tree trunks in southern Bugti Hills in early Oligocene with more open drier habitat in later Oligocene (Marivaux *et al*., 2001, 2005; De Franceschi *et al*., 2008). Martin *et al.*, (2011) interpreted the Bugti Hills region dry but densely forested under a temperate to subtropical climate. Although the confirmed Oligocene deposits are only known from the Bugti Hills, but it is likely that other parts of the Himalayan Foreland belt were also having the same tropical to subtropical climate (Awasthi, 1982; Mathur, 1984; Roddaz *et al*., 2011).

2) Early Miocene (23-15 Myr)

The Bugti Hill mammalian fauna record substantial diversity at the beginning of the Miocene, especially in the herbivores suggesting fair abundance of vegetation. The oxygen and carbon isotopes values of Rhinocerotids tooth enamel as well as the floral evidences suggest a wetter environment with tropical forest. A similar pattern of warm and moist climates conditions have been noted in the Early Miocene paleoflora in Nepal and other parts of Asia (Morley, 1998; Songtham *et al*., 2003). Martin *et al*. (2011) linked it with the development of the Asian Monsoon system with a substantial increase in the rainfall compared to the previous period. The initiation of the monsoon system is related with uplift of the Himalayan-Tibetan Plateau and shrinkage of the Para-Tethys Sea (Tapponnier *et al*., 2001; Rogl, 1998). However, Hossain *et al*. (2013) suggested arid climatic conditions for the Himalayans highlands with common occurrences of low temperature wildfire in the catchment area during the Late Eocene to Early Miocene period.

3) Middle Miocene (15-10 Myr)

The carbon isotopic values of tooth enamel of Bugti large mammals, mainly rhinocerotids (e.g. *Brachypotherium fatehjangense*, *B*. sp., Rhinocerotidae indet., etc.), indicate that these mammals were browsers subsisting predominantly on C_3 plants in a tropical relatively closed canopy rainforest (Martin *et al*., 2011). The tropical evergreen forest was extending through the entire Himalayan Foreland during the Middle Miocene are indicated by the presence of fossil wood

from Indian Siwaliks and the plants found in the Nepal Siwaliks (Parsad, 1993). However, there are indications that C_4 plants were expanding in Peninsular India at around 15-11 Myr (Tipple and Pagani, 2007).

4) Late Miocene (10-6 Myr)

This is the time of substantial mammalian faunal changes recorded from the Siwalik of the Potwar Plateau as well as from the Siwaliks of northern India (Barry *et al*., 2002). The three-toed equid *Hipparion* appeared in the Siwalik fauna around 10 Myr and has become the most common element. Himalayan uplift became quite intense and the reorganization for the paelodrainage system, precursor of the modern Indus-Ganges river system, began to take shape around 10-6 Myr (Badgley *et al*., 2008; Barry *et al*., 2002; Behrensmeyer *et al*., 2007; Morgan *et al*., 2009; Martin *et al*., 2011; Quade and Cerling, 1995). The C_4 grass components appeared around 10-9 Myr and increased to almost 60% by 7.5 Myr (Martin *et al*., 2011).

Hipparion were perhaps a mixed consumer of C_4 and C_3 plants whereas the elephantoides and rhinos were still pure browsers. The isotopic composition and microwear of several fossil mammalian teeth from Siwalik faunal assemblages of the Potwar Plateau suggest expansion of C_4 grasses, decrease in rainfall, warmer temperatures, and strong seasonality; all these changes are interpreted to be as a consequence of intensification monsoonal system in South Asia (Nelson, 2007; Behrensmeyer *et al*., 2007). The major climate change event has been proposed to explain the Late Miocene replacement of cricetid rodents with Murids (Patnaik, 2003) and the increased 7.3 to 7.0 Myr faunal turnover found in the Siwalik (Barry *et al*., 2002). One explanation of the Late Miocene monsoon intensification is a pulse of Tibetan uplift, well-documented at 9 Myr from sediments influx in the Indus and Bengal Fans (Quade *et al*., 1997; Xu *et al*., 2012).

5) Pliocene (~6-2 Myr)

The climatic cooling trend started in the Late Miocene continued in the Pliocene, with subtropical regions shrinking equatorially and the Antarctica Ice cap expanded. Intensified humid and seasonal climate arising from the Himalayan monsoon decreased the incidence and frequency of general wildfires, but increased the ratio of large to small wildfires (Hossain *et al*., 2013). A new set of mammalian fauna with dominance of grazers and open habitat dwellers appeared in the Upper Siwaliks sequence (i.e. the 'Pinjor fauna'). This was the beginning of modern-day South Asian biodiversity (Hussain *et al*., 1992; Nanda, 2008).

5.3 Rhinocerotid Hypoplasia and Climate Change

The literature review, presented earlier, revealed that all the previous studies of Enamel Hypoplasia on fossil teeth were carried out on one or two closely-related species accumulated in a very brief time span (e.g. Mead, 1999; Franz-Odendaal *et al*., 2004). The present study is the only of its kind where several species of a family (Rhinocerotidae) were examined over 30 million years' time span. Rhinocerotid's first appearance in South Asia is form the Oligocene beds of the Bugti Hills and since then Rhino fossils are one of the most common occurrences in the Neogene Siwaliks sequence everywhere in the outcrop belt. Figure 5.1 shows the ranges of 34 species in which 11 species have hypoplasia at one or more time period in their total range. It is difficult to correlate the hypoplasia occurrences with climate changes but there exists some relationship which is discussed here.

The Rhino species with EH are apparently more prevalent at four time periods; around 22-20 Myr, ~16 Myr, 12-8 Myr and ~2 Myr in the Pliocene. It is noteworthy that there were at least 9 species of Rhinocerotids in the 23-20 Myr interval, but only 3 of them, namely *Brachypotherium fatehjangense, Pleuroceros blanfordi* and *Mesaceratheruim welcommi*, were found to have hypoplasia. It can be postulated that the low incidence of hypoplasia may be related to stable subtropical to tropical climatic conditions during the Early Miocene time. The maximum number of 6 species out of 15 reported between 12-8 Myr period have hypoplasia. The Middle Miocene was a period of intense climatic changes including the appearance and expansion of the C_4 plants; visible signs of seasonality and the establishment of South Asian monsoonal system (Badgley *et al*., 2008 and references therein). The Siwalik fauna from the Potwar Plateau also show major faunal turnover during this period (e.g. see Barry *et al*., 2002). Rhinos being dominantly browsers must have suffered the most as the habitats shrank. *Brachypotherium fatehjangense*, though a long ranging species since 23 Myr showed more incidence of Enamel Hypoplasia, had apparently could not cope with the changing environment and got extinct at around 8 Myr. Studies done on microwear and oxygen & carbon isotopes on tooth enamel on other mammals (e.g. bovids, *Hipparion*, Hominoids *Sivapithecus*, etc) also point towards stress time for these animals (e.g. See Nelson, 2007; Morgan *et al*., 1994).

The Pliocene changing environment affected three species, *Rhinoceros sondaicus*, *R. sivalensis*, and *P. platyrhinus*, showing EH, whereas the teeth examined of the other two *R. unicornis* and *P. plaeindicus* did not have hypoplasia. It can be argued that climate, especially seasonality with prolonged drought periods, might have been the cause of stress for these animals. It would bring credence to the hypothesis proposed here that climate change has caused the EH in Rhinos if other mammalian taxa are also examined for the same time span.

REFERENCES

ANTOINE, P. -O. AND WELCOMME, J. -L., 2000. A new rhinoceros from the lower Miocene of the Bugti Hills, Baluchistan, Pakistan: the earliest elasmotheriine. *Palaeontology*, **43** (5): 795-816.

ANTOINE, P. -O., 2002a. Phyloge`nie et `evolution des Elasmotheriina (Mammalia, Rhinocerotidae). *Memoires du Mus`eum National d`Histoire Naturelle*, **188**: 359 p.

ANTOINE, P. -O., 2002b. Middle Miocene elasmotheriine Rhinocerotidae from Chinji and Mongolia: taxonomic revision and phylogenetic relationships. *Zoologica Scripta*, *The Norwegian Academy of Science and Letters*, **32** (2): 97.

ANTOINE, P. -O., SHAH, S. M. I., CHEEMA, I. U., CROCHET, J. Y., DE FRANCESCHI, D., MARIVAUX, L., MÉTAIS, G. AND WELCOMME, J. L., 2004. New remains of the baluchithere *Paraceratherium bugtiense* (Pilgrim, 1910) from the Late/latest Oligocene of the Bugti Hills, Balochistan, Pakistan. *Journal of Asian Earth Sciences*. **24**: 71-77.

ANTOINE, P. -O., DOWNING, K. F., CROCHET, J. -Y., DURANTHON, F., FLYNN, L. J., MARIVAUX, L., MÉTAIS, G., RAJPAR, A. R. AND ROOHI, G. 2010. A revision of *Aceratherium blanfordi* Lydekker, 1884 (Mammalia: Rhinocerotidae) from the early Miocene of Pakistan: postcranials as a key. *Zoological Journal of the Linnean Society*. **160**: 139-194.

ANTOINE, P. -O., MÉTAIS, G., ORLIAC, M. J., CROCHET, J. -Y., FLYNN, L. J., MARIVAUX, L., RAJPAR, A. R., ROOHI, G. AND WELCOMME, J. -L., 2013. Mammalian Neogene biostratigraphy of the Sulaiman Province, Pakistan. In: Wang Xiaoming, L. J. Flynn and M. Fortelius, (eds.), Fossil Mammals of Asia; Neogene Biostratigraphy and Chronology. Columbia University Press. 752 p.

AWASTHI, P., LORD, J. M. AND NESBIT-EVANS, E. M., 1982. Tertiary plant megafossils from the Himalaya--- a review. *The Palaeobotanist*, **30** (3): 254-267.

BADGLEY, C. AND BEHRENSMEYER, A. K., 1980. Paleoecology of middle Siwalik sediments and faunas, northern Pakistan. *Palaeogeography, Palaeoclimatology, Palaeoecolog*, **30**: 133-155.

BADGLEY, C., BARTELS, W. S., MORGAN, M. E., BEHRENSMEYER, A. K. AND RAZA, S. M., 1995. Taphonomy of vertebrate assemblages from the Paleogene of northwestern Wyoming and the Neogene of northern Pakistan. *Palaeogeography, Palaeoclimatology, Palaeoecology*, **115**: 157-180.

BADGLEY, C., BARRY, J. C., MORGAN, M. E., NELSON, S. V., BEHRENSMEYER, A. K., CERLING, T. E. AND PILBEAM, D., 2008. Ecological changes in Miocene mammalian record show impact of prolonged climatic forcing. *Proceedings of the National Academy of Sciences*, **105** (34): 12145-12149.

BALASSE, M., AMBROSE, S. H., SMITH, A. B. AND PRICE, T. D., 2002. The seasonal mobility model for prehistoric herders in the South-western Cape of South Africa assessed by isotopic analysis of sheep tooth enamel. *Journal of Archaeological sciences*, **29**: 917-932.

BARRY, J. C., LINDSAY, E. H. AND JACOBS, L. L., 1982. Biostratigraphic zonation of the middle and upper Siwaliks of the Potwar Plateau of Northern Pakistan. *Palaeogeography, Palaeoclimatology, Palaeoecology*, **37**: 95-130.

BARRY, J. C., MORGAN, M. E., FLYNN, L. J., PILBEAM, D., BEHRENSMEYER, A. K., RAZA, M. S., KHAN, I. A., BADGLEY, C., HICKS, J. AND KELLEY, J., 2002. Faunal and Environmental change in the Late Miocene Siwaliks of Northern Pakistan. *Paleobiology Memoir.* **28** (2): 1-72.

BARRY, J. C., COTE, S., MACLATCHY, L., LINDSAY, E. H., KITYO, R. AND RAJPAR, A. R., 2005. Oligocene and early Miocene ruminants (Mammalia, Artiodactyls) from Pakistan and Uganda. *Palaeontologia Electronica*, **8** (21A): 1–29.

BECK, R. A., BURBANK, D. W., SERCOMBE, W. J., RILEY, G. W., BARNDT, J. K., BERRY, J. R., AFZAL, J., KHAN, A. M., JURGEN, H., METJE, J., CHEEMA, A.,

SHAFIQUE, N. A., LAWRENCE, R. D. AND KHAN, M. A., 1995. Stratigraphic evidence for an early collision between northwest India and Asia. *Nature*, **373**: 55–58.

BEHRENSMEYER, A. K. AND BARRY, J. C., 2005. Biostratigraphic Surveys in the Siwaliks of Pakistan: A method for Standardized Surface Sampling of the Vertebrate Fossil Record. *Palaeontologia Electronica*, **8** (15A): 1-24.

BEHRENSMEYER, A. K., QUADE, J., CERLING, T. E., KAPPELMAN, J., KHAN, I. A., COPELAND, P., ROE, L., HICKS, J., STUBBLEFIELD, P., WILLIS, B. J. AND LATORRE, C., 2007. The structure and rate of late Miocene expansion of C4 plants: Evidence from lateral variation in stable isotopes in paleosols of the Siwalik Group, northern Pakistan. *Geological Society of America Bulletin*, **119**: 1486-1505.

BERTEN, J., 1895. Hypoplasie des Schmelzes (Congenitale Schmelzdefects; Erosionen), *Deutsche Monatsschrift fur Zahnheilkunde*, **13**: 425-600.

BILLUPS, K. AND SCHRAG, D. P., 2002. Paleotemperatures and ice volume of past 27 Myr revisited with paired Mg/Ca and $^{18}O/^{16}O$ measurements on benthic foraminifera. *Paleoceanography*, **17** (1): 3.1-3.11.

BLANFORD, W. T., 1879. The geology of Sindh. *Memoirs of the Geological Survey of India*, **18**: 1–196.

BLANFORD, W. T., 1883. Geological notes on the hills in the neighborhood of the Sind and Punjab frontier between Quetta and Dera Ghazi Khan. *Memoirs of the Geological Survey of India*, **20**:1-136.

BRATLUND, B., 1999. Taubach revisited, Jahrbuch des Romisch-Germanischen Zentralmuseums Mainz, **46**: 67-147.

BRYANT, J. D., LUZ, B. AND FROELICH, P. N., 1994. Oxygen isotopic composition of fossil horse tooth phosphate as a record of continental. *Palaeogeography, Palaeoclimatology, Palaeoecology*, **107**: 303-316.

BURBANK, D. W., DERRY, L. A. AND FRANCE-LANORD, C., 1993. Reduced Himalayan sediment production 8 Myr ago despite an intensified monsoon. *Nature*, **364**: 48-50.

CERDENO, E., 1998. Diversity and evolutionary trends of the family Rhinocerotidae (Perissodactyla). *Palaeogeography, Palaeoclimatology, Palaeoecology*, **141**: 13-34.

CERLING, T. E., HARRIS, J. M., MACFADDEN, B. J., LEAKEY, M. G., QUADE, J., EISENMANN, V. AND EHLERINGER, J. R., 1997. Global vegetation change through the Miocene/Pliocene boundary. *Nature*, **389**: 153–158.

CHEEMA, M. R., RAZA, S. M. AND AHMAD, H., 1977. Cenozoic. In S. M. I. Shah, Ed. Stratigraphy of Pakistan. *Memoirs of the Geological Survey of Pakistan*, **12**: 56-98.

COLBERT, E.H., 1935. Siwalik mammals in the American Museum of Natural History. *Transactions of the American Philosophical Society* (New Series), **26**: 1-401.

COTTER, G. P., 1933. The geology of the part of the Attock district, West of Longitude 72° 45 E. *India Geol. Surv. Mem*., **55**: 63-161.

CROCHET, J. -Y., ANTOINE, P. -O., MARIVAUX, L., MÉTAIS, G. AND WELCOMME, J. -L., 2009. Premieres descriptions de peintures et gravures rupestres au Balochistan (Pakistan). *International Newsletter on Rock Art,* **55**.

DE FRANCESCHI, D., HOORN, C., ANTOINE, P. -O., CHEEMA, I. U., FLYNN, L. J., LINDSAY, E. H., MARIVAUX, L., MÉTAIS, G., RAJPAR, A. R. AND WELCOMME, J. -L., 2008. Floral Data from the Mid-Cenozoic of central Pakistan. *Review of Palaeobotany and Palynology*, **150** (1-4): 115–129.

DOBNEY, K. AND ERVYNCK, A., 2000. Interpreting developmental stress in archaeological pigs: the chronology of linear enamel hypoplasia. *Journal of Archaeological Science*, **27**: 597–607.

DOBNEY, K., ERVYNCK, A., ALBARELLA, U. AND ROWLEY-CONWAY, P., 2004. The chronology and frequency of a stress maker (linear enamel hypoplasia) in recent and archeological populations of Sus scorfa in north-west Europe, and the effects of early domestication. *Journal of Zoology* (London), **264**: 197-208.

DOWNING, K. F., LINDSAY, E. H., DOWNS, W. R. AND SPEYER, S. E., 1993. Lithostratigraphy and vertebrate biostratigraphy of the early Miocene Himalayan Foreland, Zinda Pir Dome, Pakistan. *Sedimentary Geology*, **87**: 25–37.

DOWNING, K. F. AND LINDSAY, E. H., 2005. Relationship of Chitarwata Formation paleodrainage and paleoenvironments to Himalayan Tectonics and Indus River paleogeography. *Palaeontologia Electronica*, **8** (20A): 1–12.

EL-NAJJAR, M. Y., DESANTI, M. V. AND OZEBEK, L., 1978. Prevalence and Possible Etiology of Dental Hypoplasia. *American Journal of Physical Anthropology*, **48**: 185-192.

ENSOR, B. E. AND IRISH, J. D., 1995. Hypoplastic area method for analyzing dental enamel hypoplasia. *American Journal of Physical Anthropology*, **98**: 507–517.

FALCONER, H., 1832. Dehraudun fossil remains. *J. Asiatic Soc.* Bengal, **1**: 249 p.

FALCONER, H. AND CAUTLEY, P. T., 1868. Introductory observations on the geography, geological structure, and fossil remains of the Siwalik Hills. *Palaeont. Mems.* London, **1**: 1-29.

FATMI, A. N., 1973. Lithostratigraphic units of Kohat-Potwar Province-Indus Basin, Pakistan. *Geol. Surv. Pakistan. Mem*., **10**: 80 p.

FEDERATION DENTAIRE INTERNATIONAL, 1982. An epidemiological index of developmental defects of dental enamel (DDE Index). *International Dental Journal*, **32**: 159–167.

FERANEC, R. S. AND MACFADDEN, B. J., 2000. Evolution of the grazing niche in Pleistocene mammals from Florida: evidence from stable isotopes. *Palaeogeography, Palaeoclimatology, Palaeoecology*, **162**: 155-169.

FLOWER, B. D. AND KENNETT, J. P., 1994. The middle Miocene climatic transition: East Antarctic ice sheet development, deep ocean circulation and global carbon cycling. *Palaeogeography, Palaeoclimatology, Palaeoecology*, **108** (3-4): 537-555.

FLOWER, B. D. AND KENNETT, J. P., 1995. Middle Miocene deepwater paleoocenagraphy in the Southwest Pacific: relations with East Antarctic Ice sheet developments. *Paleoceanography*, **10** (6): 1095-1112.

FLYNN, L. J., JACOBS, L. L. AND CHEEMA, I. U., 1986. Baluchimyinae, a new ctenodactyloid rodent subfamily from the Miocene of Baluchistan. *American Museum Novitates*, **284**: 1–58.

FLYNN, L. J., BARRY, J. C., MORGAN, M. E., PILBEAM, D., JACOBS, L. L. AND LINDSAY, E. H., 1995. Neogene Siwalik Mammalian Lineages: Species longevities, rates of changes, and modes of speciation. *Palaeogeography, Palaeoclimatology, Palaeoecology*, **115**: 249-264.

FLYNN, L. J., DOWNS, W. R., OPDYKE, N. O., HUANG, K., LINDSAY, E. H., YE, J., XIE, G. AND WANG, X., 1999. Recent advances in the small mammal biostratigraphy and magnetostratigraphy of Lanzhou Basin, p. 105-118. In Fang, X.-m. and Nettleton, D. (eds.), International Symposium and Field Workshop on Paleosols and Climatic Change. Science in China Press, Lanzhou, China, 105-118.

FORSTER-COOPER, C., 1934. The extinct rhinoceroses of Baluchistan. *Philosophical Transactions of the Royal Society of London*, Series B. **223**: 569-616.

FORSTER-COOPER, M. A., 1924. The Anthracotheriidae of the Dera Bugti deposits in Baluchistan. *Memoirs of the Geological Survey of India*, **4**: 1–59.

FRANZ-ODENDAAL, T. A., LEE-THORP, J. A. AND CHINSAMY, A., 2003. Insights from stable isotopes on enamel defects and weaning in Pliocene herbivores. *Journal of Bioscience*, **28** (6): 765-773.

FRANZ-ODENDAAL, T. A., 2004. Enamel hypoplasia provides insights into early systematic stress in wild and captive giraffes (*Giraffa camelopardalis*). *Journal of Zoology* (London), **263**: 197-206.

FRANZ-ODENDAAL, T. A., CHINSAMY, A. AND LEE-THORP, J., 2004. High prevalence of enamel hypoplasia in an early Pliocene giraffid (*Sivatherium hendeyi*) from South Africa. *Journal of Vertebrate Paleontology*, **24** (1): 235-244.

FRICKE, H. C. AND O'NEIL, J. R., 1996. Inter- and Intra-tooth variation in the oxygen isotopic composition of mammalian tooth enamel phosphate implications for palaeoclimatological and palaeobiological research. *Palaeogeography, Palaeoclimatology, Palaeoecology*, **126**: 91-99.

FRIEDMAN, R., GEE, J., TAUXE, L., DOWNING, K. AND LINDSAY, E., 1992. The magnetostratigraphy of the Chiterwata and lower Vihowa formations of the Dera Ghazi Khan area, Pakistan. *Sedimentary Geology*, **81**: 253-268.

FRIEND, P. F., RAZA, S. M., GEEHAN, G. AND SHIEKH, K. A., 2001. Intermediate-scale architectural features of the fluvial Chinji Formation (Miocene), Siwalik Group, Northern Pakistan. *Journal of Geological Society*, London, **158** (1): 163-177.

GOODMAN A. H., ARMELAGOS, G. J. AND ROSE, J. C., 1980. Enamel hypoplasias as indicators of stress in three prehistoric populations from Illinois. *Human Biology*, **52**: 515–528.

GOODMAN, A. H. AND ROSE, J. C., 1990. The assessment of systemic physiological pertubations from dental enamel hypoplasias and associated histological structures. *Yearbook of Physical Anthropology*, **33**: 59–110.

GOODMAN, A.H. AND ROSE, J. C., 1991. Dental enamel hypoplasias as indicators of nutritional status. In (M. Kelly & C. Larsen, Eds) *Advances in Dental Anthropology*. New York: Wiley-Liss, 279-293.

GORLIN, R. J. AND GOLDMAN, H. M., 1970. Thoma's Oral Pathology. The C. V. Mosby Co., St. Louis.

GUATELLI-STEINBERG, D., 2000. Linear enamel hypoplasia in gibbons (Hylobates lar carpenteri). *American Journal of Physical Anthropology*, **112**: 395-410.

GUATELLI-STEINBERG, D., 2003. Macroscopic and microscopic analysis of linier enamel hypoplasia in Plio-Pleistocene South African hominins with respect to aspects of enamel development and morphology. *American Journal of Physical Anthropology*, **120**: 309-322.

GUATELLI-STEINBERG, D., 2004. Analysis and significance of linear enamel hypoplasia in Plio-Pleistocene hominins. *American journal of Physical Anthropology*, **123**: 199-215.

GUITA, J. L., 1984. Oral Pathology, 2nd Ed. Baltimore: Williams and Wilkins.

HARRISON., T. M., COPELAND., P., HALL., S. A., QUADE., J., BURNER., S., OJAH., T. P. AND KIDD., W. S. F., 1993. Isotopic preservation of Himalayan/Tibetan uplift, denudation, and climatic histories of two molasses deposits. *Journal of Geology*, **101**: 157-175.

HEDBERG, H. D., 1976. International Stratigraphic Guide, Ed. IUGS Commission on Stratigraphy. J. Wiley and Sons, New York, 200 p.

HEISSIG, K., 1972. Palaontologische und geologische untersuchungen im tertiar von Pakistan. Rhinocerotidae (Mamm.) aus den unteren und mittleren Siwalik- Schichten. Abh. Bayer. Akad. Wiss., Munich (NF)., **152**: 1-112.

HEISSIG, K., 2003. Change and Continuity in Rhinoceros faunas of Western Eurasia from the Middle to the Upper Miocene. EEDEN, *Stará Lesná*, 35-37.

HEMPHILL, W. R. AND KIDWAI, A. H., 1973. Stratigraphy of the Bannu and Dera Ismail Khan Areas, Pakistan. *United States Geological Survey Professional Paper*, **716**-B: 1–36.

HILLMAN-SMITH, A. K. K., OWEN-SMITH, N., ANDERSON, J. L., HALL-MARTIN, A. J. AND SELALADI J. P., 1986. Age estimation of the White rhinoceros (*Ceratotherium simum*). *Journal of Zoology*, London, **210**: 355-379.

HILLSON, S., 1986. Teeth. Cambridge University Press, Cambridge, 376 p.

HILLSON, S., 1996. Dental Anthropology, Cambridge University Press, Cambridge.

HILLSON, S. AND Bond, S., 1997. Relationship of enamel hypoplasia to the pattern of tooth crown growth: a discussion. *American journal of Physical Anthropology*, **104**: 89-103.

HILLSON, S., 2005. Teeth, second ed., Cambridge University Press, Cambridge.

HODELL, D. A., ELMSTRON, K. M. AND KENNETT, J. P., 1986. Latest Miocene benthic d180 changes, global ice volume, sea level and the "Messinian salinity crisis*". Nature*, **320**: 411-414.

HODGES, K. V., 2000. Tectonics of the Himalayas and southern Tibet from two perspectives. *Geological Society of America Bulletin*, **112** (3): 324-350.

HOSSAIN, H. M. Z., SAMPEI, Y. AND ROSER, B. P., 2013. Polycyclic aromatic hydrocarbons (PAHs) in late Eocene to early Pleistocene mudstones of the Sylhet succession, NE Bengal Basin, Bangladesh: Implications for source and paleoclimate conditions during Himalayan uplift. *Organic Geochemistry*, **56**: 25-39.

HUSSAIN, S. T. AND SONDAAR, P. Y., 1968. Some anomalous features in Euroasiatic *Hipparion* dentition. *Koninkl Nederl Akademie Van Wetenschappen*, **71** (2): 137-143.

HUSSAIN, S. T., VAN DEN BERGH, G. D., STEENSMA, K. J., DE VISSER, J. A., DE VOS, J., ARIF, M., VAN DAAM, J., SONDAAR, P. Y. AND MALIK, S. B., 1992. Biostratigraphy of the Plio-Pleistocene continental sediments (Upper Siwaliks) of the Mangla-Samwal anticline, Azad Kashmir, Pakistan. *Koninklijke Nederlans Akad. Van wet*., **95** (1): 65-80.

JACBOS, L. L., CHEEMA, I. U. AND SHAH, S. M. I., 1981. Zoogeographic implications of early Miocene rodents from the Bugti Beds, Baluchistan, Pakistan. *Geobios*, **15**: 101-103.

JANIS, C., 1993. Tertiary Mammal Evolution in the context of Changing Climates, Vegetation, and Tectonic Events. *Annu. Rev. Ecol. Syst*, **24**: 467-500.

KENNETT, J. P., 1986. 42. Miocene to early Pliocene oxygen and carbon isotope stratigraphy in the Southwest Pacific, Deep Sea Drilling Project Leg 90. *Initial reports of the Deep Sea Drilling Program*, **90**: 1383-1411.

KHAN, I. A., BRIDGE, J. S., KAPPELMANT, J. AND WILSONT, R., 1997. Evolution of Miocene fluvial environments, eastern Potwar plateau, northern Pakistan. *Sedimentology*, **44**: 221-251.

KHAN, A. M., 2009. Taxonomy and distribution of rhinoceroses from the Siwalik Hills of Pakistan. Unpublished PhD Thesis, Punjab University, Lahore, 180 p.

KIERDORF, H., ZEILER, J. AND KIERDORF, U., 2006. Problems and pitfalls in the diagnosis of linear enamel hypoplasia in check teeth of cattle. *Journal of Archaeological Sciences*, **33**: 1690-1695.

KING, T., HILLSON, S. AND HUMPHERY, L. T., 2002. A detailed study of enamel hypoplasia in a post-medieval adolescent of known age and sex. *Archives of oral Biology*, **47**: 29-39.

KOCH, P. L., FISHER, D. C. AND DETTMAN, D., 1989. Oxygen Isotope Variation in the tusks of extinct proboscideans: A measure of season of death and seasonality. *Geology*, **17**: 515-519.

LAKHANPAL, R. N., 1970. Tertiary Floras of India and Their Bearing on the Historical Geology of the Region. *Taxon*, **19** (5): 675-694.

LARSEN, C.S., 1997. Bioarchaeology, Cambridge University Press, Cambridge.

LEWIS, G. E., 1937. Taxonomic syllabus of Siwalik fossil Anthropods (India). *American Jour. Sci*., **237** (4): 275-280.

LEWIS, G. E., 1937a. A new Siwalik correlation (India). *American Jour. Sci*., **33** (5): 191-204.

Lindsay, E.H. AND Downs, W.R., 2000. Age assessment of the Chitarwata Formation. *Himal. Geol*., **21**: 99-107.

LINDSAY, E. H., FLYNN, L. J., CHEEMA, I. U., BARRY, J. C., DOWNING, K. F., RAJPAR, A. R. AND RAZA, S. M., 2005. Will Downs and the Zinda Pir Dome. *Palaeontologia Electronica*, **8** (21A): 1–19.

LUKACS, J. R., 2001. Enamel hypoplasia in the deciduous teeth of early Miocene catarrhines: evidence of perinatal physiological stress. *Journal of Human Evolution*, **40**: 319–329.

MARTIN, C., BENTALEB, I. AND ANTOINE, P. –O., 2011. Pakistan mammal tooth stable isotopes show paleoclimatic and paleoenvironmental changes since the early Oligocene. *Palaeogeography, Palaeoclimatology, Palaeoecology*, **31**(1-2): 19-29.

MARIVAUX, L., WELCOMME, J. -L., ANTOINE, P. -O., MÉTAIS, G., BALOCH, I. M., BENAMMI, M., CHAIMANEE, Y., DUCROCQ, S., JAEGER, J. -J., 2001. A fossil Lemur from the Oligocene of Pakistan. *Science*, **294**: 587–591.

MARIVAUX, L., ANTOINE, P, BAQRI, S. R. H., BENAMMI, M., CHAIMANEE, Y., CROCHET, J., FRANCESCHI, D., IQBAL, N., JAEGER, J. -J., METAIS, G., ROOHI, G. AND WLECOMME, J. 2005. Anthropoid primates from the Oligocene of Pakistan (Bugti Hills): Data on early anthropoid evolution and biogeography. *Proceedings of the National Academy of Sciences of the USA*, (PNAS), **102** (24): 8436-8441.

MATHUR, Y. K., 1984. Cenozoic palynofossils, vegetation, ecology and climate of the north and northwestern sub-himalayan region, India. In R. O. Whyte (ed.), The evolution of the South Asian environment, pp. 504-551. Hong Kong, University Hong Kong.

MEAD, A. J., 1999. Enamel hypoplasia in Miocene rhinoceroses (*Teleoceras*) from Nebraska: evidence of severe physiological stress. *Journal of Vertebrate Paleontology*, **19** (2): 391–397.

MEDLICOTT, H. B., 1864. On the geological structure and relations of the Southern portion of the Himalayan range between the Rivers Ganges and Ravee. *Geol. Surv. India, Mem.* III.

METAIS, G., ANTOINE, P. -O., BAQRI, S. R. H., CORCHET, J. -Y., FRANCESCHI, D., MARIVAUX, L. AND WELCOMME, J.-L., 2009. Lithofacies, depositional environments, regional biostratigraphy and age of the Chiterwata Formation in the Bugti Hills, Balochistan, Pakistan. *Journal of Asian Earth Sciences*, **34**: 154-167.

MORGAN, M. E., KINGSTON, J. D. AND MARINO, B. D., 1994. Carbon isotopic evidence for the emergence of C_4 plants in the Neogene from Pakistan and Kenya. *Nature*. **367**: 162-165.

MORGAN, M. E., BEHRENSMEYER, A. K., BADGLEY, J., BARRY, J. C., NELSON, S. AND PILBEAM, D., 2009. Lateral trends in carbon isotope ratios reveal a Miocene vegetation gradient in the Siwaliks of Pakistan. *Geology*, **37** (2):103-106.

MOGGI-CECCHI, J. AND CRIVELLA, S., 1991. Occurrence of enamel hypoplasia in the dentitions of simians primates. *Folia Primatologia*, **57**: 106-110.

MOLNAR, P., 2005. Mio-Pliocene Growth of the Tibetan Plateau and Evolution of the East Asian Climate. *Palaeontologia Electronica*, **8**: 23 p.

MORLEY, R.J., 1998. Palynological evidence for Tertiary plant dispersal in the SE Asian region in relation to plate tectonics and climate. In: R. Hall, J.D. Holloway (Eds), *Biogeography and geological evolution of SE Asia*. Backhuys. Leiden, pp. 211-234.

NANDA A. C., 2008. Comments on the Pinjor Mammalian Fauna of the Siwalik Group in relation to the post-Siwalik faunas of Peninsular India and Indo-Gangetic Plain. *Quaternary International*, **192**: 6–13.

NEIBURGER, E. J., 1990. Enamel hypoplasia: poor indicators of dietary stress. *American Journal of Physical Anthropology*, **82**: 231–232.

NELSON, S.V., 2007. Isotopic reconstructions of habitat change surrounding the extinction of *Sivapithecus*, a Miocene hominoid, in the Siwalik Group of Pakistan: *Palaeogeography, Palaeoclimatology, Palaeoecology*, **243** (1–2): 204–222.

NIVEN, L. B., EGELAND, C.P. AND TODD, L.C., 2004. An inter-site comparison of enamel hypoplasia in bison: implications for paleoecology and modeling Late Plains Archaic subsistence. *Journal of Archeological Science*, **31**: 1783-1794.

ORLIAC, M. J., ANTOINE, P, -O., METAIS, G., CROCHET, J. -Y., MARIVAUX, L., ROOHI, G. AND WELCOMME, J. -L., 2009. *Listridon guptai* Pilgrim, 1926 (Mammalia, Suidae) from the early Miocene of the Bugti Hills, Balochistan, Pakistan: New insights into early Listriodontinae evolution and biogeography. *Naturwissenschaften*, DOI 10.1007/s00114-009-0547-4.

OSBORN. H.F., 1936. Proboscidea, 1. American Museum Press, New York, 802 p.

PASCOE, E. H., 1920. Early history of the Indus, Brahamaputra, and Ganges. *Geol. Soc. London., Quart. Jour*., **75**: 138-158.

PATNAIK, R., 2003. Reconstruction of Upper Siwalik palaeoecology and palaeoclimatology using microfossil palaeocommunities. *Palaeography, Palaeoclimatology, Palaeoecology*, **197** (1-2): 133-150.

PATNAIK, R., 2013. Indian Neogene Siwalik Mammalian Biostratigraphy: An Overview. In: Wang Xiaoming, L.J. Flynn and M. Fortelius, (eds.), Fossil Mammals of Asia; Neogene Biostratigraphy and Chronology. Columbia University Press. 752 p.

PICKFORD, M., 1982. Miocene Chalicotheriidae of the Potwar Plateau, Pakistan. *Tertiary Res*, **4**: 13-29.

PILBEAM, D. R., BARRY, J. C., MEYER, G. E., SHAH, S. M. I., PICKFORD, M. H. L., BISHOP, W. W., THOMAS, H. AND JACOBS, L. L., 1977. Geology and paleontology of Neogene strata of Pakistan. *Nature*, **270**: 684-689.

PILBEAM, D. R., MEYER, G. E., BADGLEY, C. ROSE, M. D., PICKFORD, M. H. L., BEHRENSMSYER, A. K. AND SHAH, S. M. I., 1977b. New hominoid primates from the Siwaliks of Pakistan and their bearing on hominoid evolution. *Nature*, **270**: 689-695.

PILBEAM, D. R., BEHRENSMEYER, A. K., BARRY, J. C. AND SHAH, S. M. I., 1979. Miocene sediments and faunas of Pakistan. *Postilla*, **179**: 1-45.

PILBEAM, D. R., MORGAN, M., BARRY, J. C. AND FLYNN, L., 1996. European MN units and the Siwalik faunal sequence of Pakistan. S. Rietschel, eds. Evolution of Neogene Continental biotopes in Central Europe and the eastern Mediterranean. New York, Columbia University Press, pp. 96-105.

PILGRIM , G. E., 1910. Notices of new Mammalian genera and species from the Tertieries of India, Calcutta. *Rec. Geol. Surv. India*, **40**: 63-71.

PILGRIM, G.E., 1910b. Preliminary note on a revised classification of the Tertiary freshwater deposits of India. *Records of the Geological Survey of India*, **40**: 185–205.

PILGRIM, G.E., 1912. The vertebrate fauna of the Gaj series in the Bugti hills and the Punjab. *Memoirs of the Geological Survey of India*, **4**: 1–83.

PILGRIM , G. E., 1913. The correlation of the Siwaliks with the mammalian horizons of Europe. *Rec. Geol. Surv. India*, **43**: 264–326.

PINFOLD, E. S., 1918. Notes on structure and stratigraphy in the northwest Punjab. *Geol. Surv. India. Rec*., b (3): 137-160.

PARSAD, M., 1993. Siwalik (Middle Miocene) woods from the Kalagarh area in the Himalayan foot hills and their bearing on paleoclimate and phytography. *Review of Paleobotany and Palynology*, **76**: 49-82.

POTTS, R. AND BEHRENSMEYER, A. K., 1992. Late Cenozoic Terrestrial Ecosystems. *Terrestrial ecosystems through time*, pp. 419-451.

PRASAD, K. N., 1964. Upper Miocene Anthropoids from the Siwalik beds of Haritalyangar area, H. P., India. *Paleontology*, **7**: 124-134.

QUADE, J. AND CERLING, T.E., 1995, Expansion of C_4 grasses in the late Miocene of northern Pakistan: evidence from stable isotopes in paleosols. *Palaeogeography, Palaeoclimatology, Palaeoecology*, **115**: 91-116.

QUADE, J., ROE, L., DE CELLES, P.G. AND OJHA, T.P., 1997. The late Neogene $^{87}Sr/^{86}Sr$ record of lowland Himalayan Rivers. *Science*, **276**: 1828-1831.

RAZA, S. M., 1983. Taphonomy and paleoecology of middle Miocene vertebrate assemblages, southern Potwar Plateau, Pakistan. Thesis. Yale Univ., New Haven, USA, 414 p.

RAZA, S. M. AND MEYER, G. E., 1984. Early Miocene geology and paleontology of the Bugti Hills. *Geological Survey of Pakistan*, 11: 43–63.

RAZA, S. M., BARRY, J. C., MEYER, G. E. AND MARTIN, L. D., 1984. Preliminary report on the geology and vertebrate fauna of the Miocene Manchar Formation, Sind, Pakistan. *Journal of Vertebrate Paleontology*, **4**: 584–599.

RAZA, S. M., CHEEMA, I. U., DOWNS, W. R., RAJPAR, A. R. AND WARD, S. C., 2002. Miocene stratigraphy and mammal fauna from the Sulaiman Range, Southwestern Himalayas, Pakistan. *Palaeogeography, Palaeoclimatology, Palaeoecology*, **186**: 185–197.

ROBERTS, T. J. 1997. The mammals of Pakistan. Oxford University Press. Karachi. 425 p.

RODDAZ, M., SAID., GUILLOT, S., ANTOINE, P. -O. MONTEL, J. -M. AND MARTIN, F., 2011. Provenance of Eocene-Early Miocene Pakistan foreland basin sediments: implication for the exhumation of the Higher Himalaya and climatic change. *Journal of the Geological Society of London*, **168**: 499-516.

ROGL, C. F., 1998. Palaeogeographic considerations for Mediterranean and Paratethys seaways (Oligocene to Miocene). *Annalen des Naturhistorischen,* Museums in Wien, **99** A: 279-310.

ROWLEY, D. B., 1996. Age of initiation of collision between India and Asia: a review of biostratigraphy data. *Earth and Planetary Science Letters*, **145**: 1-13.

SAHNI, M. R. AND MATHUR, L. P., 1964. Stratigraphy of the Siwalik Group. *International Geol. Congr., 22nd, New Delhi, Procs*., 1-24 p.

SHAFER, W. G., HINE, M. K. AND LEVY, B. M. A., 1983. Text book of Oral Pathology, 4th ed. Philadelphia: WB Saunders.

SHAH, S. M. I., 1977. Stratigraphy of Pakistan. *Memoirs of the Geological Survey of Pakistan*, **12**: 1-138.

SHAH, S. M. I., 2009. Stratigraphy of Pakistan. *Memoirs of the Geological Survey of Pakistan*, **22**: 1-381.

SKINNER, M. F., 1986. An enigmatic hypoplastic defect of the deciduous canine. *American Journal of Physical Anthropology*, **69**: 59–69.

SKINNER, M. F. AND HUNG, J. T. W., 1989. Social and biological correlates of localized enamel hypoplasia of the human deciduous canine tooth. *American Journal of Physical Anthropology*, **79**: 159–175.

SKINNER, M. AND GOODMAN, A. H., 1992. Anthropological uses of developmental defects of enamel; pp. 153-174 in Saunders, S. R. & Katzenberg, M. A. (eds.), *Skeletal biology of past peoples*: Research Methods. Wiley-Liss, Inc., New York.

SKINNER, M.F. AND HOPWOOD, D., 2004. Hypothesis for the cause and periodicity of repetitive enamel hypoplasia in large, wild African (*Pan torglodates* and *Gorilla gorilla*) and Asian (*Pongo pygmaeus*) apes. *American Journal of Physical Anthroplogy*, **123**: 216-235.

SONGTHAM, W., RATANASTHEIN, B., MILDENHALL, D.C., SINGHARAJWARAPAN, S. AND KANDHAROSA, W., 2003. Oligocene-Miocene climatic changes in Northern Thailand resulting from extrusion tectonics of southeast Asian landmass. *Science Asia*, **29**: 221-233.

STEWART, R. E. AND POOLE, A. E., 1982. The orofacial structures and their association with congenital abnormalities. *Pediatric Clinic North America*, **29**: 547–584.

STUART-WILLIAMS, H. L. AND SCHWARCZ, H. P., 1997. Oxygen isotopic determination of climate variation using phosphate from beaver bone, tooth enamel, and dentine. *Geochem. Cosmochim. Acta*, **61**: 2539-2550.

SUCKLING, G. W., 1989. Developmental defects of enamel – historical and present-day perspectives of their pathogenesis. *Advances in Dental Research.* **3** (2): 87–94.

TAPPONNIER, P., ZHIQIN, X., ROGER, F., MEYER, B., ARNAUD, N., WITTLINGER, G. AND JINGSUI, Y., 2001. Oblique stepwise rise and growth of Tibet Plateau. *Science*, **194**: 1671-1677.

TIPPLE, B. J. AND PAGANI, M., 2007. The early origins of terrestrial C_4 photosynthesis. *Annual Reviews of Earth and Planetary Sciences*, **35**: 435-461.

TONG, H., 2001. Age Profiles of Rhino Fauna from the Middle Pleistocene Nanjing Man Site, South China---Explained by Rhino Specimens of living species. *International Journal of Osteoarchaeology*, **11**: 231-237.

VINCENT, E., KILLINGLEY, S. J. AND BERGER, W. H., 1985. Miocene oxygen and carbon isotope stratigraphy of the tropical Indian ocean. In J. P. Kennett (ed.), The Miocene Ocean: paleoceanography and biogeography. *Geol. Soc. Am. Mem.*, pp. 103-130.

WELCOMME, J. -L. AND GINSBURG, L., 1997. Miseen evidenced el'Oligocène sur leterritoire des Bugti (Balouchistan, Pakistan). *Comptes Rendus de l'Académie des Sciences de Paris*, série IIa, **325**: 999–1004.

WELCOMME, J. -L., ANTOINE, P. -O., DURANTHON, F., MEIN, P. AND GINSBURG, L., 1997. Nouvelles découvertes de vertébrés miocènes dans le synclinal de Dera Bugti (Balouchistan, Pakistan). *Comptes Rendus de l'Académie des Sciences de Paris*, série IIa, **325**: 531–536.

WELCOMME, J.-L., MARIVAUX, L., ANTOINE, P.-O. AND BENAMMI, M., 1999. Mammiferes fossils des Collines Bugti (Baluchistan, Pakistan). Nouvelles données. *Bulletin de la Société d'Histoire Naturelle de Toulouse*, **135**: 135–139.

WELCOMME, J. -L., BENAMMI, M., CROCHET, J. -Y., MARIVAUX, L., MÉTAIS, G., ANTOINE, P. -O. AND BALOCH, I. S., 2001. Himalayan Forelands: paleontological evidence for Oligocene detrital deposits in the Bugti Hills (Balochistan, Pakistan). *Geological Magazine*, **138**: 397–405.

WADIA, D. N., 1928. The geology of the Poonch State (Kashmir) and adjacent portions of the Punjab. *Geol. Surv. India, Mem*., **51** (2): 185-370.

WYNNE, A. B., 1877. Note on the Tertiary zone and the underlying rocks in the northwest Punjab. *Geol. Surv. India. Rec.*, **10**: 107-132.

XU, Y., ZHANG, K., WANG, G., JIANG, S., CHEN, F., XIANG, S., DUPONT-NIVET, G. AND HOORN, C., 2012. Extended stratigraphy, palynology and depositional environments record the initiation of the Himalayan Gyirong Basin (Neogene China): *Journal of Asian Earth Sciences*, **44**: 77-93.

ZACHOS, J.C., PAGANI, M., SLOAN, L., THOMAS, E. AND BILLUPS, K., 2001. Trends, rhythms, and aberrations in global climate 65 Ma to present. *Science*, **292**: 686-693.

YAEGER, J., 1980. Enamel. In SN Bhaskar (ed): Orban's Oral Histology and Embryology (9^{th} Ed). St. Louis: C. V. Mosby, pp. 46-106.

Appendix 1

PUBLISHED MATERIAL

THE LINNEAN SOCIETY of London ZOOLOGICAL Journal of the Linnean Society

Zoological Journal of the Linnean Society, 2010, **160**, 139–194. With 13 figures

A revision of *Aceratherium blanfordi* Lydekker, 1884 (Mammalia: Rhinocerotidae) from the Early Miocene of Pakistan: postcranials as a key

PIERRE-OLIVIER ANTOINE[1,2,3]*, KEVIN F. DOWNING[4], JEAN-YVES CROCHET[5], FRANCIS DURANTHON[6], LAWRENCE J. FLYNN[7], LAURENT MARIVAUX[5], GRÉGOIRE MÉTAIS[8], ABDUL RAHIM RAJPAR[9] and GHAZALA ROOHI[9]

[1]*Université de Toulouse, UPS (SVT-OMP), LMTG, 14 Avenue Édouard Belin, F-31400 Toulouse, France*

[2]*CNRS, LMTG, 14 Avenue Édouard Belin, F-31400 Toulouse, France* [3]*IRD, LMTG, 14 Avenue Édouard Belin, F-31400 Toulouse, France* [4]*DePaul University, Chicago, IL 60604, USA*
[5]*Département de Paléontologie, Institut des Sciences de l'Évolution (CNRS-UMR 5554) Université Montpellier 2, c.c. 064, Place Eugène Bataillon, F-34095 Montpellier Cedex 5, France*
[6]*Laboratoire d'Étude et de Conservation du Patrimoine, Muséum d'Histoire naturelle de Toulouse, 39 allées Jules Guesde, F-31000 Toulouse, France*
[7]*Department of Anthropology and Peabody Museum, Harvard University, Cambridge, MA 02138, USA* [8]*Laboratoire de Paléontologie, UMR 5143 CNRS, Muséum National d'Histoire Naturelle, 8 rue Buffon, F-75005 Paris, France*

[9]*Earth Sciences Division, Pakistan Museum of Natural History, Garden Avenue, Shakarparian, 44000 Islamabad, Pakistan*

Received 22 January 2009; accepted for publication 28 April 2009

Rhinocerotids are particularly abundant and diversified in Neogene deposits of the Indian subcontinent, but their systematics is far from being well defined. Based on the revision of old collections and new findings from the Early Miocene of the Bugti Hills and Zinda Pir, Pakistan, '*Aceratherium blanfordi* Lydekker, 1884' is a chimera, consisting of two dentally convergent but postcranially distinct rhinocerotid taxa: *Pleuroceros blanfordi* and ***Mesaceratherium welcommi* sp. nov.** Postcranial features appear to be much more diagnostic than craniodental morphology in this case. A phylogenetic analysis based on 282 morphological characters scored for 28 taxa (four outgroups and ingroup including both taxa of interest and a 'branching group') strengthens this statement and supports *Pleuroceros* and *Mesaceratherium* as monophyletic genera within Rhinocerotinae. Both genera are recognized for the first time outside Europe. In the Bugti Hills, *P. blanfordi* and *M. welcommi* are part of an exceptionally diversified rhinocerotid fauna, with up to nine species associated in the same locality (Kumbi 4f). This rhinocerotid assemblage confirms the earliest Miocene age (Agenian/Aquitanian) of the upper member of the Chitarwata Formation as a whole. Coeval homotaxic rhinocerotid faunas from Europe (France, Czech Republic) and East Africa (Uganda, Kenya) support broad and sustainable rhinocerotid interchanges amongst South Asia, Europe, and Africa under compatible environmental conditions throughout earliest Miocene times.

ADDITIONAL KEYWORDS: Bugti Hills – Chitarwata Formation – cladistics – Indian subcontinent – *Mesaceratherium* – palaeobiogeography – Perissodactyla – *Pleuroceros* – Zinda Pir.

*Corresponding author. E-mail: poa@lmtg.obs-mip.fr

INTRODUCTION

The Tertiary deposits of the Bugti Hills (Balochistan, Pakistan; Fig. 1) have yielded innumerable fossil ver-tebrates, amongst which rhinocerotoids are particu-larly abundant and diversified. Despite the high productivity of fossil vertebrates, most of the recorded fossils were studied around a century ago (Blanford, 1876, 1879; Lydekker, 1881, 1884, 1886; Pilgrim, 1910, 1912; Forster-Cooper, 1924, 1934). Amongst Bugti Hills Rhinocerotidae, '*Aceratherium*' *blanfordi* Lydekker, 1884 is widely represented in original, classic collections (Natural History Museum, London; Indian Museum, Calcutta). Lydekker (1884: 2) named '*Aceratherium blanfordi*, n. sp., *nobis*' (his nomencla-ture) on the basis of a P4–M2 series from the 'Siwa-liks of Punjab', which was originally referred to *Rhinoceros palaeindicus* by Lydekker (1881), and a few dental remains originating from the Bugti Hills area (Dera Bugti and Gandoi localities). Lydekker (1884: 2–11) split its hypodigm into two classes, including a 'larger race' and a 'smaller race'. Later, Pilgrim (1910: 66) proposed restriction of the species *A. blanfordi* Lydekker, 1884 to the hypodigm of the

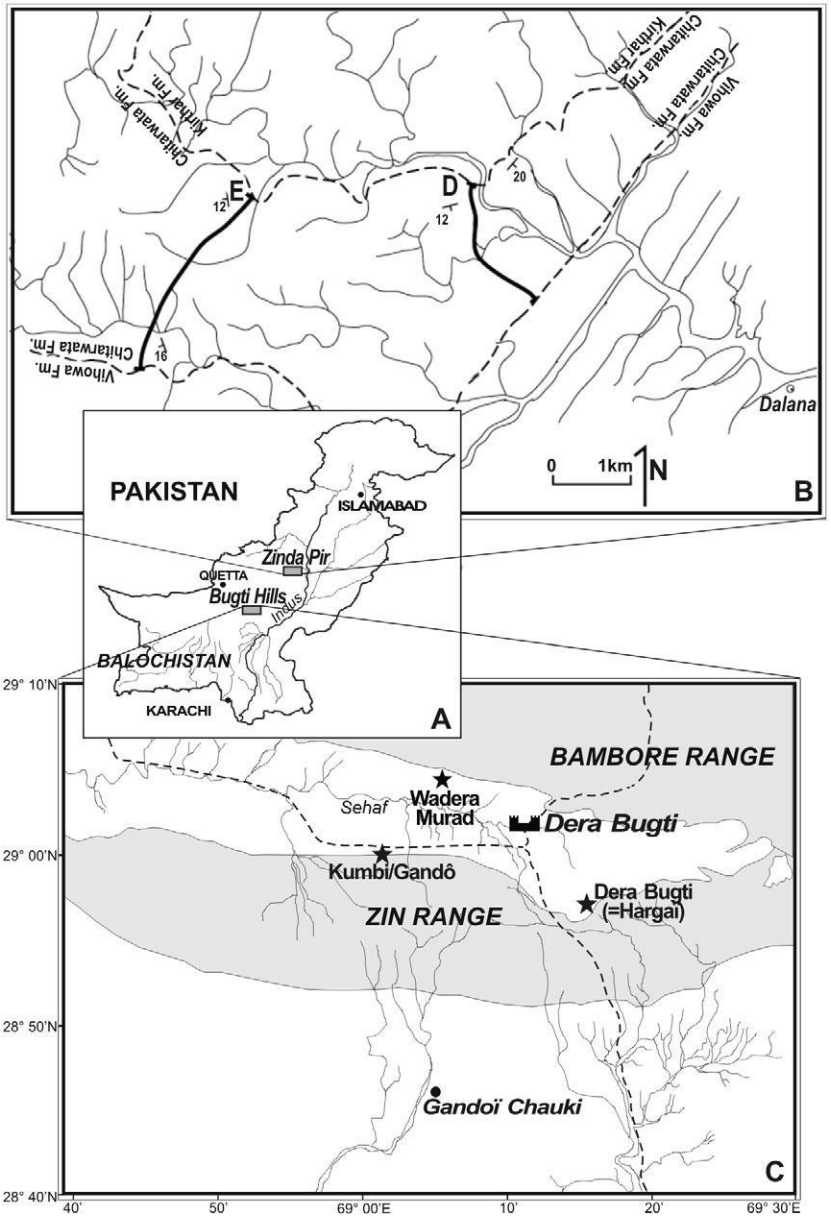

Figure 1. A, Index map of south-western Pakistan, showing the location of the main areas discussed in the text; B, enlargement of the Zinda Pir Dome area; C, enlargement of the Bugti area, with detailed location of mentioned localities.

larger series, via the awkward '*A. blanfordi* var. *majus* (probably a *Teleoceras*)'. This author then erected the new species '*Diceratherium naricum* Pilgrim, 1910' on the base of '*A. blanfordi* var. *minus* Lydekker (1884)'. In recent works (Antoine & Welcomme, 2000; Antoine *et al.*, 2003a; Antoine, Duranthon & Welcomme, 2003b; Métais *et al.*, 2009) the latter species was excluded from the waste-basket taxon *Diceratherium* Marsh, 1875 and referred to the genus *Plesiaceratherium* Young, 1937, owing to new interpretations of better fossil collections. However, the splitting proposed by Pilgrim (1910) did not clarify the affinities of the larger form, '*A. blanfordi*' *sensu stricto*, nor did it stabilize its generic assign-ment. In fact, this species was successively referred to *Teleoceras* Hatcher, 1894 by Pilgrim (1912), to *Chilotherium* Ringström, 1924 by Ringström (1924), Matthew (1929), and Forster-Cooper (1934), to *Acer-atherium* Kaup, 1832 by Heissig (1972), to *Aprotodon* Forster-Cooper, 1915 by Welcomme *et al.* (1997), and to *Rhinoceros* von Linnaeus, 1758 by Downing (2005).

Recent fieldwork campaigns in the same area by a French–Balochi team (*Mission Paléontologique Franco-Balouche*, 1995–2004) led to the recovery of hundreds of new cranial, dental, and postcranial remains referred to hyracodontids, amynodontids, and rhinocerotids in a stratigraphically controlled context (Welcomme *et al.*, 1997, 1999, 2001; Antoine & Welcomme, 2000; Antoine *et al.*, 2003a, b, 2004; Métais *et al.*, 2009). As previously argued by Welcomme & Ginsburg (1997), the new stratigraphi-cal framework in the field proved that the so-called 'Bugti fauna' was a set of distinct faunas from suc-cessive levels in this rock unit, ranging from the Early Oligocene up to the Late Miocene (Welcomme *et al.*, 1999, 2001; Antoine *et al.*, 2003b; Métais *et al.*, 2009). Thanks to these new findings, postcranials were for the first time attributed to '*A.*' *blanfordi* with confidence, some of them being recovered in associa-tion with both cranial and dental remains. Further comparison of these specimens has revealed wide morphological and metrical discrepancies, especially in the postcranial skeleton: the largest teeth (with thick enamel) are always associated with long and slender limb bones, whereas the smallest teeth (with thinner enamel) occur with somewhat shorter and more robust limbs. Comparison with the previously described specimens (including types), stored in the Natural History Museum, London, and with new material from the upper member of the Chitarwata Formation (Fm.) in the Zinda Pir (Downing, 2005; Lindsay *et al.*, 2005) confirms such a mismatch, and reveals that '*A.*' *blanfordi* is most probably a chimera, including two dentally convergent but postcranially distinct taxa that we describe and compare in this paper.

MATERIAL AND METHODS

STRATIGRAPHICAL CONTEXT

In the Bugti Hills, the outcrops usually extend over dozens of kilometres, so that several loci may docu-ment each fossiliferous level. For instance, different localities within Level 4 (earliest Miocene; Fig. 2) bear the name of the nearest spring or village (Dera Bugti, Kumbi, Gandô), associated with the number 4. As such, Dera Bugti 4, Kumbi 4a, Kumbi 4f, and Gandô 4 are laterally equivalent and considered as coeval. The same principle is applied for other levels or loci located in the Dera Bugti syncline (from 0 up to 7). Correlations get more complicated when consid-ering coeval loci situated in the Gandoï Chauki syn-cline, i.e. south to the Zin Koh anticline (Fig. 1). In this area, the levels are also sorted chronostrati-graphically, but they are labelled with letters rather than with numbers. Hypotheses of stratigraphical equivalences are summarized in Figure 2.

The fossiliferous levels document a long time range, spanning the Oligocene epoch and most of the Miocene times (Antoine *et al.*, 2003b). The lowest levels [Level 0 (= 0) to Level 3 (= J2)] correspond to Oligocene deltaic then fluvial deposits referred to the Bugti Member of the Chitarwata Fm. (Métais *et al.*, 2009); upper in the series, the levels 3bis (= M) and 4 (= Q) consist of river-lacustrine deposits attributed to the upper Member of the Chitarwata Fm., and referred to the earliest Miocene (Welcomme *et al.*, 2001; Antoine *et al.*, 2003a, b, 2004); overlying fossil-iferous strata are Levels 5 (= T), 6, and 6sup (Welcomme *et al.*, 2001; Métais *et al.*, 2009) from the lowest deposits referred to the Vihowa Fm. (late Early Miocene), and considered as coeval to the Kamlial Fm. from the Potwar Plateau series (Welcomme *et al.*, 1997, 2001; Barry *et al.*, 2002; Lindsay *et al.*, 2005; Métais *et al.*, 2009). Much higher in the series another rhino-bearing locality is referred to as Sartaaf (= Djigani, Level 7), the mammal fauna of which indicates a Late Miocene age, equivalent to the Dhok Pathan Fm. of the Potwar Plateau (Antoine *et al.*, 2003b).

The new Bugti specimens mainly originate from localities referred to the upper member of the Chitar-wata Fm. (level 4, earliest Miocene; Fig. 2); a few other were unearthed in the base of the overlying Vihowa Fm. (levels 5–6sup, Early Miocene; Fig. 2).

The specimens unearthed in the Zinda Pir area and described herein were recovered in distinct levels of sections D and E, in the Dalana area (Fig. 1; Lindsay *et al.*, 2005: fig. 3). They occur throughout the upper member of the Chitarwata Fm., which is tentatively parallelized with the Agenian European Land Mammal Age (Fig. 2; Downing, 2005; Lindsay *et al.*, 2005; Métais *et al.*, 2009). This period roughly

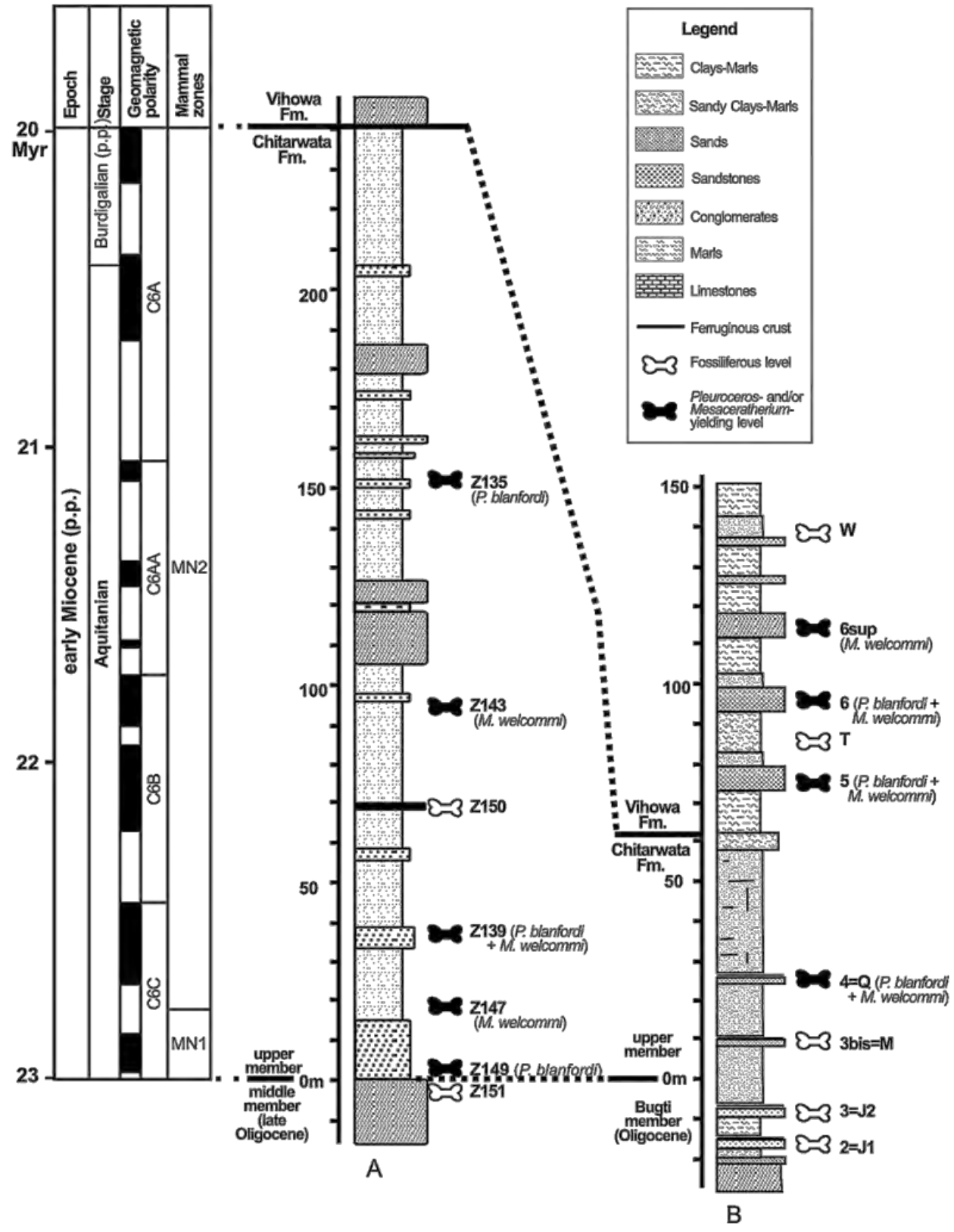
Epoch
Stage
Geomagnetic polarity
Mammal zones
20 Myr
21
22
23
early Miocene (p.p.)
Aquitanian
Burdigalian (p.p.)
C6A
C6AA
C6B
C6C
MN2
MN1
Legend
Clays-Marls
Sandy Clays-Marls
Sands
Sandstones
Conglomerates
Marls
Limestones
Ferruginous crust
Fossiliferous level
Pleuroceros- and/or Mesaceratherium-yielding level
Vihowa Fm.
Chitarwata Fm.
200
150
100
50
Z135 (P. blanfordi)
Z143 (M. welcommi)
Z150
Z139 (P. blanfordi + M. welcommi)
Z147 (M. welcommi)
Z149 (P. blanfordi)
Z151
upper member
0m
middle member (late Oligocene)
A
W
6sup (M. welcommi)
6 (P. blanfordi + M. welcommi)
T
5 (P. blanfordi + M. welcommi)
4=Q (P. blanfordi + M. welcommi)
3bis=M
3=J2
2=J1
Bugti member (Oligocene)
B

Figure 2. Synthetic stratigraphical sections and ranges of the rhinocerotids discussed in the text, in the Zinda Pir area (A) and the Bugti area (B). (A) is a composite section of the upper member of the Chitarwata Fm. based on sections D and E of Downing (2005: fig. 1) and Lindsay *et al.* (2005: fig. 3). (B) is modified from Welcomme *et al.* (2001), Antoine *et al.* (2003b, 2004) and Métais *et al.* (2009). Filled bone symbols indicate *Pleuroceros*- and/or *Mesaceratherium*-yielding levels whereas open bone symbols represent other fossiliferous levels. The upper member of the Chitarwata Formation corresponds to the classic 'Dera Bugti Fauna', which is correlated to the earliest Miocene (Aquitanian stage) based on fossil assemblages from levels 3bis-M and 4-Q. Comparisons between the Bugti faunas and biochronologic data from the Dalana area sections at Zinda Pir suggest that the best correlation is consistent with 'correlation B' of Lindsay *et al.* (2005: fig. 6B), which was also taken into account by Métais *et al.* (2009). Correlation of the Bugti and Zinda Pir faunas with standard European Neogene Mammal Zones (Steininger, 1999; Gradstein *et al.*, 2005) and with the Global Polarity Time

Scale (Gradstein *et al.*, 2005; Lindsay *et al.*, 2005) is tentative and mostly based on rodent and perissodactyl assemblages.

corresponds to the Aquitanian stage (*c*. 23–20 Myr; Gradstein, Ogg & Smith, 2005). The available sample from the Zinda Pir (12 specimens) is much smaller than the one from the Bugtis, which may explain the shorter range observed in the former area.

The biochronological framework as it appears in Figure 2 is based on the geological time scale revised in 2004 (Gradstein *et al.*, 2005), whereas lithostrati-graphical and magnetostratigraphical correlations between the Zinda Pir and Bugti areas follow 'inter-pretation B' of Lindsay *et al.* (2005: fig. 6) and the conclusions of Métais *et al.* (2009).

Field sampling: cranial/dental/postcranial associations

Most specimens were recovered isolated in the Dera Bugti and Zinda Pir areas. Thus postcranials had scarcely been identified in the past (Pilgrim, 1912; Forster-Cooper, 1934). Yet, recent collects in the Dera Bugti area have revealed several series associating cranial and dental and/or dental and postcranial remains: as an example, the association between the upper and lower dentitions has been established owing to the series Pak 1031, which includes both dentitions from the same individual. On account of the high specific diversity, we have classified the postcranial specimens after their dimensions, propor-tions, and morphology (structures, facets, and mus-cular insertions). A supplemental control was made owing to 'bone-to-bone' connections and associations.

Material for comparison

The fossils were further associated and determined by direct comparison with reference series: the 'histori-cal' specimens from the Bugti Hills (Falconer & Cautley collection; Forster-Cooper collection; casts of the Pilgrim collection) stored in the Natural History Museum, London; the Early and Middle Miocene rhi-nocerotid faunas from the Aquitaine Basin, stored in the Muséum d'Histoire Naturelle, Toulouse (Antoine, Duranthon & Tassy, 1997) and in the Natural History Museum, London; the Oligocene and Early Miocene rhinocerotid faunas from western Europe stored in Lyon (Muséum d'Histoire naturelle; Laboratoire de Paléontologie, Claude-Bernard University) and Paris (Muséum National d'Histoire Naturelle); the Oli-gocene and Miocene rhinocerotids from Asia and North America stored in the American Museum of Natural History (New York); and the Late Oligocene and earliest Miocene rhinocerotids from Gannat, France (Rhinopolis).

Descriptions of rhinocerotids from the Miocene of Africa (Hooijer, 1966, 1971, 1973), Pakistan (Lydek-ker, 1881, 1884; Pilgrim, 1910, 1912; Heissig, 1972), Anatolia (Heissig, 1976), Arabia (Gentry, 1987), western Europe (Osborn, 1900; Guérin, 1980), and south-western France (de Bonis, 1973; Antoine *et al.*, 2006) provided further useful comparisons.

The specimens stored in the Natural History Museum (London) originate from the Cambridge-Sedgwick Museum Expeditions in the Bugti area, headed by Forster-Cooper in 1910–1911. Their labels generally mention only 'Near Dera Bugti', so it is impossible to determine the precise level(s) from which they were collected.

New specimens from the Dera Bugti area were collected by the French Paleontological Expeditions in Balochistan in 1995–1999. They are currently housed in the Muséum d'Histoire Naturelle in Toulouse, France.

Specimens originating from the Chitarwata Fm. in the vicinity of Dalana, in the Zinda Pir Dome, have their permanent repository in the Pakistan Museum of Natural History. Some of them are temporarily deposited in the Department of Anthropology and Peabody Museum (Harvard University, Cambridge, USA).

Anatomical terminology and phylogenetic characters

Capital letters are used for the upper teeth (I, incisor; C, canine; D, deciduous molar; P, premolar; M, molar), whereas lower case letters indicate lower teeth (i, c, d,

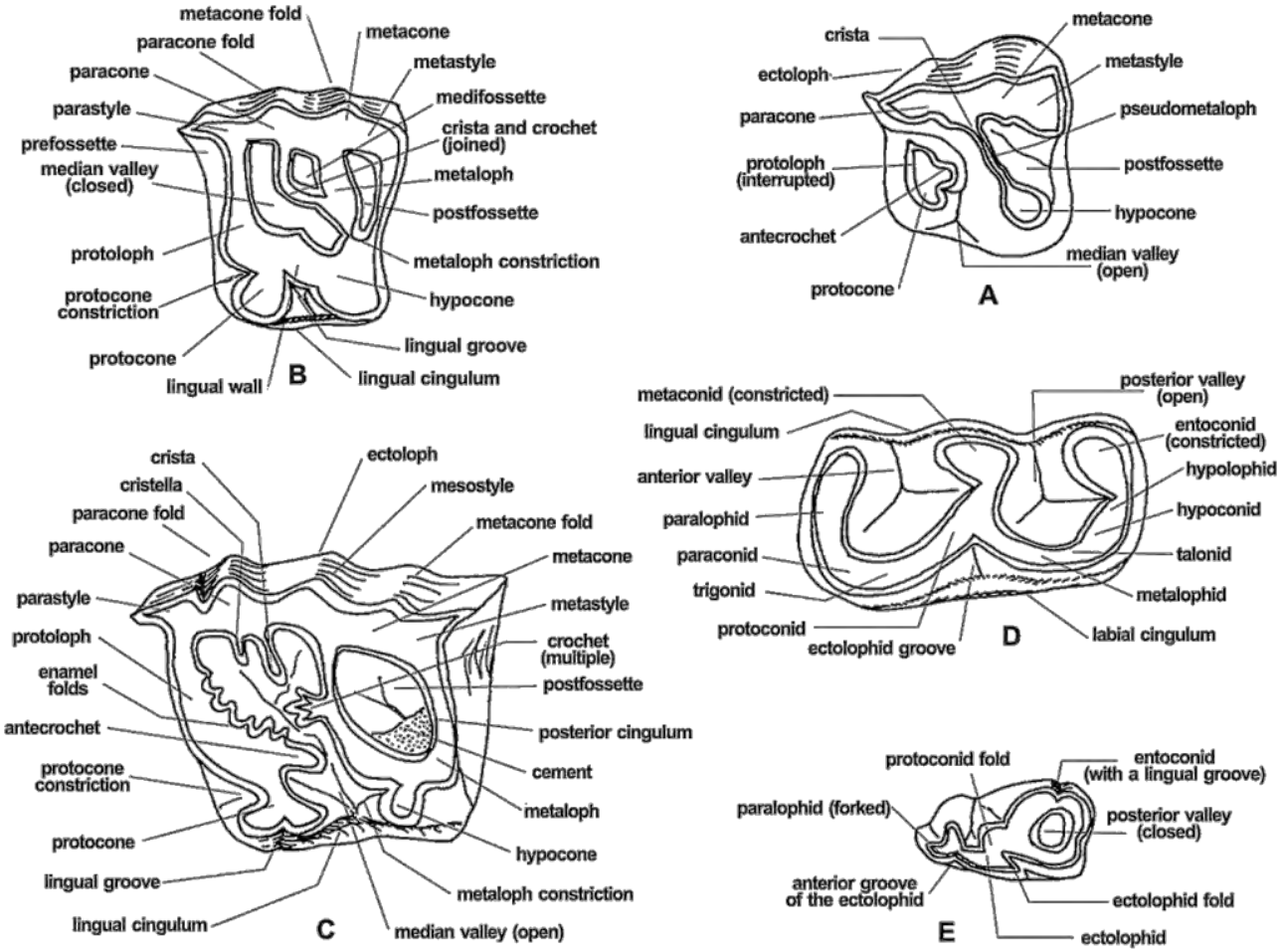

Figure 3. Dental terminology used for rhinocerotids. A, left P2 (hypothetical); B, left P3 or P4 (hypothetical); C, left upper molar (hypothetical); D, left lower molar (hypothetical); E, left d2. Modified from Antoine (2002, fig. 72).

p, m, respectively). Except when mentioned, the dimensions are given in mm.

Rhinocerotid dental terminology follows Heissig (1969: 11–12), Uhlig (1999: 15–16), and Antoine (2002: 122), as summarized in Figure 3; osteological and dental features described correspond bas-ically to cladistic characters used and listed by Antoine (2002, 2003) and Antoine *et al.* (2003b). Post-cranial dimensions follow the protocol defined by Guérin (1980).

Abbreviations

Anatomical orientation

ant, anterior; post, posterior; l, left; r, right; APD, anteroposterior diameter; H, height; L, length; TD, transversal diameter; W, width.

Institutions

BSP, Bayerische Staatssammlung für Paläontologie, Munich; IMC, Indian Museum, Calcutta; MHNT, Muséum d'Histoire naturelle, Toulouse; MNHN, Muséum National d'Histoire Naturelle, Paris; NHM, The Natural History Museum, London; PMNH, Paki-stan Museum of Natural History, Islamabad.

Localities

DB, Dera Bugti; G, Gandô; K, Kumbi.

Taxa

P. b., *Pleuroceros blanfordi*; *M. w.*, *Mesaceratherium welcommi*.

SYSTEMATIC PALAEONTOLOGY

The suprageneric systematics within Rhinocerotidae follows the arrangement of the current phylogenetic analysis (see Phylogenetic relationships).

ORDER PERISSODACTYLA OWEN, 1848
SUPERFAMILY RHINOCEROTOIDEA GRAY, 1821
FAMILY RHINOCEROTIDAE GRAY, 1821
SUBFAMILY RHINOCEROTINAE GRAY, 1821
UNNAMED CLADE
PLEUROCEROS ROGER, 1898

Emended diagnosis: Short-limbed rhinocerotine with a concave occipital crest in dorsal view, a nearly horizontal mandibular symphysis, a reduced lingual cingulum on upper premolars, a strong antecrochet on P4, a protocone deeply constricted and a low and reduced posterior cingulum on M1–2, a smooth and U-shaped external groove on lower cheek teeth, a continuous lingual cingulum on lower premolars, a tridactyl manus (vestigial metacarpal V), a prominent insertion of the m. extensor carpalis on metacarpals, a slender tuber calcanei, and a short insertion of the m. interossei on lateral metapodials.

Type species: Pleuroceros pleuroceros (Duvernoy, 1853)

PLEUROCEROS BLANFORDI (LYDEKKER, 1884)
COMB. NOV. (FIGS 4–7, 11A, 12A)

Rhinoceros palaeindicus Lydekker, 1881: 44–45; pl. 6, fig. 1

Aceratherium blanfordi sp. nov., *nobis* Lydekker, 1884: 2–11, text-fig. 2; pl. 2, figs 1–3
Aceratherium blanfordi var. *majus* Lydekker, 1884: 10; pl. 1, 1–2
Rhinoceros blanfordi var. *majus* Lydekker, 1886: 154
Aceratherium blanfordi Lyd. Pilgrim, 1908: 149 *Aceratherium blanfordi* var. *majus* Pilgrim, 1910: 66
Teleoceras blanfordi Lydekker Pilgrim, 1912: 3, 30–32, pl. 7, figs 4–7
Chilotherium blanfordi Ringström, 1924: 75
Chilotherium blanfordi Matthew, 1929: 508
Chilotherium blandfordi Forster-Cooper, 1934: 589– 594; text-fig. 9, 12C; pl. 67, figs 34–38
« *Dicerorhinus* » cf. *abeli* (partim) Welcomme *et al.*, 1997: 532, 535
? « *Dicerorhinus* » cf. *abeli* (partim) Welcomme *et al.*, 1997: 534, 535, 536
Aprotodon blanfordi Welcomme & Ginsburg, 1997: 1001, table
Pleuroceros blanfordi Lindsay *et al.*, 2005: table 1 '*Aprotodon*'
blanfordi Métais *et al.* 2009: 163, 164; table 2, fig. 5

Emended diagnosis: Differs from *P. pleuroceros* by its larger size (*c*. 15%), the presence of a posterior hori-zontal groove on the processus zygomaticus of the squamosal, the absence of a sagittal lingual groove on the corpus mandibulare, a shortened premolar series, higher tooth crowns, the abundance of coronary cement, a weaker labial cingulum, a multiple crochet always present, an unconstricted metaloph, a con-tinuous lingual cingulum, and a thick lingual bridge on upper premolars, a transverse metaloph and a reduced protocone on P2, and the usually constricted protocone on P3–4, the absence of a crista on P3, the unconstricted metaloph on P4, the usual presence of a lingual cingulum (occasional in *P. pleuroceros*) on upper molars, a deep protocone constriction and the presence of a metacone fold on M1–2, a strong meso-style on M2, a constricted metaconid on lower decidu-ous teeth, the absence of a posterior McIII-facet on McII, the absence of a fibula-facet on the calcaneus, and the concave proximal border of MtIII.

Lectotype: Right P4–M2 series unearthed in Gandoï, Bugti Hills (IMC C. 268) and figured by Lydekker (1884: pl. 1, fig. 1), proposed as a lectotype by Pilgrim (1912: 31).

Type locality: Gandoï, Bugti Hills, Pakistan (Early Miocene?).

Stratigraphical range: Chitarwata Fm. (Bugti and Zinda Pir areas) and base of the Vihowa Fm. (Bugti area). Early Miocene (*c*. 23–18.5 Myr; Lindsay *et al.*, 2005; Métais *et al.*, 2009).

Geographical range: Bugti and Zinda Pir area, Sulaiman Lobe, Balochistan, Pakistan.

Referred material
Old collections: 'Siwaliks of the Punjab' [?Early Miocene]. Left maxilla with P4–M2 IMC-without number; Gandoi [?Early Miocene, Bugti Hills]. Right mandible with p3–m1 and m2–3 salient (IMC C. 271); left M2 (IMC C. 259); right M1 or M2, worn (IMC C. 262); part of a right juvenile mandible, with d3 (IMC C. 267). Dera Bugti [?Early Miocene]. Part of left maxilla with M1–3 (IMC C. 268). 'Gaj of the Bugti Hills' [?Early Miocene]. M1–3 (IMC C. 266). 'Near Dera Bugti' [locality and age unknown]. Germ of a left P2 (NHM M 15335); left P2 and P3 from the same individual (NHM M without number [w.n.]); left P3 and P4 from the same individual (NHM M w.n.); fragment of a right maxilla with D2–4 and M1 (NHM M 15367) and germ of P3 extracted from the maxilla (NHM M 15368); right P2 (NHM M 15337); right P3 (NHM M 15338); left P3 and P4 from the same individual (NHM M 15333); right P3 and P4 from the

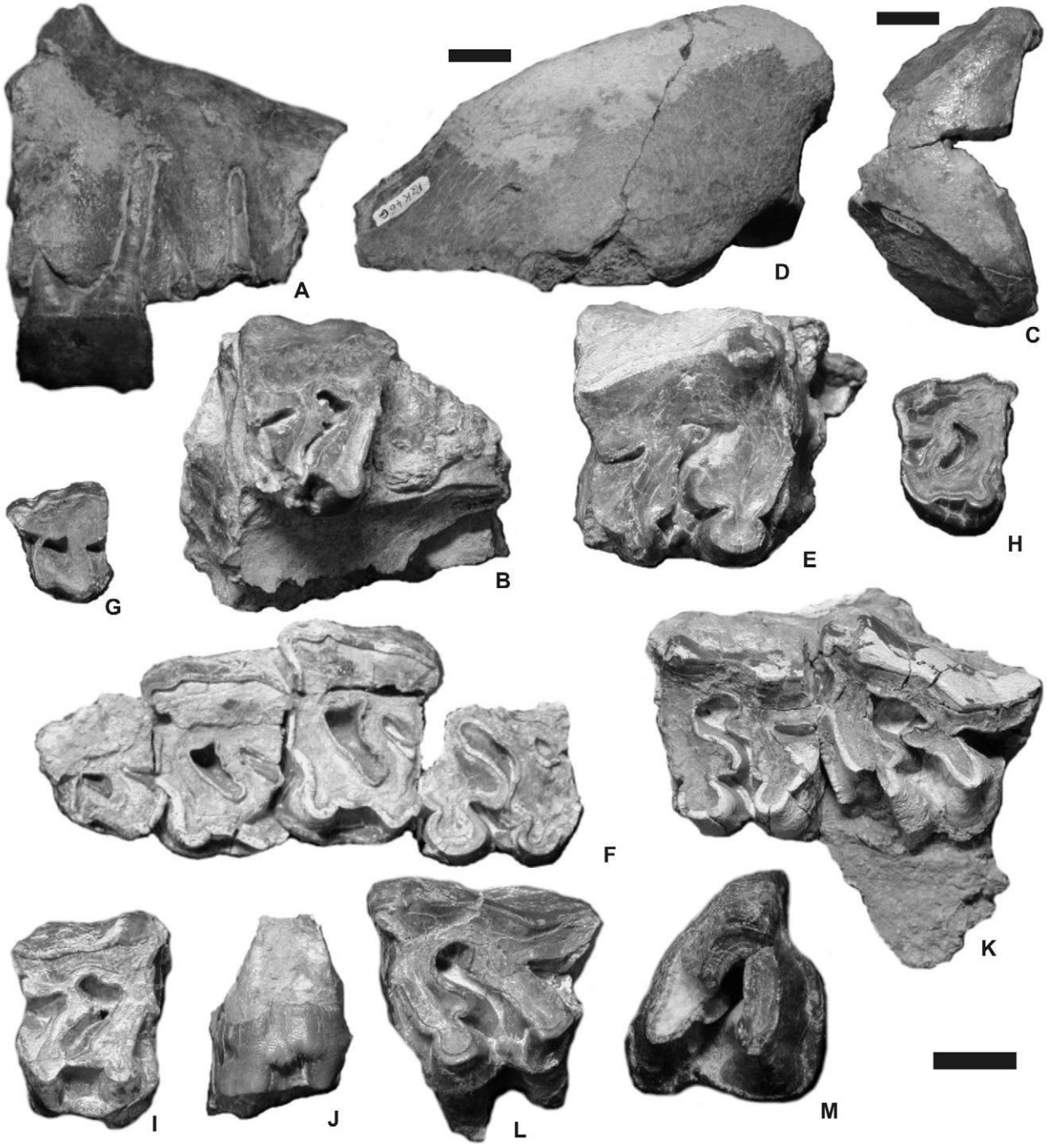

Figure 4. *Pleuroceros blanfordi* (Lydekker, 1884) from the Early Miocene of the Bugti Hills, Balochistan, Pakistan: cranial material and upper teeth. A, right fragmentary maxilla with P3 (MHNT Pak 46), lateral view. B, same, occlusal view; C, occipital crest (MHNT Pak 46A), dorsal view; D, left zygomatic arch and squamosal (MHNT Pak 46G), lateral view; E, right M1 (MHNT Pak 46D), occlusal view. The specimens illustrated in A–E belong to a single skull, from Kumbi 4a. F, left P2–M1 series (MHNT Pak 1031), occlusal view. Kumbi 4a; G, left P2 (MHNT Pak 751), occlusal view. Kumbi 4b; H, right P3 (MHNT Pak 1024), occlusal view. Kumbi 4a; I, right P4 (MHNT Pak 1046), occlusal view. Kumbi 4a; J, same, lingual view; K, left M1–M2 series (MHNT Pak 1022), occlusal view. Kumbi 4c; L, left M2 (MHNT Pak w/n), occlusal view; M, right M3 (MHNT Pak 918), occlusal view. Kumbi 4b. Scale bars = 2 cm.

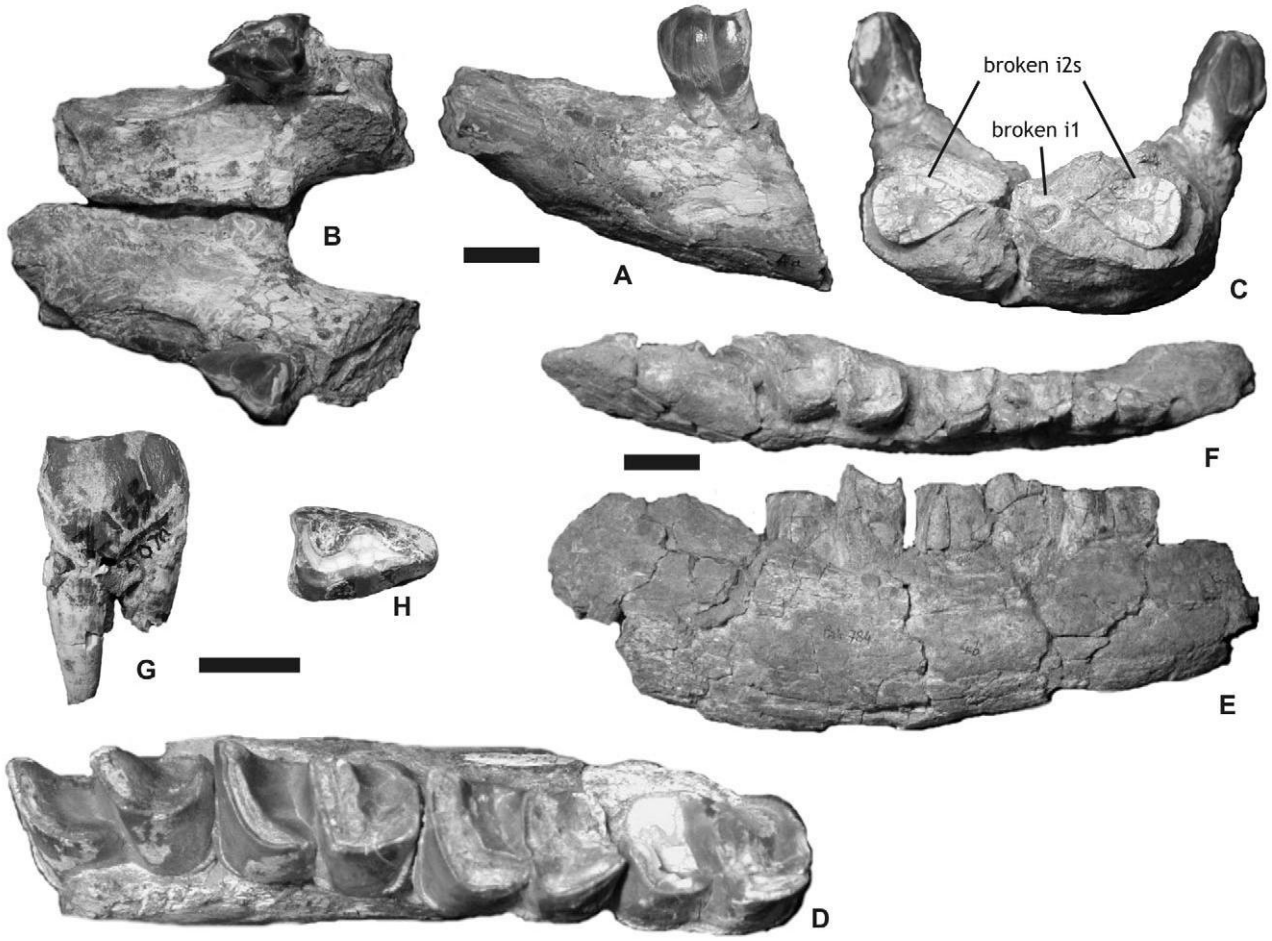

Figure 5. *Pleuroceros blanfordi* (Lydekker, 1884) from the Early Miocene of the Bugti Hills, Balochistan and of the Zinda Pir dome, Sind, Pakistan: mandibular material and lower teeth. A, mandibular symphysis with left and right p2 and alveoli of i2 (MHNT Pak 1038), lateral view; B, same, occlusal view. C, same, anterior view; D, right p4–m3 series from the same mandible, occlusal view. Kumbi 4a; E, right juvenile mandible with d2–d4 (MHNT Pak 784), lateral view. Kumbi 4b; F, same, occlusal view; G, right p2 (PMNH Z2070), lateral view. Z135 locus, Zinda Pir; H, same, occlusal view. Scale bars = 2 cm.

same individual (NHM M 15366); palate with left P2–M3 and right M1–2 (NHM M 15365).

New material

Bugti Hills (Figs 1, 2)

Kumbi 4a (Level 4, earliest Miocene). Mandible from a young adult, in three parts: left corpus with p4–m1, right corpus with p4–m3 and symphysis bearing left i1 and left and right i2, all of them broken (MHNT Pak 1038); fragment of a left mandible with p2 (broken) and p3 (MHNT Pak 1037); fragment of an toothless symphysis (MHNT Pak 1073); fragment of a right mandible with m3 (MHNT Pak 1068); fragment of a left maxilla with P2–P4, M1 without ectoloph and fragments of i2 and right p2 from the same individual (MHNT Pak 1031); right P3 (MHNT Pak 1024); right P3 (MHNT Pak 1059); left P4 (MHNT Pak 1058); right P4 d (MHNT Pak 1046); right P4 without ectol-oph (MHNT Pak 1050); fragment of a left maxilla with M1–2 (MHNT Pak 1022), from the same indi-vidual as a right M2 (MHNT Pak 1019); right M1 (MHNT Pak 1061); fragment of a right M1 on a maxilla (MHNT Pak 1035); lingual fragment of a right M1 (MHNT Pak 1064); left crushed M2 (MHNT Pak 1045); lingual fragment of a right M2 (MHNT Pak 1027); left M3 (MHNT Pak 1013); right M3 (MHNT Pak 1014); rostral fragment of a left i2 (MHNT Pak 1021); lingual fragment of a right p3 (MHNT Pak w. n.); posterior fragment of a right m3 (MHNT Pak 1020); fragment of a humeral distal end (MHNT Pak 1085); fragment of a left humeral distal end (Pal 1198); proximal end of a left radius (MHNT Pak 1088); proximal end of a right radius (MHNT Pak 1087); proximal end of a right

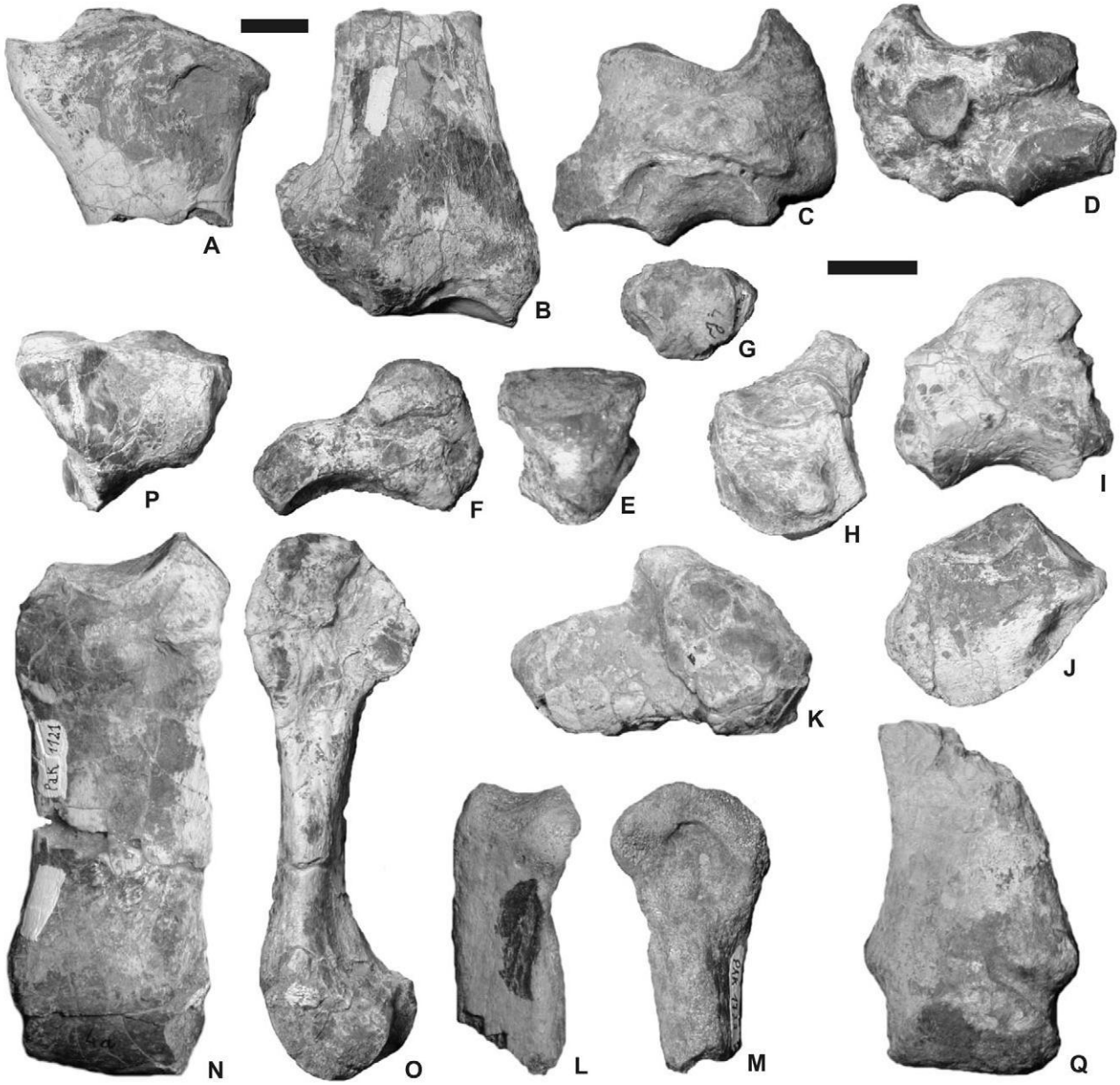

Figure 6. *Pleuroceros blanfordi* (Lydekker, 1884) from the Early Miocene of the Bugti Hills, Balochistan, Pakistan: Forelimb remains. A, right radius, proximal end (MHNT Pak 1089), anterior view. Kumbi 4a; B, right radius, distal end (MHNT Pak 1090), anterior view. Kumbi 4a; C, right scaphoid (MHNT Pak 785), anteromedial view. Kumbi 4b; D, right scaphoid (MHNT Pak 1098), posterolateral view. Kumbi 4a; E, right semilunate (MHNT Pak 1101), anterior view. Kumbi 4a; F, same, lateral view; G, right trapezoid (MHNT Pak 787), dorsal view. Kumbi 4b; H, left magnum (MHNT Pak 1110), anterior view. Kumbi 4a; I, same, lateral view; J, right unciform (MHNT Pak 1114), anterior view. Kumbi 4a; K, left unciform (MHNT Pak 1112), dorsal view. Kumbi 4a; L, left McII (MHNT Pak 1733), anterior view. Kumbi 4f; M, same, lateral view; N, left McIII (MHNT Pak 1121), anterior view. Kumbi 4a; O, same, lateral view; P, same, dorsal view; Q, right McIII, distal end (MHNT Pak 1193), anterior view. Kumbi 4a. Scale bars = 2 cm.

radius (MHNT Pak 1089); distal end of a left radius (MHNT Pak 1091); distal end of a right radius (MHNT Pak 1090); distal end of a right radius (MHNT Pak 1206); right scaphoid (MHNT Pak 1098); right semilunate (MHNT Pak 1101); left magnum (MHNT Pak 1110); right magnum (MHNT Pak 1093); left unciform (MHNT Pak 1112); right unciform (MHNT Pak 1094); right unciform (MHNT Pak 1113); right unciform without posterior tuberosity (MHNT Pak 1114); proximal end of a left McIII (MHNT Pak

1118); proximal end of a left McIII (MHNT Pak 1119); proximal end of a left McIII (MHNT Pak 1120); left McIII (MHNT Pak 1121); right Mc III without distal end (MHNT Pak 1117); distal end of a right Mc III (MHNT Pak 1193); left patella (MHNT Pak 1131); left patella (MHNT Pak 1132); distal end of a left tibia (MHNT Pak 1124); distal end of a left tibia (MHNT Pak 1126); distal end of a right tibia (MHNT Pak 1127); distal end of a right tibia (MHNT Pak 1128); distal end of a right fibula (MHNT Pak 1129); left astragalus (MHNT Pak 1137); left astragalus (MHNT Pak 1138); left astragalus (MHNT Pak 1139); medial fragment of a left astragalus (MHNT Pak 1143); right astragalus (MHNT Pak 1140); right astragalus (MHNT Pak 1141); right tuber calcanei (MHNT Pak 1104); right calcaneus (MHNT Pak 1150; right calcaneus (MHNT Pak 1151); right calcaneus (MHNT Pak 1152); left navicular (MHNT Pak 1154); posterior fragment of a left navicu-lar (MHNT Pak 1156); right cuboid (MHNT Pak 1158); right cuboid (MHNT Pak 1159); right ectocuneiform (MHNT Pak 1160); fragment of a left ectocuneiform (MHNT Pak 1161); right mesocuneiform (MHNT Pak 1590); proximal end of a left MtII (MHNT Pak 1163); distal end of a left MtII (MHNT Pak 1191); right MtII (MHNT Pak 1162); proximal end of a right MtIII (MHNT Pak 1096); distal end of a right MtIII (MHNT Pak 1192); distal end of a right MtIII (MHNT Pak 1194); right MtIII without proximal end (MHNT Pak 1195); distal end of a right MtIV (MHNT Pak 1097); right Mt IV (MHNT Pak 1165); proximal end of a right MtIV (MHNT Pak 1166); proximal end of a right MtIV (MHNT Pak 1167).

Kumbi 4b (Level 4, earliest Miocene). Fragment of an eroded right mandible with erupting m3 (MHNT Pak 772); right juvenile mandible with d2–4, m1 in the dentary and alveolus of d1 (MHNT Pak 784); left P2 (MHNT Pak 751); right P2 (MHNT Pak 844); left P3 without an ectoloph (MHNT Pak 842); right P3 without an ectoloph (MHNT Pak 758); fragment of a left M2 (MHNT Pak 760); fragment of a protoloph of left M3 (MHNT Pak 761); left M3 without a protoloph (MHNT Pak 763); right M3 (MHNT Pak 918); slightly worn left m3 (MHNT Pak 917); fragment of a left m3 (MHNT Pak 774); right scaphoid (MHNT Pak 785), fragment of a right semilunate (MHNT Pak 786) and right trapezoid (MHNT Pak 787) probably from the same individual; distal end of a left McII (MHNT Pak 789); distal end of a left MtII (MHNT Pak 790).

Kumbi 4c (Level 4, earliest Miocene). Right P2 (MHNT Pak 844); left P3 without an ectoloph (MHNT Pak 845); left M2 (MHNT Pak w. n.); left damaged patella (MHNT Pak 86); distal end of a right tibia (MHNT Pak 71).

Kumbi 4d (Level 4, earliest Miocene). Fragmentary skull with left and right squamosals (processus zygo-maticus), left postglenoid apophysis, occipital, left and right maxilla bearing P3, right M1 and the alveoli of right P1–2, fragments of right M2–3 and undeter-mined fragments (MHNT Pak 46).

Kumbi 4f (Level 4, earliest Miocene). fragment of a right M3 (MHNT Pak 1676); proximal end of a left McII (MHNT Pak 1733); right patella (MHNT Pak 1687).

Gandô 4 (Level 4, earliest Miocene). Fragment of a right M3 (MHNT Pak 1864); left p3 (MHNT Pak 1862).

Dera Bugti 4 (Level 4, earliest Miocene). Fragment of a left P4 (MHNT Pak 1967); right P4 (MHNT Pak 1964).

Dera Bugti 5 (Level 5, Early Miocene). Posterolin-gual fragment of a left M2 (MHNT Pak 1258).

Dera Bugti 6 (Level 6, Early Miocene). left M2 g (MHNT Pak 1012a); lingual fragment of a right M3 (MHNT Pak 1444); lingual fragment of a left m1 (MHNT Pak 2215); damaged right astragalus (MHNT Pak 2235).

Wadera Murad (Early Miocene, northern side of the Dera Bugti syncline). Fragment of a left P4 (MHNT Pak 2458).

Zinda Pir Dome (Fig. 1)

Z149 (earliest Miocene). Left astragalus (PMNH Z2043); Z139 (earliest Miocene). Right fragmentary astragalus (PMNH Z2047). Z135 (earliest Miocene). Right p2 (PMNH Z2070).

Cranial material: The adult skull MHNT Pak 46 is fragmentary. The occipital, fragments of maxillae, squamosals (processus zygomaticus), and a postgle-noid apophysis are preserved (Fig. 4A–D). The palate NHM M 15365 shows identical features. The foramen infraorbitalis was located above P4 and the nasal incisure above the middle of P3. The anterior border of the orbit is above M1. The zygomatic arch was high and thick (Fig. 4D). No processus postorbitalis is present on the dorsal border of the processus zygo-maticus of the squamosal. The squamosal–jugal suture is smooth and regular. The caudal border of the processus zygomaticus is depressed by a trans-verse gutter-like groove (Fig. 4D). The articular tubercle is salient and regularly convex. The postgle-noid apophysis, straight in anterior view, has a tri-angular cross-section, with a convex articular surface. The nuchal tubercle is prominent. The caudal border of the occipital crest is slightly concave. The fronto-parietal crests converge rostrally, but their junction cannot be observed on this fragmentary specimen. The dorsal half of the occipital side is depressed. The dorsal side of the skull was narrow: the occipital crest is about 100 mm wide. The junction between the nuchal and temporal crests was very close to the auditory pseudomeatus. The foramen magnum is

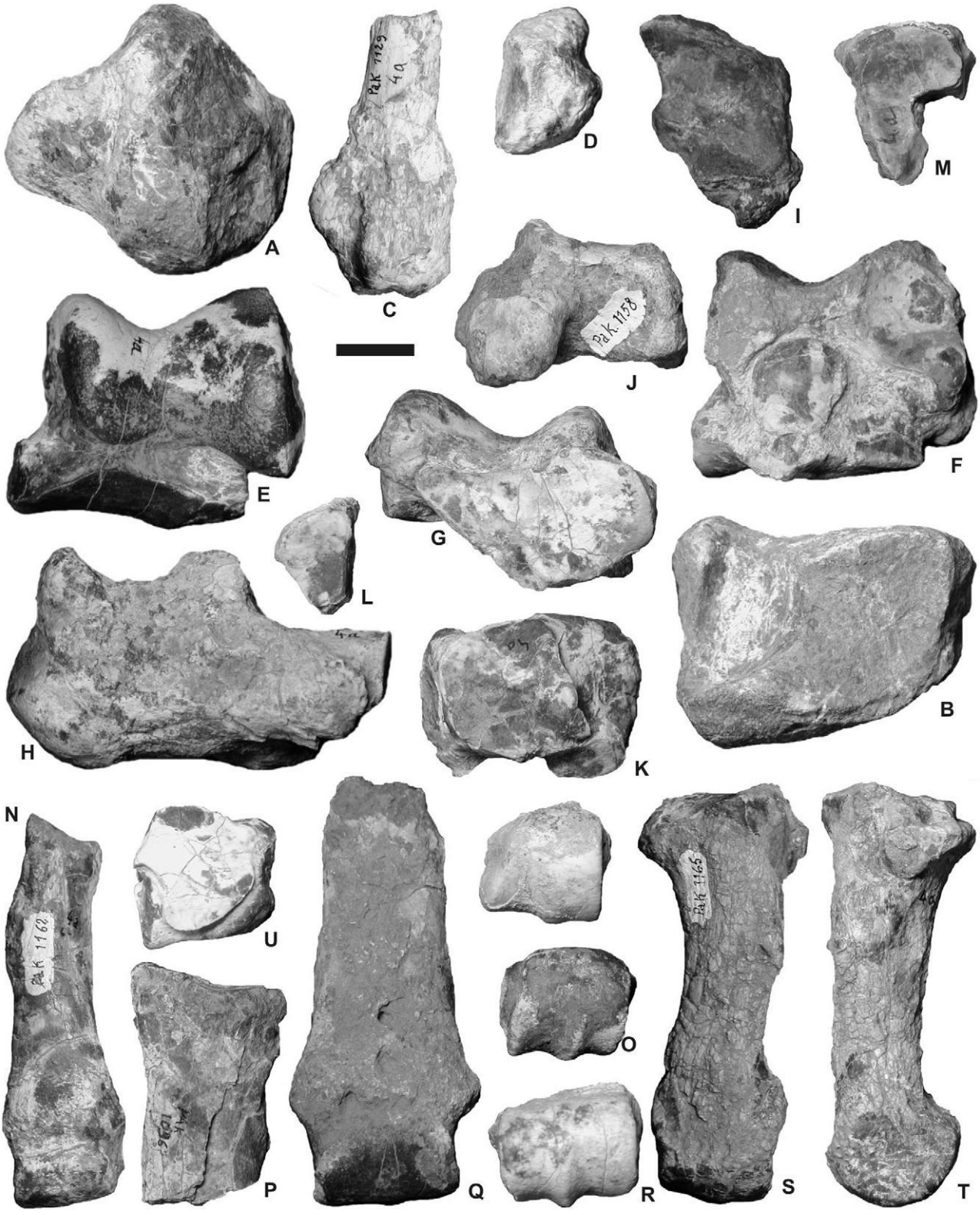
A
C
D
I
M
J
E
F
G
L
H
K
B
N
U
P
Q
O
R
S
T

Figure 7. *Pleuroceros blanfordi* (Lydekker, 1884) from the Early Miocene of the Bugti Hills, Balochistan, Pakistan: Hind limb remains. A, left patella (MHNT Pak 1132), anterior view; B, left tibia, distal end (MHNT Pak 1124), distal view; C, right fibula, distal end (MHNT Pak 1129), lateral view; D, same, distal view; E, left astragalus (MHNT Pak 1140), anterior view; F, right astragalus (MHNT Pak 1138), posterior view; G, same, distal view; H, right calcaneus (MHNT Pak 1150), lateral view; I, left navicular (MHNT Pak 1154), dorsal view; J, right cuboid (MHNT Pak 1158), lateral view; K, right cuboid (MHNT Pak 1159), dorsal view; L, right mesocuneiform (MHNT Pak 1590), dorsal view; M, right ectocuneiform (MHNT Pak 1160), dorsal view; N, right MtII (MHNT Pak 1162), anterior view; O, left MtII, distal end (MHNT Pak 1191), distal view; P, right MtIII, proximal end (MHNT Pak 1096), anterior view; Q, right MtIII without proximal end (MHNT Pak 1095), anterior view; R, right MtIII, distal end (MHNT Pak 1194), distal view; S, right MtIV (MHNT Pak 1165), anterior view; T, same, medial view; U, right MtIV (MHNT Pak 1167), proximal view; V, right MtIV, distal end (MHNT Pak 1097), distal view. A–V from Kumbi 4a. Scale bar = 2 cm.

Table 1. *Pleuroceros blanfordi* (Lydekker, 1884) and ***Mesaceratherium welcommi* sp. nov.** Compared dimensions of mandibular fragments (range, number of specimens in square brackets, and mean, in mm) from the Early Miocene of the Dera Bugti area (Balochistan, Pakistan)

	H corpus mandibulae						TD *corpus*			
Taxon	p2–3	p3–4	p4–m1	m1–2	m2–3	post m3	p4–m1	m2–3	L symphysis	H proc. coron.
M. w.	58–63	69–66	73–79	78–87	–	(81)	34.5–39	42	> 108	> 223
Mean	60.5 [2]	67.5 [2]	75.7 [3]	82.5 [2]	–	–	37.3 [3]	–	–	–
P. b.	50–53	(55)	70	75	71	–	37	(37)–41.5	(> 91)	–
Mean	51.5 [2]	–	–	–	–	–	–	–	–	–

H, height; L, length, *M. w.*; *M. welcommi*; *P. b.*, *P. blanfordi*; post, posterior; proc. coron., processus coronoideus; TD, transverse diameter. Approximate dimensions appear between brackets.

subcircular. A horizontal median ridge splits the occipital condyle into two parts. No medial truncation is visible on the latter.

Mandibular material: The most complete specimen is the mandible MHNT Pak 1038 (Fig. 5A–D). The sym-physis, nearly horizontal, forms a plateau continuing the corpus mandibulae. It is thick and rather wide, lacking any lateral constriction at the diastema level. In anterior view, the lingual border of the symphysis is regularly concave and the ventral border is flat-tened, without a median depression. A sharp and winding ridge separates the lingual and labial borders of the symphysis, between the i2 and the lingual side of p1. The posterior border of the sym-physis reaches the middle of p2, as does the wide foramen mentale. The latter is associated with acces-sory foramina, all along the ventral border of the symphysis. The spatium intermandibulare is very wide – from 32–40 mm between p2 and p3 according to the specimen. In frontal view the tooth rows are strongly divergent, the corpus mandibulae being very oblique (Fig. 5C). The corpus mandibulae gets regu-larly higher from the symphysis to m1, and notably lower backwards (MHNT Pak 1038, IMC C. 271; Table 1). There is no median sagittal groove (sulcus mylohyoideus) on the lingual side of the corpus mandibulae either in adults (MHNT Pak 1037, 1038, and 1068) or juveniles (MHNT Pak 784, IMC C. 267). The ramus is unknown, but Lydekker (1884: 6, fig. 2) figured a prominent angulus mandibulae (IMC C. 271). The mandible MHNT Pak 784 bears the alveo-lus of d1, the functional d2–4 series and the m1 included in the pars molaris (Fig. 5D–E). It belongs to a calf, referred to *P. blanfordi* owing to the shape of m1.

Dental material: The upper incisors are not known with certainty, but the flat wear surface on i2s is most probably because of large I1s. However, the mandibu-lar symphysis MHNT Pak 1038, which is broken in its anterior part, bears cross-sections of the left i1 and both i2s (Fig. 5C). The former has an oval cross-section (5.5 ¥ 7 mm) and it was located below the horizontal line defined by the i2s. The i2s, 22 mm away one from another, have a drop-shaped cross-section, as do the complete i2s MHNT Pak 1021 and 1031. A thin layer of enamel covers the crown. This enamel is fluted in the labial part of the crown. The i2s do not diverge.

The cheek teeth formula is 4P–3M, 4p–3m. No P1 or persistent D1 can be referred to this taxon. However, the maxilla MHNT Pak 46 bears the broken roots of a small triangular tooth in front of P2

Table 2. *Pleuroceros blanfordi* (Lydekker, 1884) (Early Miocene of the Bugti Hills, Balochistan, Pakistan) and *Pleuroceros pleuroceros* (Duvernoy, 1853) from Laugnac and Saint-Gérand-le-Puy (Early Miocene, France). Compared dimensions of the upper dentition (permanent and deciduous cheek teeth; range, mean, and number of specimens in square brackets, in mm)

	L		ant W		post W		H	
Tooth	*P. b.*	*P. p.*	*P. b.*	*P. p.*	*P. b.*	*P. p.*	*P. b.*	*P. p.*
P2	21–29.5	24–25	23–31	28–28	27–35	28–28	11–37	20–20
Mean	24.0 [6]	24.5 [2]	27.4 [7]	28.0 [2]	31.4 [5]	28.0 [2]	19.5 [4]	20.0 [2]
P3	25.5–35	29–29	38–47	36–36	37–48	33–33	14–27	23–23
Mean	31.3 [12]	29.0 [2]	43.0 [12]	36.0 [2]	42.4 [10]	33.0 [2]	20.4 [5]	23.0 [2]
P4	31.5–38.5	30–31	44.5–53	39	44.5–54	36	22–33	26–26
Mean	34.7 [6]	30.5 [2]	50.2 [6]	–	49.2 [5]	–	26.0 [3]	26.0 [2]
M1	42–56	36–36.5	53–57	41	50–56.5	36.5	34–60	20–21
Mean	49.0 [5]	36.2 [2]	55.4 [5]	–	53.2 [6]	–	45.1 [4]	20.5 [2]
M2	54–56	40–42	58–62	40–47	50–53	36–42.5	38–57	25–29
Mean	55.0 [4]	40.7 [3]	59.5 [4]	42.5 [4]	51.7 [5]	38.1 [4]	48.0 [3]	26.7 [4]
M3	44.5–48.5	33–36	53–57.5	32–41	L_{ect} = 57–60.5	40.5–45	21–55.5	23–30.5
Mean	47.2 [4]	34.7 [3]	54.8 [3]	37.7 [3]	58.2 [3]	41.8 [3]	36.1 [4]	26.8 [3]
D2	31.5	–	28	–	–	–	–	–
D3	35	–	38.5	–	37	–	–	–
D4	46	–	44	–	39	–	–	–

ant, anterior; H, height; L, length; L_{ect}, length of the ectometaloph; *P. b.*, *P. blanfordi*; *P. p.*, *P. pleuroceros*; post, posterior; W, width.

(Fig. 4B). The premolar row is short with respect to the molar one [($L_{P3–4}/L_{M1–3}$) ¥ 100 = 46]. There is no enamel folding (Fig. 4F, K). The cement is abundant, covering the ectolophs and filling the valleys. The enamel is thinly wrinkled vertically and even squared because of horizontal striae (MHNT Pak 751, 1024, 1058; NHM M 15337). The crowns are high but still conical, with a strongly oblique ectoloph. The roots are thinly joined, long, and divergent (Fig. 4A).

P2 is trapezoid, wider in its posterior part (Fig. 4F–G; Table 2). The P3–4s are rectangular, wider than long. The labial cingulum is generally absent (ten P2–4 out of 11), but it forms a low ridge on the P3 MHNT Pak 1024 (Fig. 4H). The lingual cingulum is always strongly developed on P2–4 (Fig. 4F). Generally interrupted on the protocone and/or the hypocone (13/16 specimens), it can be con-tinuous (three specimens out of 16). The crochet is lacking on every available P2 (Fig. 4G) and two worn P3s (MHNT Pak 758, 845). Yet, it is present and always multiple on the eight remaining P3s and the ten available P4s. The crochet is restricted to the top end of the crown, therefore vanishing with wear (Fig. 4B, F–H). The metaloph is complete, V-shaped in occlusal view, and without a constriction. The post-fossette is narrow and deep. The median valley is still deeper. The antecrochet, lacking on P2–3, is always strongly developed on P4 (Fig. 4I). There is a lingual bridge joining the lingual cusps on P2–3 and joining the antecrochet with the hypocone on P4 (Fig. 4F). This bridge is thin in Early stages of wear, and it thickens in later stages. On P2, the metaloph is transverse and the protocone is less developed than the hypocone. The protoloph is narrow but continuous on every P2. There is no medifossette on the upper premolars (Fig. 4B, F–I), except for P4 MHNT Pak 1964. On P3–4, the anterior constriction of the pro-tocone is generally present; the continuous metaloph forms a dihedron open backwards, in which the crochet is the anterior angle; the hypocone is posterior to the metacone. On P3, the protoloph is continuous and there is no crista. The parastyle is sagittal. The paracone and the metacone folds are always present on P2–4, the former being thicker.

The upper molars are generally lacking a labial cingulum: only two M2 have a cingular bulge very reduced, at the neck. The antecrochet and the crochet are always well developed, except on worn teeth, where the crochet may vanish (MHNT Pak 1031). The anterior constriction of the protocone is always deep, both in M1–2 and M3 (Fig. 4E–F, K–M). Therefore, the protoloph is ‘trefoil-shaped’ (*sensu* Antoine, 2003). The crochet is sagittally orientated and generally simple on the upper molars (11 specimens out of 15). Yet, the crochet is sometimes double in the top of the crown (MHNT Pak 760, 1012a, 1045, 1258). No crista

Table 3. *Pleuroceros blanfordi* (Lydekker, 1884) (Early Miocene of the Bugti Hills and of the Zinda Pir Dome, Pakistan) and *P. pleuroceros* (Duvernoy, 1853) from Laugnac and Saint-Gérand-le-Puy (Early Miocene, France). Compared dimen-sions of the lower dentition (permanent and deciduous cheek teeth; range, mean, and number of specimens in square brackets) in mm

	L		ant W		post W		H	
Tooth	*P. b.*	*P. p.*	*P. b.*	*P. p.*	*P. b.*	*P. p.*	*P. b.*	*P. p.*
p2	28–30	20–20.5	17–19	14–14	20–21	15–15	23–25	15–17
Mean	28.8 [3]	20.3 [3]	17.8 [3]	14.0 [3]	20.3 [3]	15.0 [3]	24 [3]	16.0 [2]
p3	(27)–32	26–28	17	16.5–18	19	18–19	19	12–18
Mean	–	26.8 [4]	–	17.4 [4]	–	18.3 [4]	–	16.5 [3]
p4	(35)–37	30–34	26–27	20–21	26–27.5	20.5–23	33–34	17–22
Mean	36.7 [3]	31.7 [3]	26.5 [2]	20.3 [3]	26.7 [2]	21.5 [3]	33.5 [2]	19.5 [2]
m1	(37)–38	31–34	25–26.5	20–23	27	20–24	24–28	12–23
Mean	–	32.7 [3]	25.7 [2]	21.0 [3]	–	21.7 [3]	26 [2]	17.5 [2]
m2	41.5	38–(40)	28	22–24.5	25–26	22–25	26–32	14–26
Mean	–	38.5 [2]	–	23.2 [2]	25.5 [2]	23.0 [3]	29 [2]	20.0 [2]
m3	45–46	38–40	26–27.5	22–24	25–29	20–22.5	19–45	16–28
Mean	45.5 [2]	39.0 [3]	26.7 [2]	22.7 [3]	26.5 [3]	20.8 [3]	28.3 [3]	22.0 [3]
d2	26.5	–	9	–	12	–	13	–
d3	(39)	–	(15)	–	(19)	–	18	–
d4 r	38.5	–	18.5	–	22	–	29	–

ant, anterior; H, height; L, length; *P. b.*, *P. blanfordi*; *P. p.*, *P. pleuroceros*; post, posterior; W, width. Approximate dimensions appear between brackets.

is present on M1–3, except on M2 MHNT Pak 1027. There is neither medifossette nor cristella. The lingual cingulum is generally reduced, determining a tubercle more or less developed, located at the entrance of the median valley. It forms a thin ridge on the protocone of two M3 (MHNT Pak 761, 918), but is absent from other molars (MHNT Pak 1019, 1022). The ectoloph is nearly straight on M1–2, with a sagittal parastyle, a weakly developed paracone fold, a weak mesostyle but no metacone fold. The metaloph is long on M1–2. A deep constriction notches the anterior side of the hypocone. This constriction is restricted to the base of the crown, deeper on M1 than on M2 (Fig. 4K–L). It is absent on M3, except on MHNT Pak 918. There is a shallow groove on the posterior side of the hypocone, close to the lingual tip of the posterior cingulum on M1–2. There is no junc-tion between the antecrochet and the hypocone, even on worn molars. The postfossette is always present, deep and narrow. No lingual groove notches the pro-tocone of M2. On M3, the ectoloph and the metaloph are fused into an ectometaloph (Fig. 4M). The poste-rior cingulum forms a thick spur restricted to the lingual half of the latter. Yet, M3 has a trapezoid outline, with a wide posterior side – corresponding to the remnant metaloph – supported by two divergent roots. The protoloph of M3 is sagittal and transverse.

The morphology of p1 is unknown. However, the size comparison between the alveolus of d1 (juvenile mandible MHNT Pak 784) and the one present in the adult mandible MHNT Pak 1038 leads us to assume the occurrence of true p1s in adults (Table 3). This p1 was single-rooted, with a cylindrical root section. The ectolophid of p2 is covered by vertical rugosities con-tinuing the labial cingulum (PMNH Z2070, Fig. 5A, G). On p3–4, such rugosities are replaced by a sinuous and continuous cingulum. The external groove is shallow, U-shaped on every lower cheek tooth, vanishing above the neck. The trigonid is angular and forms a right or obtuse dihedron (Fig. 5D). The metaconid is constricted, contrary to the entoconid. The posterior valley is wide and V-shaped. The lingual cingulum, always present, is restricted to the anterior part of the lower cheek teeth. Continuing the anterior cingulum, it forms a thick ridge interrupted at the metaconide level. The labial cingulum is high and continuous on lower pre-molars, and reduced on lower molars, forming a short ridge in the external groove. The p2 has an isolated spur-like paralophid (Fig. 5B). The paraconid is devel-oped and globular. The posterior valley of p2 is open. The base of the metaconid – between the roots – is depressed on the available specimens. The hypolophid of the lower molars is oblique. There is no lingual groove on the entoconid of m2–3.

The juvenile mandible MHNT Pak 784 bears no alveolus for deciduous incisors. d1 is one-rooted. The deciduous teeth are damaged, but the metaconid and

the entoconid seem to be constricted (Fig. 5E–F). It is impossible to observe the protoconid fold. d2–4 lack both labial and lingual cingula and external rough-ness. There is no ectolophid fold, but an anterior groove is present on the ectolophid of d2–3. The paralophid of d2 is simple and spur-like. The poste-rior valley of d2 is lingually open, but a thick oblique ridge lays posteriorly to the metaconid. The paral-ophid of d3 is double. There is no lingual groove on the entoconid of d3–4.

Postcranial skeleton: The material is very abundant, particularly in the Kumbi 4a locality. Postcranials are small- to medium-sized, very homogeneous in size and proportions (Tables 5–7, 9–13, 15–21, 23– 27).

From the humerus, only two distal fragments are referred to this taxon (MHNT Pak 1085, 1198). The fossa olecrani is high. The trochlea is very constricted in its median part. The lateral lip is narrow (TD). Available dimensions are (mm): APD distal extrem-ity = 86; APD trochlea = 71 (medial) (42) (middle), and 49.5 (lateral). The epicondyle is weakly developed and lacking any distal gutter.

No complete radius is preserved, but proximal and distal fragments are available (Fig. 6A–B; Table 5). In anterior view, the proximal end is much wider than the shaft. The proximal border is sigmoid, with a low medial border and high median part and lateral border. The weak insertion for the m. biceps brachii is slightly depressed medially. In proximal view, the anterior border of the proximal end is straight and the lateral lip of the cochlea forms a deep basin. The proximomedial ulna-facet is low and halfmoon-shaped. The proximolateral ulna-facet is high and concave. It is impossible to state whether they are fused or separate. Ulna and radius are independent all along the diaphysis. The distal end of the radius MHNT Pak 1090 (Fig. 6B) bears a huge lateral expan-sion, which supports the ulnar articular surface and takes the diaphyses away one from another. The diaphysis is slender and dorsoventrally flattened. The gutter for the m. extensor carpi is wide and deepened by a strong anterolateral tuberosity, above the semilunate-facet. The distal end is wide (TD) and flattened dorsoventrally. In anterior view, the distal border is oblique, much lower medially than laterally; the limit between the scaphoid- and the semilunate-facet is marked by a salient ridge. The scaphoid-facet, deep and sagittally shortened, is posteriorly extended by a medial high and triangular expansion. On the lateral side of the distal end, only one ulna-facet is present. Based on the available specimens, it is impossible to state the presence/absence of a pyramidal-facet.

The ulna is unknown.

The carpus is massive, with thick tuberosities and muscular insertions, especially on the scaphoid, the magnum and the unciform (Fig. 6C–K). The scaphoid is low and robust, with a large transverse diameter (Fig. 6C–D; Table 6). Its posterior height widely exceeds the anterior height. The medial side, short of articular facets, bears a very salient tuberosity in its posterior half. Such a tuberosity extends beyond the trapezium-facet. The latter is small and vertically developed. The scaphoid lacks a posteroproximal semilunate-facet, which is replaced by a thick tubercle. The trapezoid-facet is very wide (TD > APD). The magnum-facet, triangular, is sagittally concave and convex transversally. Its anterior end is located very rostrally with respect to the proximal articulation.

The semilunate MHNT Pak 1101 has no ulna-facet, which indicates the presence of a pyramidal-radius articulation (Fig. 6E–F). The proximal facet is convex and short sagittally. The posterior border of the distal pyramidal-facet is twisted posteriorly. The anterior side is smooth, with a rounded distal border. The magnum-facet does not reach the anterior side.

No pyramidal is preserved, neither the pisiform nor the trapezium.

The trapezoid is small and robust (Table 9). Its anterior side is as wide as high, with a proximal edge regularly convex (Fig. 6G).

The available magnums are broken: no posterior tuberosity is preserved (Fig. 6H–I). The anterior side is as wide as high (Table 10). Its proximal border is straight in anterior view. The articular process for the semilunate is semicircular in lateral view (diameter = 20 mm). On the medial side, the articular facets are not well separated, the anterior incisure being very shallow. Both facets form subvertical strips elongated sagittally. On the lateral side, the unciform-facet is rectangular and narrow sagittally. The distal McIII-facet is trapezoid.

The unciform is represented by four specimens, of which three are complete (Fig. 6J–K). This bone is low and wide in anterior view (Table 11). A strong tuberosity lies along the distal border of the anterior side; this tuberosity is more developed medially. The pyramidal- and McV-facets are always independent but close, especially on MHNT Pak 1113. The poste-rolateral expansion of the pyramidal-facet is present in this only specimen. In anterior view, the semilunate-facet is concave (MHNT Pak 1113, 1114) or flat (MHNT Pak 1094, 1112). In proximal view, the posterior tuberosity is slightly longer than the articu-lar part. The former is wide and low. The distal facet has a wide articular surface for the magnum, McIII, McIV, and McV. The latter is regularly concave sag-ittally and forms an angle about 60° from the hori-zontal line, indicating a tridactyl manus (i.e. with a vestigial McV).

The metacarpals are small and robust, sagittally flattened, with wide diaphyses and salient insertions for the m. extensor carpalis (Tables 12–13).

McII is only represented by an eroded proximal end (MHNT Pak 1733; Fig. 6L–M) and a distal half (MHNT Pak 789). The proximal articulation has a quarter-circle outline in proximal view. The magnum-facet is curved in proximal and lateral views. It is impossible to state the presence/absence of a trapezium-facet. The distal end is wide, with a strong lateral tubercle close to the anteroproximal border of the distal articulation. According to the preserved region of the bone, the diaphysis was curved. The distal articulation is very wide, almost symmetrical, and slightly twisted posteromedially. The keel (or intermediate relief) is high and sharp.

Six McIII are preserved (Fig. 6N–Q). One is com-plete (Table 13). The proximal end is not widened with respect to the diaphysis. The wide McII-facet is comma-like, elongated sagittally. The magnum-facet is narrow and triangular in proximal view. It is visible in anterior view. The unciform-facet forms a narrow and elongated rectangle triangle. The insertion for the m. extensor carpalis is strikingly salient, with two huge tuberosities (medial and lateral). Thus, the lateral border of the diaphysis is laterally displaced in its proximal quarter (30–40 mm long). In anterior view, the diaphysis is slightly curved inwards, without distal widening. The intermediate relief, high and acute, is visible in anterior view. It is particularly salient in its posterior half. The anteroproximal border of the distal articulation is hardly separate from the diaphysis. No posterodistal tubercle is present on the diaphysis.

McIV and McV are not preserved. However, the tridactyly of the manus can be assumed owing to the shape of the unciform (Fig. 6J), especially from the orientation of the McV-facet, as argued by Antoine & Welcomme (2000) and Antoine (2002).

The coxal and the femur are unknown.

The patella is wide, i.e. as wide as high (Fig. 7A; Table 15). The muscular insertions are smooth on the anterior side. The most prominent one corresponds to the m. fascia lata. That for the m. rectus femoris is flat. On the articular side, the medial lip is wide, low, and shallow (MHNT Pak 1131). The proximal border of the articular surface is straight. The distal tip is smooth. The lateral lip is weakly notched transversally.

The tibia is represented by five distal ends (Table 16). There is no anterior groove on the anterior side (Fig. 7B). An oblique gutter notches the median part of the posterior side. The gutter corresponding to the m. tibialis posterior is always present and is deep and narrow. It is located on the posterior third of the medial side. The tibia and the fibula are independent, as the absence of any synostosis on the lateral border of the diaphysis indicates. The diaphysis has a drop-shaped cross-section (MHNT Pak 1126, 1128). The posterodistal apophysis is high and rounded. In distal view, the distal end has a trapezoid outline. The medial border of the cochlea is narrow and very deep. The lateral lip, much wider than the medial one, is almost flat transversally. The distal fibula-facet is semicircular. The contact area does not exceed 40 mm high.

Only one distal half of a fibula can be referred to this taxon (MHNT Pak 1129). The diaphysis is slender, short of any contact with the tibia. The distal end is robust, with a deep lateral gutter for the m. fibularis (Fig. 7C–D; Table 17). This vertical gutter is located in the posterior third of the head. The astragalus-facet is flat dorsoventrally, subvertical, and slightly concave sagittally.

Eight astragali are preserved (Fig. 7E–G; Table 18). They are morphologically and metrically homoge-neous, wider than high (TD/H = 1.16) and deep (APD/ H = 0.76). The fibula-facet is subvertical and flat transversally. It is very developed anteroposteriorly. The collum tali is high. The posteroproximal border of the trochlea is nearly straight. The trochlea is very oblique with respect to the distal articulation. The lateral lip is very prominent. The laterodistal expan-sion of calcaneus-facet 1 (*sensu* Heissig, 1972) is always present and is high and narrow. This facet is very deep sagittally. Calcaneus-facet 2 is flat and oval, higher than wide. Calcaneus-facet 3 is small (MHNT Pak 1140). Calcaneus-facets 2 and 3 are not connected and are separated by a deep notch. On the distal side, the posterior border of the cuboid-facet bears a strong and abrupt inflection. This facet is wide and short. The medial tubercle is salient, overhanging the medial border of the trochlea by about 15 mm.

The four available calcanei are robust, wide, and low (Table 19). They lack both fibular and tibial facets. The insertion for the m. fibularis longus is marked, forming a deep notch trimmed by a circular ridge (Fig. 7H). The tuber calcanei is high, slender, and oblique with respect to the processus calcanei. The latter is short and very thick (TD). The beak (rostrum calcanei) is low. The sustentaculum tali is wide. The cuboid-facet is sagittally flat and very deep transversally.

From the second tarsal row, two naviculars, two cuboids, a mesocuneiform, and two ectocuneiforms are preserved. The navicular is low (Table 20), with a lozengic outline in vertical view (Fig. 7I). The inser-tions for muscles and tendons are developed, espe-cially towards the posteromedial tip, which bears a thick tubercle. The proximal articular surface for the astragalus is laterally displaced and splits into two parts because of a sharp transverse ridge (MHNT Pak 1154).

The cuboid is robust, wide (TD), and short (APD; Table 21). The anterior side, square in anterior view, is oblique with respect to a vertical transverse plane. The proximal facet, oval to lozengic, is split into two equal parts by a sagittal groove: the astragalus-facet is more posterior than the calcaneus-facet (Fig. 7K). The posterior tuberosity is well developed, with an oblique posterior border (Fig. 7J). The distal tip of this tuberosity overhangs the distal articulation by a few millimetres. The distal MtIV-facet is triangular (MHNT Pak 1158) or trapezoid (MHNT Pak 1159). In both cases, it is deeper than wide (APD > TD).

The mesocuneiform is wide, forming an isosceles triangle in proximal view (Fig. 7L; Table 23).

The ectocuneiform is high and narrow and is L-shaped in proximal view (Table 24). It lacks any posterolateral expansion (Fig. 7M). The distal border is regularly convex in anterior view.

The metatarsus is more slender than the metacar-pus (Fig. 7N–V). The lateral metatarsals are almost as developed as MtIII. The insertions for the m. interossei are short and restricted to the proximal half of the shaft (Fig. 7N, S–T). Mt II bears a narrow proximal end, sagittally elongated (Fig. 7N; Table 25). Its outline forms a quarter oval. The mesocuneiform-facet is triangular (isosceles triangle). An oval pos-teromedial entocuneiform-facet nearly joins the proximal facet. On the lateral side, the anterior MtIII-facet is well developed, flat, and vertical. The diaphysis has a circular cross-section. The distal end is the most robust part of the bone. The distal articu-lation is roughly square in distal view (Fig. 7O). It is wide, nearly flat transversally, with a posteromedial expansion. The intermediate relief is salient, espe-cially with respect to the medial lip of the pulley.

No complete MtIII has been recovered, but this bone was rather slender, according to the available fragmentary specimens (Fig. 7P–Q; Table 26). In proximal view, the anterior border of the articular facet is regularly convex. This facet is only for the ectocuneiform: there is no cuboid-facet. The proximal border of the anterior side is concave in anterior view. There are two flat and well-developed MtII-facets on the medial side of MtIII MHNT Pak 196. On the lateral side, the MtIV-facets are independent. The posterior facet is distally displaced with respect to the anterior one. The diaphysis widens distally (MHNT Pak 1194, 1195), reaching its maximal width (TD) immediately above the distal articulation: two sym-metrical tuberosities considerably widen the diaphy-sis. The intermediate relief is displaced laterally. The medial lip of the trochlea is thus wider than the lateral one (Fig. 7R). No posterodistal tubercle is present on the diaphysis.

MtIV is robust, with thick ends and a cylindrical diaphysis (Fig. 7S–V; Table 27). In proximal view, the proximal end is trapezoid, with a right angle defined by its anterior and medial sides (Fig. 7U). The angle between the other sides exceeds 90°. The articular side is roughly triangular, even if the posterolateral border is strongly convex. The medial border is notched in its median part. The posterolateral tuber-osity forms a strip and is split into two equal parts by a tendinous gutter (MHNT Pak 1166). On the medial side, the articular facets are flat and widely separate. They form an angle of about 150°. The posterior facet is oval and sagittally elongated. Its posterior end reaches the posterior tip of the bone. The diaphysis is curved outwards. The brutal curvature occurs at the distal end of the insertion for the m. interossei, in the proximal half of the shaft (Fig. 7S). The diaphysis is widened by a medial tubercle (muscular insertion), just above the distal articulation. The latter is wide and deeper (APD) than those of the other metatar-sals. It is flat transversally in its medial part and concave in its lateral part. The intermediate relief is low and smooth (Fig. 7V).

Discussion

In the field, the fossil specimens here referred to *P. blanfordi* represent thus far the most abundant small to medium-sized rhinocerotid specimens, especially in Level 4 (earliest Miocene, *c*. 22.5 Myr; Fig. 2). The dimensions of the fragmentary skull MHNT Pak 46 fit with those of the palate NHM M 15365 figured by Forster-Cooper (1934: pl. 67, fig. 34).

Since its initial discovery through dental and frag-mentary craniomandibular remains, this species has been referred to half a dozen distinct genera, which range from Recent times (*Rhinoceros* and *Diceror-hinus*) back to the Late Miocene (*Aceratherium*,
Chilotherium, and *Teleoceras*), and even to the Late Oligocene (*Aprotodon*). However, to our knowledge, no comparison has been made with coeval rhinocerotid genera, such as the teleoceratine *Diaceratherium*, the aceratheres (*sensu lato*) *Mesaceratherium* and
Protaceratherium, and the puzzling pair-horned *Pleu-roceros*, which were abundant around the Oligocene– Miocene transition in Europe (Antoine *et al.*, 2003a). At first glance, the morphological similarity is strik-ing with the type and only species of *Pleuroceros*, *P. pleuroceros*, as illustrated and described by Duvernoy (1854–1855) and de Bonis (1973), especially for the postcranials – which are referred to this taxon for the very first time in the present work.

Compared with the cranial features observable in both *P. blanfordi* and *P. pleuroceros* from France (Gannat, Laugnac, and Paulhiac localities; Duvernoy, 1854–1855; de Bonis, 1973), the Pakistani material is *c*. 15% larger. Both taxa share a concave occipital crest in dorsal view and they only differ by the hori-zontal posterior groove on the processus zygomaticus

of the squamosal, which is present in *P. blanfordi* and absent in *P. pleuroceros*, and by the nasal incision longer in *P. blanfordi*. The zygomatic arch is high, the processus postglenoidalis is thin and narrow, the fron-toparietal crests converge similarly, and the distal border of the nuchal crest is irregular in both species. The occipital side (shape, orientation) and condyle (sigmoid medial border in occipital view) are identical.

The mandible of *P. blanfordi* is strongly reminiscent of that of *P. pleuroceros*: all observable mandibular characters are shared by *P. blanfordi* and *P. pleuroc-eros* (e.g. a nearly horizontal symphysis, with sharp sagittal edges running dorsally along the diastema, and a posterior border at the level of p2), with the exception of the lingual mandibular groove.

It is still more striking on the postcranial skeleton, with highly similar carpus, tarsus, and metapodials in terms of proportions, articular facets, tuberosities, and trochleae (Figs 11A–B, 12A–B). It may be noticed that *P. blanfordi* was most probably tridactyl, as is *P. pleuroceros* (de Bonis, 1973: 153, text-fig. 44.7). In both species, the metacarpals have a prominent inser-tion for the m. extensor carpalis, the tuber calcanei is elevated and slender, and the insertion of the m. interossei on the lateral metapodials is short. The astragali are identical (Fig. 12A–B). The only postcranial differences between both species are the stronger mediodistal tuberosity on the scaphoid in *P. blanfordi* (Fig. 11A–B) and on McII, the posterior McIII-facet on McII and the fibula-facet on the calca-neus (absent in *P. blanfordi*), and the proximal border of MtIII, which is concave in *P. blanfordi* and straight in *P. pleuroceros*.

Pleuroceros blanfordi and *P. pleuroceros* primarily differ in their dental characters, mainly the upper cheek teeth: in *P. blanfordi* larger dimensions (up to 30% larger; Table 2), a shortened premolar series, higher tooth crowns, abundant coronary cement, a weaker labial cingulum, a multiple crochet (only occa-sionally observed in *P. pleuroceros*), an unconstricted metaloph, a continuous lingual cingulum, the pres-ence of a thick lingual bridge on the upper premolars, a transverse metaloph and a reduced protocone on P2, and the usually constricted protocone on P3–4, the absence of a crista on P3, the unconstricted metaloph on P4, the usual presence of a lingual cingulum (occasional in *P. pleuroceros*) on upper molars, a weak paracone fold, and the presence of a metacone fold on M1–2, a strong mesostyle on M2, and a constricted metaconid on the lower deciduous teeth.

Nevertheless, both species share several characters considered as synapomorphies in the phylogenetic analysis performed here (see Phylogenetic relation-ships): a reduced lingual cingulum on upper premo-lars, a strong antecrochet on P4, an occasional crista on upper molars, a strongly constricted protocone and a low reduced posterior cingulum on M1–2, a con-stricted hypocone on M1, a smooth and U-shaped external groove on lower cheek teeth, and a continu-ous lingual cingulum on lower premolars.

The mandibular symphysis figured by Forster-Cooper (1934: text-fig. 10A) is strongly similar to MHNT Pak 1038, especially for the wide spatium intermandibulare. None of these symphyses is very massive, neither enlarged rostrally nor displaying highly diverging incisors (i2). First lower incisors are retained. The foramen mentale is located under p2 in *P. blanfordi*, whereas it is situated in front of it in *Aprotodon*. An occasional postfossette occurs on the upper cheek teeth. The protoloph joins the ectoloph on P2. The protocone is deeply constricted on the upper molars. The posterior part of the ectoloph is concave on M1–2. A deep anterolingual groove marks the hypocone on M2. The external groove is smooth and U-shaped, and the trigonid is angular and sharp on the lower cheek teeth. The lingual opening of the posterior valley is deep, narrow, and V-shaped on the lower premolars, in lingual view. All of these man-dibular and dental features make *P. blanfordi* differ from the species referred to *Aprotodon* Forster-Cooper, 1915. To our knowledge, no postcranial remain is referred to the latter genus (Forster-Cooper, 1915, 1934; Borissiak, 1944; Beliajeva, 1954; Qiu & Xie, 1997).

More features will be discussed in the phylogenetic analysis section, including differences with type species of some genera that *P. blanfordi* had been referred to, such as *Aceratherium* and *Chilotherium*.

MESACERATHERIUM HEISSIG, 1969: 90

Emended diagnosis: Medium-sized hornless rhinoc-erotine with a strong paracone fold on M1–2, a pos-terior McIII-facet on McII, no posterior MtII-facet on MtIII, and slender limbs.

Type species: Mesaceratherium gaimersheimense Heissig, 1969.

Included species: M. paulhiacense (Richard, 1937)

MESACERATHERIUM WELCOMMI ANTOINE & DOWNING **SP. NOV.** (FIGS 8–10, 11C, 12C)

Rhinoceros Falconer & Cautley, 1846: pl. 76, figs 12, 12a, 12b

Teleoceras blanfordi (partim) Pilgrim, 1912: 3, 30–32; pl. 7, figs 4, 7

Rhinoceros blandfordi (partim) Forster-Cooper, 1934: 589–594, text-figs 9A, 9C, 9E.

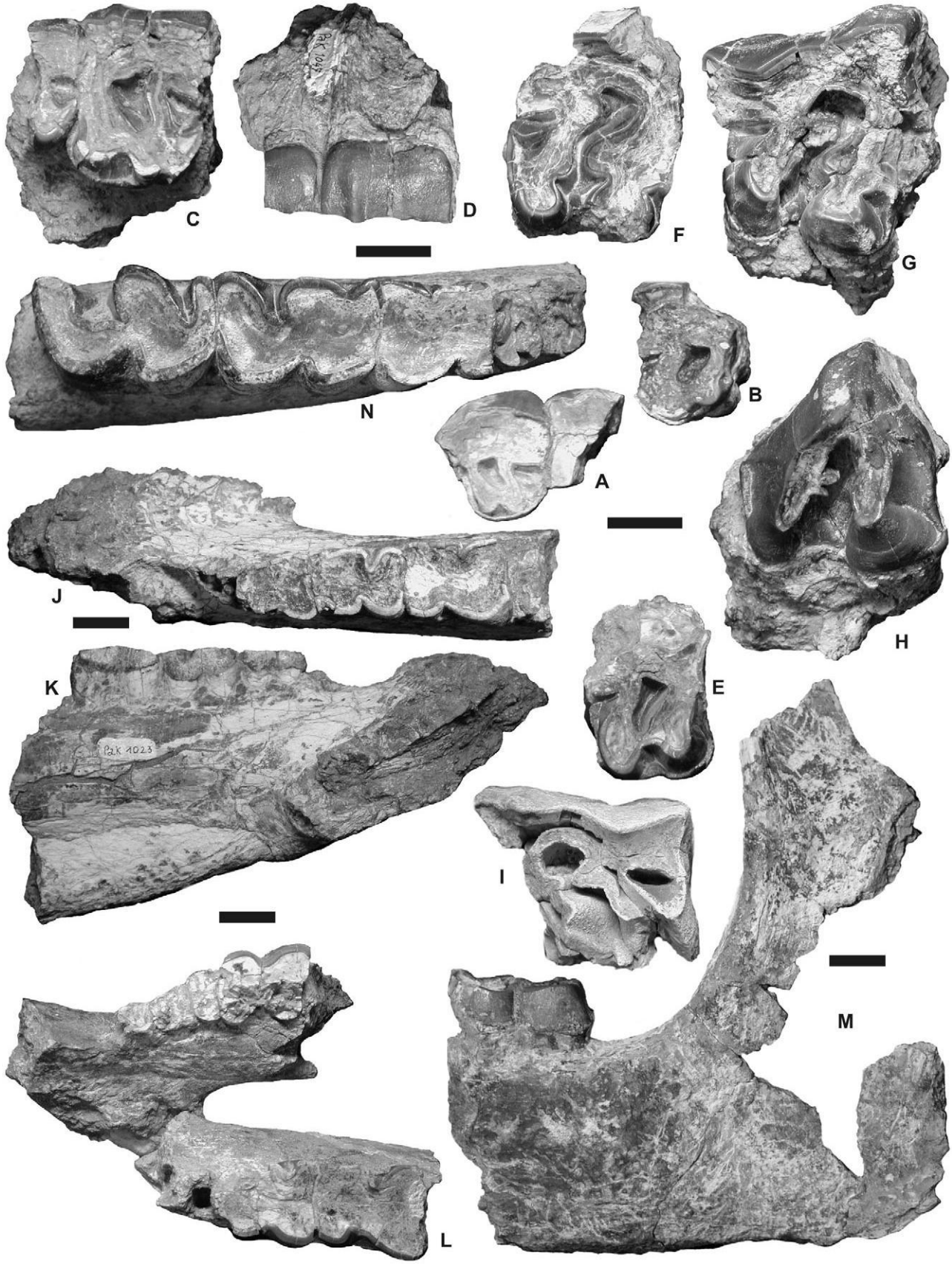
C
D
F
G
N
B
A
J
H
K
E
I
M
L

Figure 8. ***Mesaceratherium welcommi*** **sp. nov.** from the Early Miocene of the Bugti Hills, Balochistan, Pakistan: Cranial, mandibular, and dental remains. A, left P2 and fragmentary P3 (MHNT Pak 1044), occlusal view. Kumbi 4a; B, right P2 (MHNT Pak 1038bis), occlusal view. Kumbi 4a; C, left maxilla fragment, with posterior part of P2, and P3 (MHNT Pak 1047), occlusal view. Kumbi 4a; D, same, labial view; E, right P4 without ectoloph (MHNT Pak 1025), occlusal view. Kumbi 4a; F, broken right M1 (MHNT Pak 1060), occlusal view. Kumbi 4a; G, right M2 (MHNT Pak 1032A), occlusal view (holotype). Kumbi 4a; H, right M3 from the same individual as MHNT Pak 1032A (MHNT Pak 1032B), occlusal view (holotype); I, broken left M2 (MHNT Pak 2203), occlusal view (DB6); J, anterior part of a left hemimandible with p3–m1 and alveoli of i2, p1, and p2 (MHNT Pak 1023), occlusal view. Kumbi 4a; K, same, lingual view; L, fragment of a mandible with symphysis, left p4–m2, fragment of right p4, m1, m3, and alveoli of left and right p2–p3 (MHNT Pak 1054), occlusal view (paratype). Kumbi 4a; M, fragment of a left hemimandible with m3 and vertical ramus (MHNT Pak 1196), labial view. Kumbi 4a; N, fragment of a right hemimandible with m1–m3 (MHNT Pak 1648), occlusal view. Gandô 4. Scale

bars = 2 cm.

« *Dicerorhinus* » cf. *abeli* (partim) Welcomme *et al.*, 1997: 532, 535

? '*Dicerorhinus*' cf. *abeli* (partim) Welcomme *et al.*, 1997: 534, 535, 536

Rhinocerotini, indeterminate genus and species Downing, 2005: 1–8, figs 2–3

Mesaceratherium sp. Métais *et al.*, 2009: 163, 164; table 2, fig. 5

Diagnosis: Differs from other species of *Mesaceratherium* by a shorter premolar series, a hypocone posterior to the metacone, and stronger than the protocone on P2, a protocone slightly constricted on P3–4 and deeply constricted on M1–2, lower cheek teeth with a constricted entoconid, and lower premolars without labial cingulum. Further differs from *Mesaceratherium gaimersheimense* by an upraised mandibular symphysis, a foramen mentale below the middle of p3, a thick and continuous protoloph on P2, the constant presence of a crochet on upper molars, a constricted entoconid but no lingual cingulid on lower premolars, and the occasional absence of d1/p1. Differs from *Mesaceratherium paulhiacense* by the presence of a lingual bridge on upper premolars (molariform in *M. paulhiacense*), by a labial cingulum on upper molars, and the absence of a mesostyle on M2, in the curved magnum-facet and fused McIII-facets on McII, fused calcaneus-facets 2 and 3 on the astragalus, the presence of a fibula-facet on the calcaneus, the proximal border of MtIII concave in anterior view, and in the presence of a distal widening of the diaphysis on MtIII.

Nomenclatural remark: This new species must be referred to as *Mesaceratherium welcommi* Antoine and Downing, 2010, following article 50.1 and the 'recommendation 50A concerning multiple authors' of the International Code of Zoological Nomenclature (ICZN, 1999: 52, 182).

Holotype: Right M2 (MHNT Pak 1032a), right M3 (MHNT Pak 1032b), and ectometaloph of a left M3 (MHNT Pak 1051) from the same individual, unearthed in the locality of Kumbi 4a (earliest Miocene; Bugti Hills, Balochistan, Pakistan).

Paratype: Fragment of mandible with symphysis, left p4–m2, fragments of right p4, m1, m3, and alveoli of left and right p2–3 (MHNT Pak 1054) from the locality of Kumbi 4a (earliest Miocene; Bugti Hills, Balochistan, Pakistan).

Etymology: In honour of Jean-Loup Welcomme, French palaeontologist, pioneer, and leader of the French Palaeontological Expeditions in the Bugti Hills (Balochistan, Pakistan), for his prominent role in the better understanding of mid-Cenozoic vertebrate assemblages from Pakistan.

Stratum typicum: Level 4 (earliest Miocene), parallelized with the Aquitanian, or Agenian European Land Mammal Age (MN2; Lindsay *et al.*, 2005; Métais *et al.*, 2009).

Type locality: Kumbi 4a, 30 km west of Dera Bugti (Balochistan, Pakistan).

Stratigraphical range: Chitarwata Fm. (Bugti and Zinda Pir areas) and base of the Vihowa Fm. (Bugti area). Early Miocene (*c*. 23–18.5 Myr; Lindsay *et al.*, 2005; Métais *et al.*, 2009).

Geographical range: Bugti and Zinda Pir area, Sulaiman Lobe, Balochistan, Pakistan.

Referred material

Old collections

'Near Dera Bugti' (? Early Miocene). Left maxilla with P2–4 (NHM M 15332) and right P2–3 (NHM M without number) from the same individual; right P3 (NHM M 15334); left P2 (NHM M 15336); right P2 (NHM M w.n.). Beloochistan Hills (? Early Miocene).

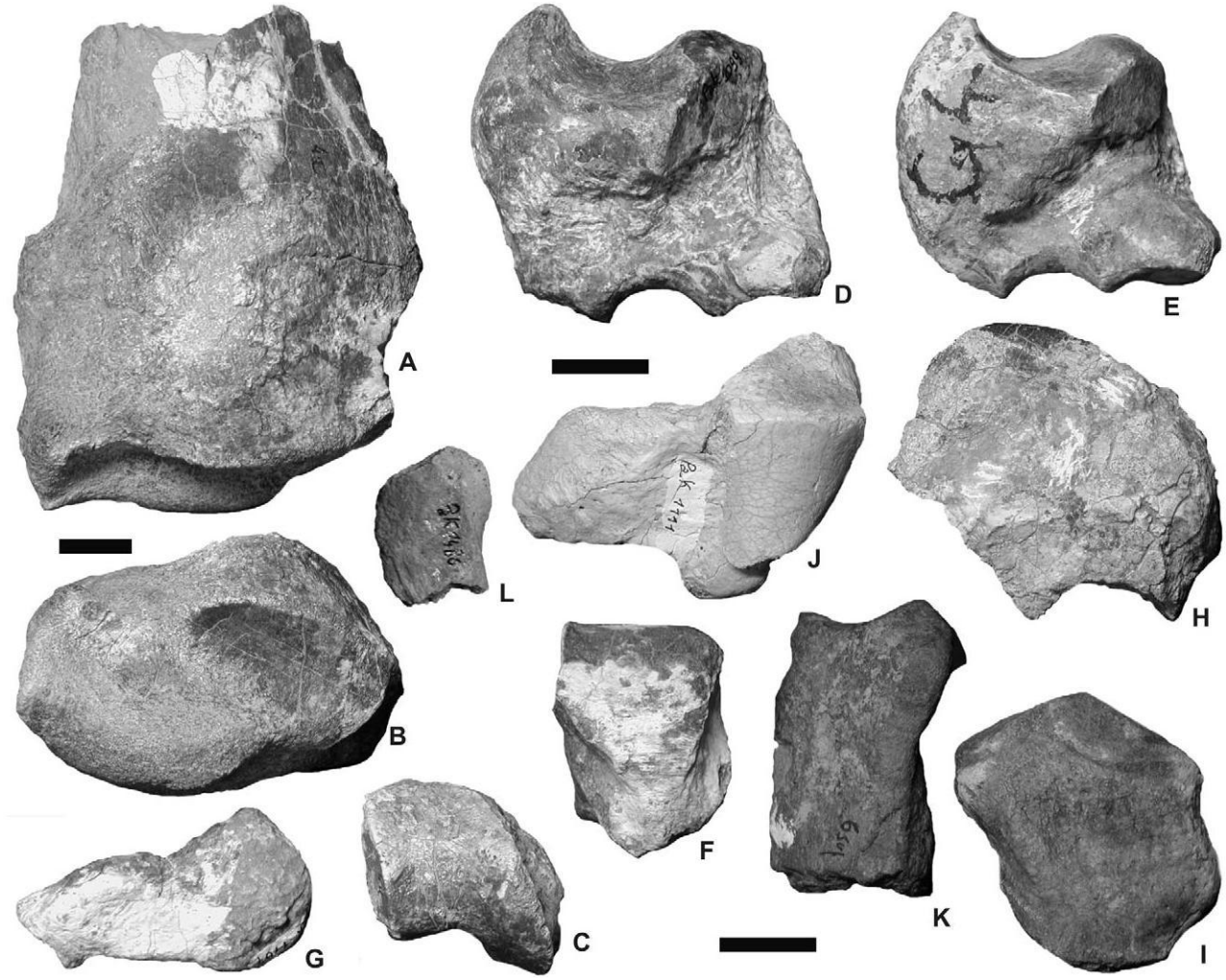

Figure 9. ***Mesaceratherium welcommi*** **sp. nov.** from the Early Miocene of the Bugti Hills, Balochistan, Pakistan: Fore limb remains. A, left radius, distal end (MHNT Pak 1092), anterior view. Kumbi 4a; B, same, distal view; C, left ulna, distal end (MHNT Pak 1184), distal view. Kumbi 4a; D, right scaphoid (MHNT Pak 1099), posteroproximal view. Kumbi 4a; E, right scaphoid (MHNT Pak 1868), posterolateral view. Gandô 4; F, left semilunate (MHNT Pak 1100), anterior view. Kumbi 4a; G, left pisiform (MHNT Pak 1107), medial view. Kumbi 4a; H, left magnum without posterior tuberosity (MHNT Pak 1109), medial view. Kumbi 4a; I, left unciform without posterior tuberosity (MHNT Pak 1709), anterior view. Kumbi 4f; J, right unciform (MHNT Pak 1111), dorsal view. Kumbi 4a; K, left McII, proximal end (MHNT Pak 1552), anterior view. Dera Bugti 6 sup; L, left McV, proximal end (MHNT Pak 1480), anterior view. Dera Bugti 6. Scale bar = 2 cm.

Distal end of a right radius (NHM M 10871). 'Gaj of the Bugti Hills' (? Early Miocene). P3 (IMC C. 295); P4 (IMC C. 311).

New material Bugti Hills (Fig. 1).

Kumbi 4a (Level 4, earliest Miocene). Fragment of left mandible with p3–m1 and alveoli of i2, p1, and p2 (MHNT Pak 1023); fragment of left mandible with m1 (MHNT Pak 1040); fragment of left mandible with m3 and vertical branch (MHNT Pak 1196), maybe from the same individual as MHNT Pak 1023; left P2 and fragment of P3 (MHNT Pak 1044); right P2 (MHNT Pak 1038bis); fragment of left maxilla with P3 and posterior part of P2 (MHNT Pak 1047); right P3 without ectoloph (MHNT Pak 1025); left P4 without ectoloph (MHNT Pak 1026); fragment of a left P4 (MHNT Pak 1062); fragment of a right M1 (MHNT Pak 1060); right M2 (MHNT Pak 1032a), right M3 (MHNT Pak 1032b) and ectometaloph of left M3 (MHNT Pak 1051) from the same individual; left M2 without ectoloph (MHNT Pak 1049); lingual fragment

Figure 10. ***Mesaceratherium welcommi*** **sp. nov.** from the Early Miocene of the Bugti Hills, Balochistan, Pakistan: Hind limb remains. A, left astragalus (MHNT Pak 1135), anterior view. Kumbi 4a; B, same, distal view; C, right astragalus (MHNT Pak 1136), posterior view. Kumbi 4a; D, right astragalus (MHNT Pak 1144), medial view. Kumbi 4a; E, left calcaneus (MHNT Pak 1147), lateral view. Kumbi 4a; F, right calcaneus (MHNT Pak 1149), proximal view. Kumbi 4a; G, right navicular (MHNT Pak 1153), proximal view. Kumbi 4a; H, same, distal view; I, right cuboid (MHNT Pak 1990), lateral view. Dera Bugti 4; J, same, distal view; K, left entocuneiform (MHNT Pak 1095), anterior view. Kumbi 4a; L, left MtII, proximal end (MHNT Pak 1164), dorsal view. Kumbi 4a; M, left fragmentary MtIII (MHNT Pak 2126), anterior view. Kumbi 5; N, left MtIV, distal end (MHNT Pak 1190), anterior view. Kumbi 4a. Scale bar = 2 cm.

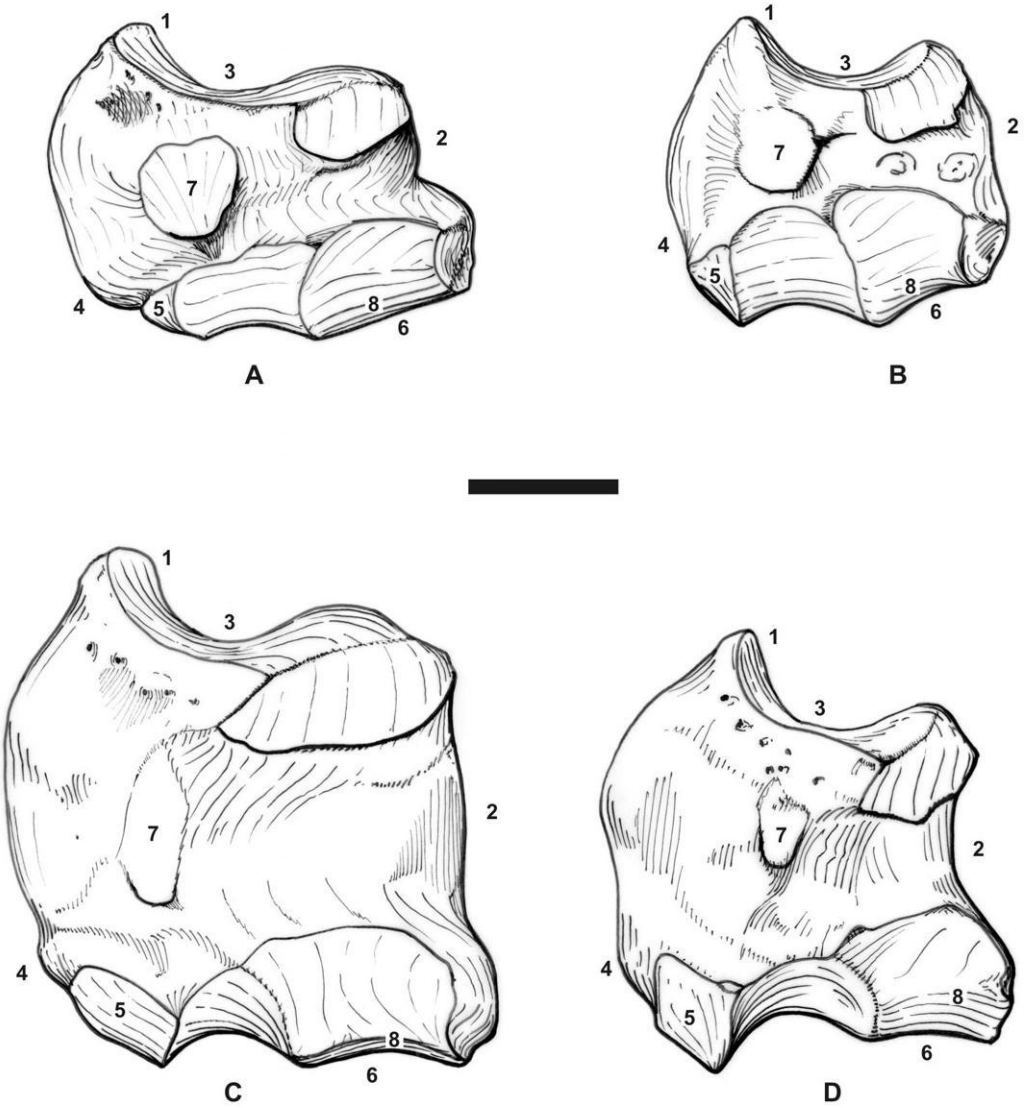

Figure 11. Morphological comparison amongst right scaphoids of four coeval fossil rhinocerotids (Early Miocene) referred to the genera *Pleuroceros* Roger, 1898 and *Mesaceratherium* Heissig, 1969, in lateral view. A, *Pleuroceros blanfordi* (Lydekker, 1884), Zinda Pir Dome, Pakistan; B, *Pleuroceros pleuroceros* (Duvernoy, 1853), Aquitaine Basin, France. 1. posterior height nearly equals anterior height; 2. robust and low bone; 3. shallow radial notch; 4. mediodistal tuberosity (thick in *P. blanfordi* but absent in *P. pleuroceros*); 5. small trapezium-facet; 6. flat magnum-facet; 7. prominent postero-proximal semilunate-facet; 8. no edge between anterodistal semilunate- and magnum-facets; C, ***Mesacerath-erium welcommi* sp. nov.**, Zinda Pir Dome, Pakistan; D, *Mesaceratherium paulhiacense* (Richard, 1937), Aquitaine Basin, France. 1. posterior height much exceeding anterior height; 2. slender and elevate bone; 3. deep radial notch; 4. small mediodistal tuberosity; 5. large trapezium-facet; 6. concave magnum-facet; 7. no posteroproximal semilunate-facet (smooth pad); 8. sharp edge between anterodistal semilunate- and magnum-facets. (B) and (D) modified after de Bonis (1973). Scale bar = 2 cm.

of right M2 (MHNT Pak 1033); fragment of a worn right M1–2 (MHNT Pak 1063); fragment of a worn left M3 (MHNT Pak 1065); protoloph of a left M3 (MHNT Pak 1066); distal end of a left radius (MHNT Pak 1092); distal end of a left ulna (MHNT Pak 1184); right scaphoid (MHNT Pak 1099); left semilunate (MHNT Pak 1100); fragment of a left semilunate (MHNT Pak 1103); left pisiform (MHNT Pak 1107); broken left magnum (MHNT Pak 1109); right unci-form (MHNT Pak 1111); distal end of a right tibia (MHNT Pak 1125); left astragalus (MHNT Pak 1134); left astragalus (MHNT Pak 1135); right astragalus (MHNT Pak 1136); medial part of a right astragalus (MHNT Pak 1144); fragment of an eroded right

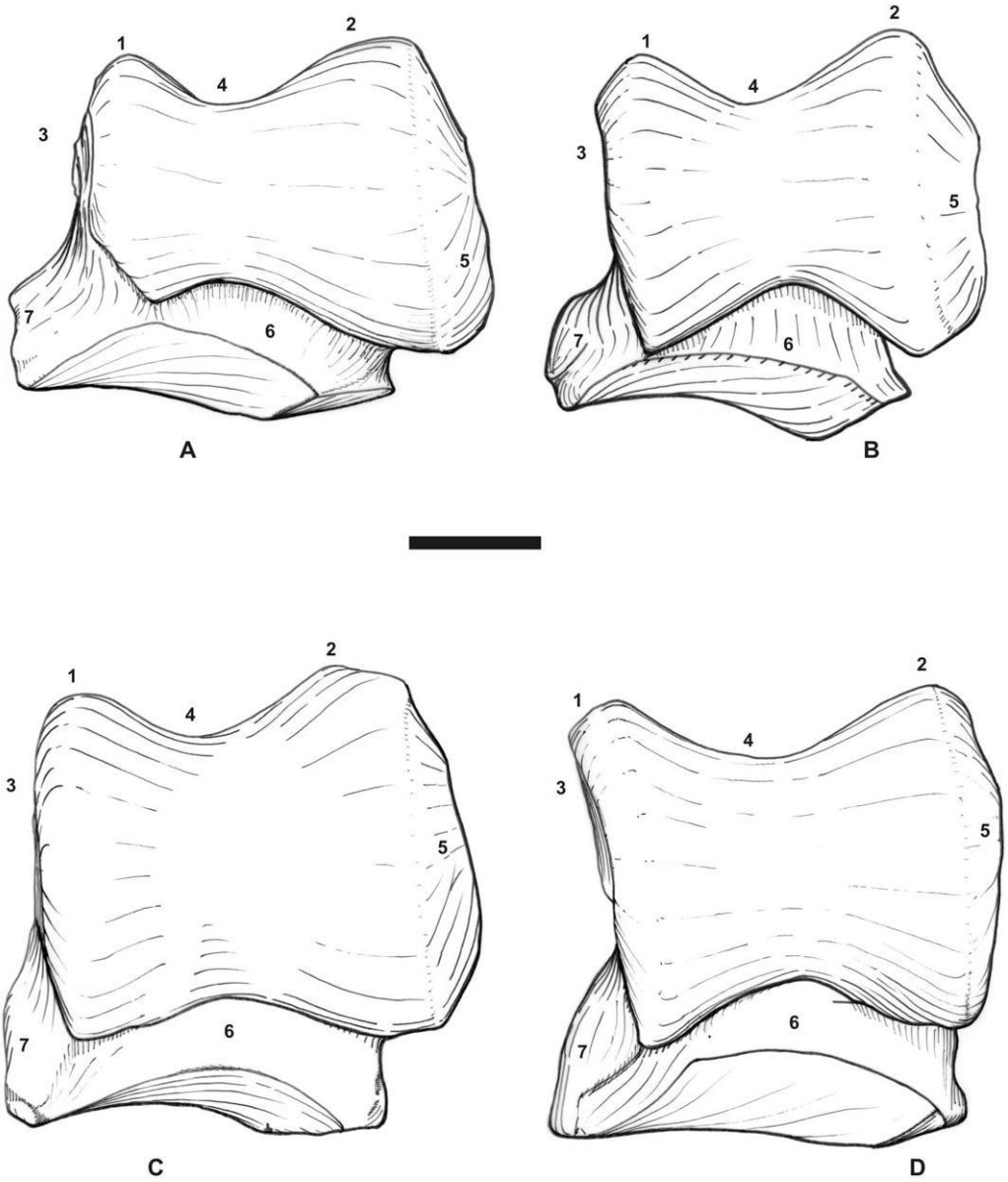

Figure 12. Morphological comparison amongst left astragali of four coeval fossil rhinocerotids (Early Miocene) referred to the genera *Pleuroceros* Roger, 1898 and *Mesaceratherium* Heissig, 1969, in lateral view. A, *Pleuroceros blanfordi* (Lydekker, 1884), Zinda Pir Dome, Pakistan; B, *Pleuroceros pleuroceros* (Duvernoy, 1853), Aquitaine Basin, France (reversed). 1. medial lip smaller than the lateral one; 2. lateral height much exceeding medial height; 3. robust, broad, and low bone; 4. deep trochlear notch; 5. broad and oblique fibula-facet; 6.high collum tali (with respect to total height); 7. medial tubercle low, salient, and laterally displaced.; C, ***Mesaceratherium welcommi* sp. nov.**, Bugti Hills, Pakistan; D, *Mesaceratherium paulhiacense* (Richard, 1937), Aquitaine Basin, France. 1. medial lip nearly equals the lateral one in size; 2. lateral height nearly equals medial height; 3. slender, narrow, and elevated bone; 4. narrow trochlear notch; 5. narrower and less oblique fibula-facet; 6.high collum tali (but lower with respect to total height); 7. medial tubercle high, smooth, and not-laterally displaced. (B) and (D) modified after de Bonis (1973). Scale bar = 2 cm.

astragalus (MHNT Pak 1145); left calcaneus (MHNT Pak 1147); right calcaneus (MHNT Pak 1149); right navicular (MHNT Pak 1153); left entocuneiform (MHNT Pak 1095); proximal end of a left Mt II (MHNT Pak 1164); distal end of a left Mt IV (MHNT Pak 1190). Kumbi 4c (Level 4, earliest Miocene). right P3 (MHNT Pak 77); distal end of a right tibia (MHNT Pak 70); right cuboid (MHNT Pak 851). Kumbi 4f (Level 4, earliest Miocene). Fragment of a right man-dible with m1–3 (MHNT Pak 1648); broken left unci-

form (MHNT Pak 1709). Gandô 4 (Level 4, earliest Miocene). Right scaphoid (MHNT Pak 1868); medial fragment of a right astragalus (MHNT Pak 1873). Dera Bugti 4 (Level 4, earliest Miocene). Right cuboid (MHNT Pak 1990); posterior tuberosity of a right cuboid (MHNT Pak 1991). Kumbi 5 (Level 5, Early Miocene). Proximal end of a right Mt III (MHNT Pak 2126). Dera Bugti 5 (Level 5, Early Miocene). Left patella (MHNT Pak 1260). Dera Bugti 6 (Level 6, Early Miocene). Right M1 without ectoloph (MHNT Pak 165); left M2 without ectoloph (MHNT Pak 1435); left broken M2 (MHNT Pak 2203); fragment of a right M2 (MHNT Pak 1438); fragment of a right M3 (MHNT Pak 1437); proximal end of a left McV (MHNT Pak 1480). Dera Bugti 6sup (Level 6, Early Miocene). Proximal end of a left McII (MHNT Pak 1552); fragment of a right patella (MHNT Pak 2234). Zinda Pir Dome (Fig. 1).

Z147 (earliest Miocene). Right M1 (PMNH Z2268).
Z139 (earliest Miocene). Right scaphoid (PMNH Z2046); left pyramidal (PMNH Z2048). Z143 (earliest Miocene). Left P2, right M2, left M3, and right M3 with 'fractured and dislocated partial maxilla' (PMNH Z2269; Downing, 2005: 3).

Description

Skull: The only available cranial element (PMNH Z2269C, from Zinda Pir) is fragmentary and dislo-cated (Downing, 2005: fig. 3). The anterior base of the zygomatic arch was high. The position of the anterior border of the orbit with respect to M3 is not observable.

Mandible: Three fragments are available (MHNT Pak 1023, 1054, 1196; Fig. 8J–M). The corpus mandibulae was about 440 mm long (from MHNT Pak 1023 + MHNT Pak 1196). The short symphysis is raised about 30° with respect to the corpus mandibu-lae, and a little more on MHNT Pak 1054 (Fig. 8K). It is thick, slightly constricted at the diastema level, and weakly widened in its anterior tip. The posterior border of the symphysis reaches the middle of p3, as does the foramen mentale (Fig. 8J–K). The latter is large, deep, and stretched sagittally. A sharp sagittal ridge runs on the dorsal border throughout the diastema, prior to joining the lingual side of the p1. The ventral side of the symphysis is convex in ante-rior view. There is a thick spina mentalis, forming a rounded axial tubercle at the caudal tip of the sym-physis (MHNT Pak 1054). The spatium interman-dibularis is very narrow near the symphysis: only 12–15 mm between the branches at the p4 level (Fig. 8L). No median sagittal groove (sulcus mylohy-oideus) is present on the lingual side of the corpus mandibulae. The latter gets regularly higher back-wards until m2, with a straight ventral border (Table 2). Behind, its height becomes constant. The horizontal branches deviate regularly. In cross-section, they are vertical. The angulus mandibulae, incompletely preserved (MHNT Pak 1196), is not very salient. The ramus mandibulae is vertical, with a processus coronoideus long and well developed sagit-tally, although broken (Fig. 8M). The foramen man-dibulare is located below the neck line.

Dentition: The presence of upper incisors and i1 cannot be confirmed from the available material. Still, the alveoli of i2 are preserved on the mandible MHNT Pak 1023 (Fig. 8K). These incisors were subcircular in cross-section, parallel, and *c.* 25 mm away from one another. The cheek teeth formula is 4P–3M and 4p–3m. No P1 (or persistent D1) is known, but each P2 bears contact facets with the former. The upper premolar series is long with respect to the molar series: $L_{P3–4}/L_{M1–3}$ ¥ 100) [a] 52. Some cement is visible on a few ectolophs, ectolophids, and in the bottom of some valleys (MHNT Pak 1648). There are no second-ary enamel foldings (Fig. 8A–I). The enamel is thick and wrinkled throughout the crowns (lower and upper teeth). The crowns are low and conical; the roots are independent, long and divergent.

The labial cingulum is totally absent on the upper teeth except for an isolated spur at the posterior tip of the ectometaloph of M3. By contrast, the lingual cingulum is always present. It is high and thickly developed on the upper premolars, sometimes inter-rupted on the protocone (MHNT Pak 1038) and/or on the hypocone (MHNT Pak 1026, 1047). This cin-gulum is reduced to a tubercle at the entrance of the median valley on all the upper molars. On M2 MHNT Pak 1438 and 2203, it forms a transverse spur that splits the valley in two parts. The anterior and posterior cingula are thick and continuous. There is neither crista, nor cristella nor medifos-sette on the upper cheek teeth. The postfossette is narrow and as deep as the median valley (Fig. 8C, E–G, I).

The upper premolars are quadrangular, short, and wide (Fig. 8A–D; Table 4). The crochet is generally lacking at the observed stages of wear (12 specimens out of 16). When present, it is restricted to a short tubercle. The metaloph is continuous, lacking any constriction, but very thin until late stages of wear. However, a thin lingual bridge connects the protocone and hypocone much earlier on the upper premolars, but there is no antecrochet. The hypocone is posterior to the metacone on all premolars. On P2, the proto-cone is weaker than the hypocone. The protoloph is thin and usually complete, except on NHM M 15336. The anterior constriction of the protocone is weak but always present on P3–4. The protoloph is continuous

Table 4. *Mesaceratherium welcommi* sp. nov. Dental dimensions (range, number of specimens in square brack-ets, and mean, in mm) from the Early Miocene of the Bugti Hills (Balochistan, Pakistan)

Tooth	L	ant W	post W	H
P2	27–32.5	31–35	37–39.5	13–17
Mean	29.4 [5]	32.7 [4]	37.5 [6]	15.3 [3]
P3	32–38	47–50	46.5–51	17–20
Mean	34.9 [4]	48.5 [4]	48.1 [4]	18.5 [2]
P4	(> 35)–39	55	52	–
M1	(> 46)	(> 63)	(59)	22
M2	57–58	68	58	35
Mean	57.5 [2]	–	–	–
M3	54	61	L_{ect} = 63–64	43–43
Mean	–	–	63.5 [2]	43 [2]
p3	25	17	22.5	7
p4	32	22.5	30.5–32	10–13
Mean	–	–	31.2 [2]	11.3 [3]
m1	31–41	23–30	27.5–33	8–25
Mean	35.5 [5]	26.7 [4]	29.1 [4]	14.7 [4]
m2	39.5–49.5	26.5–29	29.5–32	10–14
Mean	44.5 [2]	27.7 [2]	30.7 [2]	12 [2]
m3	46.5–53.5	26.5–29	26–27.5	8–19
Mean	49.2 [3]	27.8 [3]	26.5 [3]	14.3 [3]

ant, anterior; H, height; L, length; L_{ect}, length of the ectometaloph; post, posterior; W, width. Approximate dimensions appear between brackets.

and thick on P3. The paracone fold is strong on the premolars, whereas the metacone fold is poorly devel-oped or absent. The parastyle is sagittal.

The antecrochet, which is strongly detached on the upper molars, is oblique and very elongated, so that it joins the hypocone on worn molars (MHNT Pak 1049, 1063, 1065). The anterior constriction is very deep on the protocone, which gives a trefoil-shape to the pro-toloph (Fig. 8F–I). The crochet is always present, sag-ittal and generally simple (12 specimens out of 14). M3 MHNT Pak 1032b has a double crochet, whereas it is simple on the symmetric M3 of the same individual (MHNT Pak 1051) and on M3s PMNH Z2269. The ectoloph of M2 is straight, with a sagittal para-style and a weak paracone fold. Only the most pos-terior part of the ectoloph is concave. The mesostyle is lacking, as is the metacone fold. The metastyle is long on M1–2. The M1 are rectangular and the M2 sub-rectangular, with a metaloph almost as long as the protoloph is (Table 4). The protocone is elongated sagittally, with a lingual side flattened on M2 and convex on M3, but without any lingual groove. The posterior cingulum is continuous but lowered next to the postfossette. On all the upper molars, especially on M2, the hypocone is strongly constricted by a deep anterior groove, still restricted to the base of the crown. On some M2 (MHNT Pak 1032a, 1435) there is also a shallow posterolingual constriction at the base of the hypocone. A few enamel tubercles can occur at the bottom of the median valley (MHNT Pak 1033, 1065, 2203; PMNH Z2269). On M3, the ectoloph and the metaloph are fused into an ectometaloph without any remaining groove. Yet, the M3 have a quadrangular outline, with a wide posterior part sustained by two diverging transverse roots (Fig. 8H).

All the available lower cheek teeth are worn (Fig. 8J–N). The presence of a one-rooted p1, or per-sistent d1, is revealed by a small alveolus located in front of the anterior alveolus of p2 (MHNT Pak 1023). Nevertheless, there is no trace of any tooth anterior to p2 on the symphysis MHNT Pak 1054, belonging to an old individual. There is no lingual cingulid on the lower cheek teeth, except on m3 MHNT Pak 1196 (small ridge at the entrance of the posterior valley). On most specimens, the labial cingulid is also absent. If not, it is reduced to a small ridge closing the ectolophid groove (MHNT Pak 1023). This sharp groove is interrupted above the neck. The trigonid is rounded, forming a right dihedron. The metaconid lacks any constriction at the available stages of wear. The lingual side of the metaconid is flat and very elongated sagittally (as is the protocone on the upper molars), thus forming a right dihedron with the pos-terior border of this cuspid. The entoconid is constricted on the lesser worn teeth (m1 MHNT Pak 1040, m2–3 MHNT Pak 1648). The posterior valley is narrow and V-shaped on both the premolars and m1–2, whereas it is wide and U-shaped on m3. The hypolophid of the molars is almost transverse. There is no lingual groove on the entoconid of m2–3. The posterior cingulid is weak, reduced to a smooth median tubercle on m3 (Fig. 8M).

No deciduous tooth has been unearthed.

Postcranial skeleton: The bones are large and slender (Figs 9–10; Tables 5–8, 10–12, 14–16, 18–22, 25–27). The rachis, the scapula, and the humerus are unknown.

The radius is represented by a distal end (MHNT Pak 1092; Fig. 9A–B). The diaphysis has a drop-like cross-section. The radius and the ulna were indepen-dent throughout their diaphysis: no trace of contact or synostosis is visible. The distal end is not much widened with respect to the diaphysis (Table 5). Only one distal ulna-facet is present, well developed and almond-shaped. The m. extensor carpi groove is wide and deepened by the strong tuberculum dorsale lying beside it. The distal articulation is wide. The scaphoid-facet is very short in its anterior part and very convex behind. This facet is deep (APD), with a wide and low triangular posterior expansion. The semilunate-facet is narrow whereas the pyramidal-

Table 5. *Pleuroceros blanfordi* (Lydekker, 1884) and ***Mesaceratherium welcommi* sp. nov.** Compared dimensions of the radii (range, number of specimens in square brackets, and mean, in mm) from the Early Miocene of the Bugti Hills (Balochistan, Pakistan)

	prox. ext.		proximal art.			Diaphysis		dist. ext.		dist. art.	
Taxon	TD	APD	TD	medAPD	latAPD	TD	APD	TD	APD	TD	APD
P. b.	77–78.5	48.5–51.5	77	40–44	24–26	39–46	26–28	80–82.5	56	(65)	(31)–32
Mean	77.7 [2]	50 [2]	–	42 [2]	25 [2]	42.5 [2]	27 [2]	81 [3]	–	–	–
M. w.	–	–	–	–	–	–	–	80	(53)	75	(40)

APD, anteroposterior diameter; art., articulation; dist., distal; ext., extremity; lat, lateral; med, medial; *M. w.*, *M. welcommi*; *P. b.*, *P. blanfordi*; prox., proximal; TD, transverse diameter. Approximate dimensions appear between brackets.

facet is very developed, transversally and sagittally. The latter forms a wide oblique band that extends onto the posterior side.

A distal end of an ulna is preserved (MHNT Pak 1184; Fig. 9C). There is no lateral tubercle. The cross-section of the diaphysis forms a flattened lozenge. On the medial side, the only radius-facet is spindle-shaped and oblique with respect to the vertical. The distal articulation corresponds only to the pyramidal and the pisiform. The pyramidal-facet is narrow (TD = 31; APD = 48), subrectangular and more rounded behind than anteriorly. The wide pisiform-facet forms a triangle restricted to the posterior side of the bone. This facet is very high.

The carpus is high and rather slender (Figs 9D–J, 11C; Tables 6–8, 10–11).

Three scaphoids have been collected. Even though their size range reaches *c*. 15% (Table 6), the mor-phology is identical. The APD and H are similar (Figs 9D–E, 11C). There is no tubercle on the medial side, but a shallow depression hollowing its antero-distal corner. The anterior border of this medial side is straight, inclined downwards, whereas the poste-rior border is vertical and regularly convex. The radius-facet is as wide (TD) as deep (APD). It is much upraised in its posterior part, so the bone is much less elevated anteriorly than posteriorly (Fig. 11C). On the lateral side, only two semilunate-facets are present. There is neither posteroproximal facet nor tubercle. The trapezium-facet is well developed, high, and narrow (APD). In distal view, the trapezoid-facet is rectangular, longer (APD) than wide (TD). The magnum-facet forms an equilateral triangle, trans-versally flat and sagittally concave.

The semilunate is high and narrow (Fig. 9F; Table 7). The anterior side bears a thick and angulous tubercle for the m. interossei dorsales. Its distal border is sharp. The magnum-facet reaches the ante-rior side of the bone. It is weakly hollow in its pos-terior part. The unciform-facet is oval and biconcave. The posterior tuberosity is narrow and higher than wide.

The pyramidal PMNH Z2048 is badly preserved and eroded. It is roughly cubic (TD [a] 36; APD [a] 45; anterior height [a] 51). The proximal facet, for the ulna, is small. The pisiform-facet is eroded. Some parts of a strong tubercle remain on the lateral side. The medial facets for the semilunate are not preserved; yet the distal one probably had an asymmetric outline. On the distal side, the biconcave unciform-facet forms a quarter-circle in distal view.

Both trapezium and trapezoid are unknown.

The pisiform MHNT Pak 1107, doubtfully attrib-uted to this taxon, is slender and elongated sagittally (Fig. 9G; Table 8). The pyramidal-facet is comma-like, whereas the ulna-facet is semicircular. The median part, between the articular area and the posterior tuberosity, is constricted.

A broken and large-sized magnum is available (MHNT Pak 1109; Table 10). The posterior tuberosity is not preserved (Fig. 9H). The anterior side, bearing a thick tubercle surrounded by sharp ridges, is higher than wide. The proximal border is straight. The semilunate-facet reaches the anterior side. It is long (APD) and slightly convex transversally, with a 'question-mark'-like lateral profile. In proximal view, the articular apophysis bears two dissymmetrical sides. The medial side is narrow and subvertical, restricted to the anterior side of the bone. The lateral one, for the semilunate, is much more developed laterally and sagittally. On the medial side, the articular facets are connected throughout their length (APD) and delimited by a sharp ridge. This ridge is anteriorly shortened by a shallow indentation. On the lateral side, the unciform-facet forms a narrow and elongated stripe. Distally, the McIII-facet has a sigmoid lateral border.

Two unciforms are attributed to this taxon (Fig. 9I– J). The anterior side is as high as wide (Table 11). The tubercles for the m. interossei dorsales are almost lacking, except for a small mediodistal pad. The pos-terior tuberosity is very long. Thus, the proximal articular area only reaches the anterior third of the bone. The proximal facets are triangular and sagit-

Table 6. *Pleuroceros blanfordi* (Lydekker, 1884) and ***Mesaceratherium welcommi* sp. nov.** Compared dimensions of the scaphoids (range, number of specimensinsquarebrackets,andmean,inmm)fromtheEarlyMioceneoftheBugtiHillsandoftheZindaPir(Pakistan)

			Height				Trapz.-fac.		Trapzd.-fac.		Mag.-fac.		
Taxon	TD	APD	ant	mid.	post	Rad.-fac.APD	H	APD	TD	APD	TD	APD	D SL- fac.
P. b.	39–43 58–60Mean41[2]60[2]*M.w.*38.5–46.560– 66.5Mean41.7[3]63[3]		40–40 30–33 44–4440[2]31.5[2]44[2]48– 5741.5–5057–6853.3[3]46.2[3]64[3]			37–3938[2]40– (46)42.5[2]	12–16 6– 714[2]6.5 [2]23– 2510– 1324[2]11.5[2]		28–28 20–22 22–24 22 9–928[2]21[2]23[2]22[2]9[2]22–2523–2619–2418–2312– 1423.7[3]24.3[3]21.7[3]19.7[3]13[2]				

ant, anterior; APD, anteroposterior diameter; D, distance; fac., facets; H, height;posterior;Rad.,radius;TD,transversediameter;Trapzd,trapezoid.Approximate Mag., magnum; mid., middle; *M. w.*, *M. welcommi*; *P. b.*, *P. blanfordi*; post,dimensionsappearbetweenbrackets.

tally convex. The semilunate-facet is flat transver-sally on MHNT Pak 1709 and slightly concave on MHNT Pak 1111. The pyramidal-facet, lacking any posterolateral expansion, is distant from the McV-facet. The latter is about 60° to the vertical line.

The metacarpus is only represented by two proxi-mal ends (McII and McV; Fig. 9K–L).

McII MHNT Pak 1552 has a large proximal end, without any salient insertion for the m. extensor carpalis (Fig. 9K). In proximal view, the trapezoid-facet is pentagonal. The longest border is next to the lateral magnum-facet. This facet forms a curved stripe, vertical and elongated sagittally. The McIII-facets are distinct. The anterior facet is the most developed. It follows the magnum-facet, without marked edge between them. The posterior facet is reduced. A small trapezium-facet is present on the posteromedial side. It joins the proximal facet. The diaphysis has an oval cross-section, sagittally flat-tened (Table 12).

The McV was functional, with an elongated diaphy-sis (Fig. 9L; Table 14). The unciform-facet is convex and narrow sagittally. The adjoining McIV-facet is high (7 mm) and almond-shaped.

The femur and the fibula are unknown.

The patellae are damaged. The most complete (MHNT Pak 1260) is higher than wide (TD; Table 15). The muscular insertions are smooth on the anterior side. The most salient corresponds to the m. fascia lata. On the articular side, the medial lip is wide and triangular, not very hollow. The proximal border of the articular area is strongly delimited laterally. The distal tip is high and sharp, displaced outwards. The lateral lip is wide and very hollow.

Two distal ends of a tibia are preserved. They have different sizes (Table 16) but the same mor-phology. The anterior side is short of any anterodis-tal groove. At the contrary, the m. tibialis posterior groove is wide and deep on both specimens. The lateral border of the diaphysis shows high and wide (APD) rough scars corresponding to the contact with the fibula: this bone, although lacking, would have had a very developed sagittally distal end. The fibula-facet is small. The posteromedial apophysis is high and sharp. In distal view, the distal end forms a trapezium, with a straight anterior border and a high APD.

Six astragali are available, amongst which three are complete. The morphology is homogenous, but two series can be distinguished, with a size difference of *c.* 10–15% (Table 18). The astragalus is slightly wider than high (TD/H = 1.08; Figs 10A–C, 12C). It is robust in medial view (APD/H = 0.70; Fig. 10D). The fibula-facet is high, subvertical, and flat transversally. The collum tali, usually low, is high on one specimen (MHNT Pak 1135). The medial tubercle is not very

Table 7. *Pleuroceros blanfordi* (Lydekker, 1884) and ***Mesaceratherium welcommi* sp. nov**. Compared dimensions of the semilunates (mm) from the Early Miocene of the Bugti Hills (Balochistan, Pakistan)

					Magnum-fac.		Uncif.-fac.			
Taxon	TD	APD	H	post TD	TD	APD	TD	APD	D Scaph.- fac.	D Pyram.- fac.
P. b.	34	55	36	24	15	30	20	26	11	8
M. w.	(> 36)	61.5	50	27.5	16	41	25	31	–	–

ant, anterior; APD, anteroposterior diameter; D, distance; fac., facet(s); H, height; *M. w.*, *M. welcommi*; *P. b.*, *P. blanfordi*; post, posterior; Pyram., pyramidal; Scaph., scaphoid; TD, transverse diameter; Uncif., unciform. Approximate dimensions appear between brackets.

Table 8. *Mesaceratherium welcommi* sp. nov. Dimen-sions of the pisiform (mm) from the Early Miocene of the Bugti Hills (Balochistan, Pakistan)

		Tuberosity			
TD	APD	H	APD	Ulna-fac. TD	TD Pyram.-fac.
23.5	62.5	34	20	13	18

APD, anteroposterior diameter; fac., facet; H, height; Pyram., pyramidal; TD, transverse diameter.

Table 9. *Pleuroceros blanfordi* (Lydekker, 1884). Dimen-sions of the trapezoid (mm) from the Early Miocene of the Bugti Hills (Balochistan, Pakistan)

		Height			
TD	APD	ant	mid.	post	Trapz.-fac. min. APD
(21)	(30)	21	16.5	21	9

ant, anterior; APD, anteroposterior diameter; fac., facet(s); mid., middle; min, minimal; post, posterior; TD, transverse diameter; Trapz., trapezium. Approximate dimensions appear between brackets.

salient (Fig. 12C). In proximal view, the caudal border of the trochlea is nearly straight. On the posterior side, the calcaneus-facet 1 (see Heissig, 1972: pl. 13) is concave, with a long and narrow laterodistal expan-sion. The calcaneus-facets 2 and 3 are fused. In distal view, the axis of the trochlea is very oblique with respect to the distal articulation. The cuboid-facet forms an oblique stripe, posteriorly interrupted by a brutal inflexion. The navicular-facet is lozengic (Fig. 10B).

The calcaneus is robust (Table 19). The processus calcanei is short, with a wide and massive tuber calcanei (Fig. 10E–F). The latter is not very salient in lateral view, with a laterally displaced anterior tip. The beak is low, with a convex astragalus-facet, nearly angulous. There is a small fibula-facet (MHNT Pak 149), but no tibia-facet. The trochlea fibularis is marked by a sharp circular ridge. The sustentaculum tali is rather narrow. The astragalus-facets 2 and 3 are fused. On the distal side, the cuboid-facet is semicircular and biconcave.

The navicular MHNT Pak 1153 is low, with a loz-engic outline (Fig. 10G–H; Table 20). The TD and APD are similar. In proximal view, the lateral border is concave. A small articular area is isolated on the astragalus-facet, in the posterolateral corner of the proximal side. This area touches the astragalus in the extreme flexion movements.

The cuboid is large and robust (Fig. 10I–J; Table 21). The anterior side is pentagonal. This side is inclined, with a set back proximomedial border. In proximal view, the articular region is subcircular, occupying half of the APD. It is split into two equal facets, weakly separated by a shallow sagittal groove. The medial facet is damaged on all the available specimens. The navicular-facet was high. The poste-rior tuberosity is wide and very high (Table 21). Its distal tip exceeds the distal articular faced by about 15 mm. In lateral view, the posterior border is verti-cal. The distal facet is triangular, long (APD), and narrow (TD).

The mesocuneiform and ectocuneiform are unknown.

A broken entocuneiform was attributed to this taxon owing to the shape of the navicular-facet, which fits with the available naviculars (Fig. 10K). In medial view, it forms a rectangle higher than wide (Table 22). The navicular-facet is subcircular and biconcave. Contiguous to it, the mesocuneiform-facet is comma-like. A tiny MtII-facet is present in the middle of the lateral side of the bone.

The metatarsus is documented by a fragment of MtII, a damaged MtIII, and a distal end of a MtIV. The preserved diaphyseal parts indicate that the metatarsals were long, slender, and not very curved (Tables 25–27).

Table 10. *Pleuroceros blanfordi* (Lydekker, 1884) and ***Mesaceratherium welcommi* sp. nov.** Compared dimensions of the magnums (range, number of specimens in square brackets, and mean, in mm) from the Early Miocene of the Bugti Hills (Balochistan, Pakistan)

					McIII-fac.	
Taxon	TD	ant H	H	SL-fac. APD	TD	APD
P. b.	(34)–34 [2]	(24.5)–27 [2]	45–(48) [2]	39–(43) [2]	(30)–31 [2]	–
M. w.	41.5	38	(63)	58	38	–

ant, anterior; APD, anteroposterior diameter; fac., facet; H, height; *M. w.*, *M. welcommi*; *P. b.*, *P. blanfordi*; SL, semilunate; TD, transverse diameter. Approximate dimensions appear between brackets.

Table 11. *Pleuroceros blanfordi* (Lydekker, 1884) and ***Mesaceratherium welcommi* sp. nov.** Compared dimensions of the unciforms (range, number of specimens in square brackets, and mean, in mm) from the Early Miocene of the Bugti Hills (Balochistan, Pakistan)

					post tuber.		SL-fac.		Pyram.-fac.		McV-fac.	
Taxon	TD	H	max APD	APD	TD	H	TD	APD	TD	APD	TD	APD
P. b.	48–51	44–46	61–67	54–58	29–30	19–22.5	23–(26)	23–28	24–26	28–29	(19)	(21)–(26)
Mean	49.2 [4]	44.5 [4]	63.7 [3]	56 [4]	29.7 [3]	20.8 [3]	23.3 [3]	25.7 [3]	24.7 [3]	28.5 [3]	–	22 [3]
M. w.	59–60	54–55	75	63	30	22	25–27	(26)–30	31–32.5	30	20	31
Mean	59.5 [2]	54.5 [2]	–	–	–	–	26.0 [2]	[2]	31.7 [2]	–	–	–

APD, anteroposterior diameter; fac., facet; H, height; max, maximal; McV, fifth metacarpal; *M. w.*, *M. welcommi*; *P. b.*, *P. blanfordi*; post, posterior; post tuber., posterior tuberosity; Pyram., pyramidal; SL, semilunate; TD, transverse diameter. Approximate dimensions appear between brackets.

Table 12. *Pleuroceros blanfordi* (Lydekker, 1884) and ***Mesaceratherium welcommi* sp. nov.** Compared dimensions of McII (range, number of specimens in square brackets, and mean, in mm) from the Early Miocene of the Bugti Hills (Balochistan, Pakistan)

	prox. art.		Trapzd.-fac.		lat. fac. H			diaphysis		dist. art.	
Taxon	TD	APD	TD	APD	ant	mil.	post	TD	APD	TD	APD
P. b.	(25)	(33)	(19)	(29)	12	8	14	24.5	15–15	33	31
Mean	–	–	–	–	–	–	–	–	15.0 [2]	–	–
M. w.	32.5	41	25	35	20	13	18	–	–	–	–

ant, anterior; APD, anteroposterior diameter; art., articulation; dist., distal; fac., facet; H, height; lat., lateral; *M. w.*, *M. welcommi*; *P. b.*, *P. blanfordi*; post, posterior; prox., proximal; TD, transverse diameter; Trapzd, trapezoid. Approximate dimensions appear between brackets.

The proximal end of Mt II has a semicircular outline in proximal view (Fig. 10L). The mesocuneiform-facet is triangular and biconcave, with smooth angles. On the lateral side, there are two distinct MtIII-facets. The anterior facet is large, cir-cular and vertical, sagittally directed, and separated from the proximal facet. By contrast, the posterior facet joins the mesocuneiform-facet. The top of the entocuneiform-facet is preserved on the posteromedial side of the bone.

MtIII MHNT Pak 2126 bears a concave proximal border in anterior view (Fig. 10M). The proximal end is lacking any salient ligamentary insertion on its anterior side. In proximal view, the anterior border is regularly convex. The anterior MtIV-facet is vertical and triangular. The posterior one is not preserved. There is no cuboid-facet. The diaphysis widens distally. It is slender and flattened sagittally (Table 26). The insertion for the m. interossei is long, especially on the lateral side.

Table 13. *Pleuroceros blanfordi* (Lydekker, 1884). Dimensions of McIII (mean values appear in bottom line and number of specimens in square brackets) from the Early Miocene of the Bugti Hills (Balochistan, Pakistan)

	prox. art.		McIV-fac. D	Uncif.-fac.		Mag.-fac.		Diaphysis		dist. ext.	dist. art.	
L	TD	APD		TD	APD	TD	APD	TD	APD	TD	TD	APD
123	46–54	(>37)–40	7–11	30–35	37–38	14–19	18–25	37–42	14–17	47–(48)	39.5–42	33–34
–	50.2 [4]	39 [4]	11 [4]	33 [3]	37.5 [2]	16.7 [4]	21.6 [4]	39.8 [3]	15.3 [3]	–	40.7 [2]	33.5 [2]

APD, anteroposterior diameter; art., articulation; D, distance; dist., distal; ext., extremity; fac., facet; L, length; Mag., magnum; McIV, fourth metacarpal; prox., proximal; TD, transverse diameter; Uncif., unciform. Approximate dimensions appear between brackets.

Table 14. ***Mesaceratherium welcommi* sp. nov.**
Dimensions of McV (mm) from the Early Miocene of the Bugti Hills (Balochistan, Pakistan)

TD	APD	McIV-fac.		Uncif.-fac. APD
		H	APD	
20.5	23	9	17	21

APD, anteroposterior diameter; fac., facet; H, height; McIV, fourth metacarpal; TD, transverse diameter; Uncif., unciform.

The diaphysis of MtIV MHNT Pak 1190 (Fig. 10N) has a triangular to oval cross-section, medially stretched. The distal trochlea is deeper (APD) than wide (TD), with a salient and sharp intermediate relief (Table 27). This relief is located on the lateral third of the trochlea. The latter is essentially concave transversally in its medial part.

Discussion

The hypodigm of '*Aceratherium blanfordi* Lydekker, 1884' as described successively by Lydekker (1884), Pilgrim (1912), and Forster-Cooper (1934) based on Bugti Hills specimens, included only a palate, a partial mandible, and three dozen upper and lower cheek teeth. With the exception of an unusual size range and a few morphological features on upper cheek teeth (coronary cement weak/abundant; low/ high crown heights; lingual cingulum continuous/ reduced on upper premolars; metaloph oblique/ transverse on P2; antecrochet absent/present on P4; metacone fold absent/present and posterior cingulum reduced/continuous on M1–2; mesostyle absent/ present on M2), it was virtually impossible to distinguish two taxa within the available sample.

Nevertheless, Lindsay *et al.* (2005: 6) described upper teeth and a portion of maxilla from the Early Miocene of the Zinda Pir, Pakistan, and referred them to an 'enigmatic large rhinocerotid', mentioning that 'of the fossils [Forster-Cooper (1934)] discussed, the specimens assigned to *Rhinoceros blandfordi* [. . .] show the closest affinities' to it. Finally, this author concluded to their distinction, on the same grounds as discussed above, without assigning the Zinda Pir specimens to any known genus and species.

The new specimens from the Early Miocene of the Bugti Hills provide a new insight into this taxon. Associated cranials, mandibles, dentals, and postcra-nials found in the last decade by the MPFB allowed us (1) to split the sample of '*Aceratherium blanfordi* Lydekker, 1884' *sensu lato* into two consistent and homogeneous series ('*A. blanfordi*' *sensu stricto*, here referred to as *Pleuroceros blanfordi*, and a new taxon erected on the larger specimens); (2) to define further distinctive characters between them, espe-cially on postcranials (Figs 11–12); and (3) to include the enigmatic large rhino from coeval deposits of the Zinda Pir (Lindsay *et al.*, 2005) within the latter sample, formerly referred to as '*Mesaceratherium* sp.' (Métais *et al.*, 2009). As a matter of fact, based on dimensions and morphology, the concerned remains cannot be assigned to other taxa described in the same deposits as listed by Métais *et al.* (2009), such as the hippo-like teleoceratines *Brachypotherium fatehjangense* (Pilgrim, 1910), *Brachypotherium gajense* (larger and much more robust), and *Prosan-torhinus shahbazi* (small and brachypod), the tiny and minute *Protaceratherium* sp., *Plesiaceratherium naricum* (rhinocerotines), *Bugtirhinus praecursor* (elasmotheriine), and the modern-like rhinocerotines *Gaindatherium* cf. *browni* and 'Rhinocerotina indet., cf. *Rhinoceros*'.

Once its hypodigm is completed – with *c*. 80 avail-able remains – this large and slender taxon differs significantly from *P. blanfordi* in a large amount of features, amongst which are (1) a mandibular char-acter (symphysis upraised); (2) three general dental characters (cement less abundant; lower tooth crowns; distinct roots on cheek teeth); (3) 17 charac-ters of the upper dentition (neither labial cingulum nor crochet, but continuous lingual cingulum on

Table 15. *Pleuroceros blanfordi* (Lydekker, 1884) and ***Mesaceratherium welcommi* sp. nov**. Compared dimensions of the patellae (range, number of specimens in square brackets, and mean, in mm) from the Early Miocene of the Bugti Hills (Balochistan, Pakistan)

		APD			Articulation			lat. trochl.	
Taxon	TD	max.	min.	H	TD	H	TD med. trochl.	TD	H
P. b.	(73)–73.5	(33)–44	27–35	(61)–82	61	56–64	35.5	25–25.5	42
Mean	–	42.0 [3]	33.0 [4]	76.3 [4]	61	60 [2]	35.5	25.3 [3]	42
M. w.	–	53–55	(36)–(39)	(> 97)	–	–	–	29	–
Mean	–	54.0 [2]	–	–	–	–	–	–	–

APD, anteroposterior diameter; H, height; lat., lateral; max, maximal; med., medial; min, minimal; *M. w.*, *M. welcommi*; *P. b.*, *P. blanfordi*; TD, transverse diameter; trochl., trochlea. Approximate dimensions appear between brackets.

Table 16. *Pleuroceros blanfordi* (Lydekker, 1884) and ***Mesaceratherium welcommi* sp. nov**. Compared dimensions of the tibiae (range, number of specimens in square brackets, and mean, in mm) from the Early Miocene of the Bugti Hills (Balochistan, Pakistan)

					Astragalus-cochlea			
	Diaphysis		dist. ext.			APD		
Taxon	TD	APD	TD	APD	TD	med.	mid.	lat.
P. b.	47–47	33.5–36	73–78.5	(50)–57.5	59–(67)	35–39	25–32	40–(43)
Mean	47 [2]	34.5 [3]	76.1 [4]	52.9 [4]	60.0 [4]	37.0 [3]	29.7 [4]	41.2 [4]
M. w.	74	43	93	66–75.5	71	(52)–55	41.5	47
Mean	–	–	–	70.7 [2]	–	–	–	–

APD, anteroposterior diameter; dist., distal; ext., extremity; med., medial; mid., middle; *M. w.*, *M. welcommi*; *P. b.*, *P. blanfordi*; TD, transverse diameter. Approximate dimensions appear between brackets.

Table 17. *Pleuroceros blanfordi* (Lydekker, 1884). Dimen-sions of the fibula (mm) from the Early Miocene of the Bugti Hills (Balochistan, Pakistan)

Diaphysis		dist. ext.		Tibia-fac.		Astrag.-fac.	
TD	APD	TD	APD	APD	H	APD	H
12	18.5	25	37.5	17	7	26	18

APD, anteroposterior diameter; Astrag., astragalus; dist., distal; ext. extremity; fac., facet; H, height; TD, transverse diameter.

upper premolars; hypocone posterior to metacone on P2; medifossette always absent and protocone con-striction always present on P3–4; no antecrochet on P4; labial and lingual cingula always present but no crista on upper molars; continuous posterior cingu-lum and no metacone fold on M1–2; no mesostyle on M2); (4) 11 characters of the lower dentition (no lower canine; V-shaped ectolophid groove, rounded trigonid, entoconid constriction present but no metaconid constriction on lower cheek teeth; neither lingual nor labial cingulum on lower premolars; d1 usually retained in adults; lingual and labial cingula usually absent and transverse hypolophid on lower molars); and (5) 15 postcranial characters (posterior expansion of the scaphoid-facet low on the radius; large trapezium-facet on the scaphoid; distal border of the keeled anterior side acute on the lunate; no posterior expansion on the pyramidal-facet of the unciform posterior McIII-facet present on McII; functional McV; insertion of the M. extensor carpalis flat on metacar-pals; tibia and fibula in contact; posterior apophysis acute on the tibia; calcaneus-facets 2 and 3 fused and fibula-facet always present on the astragalus; tuber calcanei massive; no posterior MtII-facet on MtIII; insertion of the M. interossei long on lateral metapo-dials). About a third of these features are morpho-clines based on frequency (see the Phylogenetic relationships section below), i.e. their recognition as distinct character states necessitates a wide sample.

However, and thanks to the phylogenetic analysis detailed in the next section, this new species ap-pears to be unambiguously referable to the hornless

Table 18. *Pleuroceros blanfordi* (Lydekker, 1884) and ***Mesaceratherium welcommi* sp. nov**. Compared dimensions of the astragali (range, number of spe
mean, in mm) from the Early Miocene of the Bugti Hills (BH) and of the Zinda Pir Dome (ZP), Pakistan

				Height			Calc.-fac.1		Calc.-fac.2		distal art.
Taxon	max TD	TD trochl.	max APD	med.	mid.	lat.	TD	H	TD	H	maxTD
P. b. (BH)	71.5–75.5	59–62.5	47–49.5	54–62	48–51	(58)–64.5	26–30	43	22–25	25–33	56–62
Mean	73.6 [5]	61.0 [6]	48.1 [5]	58.1 [7]	49.5 [5]	62.5 [5]	28.5 [6]	37.0 [2]	23.7 [4]	29.0 [2]	59.4 [5]
P. b. (ZP)	(71)–73	59	44	52	48	58–(62)	(29)	42	27	–	–
Mean	–	–	–	–	–	–	–	–	–	–	–
M. w. (BH)	73–85	64–76	50.5–57	66–75	57–62	70–77	34–42	45–50	26–28	36–40	63–71
Mean	80.3 [3]	70.0 [3]	53.1 [4]	71.5 [4]	60.3 [3]	74.3 [3]	38.3 [3]	47.7 [3]	27.0 [3]	38 [3]	67.1 [4]

APD, anteroposterior diameter; art., articulation; Calc., calcaneus; Cub., cuboid, fac., facet; lat., lateral; H, height; L, length; max, maximal; med., m
welcommi; *P. b.*, *P. blanfordi*; TD, transverse diameter; W, width. Approximate dimensions appear between brackets.

Table 19. *Pleuroceros blanfordi* (Lydekker, 1884) and ***Mesaceratherium welcommi* sp. nov**. Compared dimensions of the calcanei (range, number of sp
mean, in mm) from the Early Miocene of the Bugti Hills (Balochistan, Pakistan)

			Tuberosity						Astrag.-fac.3	
Taxon	H	H art.	TD	APD	Beak APD	sust. TD	min. TD post.	min. APD post	TD	H
P. b.	(97)–105	56–59	39–44	55–63	53–(54)	(67)	30–38	41–49	22–27	8–
Mean	104.0 [2]	57.5 [2]	42.2 [3]	59.7 [3]	–	–	35.3 [3]	45.3 [2]	24.5 [2]	9.7
M. w.	122–126	73–75	45–45	59–59.5	57–57	(> 69)–70	30.5–(< 35)	50–51.5	–	12
Mean	124.0 [2]	74.0 [2]	45.0 [2]	59.2 [2]	57.0 [2]	–	–	50.7 [2]	–	–

APD, anteroposterior diameter; art., articulation; Astrag., astragalus; Cub., cuboid; fac., facet; min, minimal; H, height; *M. w.*, *M. welcommi*; *P. b.*, *P. bl*
TD, transverse diameter. Approximate dimensions appear between brackets.

Table 20. *Pleuroceros blanfordi* (Lydekker, 1884) and ***Mesaceratherium welcommi* sp. nov.** Compared dimensions of the naviculars (range, number of specimens in square brackets, and mean, in mm) from the Early Miocene of the Bugti Hills (Balochistan, Pakistan)

			Height			
Taxon	TD	APD	ant	mid.	post	prox. art. APD
P. b.	38–39	56	22	19	24–24	50.5
P. b.	38.5 [2]	–	–	–	24 [2]	–
M. w.	44	50	24	18	26	42

ant, anterior; APD, anteroposterior diameter; art., articulation; mid., middle; *M. w.*, *M. welcommi*; *P. b.*, *P. blanfordi*; post, posterior; prox., proximal; TD, transverse diameter.

Table 21. *Pleuroceros blanfordi* (Lydekker, 1884) and ***Mesaceratherium welcommi* sp. nov**. Compared dimensions of the cuboids (range, number of specimens in square brackets, and mean, in mm) from the Early Miocene of the Bugti Hills (Balochistan, Pakistan)

	TD			H		proximal art.		distal art.		Medial face	
Taxon	ant	post	APD max	ant	post	TD	APD	TD	APD	antD	postH
P. b.	34–38	39.5–39.5	53.5–61	30.5–32.5	42–42	32–32	37–37	28–30	33–36.5	12	18–20
Mean	36.0 [2]	39.5 [2]	57.2 [2]	31.5 [2]	42.0 [2]	32.0 [2]	37.0 [2]	29.0	34.7 [2]	–	19.0 [2]
M. w.	37–40	40–(41)	68	37.5–40	(53)–56	(39)–40	(39)–40	33–34	41–(43)	–	–
Mean	38.5 [2]	–	–	38.7 [2]	–	–	–	33.5 [2]	–	–	–

ant, anterior; APD, anteroposterior diameter; art., articulation; D, distance; H, height; max, maximal; *M. w.*, *M. welcommi*; *P. b.*, *P. blanfordi*; post, posterior; TD, transverse diameter. Approximate dimensions appear between brackets.

Table 22. ***Mesaceratherium welcommi* sp. nov**. Dimensions of the entocuneiform (mm) from the Early Miocene of the Bugti Hills (Balochistan, Pakistan)

			Navic.-fac.		Mesocf.-fac.		
TD	APD	H	TD	APD	TD	H	D ant. fac.
(31)	19	42	14	20	25	13	14

ant, anterior; APD, anteroposterior diameter; D, distance; fac., facets; H, height; Mesocf., mesocuneiform; Navic., navicular; TD, transverse diameter. Approximate dimensions appear between brackets.

rhinocerotine genus *Mesaceratherium* Heissig, 1969, so far restricted to the Late Oligocene and Early Miocene of western Europe, in sharing at least three synapomorphies: a strong paracone fold on M1–2, a posterior McIII-facet on McII, and no posterior MtII-facet on MtIII. Within this monophyletic genus, the Bugti species is more closely related to the Late Oligocene species *M. gaimersheimense* Heissig, 1969 in having a lingual bridge on P2–4, whereas the lingual cusps are separate in the Early Miocene species *M. paulhiacense* (Richard, 1937).

It appears as further distinct from *M. gaimershei-mense* in possessing an upraised mandibular symphy-

Table 23. *Pleuroceros blanfordi* (Lydekker, 1884). Dimen-sions of the mesocuneiform (mm) from the Early Miocene of the Bugti Hills (Balochistan, Pakistan)

			Ectocun.-fac.		Entocun.-fac.	
TD	APD	H	APD	H	TD	H
20	29.5	14	12	8	12	3

APD, anteroposterior diameter; Ectocun., ectocuneiform; Entocun., entocuneiform; fac., facet; H, height; TD, trans-verse diameter.

sis, a foramen mentale below the middle of p3, a thick and continuous protoloph on P2, a crochet on all upper molars, a constricted entoconid but no lingual cingulum on lower premolars, and occasionally no d1/p1.

Mesaceratherium welcommi sp. nov. can be distin-guished from *M. paulhiacense* (Richard, 1937) by the presence of a lingual bridge on upper premolars (molariform in *M. paulhiacense*), of a labial cingulum on upper molars, and the absence of a mesostyle on M2, in the curved magnum-facet and fused McIII-facets on McII, fused calacaneus-facets 2 and 3 on the astragalus, the presence of a fibula-facet on the cal-caneus, the proximal border of MtIII concave in ante-rior view, and in showing a distal widening of the diaphysis of MtIII. Other postcranial features are shared by both species (Figs 11C–D, 12C–D), but were not controlled in *M. gaimersheimense*, the postcranial skeleton of which is virtually unknown (Heissig, 1969; Laudet & Antoine, 2004).

Finally, *M. welcommi* sp. nov. differs from all other species of *Mesaceratherium* in having a shorter pre-molar series, a hypocone posterior to the metacone and stronger than the protocone on P2, a protocone slightly constricted on P3–4 and deeply constricted on M1–2, lower cheek teeth with a constricted entoconid, and lower premolars without labial cingulum.

Based on current phylogenetic results and contrary to what was stated by Antoine *et al.* (2006), *M. gaim-ersheimense* Heissig, 1969 cannot be considered as a junior synonym of *M. paulhiacense* (Richard, 1937): the former can be distinguished from the latter in possessing a very upraised mandibular symphysis (upraised in *M. paulhiacense*), a lingual bridge on upper premolars (lingual cusps separate), an inter-rupted protoloph on P2 (continuous), a labial cingu-lum always present (always absent) and a crochet

Table 24. *Pleuroceros blanfordi* (Lydekker, 1884). Dimen-sions of the ectocuneiform (mm) from the Early Miocene of the Bugti Hills (Balochistan, Pakistan)

			Navic.-fac.	
TD	APD	H	TD	APD
35.5	42	20	28	36

APD, anteroposterior diameter; fac., facet; H, height; Navic., navicular; TD, transverse diameter.

Table 25. *Pleuroceros blanfordi* (Lydekker, 1884) and ***Mesaceratherium welcommi* sp. nov.** Compared dimensions of MtII (range, number of specimens in square brackets, and mean, in mm) from the Early Miocene of the Bugti Hills (Balochistan, Pakistan)

		prox.art.		Mesocun.-fac.		Diaphysis		dist. art.	
Taxon	L	TD	APD	TD	APD	TD	APD	TD	APD
P. b.	101.5	(21)–22.5	34.5	16–20	26	21	19	28–30	28.5–29
Mean	–	–	–	18 [2]	–	–	–	29 [2]	28.7 [2]
M. w.	–	(24)	(35)	17	28	–	–	–	–

APD, anteroposterior diameter; art., articulation; dist., distal; L, length; Mesocun., mesocuneiform; *M. w.*, *M. welcommi*; *P. b.*, *P. blanfordi*; prox., proximal; TD, transverse diameter. Approximate dimensions appear between brackets.

Table 26. *Pleuroceros blanfordi* (Lydekker, 1884) and ***Mesaceratherium welcommi* sp. nov**. Compared dimensions of MtIII (mm) from the Early Miocene of the Bugti Hills (Balochistan, Pakistan)

	prox. art.			Diaphysis			dist. art.	
Taxon	TD	APD	TD diag.	TD	APD	max TD dia.	TD	APD
P. b.	41	(34)	24.5	32	15.5	–	–	–
P. b.	–	–	–	–	–	44	36	31.5
P. b.	–	–	–	33	16	42.5	36	30
P. b.	–	–	–	31.5	(17)	47	35	32.5
M. w.	50	–	–	39.5	–	–	–	–

APD, anteroposterior diameter; art., articulation; dia., diaphysis; diag., diagonal; dist., distal; max., maximal; *M. w.*, *M. welcommi*; *P. b.*, *P. blanfordi*; prox., proximal; TD, transverse diameter. Approximate dimensions appear between brackets.

Table 27. *Pleuroceros blanfordi* (Lydekker, 1884) and ***Mesaceratherium welcommi* sp. nov**. Compared dimensions of MtIV (range, number of specimens in square brackets, and mean, in mm) from the Early Miocene of the Bugti Hills (Balochistan, Pakistan)

	prox. ext.		prox. art.		medial facets		Diaphysis			dist. art.			
Taxon	L	TD	APD	TD	APD	antAPD	antH	postAPD	postH	TD	APD	Max TD dia.	TD	APD
P. b.	107	31–36	35.5–37.5	25–26	30–32.5	14–15	16–(18)	12–14	22–23	16–20	34–34	32–32	31–33	*P. b.*–34.0[3]36.3[3]25.7[3]31.2[3]14.7[3]13.7[3]16[2]13[3]22..5[2]18.0[2]34.0[2]32.0[2]32.0[2] *M. w.*–––––– 2920323236

ant, anterior; APD, anteroposterior diameter; art., articulation; dia., diaphysis; dist., distal; ext., extremity; H, height; L, length; max, maximal; *M. w.*, *M. welcommi*; *P. b.*, *P. blanfordi*; post, posterior; prox., proximal; TD, transverse diameter. Approximated dimensions appear between brackets.

usually absent (always present) on upper molars, and the mesostyle absent (present) on M2.

Mandibular dimensions fit the average dimensions of Recent *Dicerorhinus sumatrensis*, but postcranials are larger: their size corresponds to the mean values observed in Recent *Diceros bicornis* (Guérin, 1980). Moreover, most postcranial bones referred to *M. wel-commi* sp. nov. can be split into two series, with a size difference reaching 10–15% on the scaphoids, tibias, and astragali (Tables 6, 16, 18). This might be interpreted as a sexual dimorphism based on size, as observed in other rhinocerotoids (Antoine *et al.*, 2004; Mihlbachler, 2005). Yet, no morphologi-cal evolution has been observed between the speci-mens originating from level 4 (earliest Miocene, ª Aquitanian, ª MN2) on the one hand, and levels 5, 6, and 6sup (Early Miocene, ª Early Burdigalian', ª MN3), on the other.

PHYLOGENETIC RELATIONSHIPS

METHODS

Basically, the data set (character list, character states) is that of Antoine (2002, 2003) and Antoine *et al.* (2003b), with 282 morphological characters (52 cranial, ten mandibular, 100 on permanent cheek teeth, 20 on deciduous teeth, and 100 postcranial), originally used for proposing a phylogeny of Elasmotheriina within Rhinocerotidae.

The inclusion of intraspecifically variable charac-ters (caused either by sexual dimorphism, individual, and/or ontogenetic variations) in a cladistic analysis has been debated for decades. As they 'can contain useful phylogenetic information' (Wiens, 2001: 690), such characters have been included in the current analysis. All of them were treated the same way as character 264 (Appendix 1), which corresponds to the presence/absence of a fibula-facet on the calcaneus. This facet is always absent in several taxa (in 29 specimens of the recent rhinocerotine *Diceros bicor-nis*; Guérin, 1980: 131), always present in others [in 14 specimens of the elasmotheriine *Hispanotherium beonense* (Antoine, 1997)], and absent in 15 specimens out of 18 for *Plesiaceratherium mirallesi* (Crusafont, Villalta & Truyols, 1955). Therefore, the binary states ('0, absence; 1, presence') were replaced by multistate quantitative states based on frequency ['0, always absent (100%); 1, generally absent (50–99%); 2, gen-erally present (50–99%); 3, always present (100%)'], as detailed by Antoine (2002, 2003). The correspond-ing characters are additive and considered as mor-phoclines.

All the characters have an equal weight. Charac-ters 72, 94, 102, and 140 are unordered whereas all other characters are ordered (Wagner parsimony).

Table 28. Character coding sources (direct observation and/or literature) for each terminal taxon included within the present phylogenetic analysis

	Character coding (source)	
Terminal	Direct observation	Literature
Aceratherium incisivum Kaup, 1832	MHNT; MNHN	Kaup, 1832; Guérin, 1980; Hünermann, 1989
Alicornops simorrense (Lartet, 1851)	MHNT; MNHN; NHM	Guérin, 1980; Cerdeño & Sánchez, 2000
Brachypotherium brachypus (Lartet, 1837)	MHNT; MNHN; UCBL	Roman & Viret, 1930, 1934; Guérin, 1980; Ginsburg & Bulot, 1984; Cerdeño, 1993
Bugtirhinus praecursor Antoine & Welcomme, 2000	MHNT; pers. obs. (P.-O. A.)	Antoine & Welcomme, 2000
Diaceratherium aginense (Répelin, 1917)	MHNT; MHNH; UCBL; Rhinopolis	Répelin, 1917; de Bonis, 1973
Diceratherium armatum Marsh, 1875	AMNH	Prothero, 2005
Dicerorhinus sumatrensis (Fischer Von Waldheim, 1814)	MNHN	Cuvier, 1822; Guérin, 1980
Diceros bicornis (von Linnaeus, 1758)	MNHN	Guérin, 1980
Gaindatherium browni Colbert, 1934	AMNH; HUPM	Colbert, 1934; Heissig, 1972
Hispanotherium beonense (Antoine, 1997)	MHNT	Antoine, 2002, 2003; Antoine, Bulot & Ginsburg, 2000
Hyrachyus eximius Leidy, 1871	AMNH	Leidy, 1871
Lartetotherium sansaniense (Lartet, 1837)	MHNT; MNHN; NHM	Klaits, 1973; Guérin, 1980
Menoceras arikarense (Barbour, 1906)	AMNH	Tanner, 1969; Prothero, 2005
Mesaceratherium paulhiacense (Richard, 1937)	MHNT; Rhinopolis	Richard, 1937; de Bonis, 1973
Mesaceratherium gaimersheimense Heissig, 1969	MHNT	Heissig, 1969; Laudet & Antoine, 2004; Antoine *et al.*, 2006
***Mesaceratherium welcommi* sp. nov.**	MHNT; HUPM	Falconer & Cautley, 1846; Pilgrim, 1912; Forster-Cooper, 1934; Lindsay *et al.*, 2005
Plesiaceratherium mirallesi (Crusafont, Villalta & Truyols, 1955)	MHNT; MNHN; UCBL	Crusafont *et al.*, 1955; Yan & Heissig, 1986; Antoine *et al.*, 2000
Pleuroceros pleuroceros (Duvernoy, 1853)	MHNL; UCBL; Rhinopolis; MNHN	Duvernoy, 1853; de Bonis, 1973
Pleuroceros blanfordi (Lydekker, 1884) **comb. nov.**	MHNT; HUPM	Lydekker, 1884; Pilgrim, 1912; Forster-Cooper, 1934
Prosantorhinus douvillei (Osborn, 1900)	MHNT; MNHN; UCBL	Wermelinger, 1998; Antoine *et al.*, 2000
Protaceratherium albigense (Roman, 1912)	MHNT; FSL	Duvernoy, 1853; Roman, 1912; Antoine *et al.*, 2008; Lihoreau *et al.*, 2009
Protaceratherium minutum (Cuvier, 1822)	MHNT; MNHN; UCBL	Roman, 1924; de Bonis, 1973
Rhinoceros unicornis von Linnaeus, 1758	MNHN	Blainville, 1839; Guérin, 1980
Subhyracodon occidentalis (Leidy, 1851)	–	Scott, 1941; Prothero, 1998, 2005
Ronzotherium filholi (Osborn, 1900)	LGPH; MHNT	Osborn, 1900; Heissig, 1969; Brunet, 1979
Tapirus terrestris (von Linnaeus, 1758)	MHNT, MNHN AC	Blainville, 1839
Trigonias osborni Lucas, 1900	AMNH	Lucas, 1900; Wood, 1927; Scott, 1941; Prothero, 2005

Taxa are arranged in alphabetical order. The 'direct observation' column indicates the institution where the material is stored.

Gaps are treated as 'missing'. Using PAUP 4.0 v.10 (Swofford, 1998), starting trees were obtained via stepwise addition, and heuristic islands were avoided by multiple starts with random taxon additions (1000 replicates).

TAXONOMIC SAMPLING

Twenty-eight terminal taxa were included in the phylogenetic analysis (Table 28). Four terminals were selected as outgroups: the extant tapirid *Tapirus terrestris* von Linnaeus, 1758, the Eocene

hyrachyid rhinocerotoid *Hyrachyus eximius* Leidy, 1871, the Eocene rhinocerotid *Trigonias osborni* (Lucas, 1900) from North America, and the Oli-gocene rhinocerotid *Ronzotherium filholi* (Osborn, 1900) from Europe.

The ingroup *sensu lato* consists of both taxa of interest (in-group *sensu stricto*: exhaustive specific sampling for *Mesaceratherium* Heissig, 1969 and *Pleuroceros* Roger, 1898) and selected taxa forming a 'branching group', *sensu* Antoine (2002).

The ingroup *sensu stricto* includes *P. blanfordi* Lydekker (1884), *M. welcommi* sp. nov. (Early Miocene of Pakistan), and all other known species of *Mesaceratherium* Heissig, 1969 [*M. paulhiacense* (Richard, 1937) and *M. gaimersheimense* Heissig, 1969, from around the Oligocene–Miocene limit in Europe] and *Pleuroceros* Roger, 1898 [*P. pleuroceros* (Duvernoy, 1853), from the Early Miocene of Europe]. The branching group includes (1) type species or well-represented species of type genera of suprage-neric groups recognized within Rhinocerotidae; and

(2) early representatives of these suprageneric groups, in order to branch the taxa of interest within the Rhinocerotidae, to define their generic and suprageneric affinities, and to avoid long-branch attraction artefacts because of parallelism (e.g. late representatives of Elasmotheriinae vs. Rhinoceroti-nae; Antoine, 2002). The present branching group comprises well-known Elasmotheriinae (early Elas-motheriina: *Hispanotherium beonense* (Antoine, 1997) and *Bugtirhinus praecursor* Antoine & Welcomme, 2000 from the Early Miocene of Europe and Pakistan, respectively; Menoceratina: *Menoceras arikarense* (Barbour, 1906), from the Early Miocene of North America; 'diceratheres': *Diceratherium armatum* Marsh, 1875 and *Subhyracodon occidentalis* (Leidy, 1851), from the Oligocene of North America) and Rhinocerotinae (Rhinocerotina: *Rhinoceros unicornis* von Linnaeus, 1758, *Diceros bicornis* (von Linnaeus, 1758), and *Dicerorhinus sumatrensis* (Fischer Von Waldheim, 1814) (recent), *Lartetotherium sansaniense* (Lartet, 1837) and *Gaindatherium browni* Colbert, 1934, from the Miocene of Europe and South Asia, respectively (extinct); Teleoceratina: *Brachypoth-erium brachypus* (Lartet, 1837), *Prosantorhinus dou-villei* (Osborn, 1900), and *Diaceratherium aginense* (Répelin, 1917), from the Early and/or Middle Miocene of Europe; Aceratheriini: *Aceratherium inci-sivum* Kaup, 1832, *Alicornops simorrense* (Lartet, 1851), and *Chilotherium anderssoni* Ringström, 1924, from the middle and/or Late Miocene of Eurasia; other selected hornless rhinos ('aceratheres *sensu lato'*): *Protaceratherium minutum* (Cuvier, 1822), *Pro-taceratherium albigense* (Roman, 1912), and *Plesi-aceratherium mirallesi* (Crusafont *et al.*, 1955) from the Oligocene of Eurasia (*Protaceratherium albigense, Pr. a.*; Lihoreau *et al.*, 2009) and the Early Miocene of Europe (*Protaceratherium minutum, Pr. m.* and *Ple-siaceratherium mirallesi, Pl. m.*).

The character coding was performed through direct observation and/or the literature (Table 28).

RESULTS

Two equally parsimonious trees (1237 steps; consis-tency index = 0.27; retention index = 0.42) were obtained by using the 'mh*bb*' command of Hen-nig86, 1.5 (Farris, 1988) and the heuristic search of PAUP 4.0 v.10 (Swofford, 1998). They only differ in the relationships between the Aceratheriina included in the analysis (*Aceratherium incisivum*, *Chilothe-rium anderssoni*, and *Alicornops simorrense*; Fig. 13).

The suprageneric and interspecific phylogenetic relationships within Rhinocerotidae are discussed below, as well as the distribution of unambiguous synapomorphies, detailed in Table 29, and based on the consensus tree (1244 steps; consistency index = 0.27; retention index = 0.41) as illustrated in Figure 13. Both indexes are low, which indicates a large amount of unstructured homoplasy. The ingroup is not monophyletic, with the extra-group *Ronzothe-rium filholi* as the first offshoot of Elasmotheriinae. Nevertheless, suprageneric taxa such as Rhino-cerotidae, Elasmotheriinae, Elasmotheriini and Elasmotheriina, Rhinocerotinae, Aceratheriini, Rhi-nocerotina, and Teleoceratina are monophyletic in the consensus tree (Fig. 13). Moreover, suprageneric rela-tionships are consistent with those resulting from recent analyses with better indexes (e.g. Antoine, 2002, 2003; Antoine *et al.*, 2003b), pointing to termi-nal taxa homoplasy. Twenty-three characters are uninformative in the current analysis (cranial: 5, 7, 32, 43; dental: 64, 69, 92, 93, 106, 117, 123, 126, 127, 131, 132, 137, 141, 153, 167, 171, 175; postcranial: 217, 273; Appendix 1).

Within the available taxonomic sample, Rhinocer-otidae (Fig. 13, node 1) are characterized by 11 syna-pomorphies, of which two are nonhomoplastic (i2 tusk-like and i3 absent). The other ones are a brachycephalic skull, an upraised mandibular sym-physis, the c1 absent, the antecrochet usually absent on upper molars, the alar notch present on the atlas, the long posterior tuberosity on the magnum, the transverse diameter/height ratio between 1.0 and 1.2 on the astragalus, the anteroposterior diameter/ height ratio higher than 0.65 on the astragalus, and the proximal border of MtIII concave in anterior view.

Node 2 (Fig. 13) puts the clades Rhinocerotinae and Elasmotheriinae as sister groups. This node is defined by the absence of I3 (nonhomoplastic), a spur-like paralophid on p2 (unique reversion), a straight occipi-

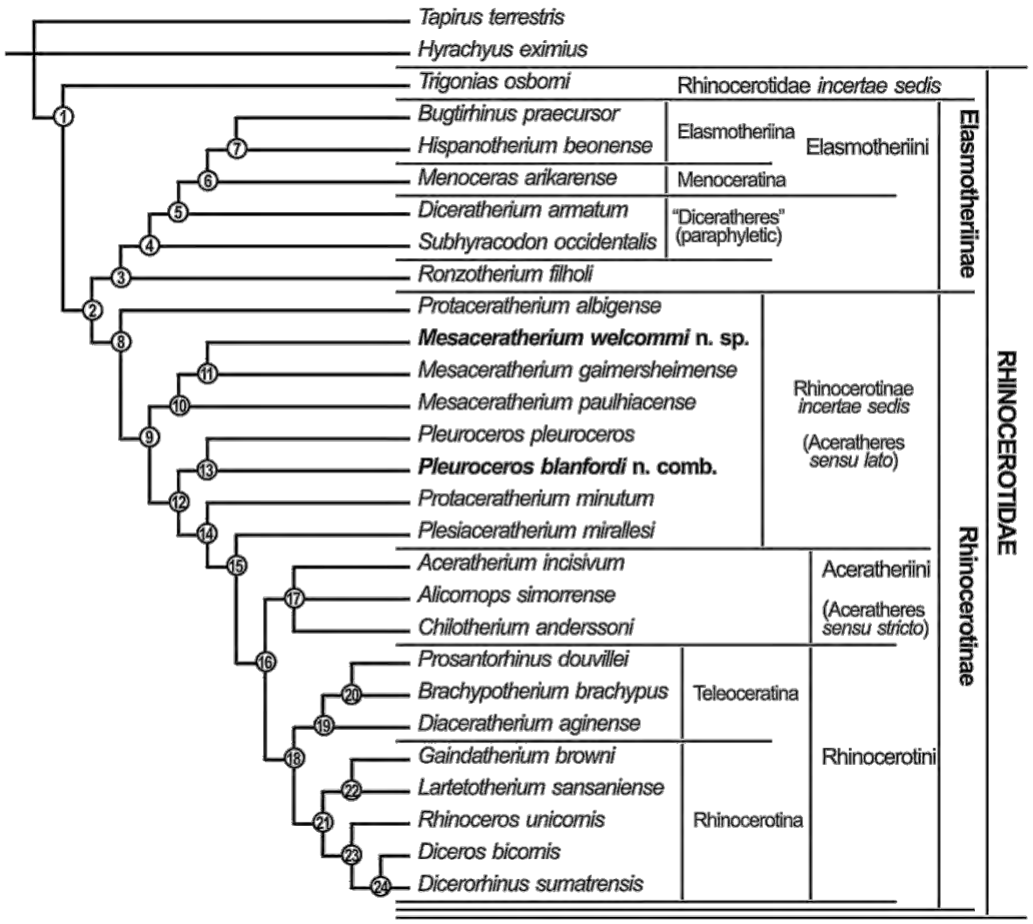

Figure 13. Strict consensus tree of two most parsimonious trees (1237 steps; consistency index = 0.27; retention index = 0.42) obtained using Hennig86 1.5 (Farris, 1988) and PAUP 4.0 v.10 (Swofford, 1998), based on 282 morphological characters, and performed on 28 rhinocerotid, rhinocerotoid, and tapirid taxa, with *Tapirus terrestris*, *Hyrachyus eximius*, *Trigonias osborni*, and *Ronzotherium filholi* as outgroups. Suprageneric group names are based on current phylogenetic relationships. Taxa of interest are in bold.

tal crest, a convex processus postglenoidalis, the absence of C1, and the antecrochet usually present on upper molars.

The controlled Elasmotheriinae (Fig. 13, node 3) have seven homoplastic synapomorphies, such as an open external auditory pseudomeatus (reversion), a rounded vomer, a lingual wall on P3–4, a forked paralophid on d2, no foramen transversarium on the atlas, fused proximal ulna-facets on the radius, and a McIV with a triangular outline in proximal view.

Node 4 (Fig. 13, unnamed clade) joins the dicerath-eres (*Subhyracodon occidentalis* + *Diceratherium armatum*; paraphyletic) and the Elasmotheriini (Elasmotheriina + Menoceratina), based on nine homoplastic features: a depressed area between tem-poral and nuchal crests on the temporal, a doli-chocephalic skull (reversion), a trigonid forming an acute dihedron on lower cheek teeth, a continuous lingual cingulum on lower premolars, d1/p1 absent in adults, an oblique hypolophid on lower molars, radius and ulna in contact or fused, a proximal fibula-surface proximally displaced on the tibia, and a proximal border of MtIII sigmoid in anterior view.

Diceratherium armatum appears as the sister group of the Menoceratina + Elasmotheriina clade because of a low anterior base of the processus zygo-maticus maxillari, a well-developed nuchal tubercle, a concave occipital crest (reversion), the presence of cement on cheek teeth, the hypocone posterior to the metacone on P3–4, the antecrochet always present on upper molars, the protocone usually constricted on M1–2, the absence of a posteroproximal lunate-facet on the scaphoid, calcaneus-facets 2 and 3 always fused on the astragalus (Antoine, 2002), and the tibia-facet always present on the calcaneus.

The Elasmotheriini (Fig. 13, node 6), i.e. Menocera-tina (*Menoceras arikarense*) + Elasmotheriina, share 20 synapomorphies (Table 29), amongst which the

Table 29. Distribution of unambiguous synapomorphies in the strict consensus tree illustrated in Figure 13

Node 1 (Rhinocerotidae): 23[1], 53[1], **79[1]**, **81[1]**, 82[1], 110[1], 184[1], 220[1], 252[1], 253[1], 271[1] Node 2
(Rhinocerotinae + Elasmotheriinae): 36[1], 42[1], **74[1]**, 75[1], 110[2], -154[0]
Node 3 (Elasmotheriinae): -18[0], 38[1], 102[3], 179[1], 188[1], 199[3], 230[2] Node 4:
17[1], -23[0], 143[1], 148[1], 151[3], 161[1], 201[1], 248[1], 271[2]
Node 5: 10[1], 20[2], -36[0], 65[1], 103[1], 110[3], 115[2], 207[1], 263[3], 265[2]
Node 6 (Elasmotheriini): 45[1], 49[1], 59[1], 84[2], 88[1], 115[3], 130[1], 140[2], 154[1], 176[1], 194[1], 234[1], 235[1], 254[1], 256[1], 259[1], 264[3], 266[1], 275[1], 278[1]
Node 7 (Elasmotheriina): 63[1], 87[1], 94[3], 95[1], 116[1], 135[2], 147[2], 149[1], 157[1], 210[1], 277[1] Node 8
(Rhinocerotinae): 46[1], 103[1], 110[3], 115[3], 125[1], 129[1], 152[2], 210[1]
Node 9: 83[2], 111[3], 138[1], 160[1], 242[1]
Node 10 (*Mesaceratherium*): 118[1], 226[2], 272[1]
Node 11 (*Mesaceratherium gaimersheimense*, *Mesaceratherium welcommi* sp. nov.): 94[1], 102[1]
Node 12: 70[1], 72[1], 84[1], 100[1], 161[1], 213[1]
Node 13 (*Pleuroceros*): -36[0], 53[2], 88[1], 107[3], 112[1], 116[1], 124[1], 140[1], 148[1], 231[1], 232[1], 266[1], 282[1] Node 14:
3[1], 84[2], 105[1], -110[2], -174[0], 207[1], 259[1]
Node 15: -11[0], 134[1], 142[1], 150[1], 151[1], **186[1]**, 196[1], -212[0], 265[2]
Node 16 (Aceratheriini + Rhinocerotini): -122[0], 147[2], 151[2], 157[1], 224[1], 232[1] Node 17
(Aceratheriini): 22[1], 37[1], 47[1], 62[1], 80[1], -85[0], 193[1], 199[1], 223[2] Node 18 (Rhinocerotini):
-3[0], 12[1], 15[1], -36[0], 67[1], 97[1], -100[0], 247[1]
Node 19 (Teleoceratina): 45[1], -105[0], -146[0], 206[1], -220[0], **229[1]**, 241[1], 257[1], **262[1]**, 282[1] Node 20: -72[0], -119[0], 144[1], 199[2], 202[1], -226[1], -238[0], 252[2], 275[1], 279[1]
Node 21 (Rhinocerotina): 24[1], 27[1], 83[3], 109[3], -110[0], 114[2], -115[2], 149[1], 154[1], 230[2], 263[2], 280[1] Node 22:
94[1], 102[1], 143[1], -151[1], 157[3], -161[0]
Node 23: 77[1], 91[1], 101[1], -111[2], 112[1], -125[0], -204[0], 216[1], 256[1], 277[1]
Node 24: -18[0], **31[1]**, 38[1], 121[1], 187[2], -210[0], 214[2], 228[2], -232[0], 234[1]

Superscript numbers correspond to character states. Reversions are preceded by '-'. Nonhomoplastic synapomorphies [consistency index = retention index (RI) = 1] are in bold; weakly homoplastic apomorphies (RI 0.80) and unique reversions are underlined. Other characters are strongly homoplastic.

less homoplastic are a crochet always present on P2–4, a protocone always constricted on M1–2, the presence of vertical external rugosities on d2–3, a medially stiff femoral head, an astragalus with a trochlea and a distal articulation sharing the same axis, and nearly anterior symmetric insertions on MtIII first phalanges.

The Elasmotheriina, represented by the Early Miocene *Bugtirhinus praecursor* and *Hispanotherium beonense*, are monophyletic (Fig. 13, node 7), and characterized by 11 derived homoplastic features, including a short premolar row, a lingual wall on P2, a protocone strongly constricted on upper molars, the absence of a labial cingulum on lower premolars, a scaphoid higher posteriorly than anteriorly, and a pad-shaped and continuous posteroproximal tuberos-ity on MtIV.

Both taxa of interest (*P. blanfordi* and *M. welcommi* sp. nov.) belong to the Rhinocerotinae (Fig. 13, node 8), with the Oligocene *Protaceratherium albigense* as the first offshoot. This Rhinocerotinae clade is defined by eight homoplastic synapomorphies: processus post-tympanicus and processus paraoccipitalis distant, hypocone posterior to metacone on P3–4, antecrochet always present on upper molars, protocone always constricted on M1–2, hypocone isolated on M1 and M2, one-rooted d1, and scaphoid higher posteriorly than anteriorly (convergence with Elasmotheriina).

Protaceratherium albigense is set well apart from the type species of the genus (*Protaceratherium minutum*; Fig. 13, node 14).

Node 9 (unnamed clade) sets *Mesaceratherium* – including its three representatives – as the sister group of other Rhinocerotinae (Fig. 13), on the basis of five dental and postcranial homoplastic synapomor-phies, such as the labial cingulum usually absent on the upper premolars, the crochet always present on upper molars, the absence of a posterior groove on the ectometaloph of M3, a reduced labial cingulum on lower molars, and the absence of an anterodistal groove on the tibia.

Node 10 sets *M. paulhiacense* as the sister group of the *M. gaimersheimense* + *M. welcommi* sp. nov. clade (Fig. 13). Therefore, *Mesaceratherium* appears as a monophyletic genus, including the three species men-tioned above, and diagnosed by a weak paracone fold, a posterior McIII-facet always present on McII, but no posterior MtII-facet on MtIII.

Mesaceratherium gaimersheimense and *M. wel-commi* sp. nov. are sister groups (Fig. 13, node 11),

based on the presence of a lingual bridge on upper premolars, which in turn confirms that *M. gaimer-sheimense* Heissig, 1969 cannot be considered as a junior synonym of *M. paulhiacense* (Richard, 1937).

The clade formed by *Pleuroceros* and more derived Rhinocerotinae (Fig. 13, node 12) is defined by upper cheek teeth with joined roots, I1s oval in cross-section, a crochet usually present on P2–4, a medi-fossette usually absent on P3–4, a hypolophid oblique on lower molars, and a smooth anterior side on the lunate.

Pleuroceros (Fig. 13, node 13) is a clade including *P. pleuroceros* and *P. blanfordi* comb. nov. Both species share 12 homoplastic synapomorphies: a concave occipital crest in dorsal view (reversion), a nearly horizontal mandibular symphysis, a reduced lingual cingulum on upper premolars, a strong antecrochet on P4, a protocone deeply constricted and a low and reduced posterior cingulum on M1–2, a smooth and U-shaped external groove on lower cheek teeth, a continuous lingual cingulum on lower premolars, a tridactyl manus (vestigial McV), a salient insertion of the m. extensor carpalis on metacarpals, a slender tuber calcanei, and a short insertion of the m. interossei on lateral metapodials.

The following node (Fig. 13, node 14) puts *Protaceratherium minutum* as the sister group of the [*Plesiaceratherium mirallesi* [Aceratheriini, Rhinoc-erotini]] clade. This node is characterized by seven synapomorphies, of which only one is weakly homoplastic (presence of a protoconid fold on lower deciduous teeth; unique reversion): nasal notch above P4–M1, crochet always present on P2–4, crista usually absent on P3, antecrochet usually present on upper molars (reversion), posteroproximal lunate-facet absent on the scaphoid, and astragalus with a trochlea and a distal articulation sharing the same axis.

Plesiaceratherium mirallesi is the sister group of the [Aceratheriini, Rhinocerotini] clade. Terminals from node 15 (Fig. 13) share kidney-like condyle-facets on the atlas (consistency index = retention index = 1), a low zygomatic arch (unique reversion), a triangular M3, a rounded trigonid on lower cheek teeth, a reduced labial cingulum on lower premolars, d1/p1 usually present in adults, a distal gutter on the lateral epicondyle of the humerus, a lunate with a rounded distal border in anterior view (reversion), and a tibia-facet always present on the calcaneus.

The next node (Fig. 13, node 16) highlights the phylogenetic relationships amongst aceratheriines, teleoceratines, and rhinocerotines: the Aceratheriini appear as the sister group of the Rhinocerotini (the latter including Rhinocerotina and Teleoceratina as sister groups). Such relationships were not solved in Antoine *et al.* (2003b: fig. 4). The concerned taxa (node 16) are defined by an unique reversion (poste-rior part of the ectoloph straight on M1–2), and five homoplastic dental and postcranial synapomorphies: lingual cingulum usually absent on lower premolars and usually present on lower molars, d1/p1 usually absent in adults, magnum-facet straight on McII, and insertion of the m. extensor carpalis salient on metac-arpals (convergence with *Pleuroceros*).

Node 17 (Fig. 13, Aceratheriini) is a polytomy with *Aceratherium incisivum*, *Alicornops simorrense*, and *Chilotherium anderssoni*. The three of them are char-acterized by a nearly vertical posterior margin on the pterygoid, a brutal anterior tip on the processus zygo-maticus maxillary in palatine view, a small processus post-tympanicus, a foramen mandibulare open above the teeth neck line, divergent i2s, simple crochets on P2–4 (reversion), a wide and low fossa olecrani on the humerus, proximal ulna-facets usually separate on the radius, and a posterior expansion usually present on the pyramidal-facet of the unciform.

The aceratheriines as classically defined, i.e. including hornless taxa such as *Plesiaceratherium*, *Mesaceratherium*, and sometimes *Protaceratherium*, along with *Aceratherium*, *Chilotherium*, and *Alicor-nops*, appear as an unnatural group. We propose the restriction of the use of 'Aceratheriini' or 'Acerath-eriina' in the current analysis to the clade (*Acerath-erium incisivum*, *Alicornops simorrense*, *Chilotherium anderssoni*) and their close relatives (such as *Hoplo-aceratherium tetradactylum* and *Acerorhinus zernowi*; Antoine *et al.*, 2003b).

The Rhinocerotini (Fig. 13, node 18) include the Teleoceratina (node 19) and the Rhinocerotina (node 21) as sister groups; they share eight synapomorphies amongst which a unique reversion (medifossette always absent on P3–4), and homoplastic features, such as a nasal notch retracted above P1–P3 (rever-sion), the processus postorbitalis absent on the zygo-matic arch, the dorsal profile of the skull concave in lateral view, the concave occipital crest (reversion), wrinkled and corrugated enamel on cheek teeth, a protocone less developed than the hypocone on P2, and a rounded posterior apophysis on the tibia.

The early Teleoceratina included in the present analysis (Fig. 13, node 19), arranged as follows: [*Diaceratherium aginense* [*Prosantorhinus douvillei*, *Brachypotherium brachypus*]], are defined by two nonhomoplastic postcranial synapomorphies (magnum-facet invisible in anterior view on McIII and calcaneus-facet 1 nearly flat on the astragalus), two unique reversions (U-shaped lingual opening of the posterior valley on lower premolars in lingual view and posterior tuberosity short on the magnum), and six homoplastic features: posterior groove present on the processus zygomaticus of the squamosal, crista always absent on P3 (reversion), anterior tubercle

present on the distal end of the ulna, proximal border of the patellar articulation straight on the femur, posterior stop absent on the cuboid-facet of the astragalus, and insertion of the m. interossei short on lateral metapodials. As usual, the Teleoceratina are essentially diagnosed by postcranial characters.

Prosantorhinus douvillei and *B. brachypus* share three unique reversions (Fig. 13, node 20; I1 almond-shaped in cross-section, metacone fold present on M1–2, and posterior McIII-facet usually absent on McII), and seven homoplastic synapomorphies: con-stricted metaconid on lower cheek teeth, proximal ulna-facets usually fused on the radius, gutter for the m. extensor carpi weak on the radius, fovea capitis high and narrow on the femur (reversion), transverse diameter/height ratio higher than 1.2 on the astraga-lus, presence of a cuboid-facet on MtIII, and short-ened limbs (brachypody). Once again, seven derived features out of ten are postcranial.

The Rhinocerotina included in this phylogenetic analysis are monophyletic (Fig. 13, node 21), and split into two clades: one-horned extinct rhinocerotines
Lartetotherium sansaniense and *Gaindatherium browni* on the one hand (Fig. 13, node 22), and Recent rhinocerotines on the other (Fig. 13, node 23). The Rhinocerotina (node 21) are notably characterized by a broad anterior tip on the nasals, the presence of a nasal horn, the antecrochet absent on upper molars and a protocone usually constricted on M1–2 (unique reversions), and the labial cingulum always absent on upper molars.

The *Lartetotherium–Gaindatherium* clade (Fig. 13, node 22) is defined by six dental features: d1/p1 usually present in adults and hypolophid transverse on lower molars (unique reversions), lingual bridge present on upper premolars, trigonid of lower cheek teeth forming an acute dihedron, and lingual cingu-lum always absent on lower molars.

The Recent rhinocerotines included in this analy-sis share ten dental and postcranial features, amongst which are two unique reversions (crochet usually present on upper molars and hypocone unconstricted on M1), a P1 usually present in adults, a collum tali low on the astragalus, a pad-shaped posteroproximal tuberosity on MtIV (conver-gence with Elasmotheriina), and several highly homoplastic characters.

The two-horned Recent rhinos included in the present work, *Diceros bicornis* and *Dicerorhinus sumatrensis*, form a clade essentially diagnosed by cranial and postcranial synapomorphies rather than by mandibular and dental features (Fig. 13, node 24), including the presence of a frontal horn (consistency index = retention index = 1), the scaphoid with equal anterior and posterior heights and the insertion of the m. extensor carpalis flat on the metacarpals (unique reversions), and a rounded vomer. The other ones are quite homoplastic (Appendix 1).

Mesaceratherium and *Pleuroceros* appear as mono-phyletic genera, quite distinct but branching at the same level in the cladogram (Fig. 13), which confirms that *M. welcommi* sp. nov. could be misidentified, as occurred throughout the last century. Both can be referred to Rhinocerotinae incertae sedis, a paraphyl-etic ensemble we propose to name ‘aceratheres *sensu lato*’.

CONCLUSION

The revision of the hypodigm of ‘*Aceratherium blan-fordi*, n. sp., *nobis* Lydekker, 1884’ led us to split up this taxon into two co-occurring but distinct species, namely *P. blanfordi* (Lydekker, 1884) comb. nov. and *M. welcommi* Antoine & Downing sp. nov. This work highlights the identificatory/discriminatory skills of postcranial skeleton elements for rhinocerotids, espe-cially for the ones which display globally similar – and therefore potentially homoplastic – dental pat-terns and features: although being associated in various localities and having comparable cheek teeth morphologies, *P. blanfordi* and *M. welcommi* can be easily distinguished thanks to their limb bones. The small, short, and robust chilothere-like postcranial bones of the tridactyl *P. blanfordi* are highly diver-gent from the large, long, and slender ones of the tetradactyl *M. welcommi*.

In the Bugti area, *P. blanfordi* and *M. welcommi* are found in association with a surprisingly diversi-fied rhinocerotid fauna, especially in the locus Kumbi 4f (Level 4, earliest Miocene, MN2; Table 30), in which they co-occur with the rhinocerotine

Gaindatherium cf. *browni*, the teleoceratines *Brachy-potherium fatehjangense* (Pilgrim, 1910), *Brachypoth-erium gajense* (Pilgrim, 1912), and *Prosantorhinus shahbazi* (Pilgrim, 1910), the aceratheriine *Plesiacer-atherium naricum* (Pilgrim, 1910), the minute *Prota-ceratherium* sp., and the early elasmotheriine *Bugtirhinus praecursor* (Antoine & Welcomme, 2000; Welcomme *et al.*, 2001; Métais *et al.*, 2009). To our knowledge, such a rhinocerotid specific diversity – up to nine coeval/associated species in the same locus – is unique in the world. It testifies notably to an exceptional food supply for the Dera Bugti area in the Early Miocene, in as far as these rhinocerotids were found associated with a diversified megaherbivore and macroherbivore fauna, including proboscideans, chalicotheriids, anthracotheriids, and ruminants (Antoine & Welcomme, 2000; Métais *et al.*, 2009). Given that the number of plant species included in a natural diet increases with the size of the herbivore(s) (Freeland, 1991) and that a reduction in available plant variety may cause the decline of megamammals

Table 30. Stratigraphical distribution of the rhinocerotids identified in the Early Miocene of the Bugti Hills (Balochistan. Pakistan), locality by locality

Formation	Chitarwata Formation (upper member)									Vihowa Formation (base)			
Levels	3bis	4								5		6	6sup
		Kumbi 4											
	DB							Gandô		Kumbi			DB
Loci	3bis	4a	4b	4c	4d	4e	4f	4	DB 4	5	DB 5	DB 6	6sup
Bugtirhinus praecursor													
Protaceratherium sp.													
Plesiaceratherium naricum										?			
Brachypotherium gajense													
Brachypotherium fatehjangense													
Gaindatherium cf. *browni*													
***Mesaceratherium welcommi* sp. nov.**													
Pleuroceros blanfordi													
Prosantorhinus shahbazi													
Rhinocerotina indet., cf. *Rhinoceros*		?											
Number of co-occurring rhinocerotid species	3	6	6	6	3	3	**9**	7	5	4	4	5	4

Modified and completed from Antoine & Welcomme (2000); Welcomme *et al.* (2001); Métais *et al.* (2009). See Material and methods for level numbers and corresponding letters (loci and levels).

(Guthrie, 1984), high plant diversity under a favour-able climate may be suspected for the Early Miocene of the Sulaiman Lobe. Yet, in the absence of available climatic, palynological, and palaeobotanical data for this period and area (Collinson & Hooker, 2003; De Franceschi *et al.*, 2008; Métais *et al.*, 2009), this hypothesis cannot yet be tested.

The co-occurrence of *P. blanfordi*, *M. welcommi*, *Protaceratherium* sp., *Plesiaceratherium naricum*, and *Brachypotherium gajense* in both the Bugti and Zinda Pir areas (our unpublished data) allows the refinement of the stratigraphical correlations pro-posed by Lindsay *et al.* (2005) and Métais *et al.* (2009) for the upper member of the Chitarwata Formation throughout the Sulaiman Lobe. The *Pleuroceros– Mesaceratherium–Protaceratherium* assemblage defines the earliest Miocene European Land Mammal Age (Agenian ELMA; MN1+MN2) in western Europe (Bruijn *et al.*, 1992; Antoine *et al.*, 2006). Hence, their co-occurrence in the Bugti Hills and Zinda Pir – recorded for the first time outside Europe – confirms the earliest Miocene age of the upper member of the Chitarwata Fm as a whole. Compatible environmen-tal conditions might have occurred at these times in both areas, although geographically remote. Heissig & Fejfar (2007) recently described a rhinocerotid fauna from the Early Miocene of Tuchoř ice (MN3) in the Czech Republic, consisting of the small teleocera-tine *Prosantorhinus laubei* sp. nov., the small and slender acerathere *Protaceratherium minutum*, and the large and slender acerathere '*Aceratherium* (*Ali-cornops*) aff. *pauliacense*'. The latter 'can not be dis-tinguished from the earlier type population [of *Mesaceratherium paulhiacense* (Richard, 1937)] from Paulhiac (MN1)' (Heissig & Fejfar, 2007: 19). The rhinocerotid assemblage recognized in Level 4 in the Bugti area (~MN2) includes notably *Prosantorhinus shahbazi*, *Protaceratherium* sp., and *M. welcommi* sp. nov. (Métais *et al.*, 2009; this work) Similarly, the teleoceratine *Brachypotherium fatehjangense* and the acerathere *Mesaceratherium welcommi* from the Sulaiman Range (Pakistan) have strong affinities to the earliest African rhinocerotids, *Brachypotherium heinzelini* and *Aceratherium acutirostratum*, respec-tively, recognized in Napak II and Songhor by Hooijer (1966, 1973) and Hooijer & Patterson (1972). More-over, the earliest elasmotheriine *Bugtirhinus praecur-sor* from the earliest Miocene of the Bugti Hills (Levels 3bis and 4; Table 30; Antoine & Welcomme, 2000) has close affinities with *Ougandatherium napa-kense* from Napak I (Guérin & Pickford, 2003). The radiometric age of Songhor is ~19.5 Myr (Pickford, 1986; Cote *et al.*, 2007) and Napak might be slightly older (Tassy, 1986; Cote *et al.*, 2007). In the light of such coeval and comparable assemblages (Pakistan/ East Africa), it might be worth revising the earliest

remains of the African 'chilothere' *Chilotheridium pattersoni* Hooijer, 1971, from the Early Miocene of Kenya and Uganda (Rusinga, Bukwa, Loperot, and Ombo; 18–16 Myr interval; Guérin & Pickford, 2003), and comparing them to both *P. blanfordi* and *M. welcommi*, with a special emphasis on referable post-cranials: (1) true chilotheres have their First Appear-ance Datum much later, i.e. during the late Middle Miocene in Eurasia, with a late Miocene climax in Asia (Hooijer, 1966; Antoine *et al.*, 2003b); (2) as a result of convergent cheek teeth patterns, '*Acerath-erium blanfordi*' as a whole had been mistakenly referred to the genus *Chilotherium* for decades; and

(3) figured teeth from Rusinga (18 Myr; Hooijer, 1966: 151, pl. 6) and Ombo (16 Myr; Hooijer, 1973: pl. 1, figs 3, 9, 10) have strong similarities to *P. blanfordi* and/or *M. welcommi*.

All these homotaxic assemblages constrain the existence of broad and sustainable rhinocerotid inter-changes amongst South Asia, Europe, and Africa under comparable environmental conditions through-out earliest Miocene times (*c*. 23–19 Myr interval).

ACKNOWLEDGEMENTS

We thank J.-L. Welcomme for his prominent role in the French-Baloch Palaeontological Expeditions 1995–2004 in the Bugti Hills, in which Léonard Gins-burg, Marc Delcorso, Jérôme Proriol, Mouloud Benammi, Jean-Jacques Jaeger, Yaowalak Chaim-anee, and Dario De Franceschi participated and suffered. Michèle E. Morgan, John C. Barry, David Pilbeam, Everett H. Lindsay, Iqbal U. Cheema, and Susanne Cote provided valuable help and discussion. We are grateful to H. E. Iqbal Akhund and Kamal Majidullah (Karachi) for their indefectible support. Jerry J. Hooker, Andy Currant, and Peter J. Whybrow (NHM, London), Sophie Hervet (Rhinopolis), Abel Prieur (UCBL, Lyon-Villeurbanne), Christine Argot, Claire Sagne, and Pascal Tassy (MNHN, Paris), Malcolm C. McKenna (AMNH, New York), and David Pilbeam and John C. Barry (Peabody Museum, Harvard University) granted access to the collections of which they are/were in charge. Peter Hayward, Hans Larsson, and an anonymous reviewer signifi-cantly improved the original manuscript. This article is dedicated to the memory of Annie Antoine, Nawab M. A. K. Bugti, Will Downs, and Malcolm C. McKenna. This research was supported by the French ANR-PALASIAFRICA Program (ANR-08-JCJC-0011-01 – ANR-ERC). MPFB publication n°38.

REFERENCES

Antoine PO. 1997. *Aegyrcitherium beonensis* nov. gen. nov. sp., nouvel élasmothère (Mammalia, Rhinocerotidae) du gisement miocène (MN 4b) de Montréal-du-Gers (Gers, France). Position phylogénétique au sein des Elasmoth-eriini. *Neues Jahrbuch für Geologie und Paläontologie, Abhandlungen* **204:** 399–414.

Antoine PO. 2002. Phylogénie et évolution des Elasmoth-eriina (Mammalia, Rhinocerotidae). *Mémoires du Muséum National d'Histoire Naturelle* **188:** 1–359.

Antoine PO. 2003. Middle Miocene elasmotheriine Rhinoc-erotidae from China and Mongolia: taxonomic revision and phylogenetic relationships. *Zoologica Scripta* **32:** 95–118.

Antoine PO, Bulot C, Ginsburg L. 2000. Une faune rare de rhinocérotidés (Mammalia, Perissodactyla) dans le Miocène inférieur de Pellecahus (Gers, France). *Geobios* **33:** 249– 255.

Antoine PO, Ducrocq S, Marivaux L, Chaimanee Y, Crochet JY, Jaeger JJ, Welcomme JL. 2003a. Early rhinocerotids (Mammalia, Perissodactyla) from South Asia and a review of the Holarctic Paleogene rhinocerotid record. *Canadian Journal of Earth Sciences* **40:** 365–374.

Antoine PO, Duranthon F, Hervet S, Fleury G. 2006. Vertébrés de l'Oligocène terminal (MP30) et du Miocène basal (MN1) du métro de Toulouse (SW de la France). *Comptes Rendus Palevol* **5:** 875–884.

Antoine PO, Duranthon F, Tassy P. 1997. L'apport des grands mammifères (Rhinocérotidés, Suoidés, Probosci-diens) à la connaissance des gisements du Miocène d'Aquitaine (France). In: Aguilar JP, Legendre S, Michaux J, eds. *Actes du Congrès biochrom'97*, Vol. 21. Montpellier: Mémoires et Travaux de l'Ecole Pratique des Hautes Etudes, Institut de Montpellier, 581–590.

Antoine PO, Duranthon F, Welcomme JL. 2003b. *Alicornops* (Mammalia, Rhinocerotidae) dans le Miocène supérieur des Collines Bugti (Balouchistan, Pakistan): implications phylogénétiques. *Geodiversitas* **25:** 575–603.

Antoine PO, Karadenizli L, Saraç G, Sen S. 2008. A giant rhinocerotoid (Mammalia, Perissodactyla) from the Late Oligocene of north-central Anatolia (Turkey). *Zoological Journal of the Linnean Society* **152:** 581–592.

Antoine PO, Shah SMI, Cheema IU, Crochet JY, de Franceschi D, Marivaux L, Métais G, Welcomme JL. 2004. New remains of the baluchithere *Paraceratherium bugtiense* (Pilgrim, 1910) from the Late/latest Oligocene of the Bugti Hills, Balochistan, Pakistan. *Journal of Asian Earth Sciences* **24:** 71–77.

Antoine PO, Welcomme JL. 2000. A new rhinoceros from the Bugti Hills, Baluchistan, Pakistan: the earliest elas-motheriine. *Palaeontology* **43:** 795–816.

Barbour EH. 1906. Notice of a new Miocene rhinoceros, *Diceratherium arikarense*. *Science New Series* **24:** 780– 781.

Barry JC, Morgan ME, Flynn LJ, Pilbeam D, Behrens-meyer A, Raza S, Khan I, Badgley C, Hicks J, Kelley J. 2002. Faunal and environmental change in the Late Miocene Siwaliks of Northern Pakistan. *Paleobiology* **28:** Memoir 3 (Supplement to Number 2), 1–71.

Beliajeva EI. 1954. New rhinoceros remains from Kazakh-stan. *Travaux de l'Institut Paléozoologique de l'Académie des Sciences de l'URSS, Moscou* **47:** 44–54 [in Russian].

de Blainville HMD. 1839–1864. *Ostéographie des mam-mifères récents et fossiles. Atlas – Tome troisième (Quater-natès)*, Paris: Baillière.

Blanford WT. 1876. On the geology of Sind. *Indian Geologi-cal Survey Records* **9:** 8–22.

Blanford WT. 1879. The geology of Sindh. *Memoirs of the Geological Survey of India* **18:** 1–196.

de Bonis L. 1973. *Contribution à l'étude des mammifères de l'Aquitanien de l'Agenais. Rongeurs-Carnivores-Périssodactyles*, Vol. 28. Paris: Mémoires du Muséum National d'Histoire Naturelle, 1–192.

Borissiak AA. 1944. *Aceratherium aralense* n. sp. *Doklady Akademiye Nauk SSSR* **43:** 30–32 [In Russian].

Brunet M. 1979. *Les grands mammifères chefs de file de l'immigration oligocène et le problème de la limite Eocène-Oligocène en Europe*, Paris: Fondation Singer-Polignac (ed.).

Cerdeño E. 1993. Etude sur *Diaceratherium aurelianense* et *Brachypotherium brachypus* (Rhinocerotidae, Mammalia) du Miocène moyen de France. *Bulletin du Muséum National d'Histoire Naturelle, Paris* **15:** 25–77.

Cerdeño E, Sánchez B. 2000. Intraspecific variation and evolutionary trends of *Alicornops simorrense* (Rhinocer-otidae) in Spain. *Zoologica Scripta* **29:** 275–305.

Colbert EH. 1934. A new rhinoceros from the Siwalik Beds of India. *American Museum Novitates* **749:** 1–13.

Collinson M, Hooker JJ. 2003. Paleogene vegetation of Eurasia: framework for mammalian faunas. *Deinsea* **10:** 41–83.

Cote S, Werdelin L, Seiffert ER, Barry JC. 2007. Addi-tional material of the enigmatic Early Miocene mammal Kelba and its relationship to the order Ptolemaiida. *Pro-ceedings of the National Academy of Sciences of the United States of America* **104:** 5510–5515.

Crusafont M, Villalta JF, Truyols J. 1955. El Burdi-galiense continental de la Cuenca del Vallés-Penedés. *Memorias y Comunicaciones del Instituto Geológico de Bar-celona, Barcelona* **12:** 1–272.

Cuvier G. 1822. *Recherches sur les ossemens fossiles*, Vol. 5, 2nd edn. Paris: Edmond d'Ocagne.

De Bruijn H, Daams R, Daxner-Höck G, Fahlbusch V, Ginsburg L, Mein P, Morales J. 1992. Report of the RCMNS working group on fossil mammals, Reisenburg 1990. *Newsletters on Stratigraphy* **26:** 65–118.

De Franceschi D, Hoorn C, Antoine PO, Cheema IU, Flynn LJ, Lindsay EH, Marivaux L, Métais G, Rajpar AR, Welcomme JL. 2008. Floral Data from the Mid-Cenozoic of central Pakistan. *Review of Palaeobotany and Palynology* **150:** 115–129.

Downing KF. 2005. A new enigmatic large rhinocerotid from the upper unit of the Chitarwata Formation at Zinda Pir Dome, Western Pakistan. *Palaeontologia Electronica* **8** (21A)**:** 1–8.

Duvernoy GL. 1853. Nouvelles études sur les rhinocéros fossiles. *Archives du Muséum d'Histoire Naturelle, Paris* **7:** 1–144.

Duvernoy GL. 1854–1855. Nouvelles études sur les rhi-nocéros fossiles. *Archives du Muséum National d'Histoire Naturelle, Paris* **7:** 1–144.

Falconer H, Cautley PT. 1846–1849. Fauna antiqua sivalensis, *being the fossil zoology of the Sewalik Hills, in the north of India*. London: Falconer H.

Farris JS. 1988. *Hennig86 reference*. Version 1.5 (software). New York: Port Jefferson Station.

Fischer von Waldheim GF. 1814. *Zoögnosia tabulis synop-ticis illustrate, in usum Paeselectionum Academiae Imperia-lis Medicochirurgae*. Moscow: Nicolai Sergeidis Vsevolozsky.

Forster-Cooper C. 1915. New genera and species of mammals from the Miocene deposits of Baluchistan. Pre-liminary notice. *Annual Magazine of Natural History* **16:** 404–410.

Forster-Cooper C. 1924. On the skull and dentition of *Paraceratherium bugtiense*: a genus of aberrant rhinoceros from the lower Miocene deposits of Dera Bugti. *Philosophi-cal Transactions of the Royal Society of London, Series B* **212:** 369–394.

Forster-Cooper C. 1934. XIII. The Extinct Rhinoceroses of Baluchistan. *Philosophical Transactions of the Royal Society of London, Series B* **223:** 569–616.

Freeland WJ. 1991. Plant secondary metabolites: biochemi-cal coevolution with herbivores. In: Palo RT, Robbins CT, eds. *Plant defenses against mammalian herbivory*. Boca Raton: CRC Press, 61–81.

Gentry AW. 1987. Rhinoceroses from the Miocene of Saudi Arabia. *Bulletin of the British Museum (of Natural History)* **41:** 409–432.

Ginsburg L, Bulot C. 1984. Les Rhinocerotidae (Perissodac-tyla, Mammalia) du Miocène de Bézian à La Romieu (Gers). *Bulletin du Muséum National d'Histoire Naturelle, Paris* **6:** 353–377.

Gradstein FM, Ogg JG, Smith AG. 2005. *A geological time scale 2004*. Cambridge: Cambridge University Press.

Gray JE. 1821. On the natural arrangements of vertebrose animals. *London Medical Repository* **15:** 296–310.

Guthrie RD. 1984. Mosaics, allelochemics and nutrients. In: Martin PS, Klein RG, eds. *Quaternary extinctions. A prehis-toric evolution*. Tucson: University of Arizona Press, 259– 298.

Guérin C. 1980. *Les Rhinocéros (Mammalia, Perissodactyla) du Miocène terminal au Pléistocène supérieur en Europe occidentale. Comparaison avec les espèces actuelles*. Lyon: Documents du Laboratoire de Géologie de l'Université de Lyon, Sciences de la Terre 79, Vol. 3.

Guérin C, Pickford M. 2003. *Ougandatherium naMHNT Pak ense* nov. gen. nov. sp., le plus ancien Rhinocerotidae Iranotheriinae d'Afrique. *Annales de Paléontologie* **89:** 1– 35.

Hatcher JB. 1894. On a small collection of vertebrate fossils from the Loup Fork beds of northwestern Nebraska, with note on the geology of the region. *American Naturalist* **28:** 236–248.

Heissig K. 1969. Die Rhinocerotidae (Mammalia) aus der oberoligozänen Spaltenfüllung von Gaimersheim. *Abhand-lungen der Bayerischen Akademie der Wissenschaften, Mathematisch-Naturwissenschaftliche Klasse* **138:** 1–133.

Heissig K. 1972. Paläontologische und geologische Untersu-chungen im Tertiär von Pakistan. 5. Rhinocerotidae

(Mamm.) aus den unteren und mittleren Siwalik-Schichten. *Abhandlungen der Bayerischen Akademie der Wissen-schaften Mathematisch-Naturwissenschaftliche Klasse* **152:** 1–112.

Heissig K. 1976. Rhinocerotidae (Mammalia) aus der *Anchitherium*-Fauna Anatoliens. *Geologisches Jahrbuch B* **19:** 3–121.

Heissig K, Fejfar O. 2007. Die Säugetiere aus dem Unter-miozän von Tuchoř ice in Nordwestböhmen. I. Die fossilen Nashörner (Mammalia, Rhinocerotidae). *Acta Musei Nationalis Pragae, Series B, Historia Naturalis, Prague* **63:** 19–64.

Hooijer DA. 1966. Miocene rhinoceroses of East Africa. *Bul-letin of the British Museum (of Natural History), Fossil Mammals of Africa* **21:** 117–190.

Hooijer DA. 1971. A new rhinoceros from the late Miocene of Loperot, Turkana District, Kenya. *Bulletin of the Museum of Comparative Zoology, Cambridge (Mass.)* **142:** 339–392.

Hooijer DA. 1973. Additional Miocene to Pleistocene rhinoc-eroses of Africa. *Zoological Mededelingen* **46:** 149–178.

Hooijer DA, Patterson B. 1972. Rhinoceroses from the Pliocene of Northwestern Kenya. *Bulletin of the Museum of Comparative Zoology, Cambridge (Mass.)* **144:** 1–26.

Hünermann KA. 1989. Die Nashornskelette (*Aceratherium incisivum* Kaup 1832) aus dem Jungtertiär vom Höwenegg im Hegau (Südwestdeutschland). *Andrias* **6:** 5–116.

International Commission On Zoological Nomencla-ture. 1999. *International Code of Zoological Nomenclature, 4ème édition*. London: The International Trust for Zoological Nomenclature.

Kaup JJ. 1832. *Description d'Ossements fossiles de Mam-mifères inconnus jusqu'à présent, qui se trouvent au Musée grand-ducal de Darmstadt*. Darmstadt: Heyer, J.G.

Klaits BG. 1973. Upper Miocene rhinoceroses from Sansan (Gers), France: the manus. *Journal of Paleontology* **47:** 315–326.

Lartet E. 1837. Note sur les ossements fossiles des terrains tertiaires de Simorre, de Sansan, etc., dans le département du Gers, et sur la découverte récente d'une mâchoire de singe fossile. *Comptes Rendus de l'Académie des Sciences, Paris* **4:** 85–93.

Lartet E. 1851. *Notice sur la colline de Sansan*. Auch: Portes.

Laudet F, Antoine PO. 2004. Des chambres de pupation de Dermestidae (Insecta : Coleoptera) sur un os de mammifère tertiaire (phosphorites du Quercy). Implications tapho-nomiques et paléoenvironnementales. *Geobios* **37:** 376– 381.

Leidy J 1851. Remarks on *Oreodon priscus* and Rhinoceros occidentalis. *Proceedings of the Academy of Natural Sciences of Philadelphia* **5:** 276.

Leidy J. 1871. Report on the vertebrate fossils of the Tertiary formations of the West. *Annals and Reports of the United States Geological and Geographic Survey, Hayden* **2:** 340– 370.

Lihoreau F, Ducrocq S, Antoine PO, Vianey-Liaud M, Rafaÿ S, Garcia G, Valentin X. 2009. First complete skulls of *Elomeryx crispus* (Gervais, 1849) and of *Protacer-atherium albigense* (Roman, 1912) from a new Oligocene locality near Moissac (SW France). *Journal of Vertebrate Paleontology* **29:** 242–253.

Lindsay EH, Flynn LJ, Cheema IU, Barry JC, Downing KF, Rajpar AR, Raza SM. 2005. Will Downs and the Zinda Pir Dome. *Palaeontologia Electronica* **8:** 1–19.

von Linnaeus C. 1758. *Systema Naturae per regna tria naturae, secundum classes, ordines, genera, species, cum characteribus, differentiis, synonymis, locis*, 10th edn, Vol. 1: *Regnum animale*. Stockholm.

Lucas FA. 1900. A new rhinoceros, *Trigonias osborni*, from the Miocene of South Dakota. *United States National Museum Proceedings* **23:** 221–224.

Lydekker R. 1881. Siwalik Rhinocerotidae. *Memoirs of the Geological Survey of India – Palaeontologica Indica* **2:** 1–62.

Lydekker R. 1884. Additional Siwalik Perissodactyla and Proboscidea. *Memoirs of the Geologcal Survey of India – Palaeontologia Indica* **3:** 1–34.

Lydekker R. 1886. *Catalogue of the fossil mammalia in the British Museum (Natural History), Part III*. London: Taylor and Francis.

Marsh OC. 1875. Notice of new Tertiary mammals. IV. *American Journal of Sciences and Arts* **109:** 239–250.

Matthew WD. 1929. Critical observations upon Siwalik mammals. *Bulletin of the American Museum of Natural History* **56:** 437–560.

Métais G, Antoine PO, Baqri SRH, Marivaux L, Welcomme JL. 2009. Lithofacies, depositional environ-ments, regional biostratigraphy, and age of the Chitarwata Formation in the Bugti Hills, Balochistan, Pakistan. *Journal of Asian Earth Sciences* **34:** 154–167.

Mihlbachler MC. 2005. Linking sexual dimorphism and soci-ality in rhinoceroses: insights from *Teleoceras proterum* and *Aphelops malacorhinus* from the late Miocene of Florida. *Bulletin of the Florida Museum of Natural History* **45:** 495–520.

Osborn HF. 1900. Phylogeny of Rhinoceroses of Europe. *Memoirs of the American Museum of Natural History* **13:** 229–267.

Owen R. 1848. *The archetype and homologies of the vertebrate skeleton*. London.

Pickford M. 1986. A revision of the Miocene Suidae and Tayassuidae (Artiodactyla, Mammalia) of Africa. *Tertiary Research, Special Papers* **7:** 1–83.

Pilgrim GE. 1908. The Tertiary and post-Tertiary fresh-water deposits of Baluchistan and Sind, with notices of new vertebrates. *Records of the Geological Survey of India* **37:** 139–166.

Pilgrim GE. 1910. Notice on new mammal genera and species from the Tertiaries of India. *Records of the Geologi-cal Survey of India* **15:** 63–71.

Pilgrim GE. 1912. The vertebrate fauna of the Gaj Series in the Bugti Hills and the Punjab. *Paleontologia Indica* **4:** 1–83.

Prothero DR. 1998. 42 Rhinocerotidae. In: Janis CM, Scott KM, Jacobs LL, eds. *Evolution of tertiary mammals of North America. Terrestrial carnivores, ungulates and ungulatelike mammals*, Vol. 1. New York: Cambridge University Press, 595–605.

Prothero DR. 2005. *The evolution of North American Rhi-noceroses*. Cambridge; New York; Melbourne: Cambridge University Press.

Qiu Z, Xie J. 1997. A new species of *Aprotodon* (Perissodac-tyla, Rhinocerotidae) from Lanzhou Basin, Gansu, China. *Vertebrata PalAsiatica* **35:** 250–267 [in Chinese and English].

Répelin J. 1917. Études paléontologiques dans le sud-ouest de la France (Mammifères). Les rhinocérotidés de l'Aquitanien supérieur de l'Agenais (Laugnac). *Annales du Muséum d'Histoire naturelle de Marseille* **16:** 1–47.

Richard M. 1937. Une nouvelle espèce de Rhinocérotidé aquitanien: *Diaceratherium pauliacensis*. *Bulletin de la Société d'Histoire Naturelle de Toulouse* **71:** 165–170.

Ringström TJ. 1924. Nashörner der *Hipparion*-Fauna Nord-Chinas. *Geological Survey of China* **11:** 1–156.

Roger O. 1898. Wirbeltierreste aus dem Dinotheriensande der bayerisch-schwäbischen Hochebene. *Bericht des Natur-wissenschaftlichen Vereins für Schwaben, Neuburg* **33:** 1–46, 383–396.

Roman F. 1912. Les rhinocérotidés de l'Oligocène d'Europe. *Archives du Musée des Sciences Naturelles de Lyon* **11:** 1– 92.

Roman F. 1924. Contribution à l'étude de la faune de mam-mifères des Littorinenkalk (Oligocène supérieur) du Bassin de Mayence. *Travaux du Laboratoire de Géologie de la Faculté de Sciences de Lyon* **VII:** 55.

Roman F, Viret J. 1930. Le Miocène continental de l'Armagnac et le gisement burdigalien de La Romieu (Gers). *Livre Jubilaire de la Société Géologique de France, Paris* **2:** 576–604.

Roman F, Viret J. 1934. *La faune de Mammifères du Bur-digalien de La Romieu (Gers)*, Vol. 21. Paris: Mémoires de la Société Géologique de France.

Scott WB. 1941. Perissodactyla. The mammalian fauna of the White River Oligocene. *Transactions of the American Philo-sophical Society* **28:** 747–980.

Steininger FF. 1999. Chronostratigraphy, geochronology and biochronology of the Miocene 'European Land Mammal Mega-Zones' (ELMMZ) and the Miocene 'Mammal-Zones' (MN). In: Rössner GE, Heissig K, eds. *The Miocene land mammals of Europe*. Munich: Pfeil, 9–24.

Swofford DL. 1998. *PAUP, Phylogenetic analysis using par-simony*, version 4.0 (software). Sunderland: Smithsonian Institution, Sinauer Associates.

Tanner LG. 1969. A new rhinoceros from the Nebraska Miocene. *Bulletin of the University of Nebraska State Museum* **8:** 395–412.

Tassy P. 1986. *Nouveaux Elephantoidea (Mammalia) dans le Miocène du kenya*. Paris: Cahiers de Paléontologie, Editions du Centre National de la Recherche Scientifique.

Uhlig U. 1999. Die Rhinocerotidae (Mammalia) aus der unteroligozänen Spaltenfüllung Möhren 13 bei Treuchtlin-gen in Bayern. *Verlag der Bayerischen Akademie der Wis-senschaften Abhandlungen*. Neue Folge **170**.

Welcomme JL, Antoine PO, Duranthon F, Mein P, Gins-burg L. 1997. Nouvelles découvertes de Vertébrés miocènes dans le synclinal de Dera Bugti (Balouchistan, Pakistan). *Comptes Rendus de l'Académie des Sciences, Sciences de la terre et des planètes* **325:** 531–536.

Welcomme JL, Benammi M, Crochet JY, Marivaux L, Métais G, Antoine PO, Baloch I. 2001. Himalayan Fore-lands: palaeontological evidence for Oligocene detritic deposits in the Bugti Hills (Baluchistan, Pakistan). *Geologi-cal Magazine* **138:** 397–405.

Welcomme JL, Ginsburg L. 1997. Mise en évidence de l'Oligocène sur le territoire des Bugti (Balouchistan, Paki-stan). *Comptes Rendus de l'Académie des Sciences, Sciences de la Terre et des Planètes* **325:** 999–1004.

Welcomme JL, Marivaux L, Antoine PO, Benammi M. 1999. Mammifères fossiles des Collines Bugti (Balouch-istan, Pakistan). Nouvelles données. *Bulletin de la Société d'Histoire Naturelle de Toulouse* **135:** 135–139.

Wermelinger M. 1998. Prosantorhinus *cf.* douvillei *(Mammalia, Rhinocerotidae), petit rhinocéros du gisement miocène (MN 4b) de Montréal-du-Gers (Gers, France). Etude ostéologique du membre thoracique*. Unpublished PhD, Uni-versity Toulouse III, France.

Wiens JJ. 2001. Character analysis in morphological phylo-genetics: problems and solutions. *Systematic Biology* **50:** 689–699.

Wood HE II. 1927. Some early Tertiary rhinoceroses and hyracodonts. *Bulletin of the American Paleontologists* **13:** 5–105.

Yan D, Heissig K. 1986. Revision and autopodial morphology of the Chinese-European rhinocerotid genus *Plesiacerath-erium* Young 1937. *Zitteliana Abhandlungen der Bayerische Staatssammlung für Paläontologie und historisches Geolo-gie, München* **14:** 81–110.

Young C-C. 1937. On a Miocene mammalian fauna from Shantung. *Bulletin of the Geological Society of China* **17:** 209–245.

APPENDIX 1

CHARACTER LISTING

This list coincides with the character list proposed by Antoine (2003) and Antoine *et al.* (2003b).

Cranium

(1) Nasal: lateral apophysis = 0, absent; 1, present
(2) Maxillary: foramen infraorbitalis = 0 above pre-molars; 1, above molars
(3) Nasal notch = 0, above P1–3; 1, above P4–M1
(4) Nasal septum = 0, never ossified; 1, ossified (even sometimes)
(5) Nasal septum: ossified = 0, partially; 1, totally
(6) Nasal/lacrymal: contact = 0, long; 1, punctual or absent
(7) Orbit: anterior border = 0, above P4–M2; 1, above M3; 2, behind M3
(8) Lacrymal: processus lacrymalis = 0, present; 1, absent

(9) Frontal: processus postorbitalis = 0, present; 1, absent
(10) Maxillary: anterior base of the processus zygo-maticus maxillari = 0, high; 1, low
(11) Zygomatic arch = 0, low; 1, high; 2, very high
(12) Zygomatic arch: processus postorbitalis = 0, present; 1, absent
(13) Zygomatic arch: processus postorbitalis = 0, on jugal; 1, on squamosal
(14) Jugal/squamosal: suture = 0, smooth; 1, rough
(15) Skull: dorsal profile = 0, flat; 1, concave; 2, very concave

(16) Sphenoid: foramen sphenorbitale and f. rotun-dum = 0, distinct; 1, fused
(17) Squamosal: area between temporal and nuchal crests = 0, flat; 1, depression
(18) External auditory pseudomeatus = 0, open; 1, partially closed; 2, closed
(19) Occipital side = 0, inclined forward; 1, vertical; 2, inclined backward
(20) Occipital: nuchal tubercle = 0, little developed; 1, developed; 2, very developed
(21) Skull: back of teeth row = 0, in the posterior half; 1, restricted to the anterior half
(22) Pterygoid: posterior margin = 0 nearly horizon-tal; 1, nearly vertical
(23) Skull = 0, dolichocephalic; 1, brachycephalic
(24) Nasal bones: rostral end = 0, narrow; 1, broad; 2, very broad
(25) Nasal bones = 0, totally separated; 1, anteriorly separated; 2, fused
(26) Nasal bones = 0, long; 1, short; 2, very long
(27) Median nasal horn = 0, absent; 1, present
(28) Median nasal horn = 0, small; 1, developed
(29) Paired nasal horns = 0, absent; 1, present
(30) Paired nasal horns = 0, terminal bumps; 1, lateral crests

(31) Frontal horn = 0, absent; 1, present (32)*Frontal horn = 0, small; 1, huge [*Elasmotherium*]
(33) Orbit: lateral projection = 0, absent; 1, present
(34) Zygomatic width/frontal width = 0, less than 1.5; 1, more than 1.5
(35) Frontal-parietal = 0, sagittal crest; 1, close fron-toparietal crests; 2, distant crests
(36) Occipital crest = 0, concave; 1, straight; 2, forked
(37) Maxillary: processus zygomaticus maxillari, anterior tip = 0, progressive; 1, brutal
(38) Vomer = 0, acute; 1, rounded
(39) Squamosal: articular tubercle = 0, smooth; 1 high

(40) Squamosal: transversal profile of articular tubercle = 0, straight; 1, concave
(41) Squamosal: foramen postglenoideum = 0, distant from the processus postglenoidalis; 1, close to it
(42) Squamosal: processus postglenoidalis = 0, flat; 1, convex; 2, dihedron
(43) Basioccipital: foramen nervi hypoglossi = 0, in the middle of the fossa; 1 shift anteroexternally
(44) Basioccipital: sagittal crest on the basilar pro-cess = 0, absent; 1, present
(45) Squamosal: posterior groove on the processus zygomaticus = 0, absent; 1, present
(46) Squamosal-occipital: processus post-tympanicus and processus paraoccipitalis = 0, fused; 1, distant

(47) Squamosal: processus post-tympanicus = 0, well developed; 1, little developed; 2, huge
(48) Occipital: processus paraoccipitalis = 0, well developed; 1, little developed
(49) Occipital: foramen magnum = 0, circular; 1, sub-triangular
(50) Basioccipital: median ridge on the condyle = 0, absent; 1, present
(51) Basioccipital: medial truncation on the condyle = 0, absent; 1, present
(52) Basioccipital: medial truncation on the condyle = 0, present at juvenile stage; 1, still present at adult stage

Mandible
(53) Symphysis = 0, very upraised; 1, upraised; 2, nearly horizontal
(54) Symphysis = 0, spindly; 1, massive; 2, very massive

(55) Symphysis: posterior margin = 0, in front of p2; 1, level of p2–4
(56) Foramen mentale = 0, in front of p2; 1, level of p2–4

(57) Corpus mandibulae: lingual groove = 0, present; 1, absent

(58) Corpus mandibulae: lingual groove = 0, still present at adult stage; 1, present at juvenile stage only

(59) Corpus mandibulae: base = 0, straight; 1, convex; 2, very convex
(60) Ramus = 0, vertical; 1, inclined forward; 2, inclined backward
(61) Ramus: processus coronoideus = 0, well devel-oped; 1, little developed
(62) Foramen mandibulare = 0, below the teeth neck; 1, above the teeth neck

Teeth
(63) Compared length of the premolars/molars rows = 0 ($100 ¥ L_{P3–4}/L_{M1–3}) > 50$; 1, $42 < (100 ¥ L_{P3–4}/L_{M1–3}) < 50$; 2 $(100 ¥ L_{P3–4}/L_{M1–3}) < 42$
(64) Cheek teeth: enamel foldings = 0, absent; 1, weak; 2, developed; 3, intense
(65) Cheek teeth: cement = 0, absent; 1, present
(66) Cheek teeth: cement = 0, weak or variable; 1, abundant

(67) Cheek teeth: shape of enamel = 0, wrinkled; 1, wrinkled and corrugated; 2, corrugated and arborescent

(68) Cheek teeth: crown = 0, low; 1, high

(69) Cheek teeth: crown = 0, high; 1, partial hyps-odonty; 2, subhypsodonty; 3, hypsodonty

(70) Cheek teeth: roots = 0, distinct; 1, joined; 2, fused

(71) I1 = 0, present; 1, absent

(72) I1: shape of the crown (cross-section) = 0, almond; 1, oval; 2, halfmoon (NA)

(73) I2 = 0, present; 1, absent

(74) I3 = 0, present; 1, absent

(75) C1 = 0, present; 1, absent

(76) i1 = 0, present; 1, absent

(77) i1: crown = 0, developed, with a pronounced neck; 1, reduced

(78) i2 = 0, present; 1, absent

(79) i2: shape = 0, incisor-like; 1, tusk-like

(80) i2: orientation = 0, parallel; 1, divergent

(81) i3 = 0, present; 1, absent

(82) c1 = 0, present; 1, absent

(83) Upper premolars: labial cingulum = 0, always present; 1, usually present; 2, usually absent; 3, always absent

(84) P2–4: crochet = 0, always absent; 1, usually present; 2, always present

(85) P2–4: crochet = 0, always simple; 1, usually simple; 2, usually multiple

(86) P2–4: metaloph constriction = 0, absent; 1, present

(87) P2–4: lingual cingulum = 0, always present; 1, usually present; 2, usually absent; 3, always absent

(88) P2–4: lingual cingulum = 0, continuous; 1, reduced

(89) P2–4: postfossette = 0, narrow; 1, wide; 2, pos-terior wall

(90) P2–3: antecrochet = 0, always absent; 1, usually absent; 2, usually present; 3, always present

(91) P1 (in adults) = 0, always present; 1, usually present; 2, always absent

(92) P1: anterolingual cingulum = 0, present; 1, absent [*Rhinoceros sondaicus*]

(93) P2 = 0, present; 1, absent

(94) P2: protocone and hypocone = 0, fused; 1, lingual bridge; 2, separated; 3, lingual wall (NA)

(95) P2: metaloph = 0, hypocone posterior to meta-cone; 1, transverse; hypocone anterior to metacone

(96) P2: lingual groove = 0, present; 1, absent

(97) P2: protocone = 0, equal or stronger than the hypocone; 1, less strong than the hypocone

(98) P2: protoloph = 0, present; 1, absent

(99) P2: protoloph = 0, joined to the ectoloph; 1, inter-rupted

(100) P3–4: medifossette = 0, always absent; 1, usually absent; 2, usually present; 3, always present

(101) P3–4: constriction of the protocone = 0, always absent; 1, usually absent; 2, usually present; 3, always present

(102) P3–4: protocone and hypocone = 0, fused; 1, lingual bridge; 2, separated; 3, lingual wall (NA)

(103) P3–4: metaloph = 0, transverse; 1, hypocone pos-terior to metacone; 2, hypocone anterior to meta-cone

(104) P3: protoloph = 0, joined to the ectoloph; 1, inter-rupted

(105) P3: crista = 0, always absent; 1, usually absent; 2, usually present; 3, always present

(106) P3: pseudometaloph = 0, always absent; 1, some-times present

(107) P4: antecrochet = 0, always absent; 1, usually absent; 2, usually present; 3, always present

(108) P4: hypocone and metacone = 0, joined; 1, sepa-rated

(109) Upper molars: labial cingulum = 0, always present; 1, usually present; 2, usually absent; 3, always absent

(110) Upper molars: antecrochet = 0, always absent; 1, usually absent; 2, usually present; 3, always present

(111) Upper molars: crochet = 0, always absent; 1, usually absent; 2, usually present; 3, always present

(112) Upper molars: crista = 0, always absent; 1, usually absent; 2, usually present; 3, always present

(113)*Upper molars: medifossette = 0, always absent; 1, usually absent [*Diceros bicornis*]; 2, usually present [*Ceratotherium simum*; *Coelodonta antiquitatis*; *Rhinoceros unicornis*]

(114) Upper molars: lingual cingulum = 0, always present; 1, usually present; 2, usually absent; 3, always absent

(115) M1–2: constriction of the protocone = 0, always absent; 1, usually absent; 2, usually present; 3, always present

(116) M1–2: constriction of the protocone = 0, weak; 1, strong

(117) M1–2: paracone fold = 0, present; 1, absent

(118) M1–2: paracone fold = 0, strong; 1, weak

(119) M1–2: metacone fold = 0, present; 1, absent

(120) M1–2: metastyle = 0, short; 1, long

(121) M1–2: metaloph = 0, long; 1, short

(122) M1–2: posterior part of the ectoloph = 0, straight; 1, concave

(123) M1–2: cristella = 0, always absent; 1, usually present; 2, always present
(124) M1–2: posterior cingulum = 0, continuous; 1, low and reduced
(125) M1: metaloph = 0, continuous; 1, hypocone iso-lated
(126) M1: antecrochet-hypocone = 0, always sepa-rated; 1, sometimes joined; 2, always joined
(127) M1: postfossette = 0, present; 1, usually absent
(128) M2: protocone, lingual groove = 0, always absent; 1, usually absent; 2, always present
(129) M2: metaloph = 0, continuous; 1, hypocone isolated
(130) M2: mesostyle = 0, absent; 1, present
(131) M2: mesostyle = 0, weak; 1, strong
(132) M2: antecrochet and hypocone = 0, separated; 1, joined
(133) M3: ectoloph and metaloph = 0, distinct; 1, fused (ectometaloph)
(134) M3: shape = 0, quadrangular; 1, triangular
(135) M3: constriction of the protocone = 0, always absent; 1, usually absent; 2, always present
(136) M3: protocone = 0, trefoil-shape; 1, indented
(137) M3: protoloph = 0, transverse; 1, lingually elon-gated
(138) M3: posterior groove on the ectometaloph = 0, present; 1, absent
(139)*p2–3: vertical external roughnesses = 0, absent; 1, present
(140) Lower cheek teeth: external groove = 0, devel-oped; 1, smooth, U-shaped; 2, angular, V-shaped (NA)
(141) Lower cheek teeth: external groove = 0, vanish-ing before the neck; 1, developed until the neck
(142) Lower cheek teeth: trigonid = 0, angular; 1, rounded
(143) Lower cheek teeth: trigonid = 0, obtuse or right dihedron; 1, acute dihedron
(144) Lower cheek teeth: metaconid = 0, joined to the metalophid; 1, constricted
(145) Lower cheek teeth: entoconid = 0, joined to the hypolophid; 1, constricted
(146) Lower premolars: lingual opening of the poste-rior valley = 0, U-shape; 1, narrow, V-shape
(147) Lower premolars: lingual cingulum = 0, always present; 1, usually present; 2, usually absent; 3, always absent
(148) Lower premolars: lingual cingulum = 0, reduced; 1, continuous
(149) Lower premolars: labial cingulum = 0, present; 1, absent
(150) Lower premolars: labial cingulum = 0, continu-ous; 1, reduced
(151) d1/p1 (in adults) = 0, always present; 1, usually present; 2, usually absent; 3, always absent
(152) d1: 0, always two-rooted; 1, usually two-rooted; 2, always one-rooted
(153) p2 = 0, always present; 1, usually present; 2, always absent
(154) p2: paralophid = 0, isolated, spur-like; 1, curved, without constriction
(155) p2: paraconid = 0, developed; 1, reduced
(156) p2: posterior valley = 0, lingually open; 1, usually closed; 2, always closed
(157) Lower molars: lingual cingulum = 0, always present; 1, usually present; 2, usually absent; 3, always absent
(158) Lower molars: lingual cingulum = 0, reduced; 1, continuous
(159) Lower molars: labial cingulum = 0, always present; 1, usually present; 2, usually absent; 3, always absent
(160) Lower molars: labial cingulum = 0, continuous; 1, reduced
(161) Lower molars: hypolophid = 0, transverse; 1, oblique; 2, almost sagittal
(162) m2–3: lingual groove of the entoconid = 0, absent; 1, present
(163)*dI1 = 0, present; 1, absent [*Ceratotherium simum*; *Coelodonta antiquitatis*]
(164)*dI2 = 0, present; 1, absent
(165) D2: mesostyle = 0, present; 1, absent
(166) D3–4: mesostyle = 0, absent; 1, present
(167) D2: lingual wall = 0, absent; 1, present
(168) D2: secondary folds = 0, absent; 1, present
(169) D2: mesoloph = 0, absent; 1, present
(170) di1 = 0, present; 1, absent
(171) di2 = 0, present; 1, absent
(172) Lower milk teeth: constriction of the meta-conid = 0, present; 1, absent
(173) Lower milk teeth: constriction of the ento-conid = 0, absent; 1, present
(174) Lower milk teeth: protoconid fold = 0, present; 1, absent
(175) d1 (in juveniles) = 0, present; 1, absent
(176) d2–3: vertical external roughnesses = 0, absent; 1, present
(177) d2–3: ectolophid fold = 0, present; 1, absent
(178) d2: anterior groove on the ectolophid = 0, absent; 1, present
(179) d2: paralophid = 0, simple; 1, double
(180) d2: posterior valley = 0, always open; 1, usually open; 2, usually closed; 3, always closed
(181) d3: paralophid = 0, double; 1, simple
(182) d3: lingual groove on the entoconid = 0, always absent; 1, usually absent; 2, always present

Postcranial skeleton

(183) Atlas: outline of the rachidian canal = 0, bulb; 1, mushroom

(184) Atlas: alar notch = 0, absent; 1, present
(185) Atlas: foramen vertebrale lateralis = 0, absent; 1, present
(186) Atlas: condyle-facets = 0, comma-like; 1, kidney-like

(187) Atlas: axis-facets = 0, straight; 1, sigmoid; 2, transversally concave (NA)
(188) Atlas: foramen transversarium = 0, present; 1, absent

(189) Atlas: foramen transversarium = beside the axis-facet; 1, hidden by the axis-facet
(190) Scapula = 0, elongated (1.5 < H/APD 2); 1, very elongated (H/APD > 2); 2, spatula-shaped (H/APD 1.5)

(191) Scapula: glenoid fossa = 0, oval; 1, medial border straight
(192) Humerus: greater trochiter = 0, high; 1, low
(193) Humerus: fossa olecrani = 0, high; 1, low
(194) Humerus: distal articulation = 0, egg cup (shallow median constriction); 1, diabolo (deep median constriction)
(195) Humerus: scar on the trochlea = 0, absent; 1, present

(196) Humerus: distal gutter on the epicondyle = 0, absent; 1, present
(197) Radius: anterior border of the proximal articu-lation = 0, straight; 1, M-shaped
(198) Radius: medial border of the diaphysis = 0, straight; 1, concave
(199) Radius: proximal ulna-facets = 0, always sepa-rated; 1, usually separated; 2, usually fused; 3, always fused

(200) Radius: insertion of the m. biceps brachii = 0, shallow; 1, deep
(201) Radius/ulna = 0, independent; 1, in contact or fused

(202) Radius: gutter for the m. extensor carpi = 0, deep and wide; 1, weak
(203) Radius/ulna: second distal articulation = 0, absent; 1, present
(204) Radius: posterior expansion of the scaphoid-facet = 0, low; 1, high
(205) Ulna: angle between diaphysis and olecra-non = 0, open; 1, closed
(206) Ulna: anterior tubercle on the distal end = 0, absent; 1, present
(207) Scaphoid: posteroproximal facet with semilu-nate = 0, present; 1, absent or contact
(208) Scaphoid: trapezium-facet = 0, large; 1, small
(209) Scaphoid: magnum-facet in lateral view = 0, concave; 1, straight
(210) Scaphoid: comparison between anterior and posterior heights = 0, equal; 1, H ant < H post
(211) Semilunate: ulna-facet = 0, absent; 1, present
(212) Semilunate: distal border of anterior side = 0, acute; 1, rounded
(213) Semilunate: anterior side = 0, keeled; 1, smooth
(214) Pyramidal: distal facet for semilunate = 0, sym-metric; 1, asymmetric; 2, L-shaped
(215) Pyramidal: distal side = 0, triangular; 1, elliptic
(216) Trapezoid: proximal border in anterior view = 0, symmetric; 1, asymmetric
(217) Magnum: proximal border of the anterior side = 0, nearly straight; 1, concave
(218) Magnum: indentation on the medial side = 0, absent; 1, present
(219) Magnum: indentation on the medial side = 0, always shallow; 1, usually shallow; 2, always deep

(220) Magnum: posterior tuberosity = 0, short; 1, long
(221) Magnum: posterior tuberosity = 0, curved; 1, straight

(222) Unciform: pyramidal-facet and McV-facet = 0, always separate; 1, usually separate; 2, always in contact

(223) Unciform: posterior expansion of the pyramidal-facet = 0, always absent; 1, usually absent; 2, usually present; 3, always present
(224) McII: magnum-facet = 0, curved; 1, straight
(225) McII: anterior McIII-facet = 0, present; 1, some-times absent
(226) McII: posterior McIII-facet = 0, always absent; 1, usually absent; 2, always present
(227) McII: anterior and posterior McIII-facets = 0, separated; 1, fused
(228) McII: trapezium-facet = 0, always present; 1, usually present; 2, always absent
(229) McIII: magnum-facet in anterior view = 0, visible; 1, invisible
(230) McIV: proximal facet, outline = 0, trapezoid; 1, pentagonal; 2, triangular
(231) McV: 0, functional; 1, vestigial
(232) Metacarpals: insertion of the m. extensor car-palis = 0, flat; 1, salient
(233) Coxal: acetabulum = 0, oval or circular; 1, sub-triangular
(234) Femur: trochanter major = 0, high; 1, low
(235) Femur: head = 0, hemispheric; 1, medially stiff
(236) Femur: surface of epiphysis of the head = 0, flat; 1, crescent-shaped
(237) Femur: fovea capitis = 0, present; 1, absent
(238) Femur: fovea capitis = 0, high and narrow; 1, low and wide
(239) Femur: third trochanter = 0, developed; 1, very developed
(240) Femur: relations between the medial lip of the trochlea and the diaphysis = 0, broken angle; 1, ramp

(241) Femur: proximal border of the patellar tro-chlea = 0, curved; 1, straight

(242) Tibia: anterodistal groove = 0, present; 1, absent

(243) Tibia: mediodistal gutter (tendon m. tibialis posterior) = 0, always present; 1, usually present; 2, always absent

(244) Tibia: mediodistal gutter = 0, shallow; 1, deep
(245) Tibia–fibula = 0, independent; 1, in contact or fused

(246) Tibia: posterior apophysis = 0, high; 1, low
(247) Tibia: posterior apophysis = 0, acute; 1, rounded
(248) Fibula: proximal articulation = 0, low; 1, high
(249) Fibula: distal end = 0, slender; 1, robust
(250) Fibula: laterodistal gutter (tendon peronaeus muscles) = 0, shallow; 1, deep
(251) Fibula: position of the laterodistal gutter = 0, posterior; 1, median
(252) Astragalus: (transverse diameter/height) ratio = 0, TD/H < 1; 1, 1 TD/H < 1.2; 2, 1.2 TD/H
(253) Astragalus: (anteroposterior diameter/height) ratio = 0, APD/H < 0.65; 1, 0.65 APD/H
(254) Astragalus: orientation of the fibula-facet = 0, subvertical; 1, oblique
(255) Astragalus: fibula-facet = 0, flat; 1, concave
(256) Astragalus: collum tali = 0, high; 1, low
(257) Astragalus: posterior stop on the cuboid-facet = 0, present; 1, absent
(258) Astragalus: caudal border of the trochlea, in proximal view = 0, sinuous; 1, nearly straight
(259) Astragalus: orientation of trochlea/distal articulation = 0, very oblique; 1, same axis
(260) Astragalus: expansion of the calcaneus-facet 1 = 0, always present; 1, usually present
(261) Astragalus: expansion of the calcaneus-facet 1 = 0, always wide and low; 1, usually wide and low; 2, always high and narrow
(262) Astragalus: calcaneus-facet 1 = 0, very concave; 1, nearly flat
(263) Astragalus: calcaneus-facets 2 and 3 = 0, always independent; 1, usually independent; 2, usually fused; 3, always fused

(264) Calcaneus: fibula-facet = 0, always absent; 1, usually absent; 2, usually present; 3, always present

(265) Calcaneus: tibia-facet = 0, always absent; 1, usually absent; 2, always present
(266) Calcaneus: tuber calcanei = 0, massive; 1, slender

(267) Calcaneus: insertion of the m. fibularis lon-gus = 0, salient; 1, invisible
(268) Navicular: cross-section = 0, lozenge; 1, rect-angle

(269) Cuboid: proximal side = 0, oval; 1, triangular
(270) Ectocuneiform: posterolateral process = 0, weak; 1, developed
(271) MtIII: proximal border of the anterior side = 0, straight; 1, concave; 2, sigmoid
(272) MtIII: posterior MtII-facet = 0, present; 1, absent
(273)*MtIII: MtIV-facets = 0, distinct; 1, sometimes joined [*Coelodonta antiquitatis*]
(274) MtIII: distal widening of the diaphysis (in adults) = 0, absent; 1, present
(275) MtIII: cuboid-facet = 0, absent; 1, present
(276) MtIII: cuboid-facet = 0, small; 1, large
(277) MtIV: posteroproximal tuberosity = 0, isolated; 1, pad-shaped and continuous
(278) Phalanx I for MtIII: symmetric insertions = 0, lateral; 1, nearly anterior
(279) Limbs = 0, slender; 1, robust (brachypod)
(280) Metapodials: intermediate relief = 0, high and acute; 1, low and smooth
(281) Central metapodials: posterodistal tubercle on the diaphysis = 0, absent; 1, present
(282) Lateral metapodials: insertion of the m. interossei = 0, long; 1, short (does not reach distal half of the shaft)

APPENDIX 2

Data matrix including 282 cranial, dental, and postcranial characters controlled on 28 terminal taxa (tapirid, rhinocerotoids, and rhinocero
Tapirus terrestris, Hyrachyus eximius, Trigonias osborni, and *Ronzotherium filholi*. The characters 72, 94, 102, 140 and 187 are non-a
and nonapplicable characters appear as '?' and '–', respectively.

	Characters
	00000000000000000000000000000000000000000000000000**0**0000000000000000000000000000
	00000000001111111111222222222233333333334444444444**5**5555555556666666666777777
	01234567890123456789012345678901234567890123456789**0**1234567890123456789012345
Taxa	
Tapirus terrestris (outgroup)	**0**0010-10000000000000100100010-0-0-0100000100000000**0**0-0010000000000--0-0000000
Hyrachyus eximius (outgroup)	**0**0000-00?0110000001020000000-0-0-00000?000000000**0**0-0001000100100-00-0000000
Trigonias osborni (outgroup)	**0**1000-1000010000?0102001000-0-0-00000?000001001010-20110000?100-00-?010000
Ronzotherium filholi (outgroup)	**0**0100-?000001-01100000010000-0-0-0011110001010000**0**0-0000010010000-00-0000110
Aceratherium incisivum	**0**0000-0000010000?10110?00000-100-01010??0??????00?**?**???21?1??000?100-?0-?000110
Alicornops simorrense	**0**0000-?000110101110220000000100-0-00101?0?0101100010111000011 0?110101102021110
Brachypotherium brachypus	**0**0000-1001101-1210012101210110-1010210110010101010**0**0-00111-2201001021011-1111
Bugthirhinus praecursor	**0**000100000001-1111001000110110-1000200111010001001**1**0?11101-0010001010-1011110
Chilotherium anderssoni	**0**0001000000000?211201011110110-0-0-0120001101010100**1**0-2111010110001011010111 0
Diaceratherium aginense	**0**0010-?0?0001001 1?1??0?10000-0-0-0020000?0201?1111**0**0?22111-0001000-10-100??10
Diceratherium armatum	**0**0000-?0101100 01?12020100000-110-0000011001010???0**0**0?201000000000 1010-1010110
Dicerorhinus sumatrensis	**0**0000-?000110001100120 1?0000-100-00?0010102011101 1**0**0?10111-1000001010-2021101
Diceros bicornis	**0**0?10-?0??00??00?1100???0000-0-0-0?010?10120010000**1**10111100 0???000-00-001??10
Gaindatherium browni	**0**0010-?0??01???0??0100?10000-0-0-0????0?0????????0?0**?**???010??100?000-10-101??10
Hispanotherium beonense	**0**0000-?000010100?01210010010-0-0-00020?00?1?0011010**0**0???1000???000-00-000111?
Lartetotherium sansaniense	**0**0000-?00001??00?00100110000-0-0-0?000?00?10000 10?**1**??110000000?00??00-0010000
Menoceras arikarense	**0**??**?**????????????001000-?010000
Mesaceratherium gaimersheimense	**0**1000-?000001-?1?12020?10100-0-0-01000??????11011**?**?01110??000?000-10-?011110
Mesaceratherium paulhiacense	**0**0000-?000001-?2?01010?1210110-0-00200??0??0111000**?**??211100000?000-10-?011110
***Mesaceratherium welcommi* sp. nov.**	**0**0000-?000101-?1?0210001110110-0-0111001????00????**?**??2111??0???001010-?01011??01111
Plesiaceratherium mirallesi	**0**0010-0000010100?11110110110-0-0-00211?????0100100**?**??2211??000?000-010?1-1111
Pleuroceros blanfordi	**0**0000-?0001000?0000110110010-0-0-0?001?10?2010110 1**0**?1111??000100??00-?011110
Pleuroceros pleuroceros	**0**?000-?????????0????????00?0-0-0-??0?1????????????**?**???22?0000???100-?0-??????1
Prosantorhinus douvillei	**0**??**?**??0110??0???000-00-0000110
Protaceratherium albigense	**0**??**?**??11?????????00???0-?0?????0
Protaceratherium minutum	**0**??**?**??11111?0000101000-0??????
Rhinoceros unicornis	**0**0000-?0000100?1?01110?00??0-110-00?01??????11000**?**??2111??00??1?????0?0?1110
Subhyracodon occidentalis	**0**?00????????1??0?????1?????????????????0??1??2??1???0**1**0?21111-0???10110101?????0

	Characters
	11111111111111111111111111111111111111111111111111111**1**1111111111111111111111111111
	00000000001111111111222222222233333333334444444444**5**5555555556666666666777777
	01234567890123456789012345678901234567890123456789**0**1234567890123456789012345678
Taxa	
Tapirus terrestris (outgroup)	**0**020000000000000-000000000-0000-0000-0-0--110000000**1**3-0100000100001000000000000
Hyrachyus eximius (outgroup)	**0**000100012000000-000010000-0000-0000-0-000001003-0**0**0001002-0000??00000???????
Trigonias osborni (outgroup)	**0**020000010100000-010000000000000-0000-0000000100201-0000002-2-00??000000000100
Ronzotherium filholi (outgroup)	**0**030020101222000-001100000000000-0000-000000000010**0**000000000000??000000?0000?
Aceratherium incisivum	**1**221010112231113001110100100010-011200101010001200**1**120000102110??000?????????
Alicornops simorrense	**1**021010202331023000110000100000-011200100001001200**0**2200003-1110??100100000000
Brachypotherium brachypus	**0**021000101230002001010000100010-0110-01010101003-0**1**2000102-0010??000101000?00
Bugthirhinus praecursor	**0**131000000330013101??1100???011001020?02001001201-3?0???101110??00000???????
Chilotherium anderssoni	**2**321020301330003101110000000001001021000001010100 1-320000103-1011110000000000
Diaceratherium aginense	**0**021000002330003000110000100000-010200?000000000??0**1**320000??011????????????00
Diceratherium armatum	**0**011000000310002001000100000010-0100-0100001000010**0**3?000001001 0??000?0??10000
Dicerorhinus sumatrensis	**1**121010003021023000111000-000100110-01000100013-1-2100002-2-10????0?????????
Diceros bicornis	**2**121010003121101001111000000000-0110-01000100013-1-2001002-2-1001100000???00
Gaindatherium browni	**0**011000003030022000110000100000-0112001000110013-1-1201003-3-00???0??????????
Hispanotherium beonense	**0**331100001330023100011101100211001020000200 11013-1-3001002-2-10??000000000001
Lartetotherium sansaniense	**0**011010003030022000110000100000-0112001000111013-1-1201003-2100??00000???????
Menoceras arikarense	**2**321030000332003000011101000001001 00-0002001001010**0**3?0100002-10??100010010001
Mesaceratherium gaimersheimense	**0**011000000310003001110100100010-0101-01?201000110 0**1**020000102100????????001??
Mesaceratherium paulhiacense	**0**021000003330003001110100100?110010??0????????????0**?**??0??????????????????????
***Mesaceratherium welcommi* sp. nov.**	**0**311000000330003101110100100010-0102001120100113-1-120???20210-??????????????????
Plesiaceratherium mirallesi	**2**021010102230013000011100000000-0110-0110010001000**1**1100000001 00??000100000001
Pleuroceros blanfordi	**1**211000302331013101010101100011001020011100010101 0**0**2000000011 0????????00?00
Pleuroceros pleuroceros	**?**??????????????????????????????????????11000?01010**0**??0???00011??????????????
Prosantorhinus douvillei	**0**021000303230023000010100000001001 10-0100010100001-2200020001111??00010??00000
Protaceratherium albigense	**0**011010000300003 0-0100100100011001020000000000101 0**0**2000000000???1???00?100
Protaceratherium minutum	**1**021020202230003000011100000010-0100-0102000101000**0**0200000011 10??00000??00000
Rhinoceros unicornis	**0**221020003022232001110000 0-0000-0110-01000101013-1-2001002-2-11????010??????0?
Subhyracodon occidentalis	**0**030000010110000-000111000000??0100-0?000010010 10**0**3200010100100000000000???00

Taxa

Tapirus terrestris (outgroup) *Hyrachyus eximius* (outgroup) *Trigonias osborni* (outgroup) *Ronzotherium filholi* (outgroup) *Aceratherium incisivum Alicornops simorrense Brachypotherium brachypus Bugthirhinus praecursor Chilotherium anderssoni Diaceratherium aginense Diceratherium armatum Dicerorhinus sumatrensis Diceros bicornis Gaindatherium browni Hispanotherium beonense Lartetotherium sansaniense Menoceras arikarense*

Mesaceratherium gaimersheimense Mesaceratherium paulhiacense
***Mesaceratherium welcommi* sp. nov.**
Plesiaceratherium mirallesi
Pleuroceros blanfordi
Pleuroceros pleuroceros Prosantorhinus douvillei Protaceratherium albigense Protaceratherium minutum Rhinoceros unicornis Subhyracodon occidentalis

Characters

222222222222222222222222222222222222222222222222**2**22222222222222222222222222222222

000000000011111111112222222222333333333344444444445555555556666666666777777777888

012345678901234567890123456789012345678901234567890123456789012345678901234567890123456789012

00000000001001000000-0000000-000000000000001010000001000100000000000000000020000-000000
01000001000111000010000000-00000000?0100000000000**0**0000000000003000000021-010000000
0000?000100000100010100100**0**-00?00000???00101-000?0**0**0110000000000??1?00?0000????0001
00000000000000000000-1???000-202?0000?000000000000**0**01?000010020101001?000000-0?0000
01001111001001001010102210212010 1?00?0100000110000**0**1111000100101000010000000-000000
1000?001?000011000??00231021 00?01?10???00??1?0???1**?**?1100001100003200000100010 0?0000
00110110011000100010001 1100-0111100000010112-00101**0**12110010100112200000?100011001001
??001?010010????????1000??????21?????????????????????**0**1111101??10003??1?1?0200110110 0?0
0???????????0???10?????????????????1?????????????????**?**?2?100???10?0???????????10??10??
01001011101011000 0-01001021010 01?00?010011??00111**?**?101001?110103?0?00020000-000001
01000001000010100010100 000-00210?000010000000011 0**0**0100001000003120010020010-000001
01100100000100201010000000202021001 0?0100101-00001**1**1110010110002320001010001010 0000
11000100000111211010100010212001001101-11010101110**1**1111010110002020100010000-100100
???**?**????????????????????????????????
11000101111100101012111200100021011110001010111110**1**12111101102033211101200110110100
01001??000110110001211 2?00200021 1?????????000101???**?**110000?01003??0010?100?0-0?0100
01000001100010100010100300200021011100100000100110**0**0111010010103321011010011001 0000
???**?**????????????????????????????????
???????000101?10101011 0?1021001 0????????????????????**?**?110000?002000?0?00021-00-??00?0
?0000?00001000?0?010??0000200??00?????????101100???**?**?110000100203300000?1101????00?0
01000001001000000010100001100010000000000010000001**1**1110010010103120000011-00-000010
00001??0101011??0010??01000-?0?11?????????101001?1**1**0110000100200001000010010-0?0001
???????0101???100010??0?002000?11?????????????????**?**?110000?00?003?1?000000?0-??0001
01101110001001000 00-0000101111011010000001110000001**0**12100010112103200000 11-010001001
01000??00010??10?01010??000-00101?????????00110 0??**?**010000102-00????1??1?0?0-??0000
0?????0110101110001 1??0?000-?00?0?1????0?00??000??**?**?1100100100011000000 2??10-?10000
01000100001000001 00-1020102000211000?0110010001101**1**1110010110002320000010010-100100
010??1001??0100??0???????????0?10000???000???0??1 0**?**?1?0000?000000010 0??2??00-??0???